# Application of a Helmholtz resonator excited by grazing flow for manipulation of a turbulent boundary layer

Farzin Ghanadi

School of Mechanical Engineering
The University of Adelaide
South Australia, 5005
Australia

A thesis submitted in fulfilment of the requirements for the degree of Ph.D. in Mechanical Engineering on the 22nd September 2014

# Abstract

In most industrial applications involving flow the Reynolds number is typically sufficiently high such that the boundary layer is turbulent. Flow instabilities within the turbulent boundary layer can result in an excessive drag penalty which is considered to be the main parameter affecting the aerodynamic efficiency in numerous applications including aircraft and pipelines. The aim of this research is manipulation of the turbulent boundary layer through the oscillatory flow created by a flow-excited Helmholtz resonator for the purpose of minimising the flow instabilities. Attention has been given here to a cylindrical Helmholtz resonator as a possible alternative flow control device. The energy required to activate the Helmholtz resonator comes from the grazing flow and it can be fitted to existing airframes with minimal manufacturing requirements. Hence it can potentially be an ideal solution for a wall-based flow control device. This research provides an insight into the behaviour of the flow in the vicinity of the resonator and assesses the capability of a flow-excited Helmholtz resonator for reduction of disturbances within the boundary layer.

The excitation of flow in the vicinity of the Helmholtz resonator is associated with both the external pressure fluctuations within the turbulent boundary layer and the acoustic response of the resonator cavity. A model of the relationship between the pressure inside the cavity and the boundary layer was developed based on a momentum balance equation and combination of the vortex sheet with discrete vortex models. A parametric study of the

resonator showed that when the orifice length is increased the pressure fluctuations within the resonator are reduced, potentially due to the larger skin friction inside the orifice. To understand the boundary layer features over a flow-excited Helmholtz resonator a Large Eddy Simulation (LES) of the three dimensional flow over a wide range of flow velocities was also conducted. It was demonstrated that when the boundary layer thickness equals the orifice length and is twice the orifice diameter, the flow suction within the orifice is greater than the flow injection area which results in a reduction in the turbulence intensity of up to 10%. Detailed investigation of the characteristics of the turbulent boundary layer downstream of the resonator has also been accomplished through an extensive experimental study in a subsonic wind tunnel with a low turbulence intensity level of 0.5%, for free stream velocities between 15 and 30m/s. Similar to the results of the numerical modelling, the experimental results showed that a resonator with an orifice length equal to the boundary layer thickness modifies near-wall structures such that the intensity of sweep is reduced by up to 5% and its duration by up to 8%. It was also demonstrated that when the orifice diameter approximately equals the thickness of the inner layer, $y^+ \approx 400$, the velocity fluctuations normal to the grazing flow can penetrate the boundary layer, which in turn causes the large eddies to transfer their energy to the smaller eddies within the logarithmic region, resulting in attenuation of turbulence production.

The results of this study provide an improved understanding for the further development of flow-excited Helmholtz resonators as a flow control device, an area that warrants further investigation in the future.

# Contents

# Declaration

I certify that this work contains no material which has been accepted for the award of any other degree or diploma in my name, in any university or other tertiary institution and, to the best of my knowledge and belief, contains no material previously published or written by another person, except where due reference has been made in the text. In addition, I certify that no part of this work will, in the future, be used in a submission in my name, for any other degree or diploma in any university or other tertiary institution without the prior approval of the University of Adelaide and where applicable, any partner institution responsible for the joint-award of this degree.

I give consent to this copy of my thesis when deposited in the University Library, being made available for loan and photocopying, subject to the provisions of the Copyright Act 1968.

The author acknowledges that copyright of published works contained within this thesis resides with the copyright holder(s) of those works.

I also give permission for the digital version of my thesis to be made available on the web, via the University's digital research repository, the Library Search and also through web search engines, unless permission has been granted by the University to restrict access for a period of time.

Farzin Ghanadi Date

# Acknowledgment

I would firstly like to acknowledge the support of my principal supervisor Dr Arjomandi for his endless support and guidance during the course of this study; I continue to learn a lot from him. I would also like to thank the co-supervisors of the project, A/Prof Ben Cazzolato and A/Prof Anthony Zander who have shared their knowledge and expertise. I thank you all sincerely.

I would also like to thank all of my friends, (of which there are many), who have supported me throughout my research endeavours.

I would like to extend my thanks to the technicians of the Mechanical and Electrical workshops in the School of Mechanical Engineering at the University of Adelaide who have assisted in the fabrication of the designed models as well as the provision of the required equipment. You have all been a source of knowledge, fun and friendliness, and to you all I express my thanks.

Finally I save the biggest thanks to my parents Nayereh Beheshti and Mohammadreza Ghanadi and to my brother Mehdi Ghanadi whose love and support led me to this point. This journey has been as much hard work for you as it has been for me and through your support we have made it. Words cannot express my thanks and appreciation.

# Nomenclature

| | |
|---|---|
| $A$ | cross-section area of the riblets groove ($m^2$) |
| $c$ | speed of sound (m/s) |
| $C_q$ | suction coefficient: $\frac{V_w}{U_\infty}$ |
| $d$ | orifice diameter (m) |
| $D$ | cavity diameter (m) |
| $f$ | frequency (Hz) |
| $f_b$ | bursting frequency (Hz) |
| $F_c$ | Coriolis force (N) |
| $F_{ext}$ | force exerted on the fluid inside the orifice (N) |
| $f_n$ | natural frequency of the resonator (Hz) |
| $f_r$ | resonance frequency of the resonator (Hz) |
| $h$ | groove depth (m) |
| $i$ | resonator mode number, imaginary number $\sqrt{-1}$ |
| $K$ | spring constant (N/m) |
| $k$ | wavenumber (rad/m) |
| $l$ | length of the orifice (mm) |
| $L$ | cavity depth (mm) |
| $l_e$ | effective length of the orifice (mm) |
| $m$ | mass of fluid (kg) |
| $Ma$ | Mach number |

| | |
|---|---|
| $n$ | compliance of the resonator |
| $P_{ext}$ | excitation pressure (Pa) |
| $P_{res}$ | resonator pressure fluctuations (Pa) |
| $P_t$ | acoustic power (W) |
| $q_o$ | spatially averaged flow rate induced by flow over the resonator orifice ($m^3$/s) |
| $q_r$ | spatially averaged acoustic volume flux through the resonator orifice ($m^3$/s) |
| $R$ | damping constant |
| $S$ | cross-section area of the orifice ($m^2$) |
| $s$ | groove spacing (m) |
| $St$ | Strouhal number |
| $t$ | time (s) |
| $T_{\mathrm{osc}}$ | period of wall oscillation (s) |
| $U$, $U_\infty$ | mean free stream velocity (m/s) |
| $u$ | streamwise flow velocity (m/s) |
| $u_a$ | acoustic particle velocity (m/s) |
| $u_c$ | convection velocity of the vortices (m/s) |
| $u_{cs}$ | propagation speed of streaks (m/s) |
| $u_\tau$ | friction velocity (m/s) |
| $T$ | time period (s) |
| $v_t$ | local velocity (m/s) |
| $v$ | cross-stream component of velocity (m/s) |
| $V_c$ | cavity volume ($m^3$) |
| $V_w$ | suction velocity (m/s) |
| $x$ | indicates the x-direction (streamwise) (m) |
| $y$ | indicates the y-direction (wall-normal direction) (m) |
| $z$ | indicates the z-direction (spanwise direction) (m) |

| | |
|---|---|
| $Z$ | spanwise spacing of streaks (m) |
| $Z_c$ | total input impedance of the resonator (N.s/m$^3$) |
| $Z_M$ | acoustic impedance (N.s/m$^3$) |

**Symbols**

| | |
|---|---|
| $\sigma$ | standard deviation |
| $\Gamma$ | circulation (m$^2$/s) |
| $\zeta$ | damping ratio |
| $\omega$ | angular frequency (rad/s) |
| $\omega_r$ | angular resonance frequency (rad/s) |
| $\Omega$ | vorticity (1/s) |
| $\rho$ | density of air (kg/m$^3$) |
| $\varphi$ | phase lag between the vortical flow and acoustic volume flow (rad) |
| $\lambda$ | acoustic wavelength (m) |
| $\upsilon$ | kinematic viscosity (m$^2$/s) |
| $\delta$ | boundary layer thickness (mm) |
| $\theta$ | momentum thickness (mm) |

**Superscripts**

| | |
|---|---|
| $()'$ | denotes the fluctuating part of () |
| $\overrightarrow{()}$ | denotes a vector |
| $\widehat{()}$ | denotes Fourier transform of () |
| $+$ | denotes time scale ($\frac{\upsilon}{{u_\tau}^2}$) or length scale ($\frac{\upsilon}{u_\tau}$) |

# Chapter 1

# Introduction

## 1.1 Background

The vast majority of boundary layers surrounding aerodynamic bodies can be categorised as turbulent boundary layers. In many situations, such as aircraft or pipelines, this kind of boundary layer is unavoidable due to flow irregularities resulting in transition. Shear interactions between a turbulent boundary layer and the wall surface generate three dimensional flow instabilities within the boundary layer, that are approximately an order of magnitude larger than those observed during laminar flows, and are considered to be the major source of the skin friction drag (Karvchenko et al. 1993; Kasagi et al. 2009). The increase in viscous or skin friction drag due to a turbulent boundary layer generally poses serious restrictions on the aerodynamic performance for various applications. For example, the skin-friction drag constitutes roughly 50% of the total drag of a commercial aircraft in steady flight condition as shown in Figure 1.1, and 90% of the drag for underwater vehicles (Marec 2000; Malik et al. 2013). Considering the sharp rise in the costs of fossil fuel during the last few years, even a small reduction in viscous drag of 10% can lead to an annual fuel saving of approximately half a billion dollars in commercial airlines (Hefner 1988; Kral

1999; Parker and Sayers 1999). Other possible benefits of viscous drag reduction include increased speed of vehicles, enhanced mixing in combustion engines, higher efficiency of heat transfer in heat exchangers, and a reduction in the duct size and pumping power in pipelines (Gad-el-Hak 2000; Kasagi et al. 2012).

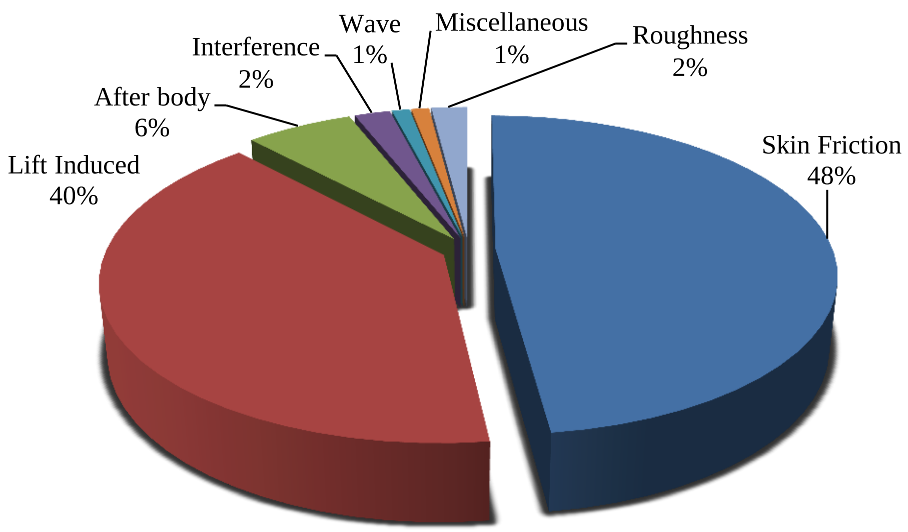


Figure 1.1: Contribution of drag types for a typical aircraft (Marec 2000& Malik et al. 2013)

Therefore, a reliable flow control strategy to reduce the skin friction drag is of paramount importance in many engineering applications, although the control is difficult due to the non-deterministic and chaotic behaviour of the turbulent boundary layer. In order to attenuate the viscous drag, it is therefore necessary to understand the creation process of the flow instabilities within the turbulent boundary layer. It is believed that streamwise vortices generated by low momentum flow within the boundary layer plays the primary role in the development of inflection points in the streamwise and spanwise velocity profiles of grazing flow (Kline et al. 1967; Adrian et al. 2000). Suppression of the instabilities due to these inflectional velocity profiles, and the corresponding Reynolds shear stresses, is an important step towards reduction of high skin friction drag in turbulent boundary layers.

An immense body of literature exists regarding drag reduction by controlling the three-dimensional instabilities in turbulent boundary layers. For example, by using riblets or small longitudinal striations on the surface on the surface of a body, Walsh (1983) managed to passively control these instabilities. The secondary vortex system within the groove valleys of the riblets are responsible for retaining streamwise vortices, thereby the total thickness of the boundary layer is decreased, while the viscous sublayer has greater thickness. It has, furthermore, been indicated that by means of these structures the local skin friction can be reduced by approximately 8% (Vukoslavcevic et al. 1992). However, challenges such as manufacturing difficulties and finding the optimal riblet size in the industrial applications still remain. Similarly, applying a specifically-designed suction technique beneath the streamwise vortices, Gad-El-Hak and Blackwelder (1989) showed a dramatic drag reduction of up to 50%. In the same way, weakening of the quasi-streamwise vortices through generating travelling waves with plasma actuators or wall oscillations has shown a reduction in the skin friction drag (Laadhari et al. 1994; Du et al. 2004). In all these methods, disrupting the streamwise vortices within the near-wall region has been achieved through addition of vortices within the boundary layer. Similarly, a more recent numerical investigation revealed that vortex generating devices such as synthetic jets can manipulate the link between streamwise vortices and the low speed flow within the inner layer of the boundary layer (Lockerby et al. 2005). However, all these active control techniques require an external energy source and, therefore, are difficult to implement in practice.

To manipulate the turbulent boundary layer an innovative technique is required with minimal problems for implementation in real applications. An appropriate flow control device should be relatively easy to construct and implement, as well as not being too expensive or heavy. Moreover, in real applications it is very important that a flow control device has minimal external energy requirements. In the present study, a cylindrical flow-excited Helmholtz resonator is introduced as a new concept for passive flow control of turbulent boundary layers. Furthermore, the characteristics and effectiveness of this device in providing a reduction in the instabilities within a turbulent boundary layer are investigated.

Under certain conditions the flow past a Helmholtz resonator results in self-sustained resonance and the flow within the resonator cavity forces the grazing flow. The flow oscillations over the Helmholtz resonator has gained renewed interest due its diverse industrial applications (Rienstra and Hirschberg 2001; Hemon et al. 2004). The flow oscillations generated by the resonator may have undesirable effects, for instance, gas fluctuations inside pipelines with closed side branches, the grazing flow over aircraft landing gear, and cabin pressure fluctuations inside a vehicle with an open window or sunroof (Bruggeman et al. 1991; Inagaki et al. 2002; Crouse et al. 2006). In most engineering applications, the flow oscillations are, therefore, deemed undesirable and thus a large amount of research focuses on active or passive methods for suppression of the unwanted excitations (Kook 1997; Alam et al. 2007; Ma et al. 2009). However, exploration of the potential benefits of a flow-excited Helmholtz resonator for separation control and manipulation of the boundary layer downstream of the resonator has received little attention (De Metz et al. 1977; Flynn et al. 1990; Lockerby 2001; Urzynicok 2003).

The motivation for this research originates from the desire to postpone the turbulent events or reduce the flow instabilities within the turbulent boundary layer using the resonator excited by the grazing flow. It is thought that at resonance flow induced pulsation in the vicinity of the resonator orifice may inhibit the growth of the coherent structures and stabilise the turbulent boundary layer. In this method, the energy required for manipulation of the low momentum flow and associated streamwise vortices is extracted from the grazing flow and is returned to it almost entirely as periodic fluctuations. The frequency and amplitude of the flow fluctuations over the resonator can be altered by changing the characteristics of the resonator, such as the cavity volume and the orifice size, and the incoming flow condition. Hence, in the present study the flow features within the resonator and in the vicinity of its orifice have been investigated to provide an insight into the potential of the flow-excited Helmholtz resonator as a flow control device.

### 1.2 Aims and objectives

The aims of the present research are to investigate the feasibility of the application of a flow-excited Helmholtz resonator to control the turbulent boundary layer for the purpose of drag reduction. Therefore, the objectives of the research can be defined as:

- to determine instantaneous pressure and velocity fields within the cavity and in the vicinity of the orifice of a flow-excited Helmholtz resonator;
- to explore the potential of the flow-excited Helmholtz resonator to attenuate or amplify the three-dimensional instabilities within a turbulent boundary layer downstream of the resonator;
- to determine the changes in turbulent energy cycles downstream of the resonator with potential to reduce the instabilities within the near wall regions of the boundary layer and to explore the streamwise and spanwise extent to which stability improvements are maintained;
- to identify the optimal parameters of the resonator, with the potential to improve the stability of a flat plate turbulent boundary layer with no pressure gradients.

In order to achieve the desired research objectives, the present study involved the following tasks:

- the development of an analytical model to predict the amplitude and frequency of the pressure fluctuations inside a cylindrical Helmholtz resonator with varying dimensions;
- the implementation of an appropriate numerical approach to study the flow behaviour inside and in the vicinity of the flow-excited resonators as well as an insight into the effects of the resonators on the turbulence structures of the downstream boundary layer;
- the design, development and manufacture of a flat plate rig system, diverse resonator configurations and measurement techniques that are able to achieve favourable experimental results.

### 1.3 Thesis outline

The current thesis is presented in a number of chapters, the sequence of which highlights the chronology of the knowledge-development and the research undertaken to meet the mentioned aims. The first chapter provides an overview of the subject matter as well as the principal aims and the tasks required for the current research. Chapter 2 gives a comprehensive and up-to-date summary of previous studies in this area and determines the gap in knowledge as well as the significance of the present research in further detail. Chapters 3 to 6 constitute the main body of the thesis and consist of six manuscripts which have been published, or are currently under review in prestigious international peer-reviewed journals. The detailed discussion of the analytical model and the simulation results along with the achievements of the experimental investigation are presented in these publications. Finally, in the last chapter of the thesis, the conclusions of the present research and recommendations for future work are given. The following is a description of how the contents of each chapter link together to achieve the specified scope of the present research.

Chapter 2 provides a comprehensive review of the characteristics of the flow within the cavity of a flow-excited Helmholtz resonator and in the vicinity of the resonator orifice. It is followed by an extensive literature review of the turbulence production mechanism in the near wall region of the boundary layer, along with a brief discussion of various control techniques that have been used to suppress the instabilities that naturally occur in the turbulent boundary layer. The review identifies the primary research gaps that have been addressed by the current work.

The main body of the research starts by examining the instantaneous pressure fields within a flow-excited Helmholtz resonator for a range of free stream velocities and resonator geometries. Chapter 3 consists of the first of the six journal papers and presents a detailed model for predicting the pressure fluctuations within the resonator cavity and in the flow exterior to the cavity as a function of the resonator geometry. The model employs a simplified momentum balance equation between the interior and exterior of the resonator. It is based on a combination of the incompressible and fully-developed flow within the resonator neck and the compressible flow inside the cavity. The validation process demonstrates that the model can successfully capture the coupled dynamics arising from the interaction of the grazing flow with the Helmholtz resonator. The parametric study showed that the pressure amplitude inside the resonator is strongly affected by the resonator shape and the properties of the incoming flow.

Chapter 4 presents a detailed numerical investigation of the three-dimensional flow over a flow-excited Helmholtz resonator. Due to the minimal dissipation effects at sub-grid scales, a Large Eddy Simulation (LES) model was utilised to predict the time dependent pressures inside the resonator and the velocity fluctuations within the shear layer over the resonator orifice. A comparison between published experimental data and the results obtained by the simulation shows that the numerical modelling provides an accurate representation of the interaction of the turbulent boundary layer with the Helmholtz resonator. The calculated sound pressure level of the acoustic response of the resonator demonstrates that at a specific range of flow velocities, strong excitation of the resonator occurs. It was also observed that the maximum velocity fluctuations normal to the grazing flow occur at frequencies close to the natural frequency of the resonator itself.

The potential of the flow-excited Helmholtz resonator to modify the flow instabilities within the turbulent boundary layer downstream of the resonator has been investigated experimentally and numerically in Chapter 5. The focus of this chapter is on the pressure fluctuations within the resonator along with the turbulence intensity and energy spectra of the streamwise velocity fluctuations downstream of the resonator orifice. The chapter aims to identify the relationship between the flow fluctuation fields downstream of the resonator with the geometric characteristics of the resonator and the properties of the grazing flow. The results indicate a reduction in the turbulence intensity and the transfer of energy from large eddies to small eddies within the boundary layer downstream of certain resonators.

Chapter 6 presents a detailed description of the attenuation of the turbulence production downstream of the resonators with the potential to reduce the turbulence intensity. An LES model and further experimental work discussed in this chapter provide an insight into the mechanisms involved in the resonator's role to attenuate the turbulence and also identifies the favourable parameters required to stabilise the downstream boundary layer. It is recommended, based on this work, that an orifice length equal to the incoming boundary layer thickness and an orifice diameter similar to the thickness of the inner layer of the boundary layer are necessary for the resonator to be used as a flow control device. Finally, the durability of the favourable effects of the resonator on the turbulence structures is also discussed in this chapter.

In the final chapter, the key conclusions that have been documented throughout the thesis will be presented. It must be noted that the investigations discussed in this thesis are only the beginning of the development of a flow-excited Helmholtz resonator as a flow control device. Consequently a significant amount of potential work still exists for future investigations.

## 1.4 Publications arising from this thesis

The research presented in this thesis has led to the generation of six journal manuscripts and five peer reviewed conference articles. The journals and conferences in which the papers are published or submitted are closely related to the field of the research of this thesis and will be cited in the following section. Following is a list of the manuscripts resulting from the current research:

### Journal papers

Ghanadi, F., Arjomandi, M., Cazzolato, B. S., and Zander, A. C. 2013 'Numerical simulation of grazing flow over a self-excited Helmholtz resonator', *Engineering Letters*, vol. 21, no 3, pp. 137-142.

Ghanadi, F., Arjomandi, M., Cazzolato, B. S., and Zander, A. C. 2013, 'Analysis of the pressure fluctuations induced by grazing flow over a Helmholtz resonator', submitted to *Journal of Fluids and Structures*.

Ghanadi, F., Arjomandi, M., Cazzolato, B. S., and Zander, A. C. 2014, 'Understanding of the flow behaviour on a Helmholtz resonator excited by grazing flow', *International Journal of Computational Fluid Dynamics,* published online (DOI: 10.1080/10618562.2014.922681).

Ghanadi, F., Arjomandi, M., Cazzolato, B. S., and Zander, A. C. 2014, ' Interaction of a flow-excited Helmholtz resonator with a grazing turbulent boundary layer', *Experimental Thermal and Fluid Science,* vol. 58, pp. 80-92.

Ghanadi, F., Arjomandi, M., Cazzolato, B. S., and Zander, A. C. 2014, 'Analysis of the turbulent boundary layer in the vicinity of a self-excited cylindrical Helmholtz resonator', submitted to *Journal of Turbulence*.

Ghanadi, F., Arjomandi, M., Cazzolato, B. S., and Zander, A. C. 2014, 'Control of turbulent boundary layer by a self-excited Helmholtz resonator', submitted to *Journal of Fluid Mechanics*.

**Refereed conference papers**

Ghanadi, F., Arjomandi, M., Cazzolato, B. S., and Zander, A. C. 2012, 'A review of skin friction drag reduction within the turbulent boundary layer', *7th Australasian Congress on Applied Mechanics*, ACAM 7, Adelaide, Australia.

Ghanadi, F., Arjomandi, M., Cazzolato, B. S., and Zander, A. C. 2013, 'Velocity fluctuations within the turbulent flow over a flow-excited Helmholtz resonator', *The 2013 International Conference on Mechanical and Materials Engineering*, Stockholm, Sweden.

Ghanadi, F., Arjomandi, M., Cazzolato, B. S., and Zander, A. C. 2013, 'Numerical simulation of grazing flow over a self-excited Helmholtz resonator', *International Conference of Mechanical Engineering*, London, U. K.

Ghanadi, F., Arjomandi, M., Cazzolato, B. S., and Zander, A. C. 2014, 'Experimental investigation of the application of a self-excited cylindrical Helmholtz resonator for turbulent drag reduction', *19th Australasian Fluid Mechanics Conference*, AFMC 2014, Melbourne, Australia.

Ghanadi, F., Arjomandi, M., Cazzolato, B. S., and Zander, A. C. 2014, 'The streamwise and spanwise effects of flow-excited Helmholtz resonators on a three-dimensional turbulent boundary layer', *9th International Symposium on Turbulence and Shear Flow Phenomena*, TSFP-9, Melbourne, Australia.

## 1.5 Format

The thesis has been submitted as a portfolio of the publications according to the formatting requirements of The University of Adelaide. The printed and online versions of this thesis are identical. The online version of the thesis is available as a PDF and can be viewed in its correct fashion using Adobe Reader 9.

## References

Adrian, R. J., Meinhart, C. D., and Tomkins, C. D. 2000, 'Vortex organisation in the outer region of the turbulent boundary layer', *Journal of Fluid Mechanics*, vol. 422, pp. 1–54.

Alam, M. M., Matsuob, S., Teramotob, K., Setoguchib, T., and Kim, H. D. 2007, 'A new method of controlling cavity-induced pressure oscillations using sub-cavity', *Journal of Mechanical Science and Technology*, vol. 21, no. 9, pp. 1398-1407.

Bruggeman, J., Hirschberg, A., Van Dongen, M., Wijnands, A., and Gorter, J. 1991, 'Self-sustained aero-acoustic pulsations in gas transport systems: experimental study of the influence of closed side branches', *Journal of Sound and Vibration*, vol. 150, no. 3, pp. 371-393.

Crouse, B., Senthooran, S., Freed, D., Balasubramanian, G., Gleason, M., Puskarz, M., Lew, P., and Mongeau, L. 2006, 'Experimental and numerical investigation of a flow induced cavity resonance with application to automobile buffeting', *27th AIAA Aeroacoustics Conference*, Massachusetts, USA.

De Metz, F. C., and Farabee, T. M. 1977 'Laminar and turbulent shear flow induced cavity resonances', *4th Aeroacoustics Conference*, Atlanta, USA.

Du, Y., Symeonidis, V., and Karniadakis, G. 2002, 'Drag reduction in wall-bounded turbulence via a transverse travelling wave', *Journal of Fluid Mechanics*, vol. 457, no. 1, pp. 1-34.

Flynn, K. P., and Panton, R. L. 1990, 'The interaction of Helmholtz resonators in a row when excited by a turbulent boundary layer', *Journal of the Acoustical Society of America*, vol. 87, no. 4, pp. 1482-1488.

Gad-el-Hak, M. 2000, 'Flow control: passive, active, and reactive flow management', Cambridge University Press.

Gad-El-Hak, M., and Blackwelder, R. F. 1989, 'Selective suction for controlling bursting events in a boundary layer', *AIAA Journal*, vol. 27, no 3, pp. 308-314.

Hefner, J. N. 1988, 'Dragging down fuel costs', *Aerospace America*, vol. 26, no. 2, pp. 14-16.

Hémon, P., Santi, F., and Amandolèse, X. 2004, 'On the pressure oscillations inside a deep cavity excited by a grazing airflow', *European Journal of Mechanics-B/Fluids*, vol. 23, no. 4, pp. 617-632.

Inagaki, M., Murata, O., Kondoh, T., and Abe, K. 2002, 'Numerical prediction of fluid-resonant oscillation at low Mach number', *AIAA Journal*, vol. 40, no. 9, pp. 1823-1829.

Kasagi, N., Hasegawa, Y., and Fukagata, K. 2009, 'Toward cost-effective control of wall turbulence for skin friction drag reduction', *Advances in Turbulence XII*, vol. 132, pp. 189-200.

Kasagi, N., Hasegawa, Y., Fukagata, K., and Iwamoto, K. 2012, 'Control of turbulent transport: Less friction and more heat transfer', *Journal of Heat Transfer,* vol. 134, no. 3, pp. 309-324.

Kline, S., Reynolds, W., Schraub, F., and Runstadler, P. 1967, 'The structure of turbulent boundary layers', *Journal of Fluid Mechanics*, vol. 30, no. 4, pp. 741-773.

Kook, H. 1997, 'Prediction and control of the interior pressure fluctuations in a flow-excited Helmholtz resonator', *Ph.D. Thesis*, Purdue University.

Kral, L. D. 1999, 'Active flow control technology', *ASME Fluids Engineering Division Newsletter*, pp 1-28.

Kravchenko, A. G., Choi, H., and Moin, P. 1993, 'On the relation of near-wall streamwise vortices to wall skin friction in turbulent boundary layers', *Physics of Fluids*, vol. 5, no. 12, pp. 3307-3309.

Laadhari, F., Skandaji, L., and Morel, R. 1994, 'Turbulence reduction in a boundary layer by a local spanwise oscillating surface', *Physics of Fluids*, vol. 6, no. 10, pp. 3218-3220.

Lockerby, D. 2001, 'Numerical simulation of boundary-layer control using MEMS actuation', *Ph.D. Thesis*, The University of Warwick.

Ma, R., Slaboch, P. E., and Morris, S. C. 2009, 'Fluid mechanics of the flow-excited Helmholtz resonator', *Journal of Fluid Mechanics*, vol. 623, no. 1, pp. 1-26.

Malik, M., Liao, W., Li, F. and Choudhari, M. 2013, 'DRE-Enhanced Swept-Wing Natural Laminar Flow at High Reynolds Numbers', *51st AIAA Aerospace Sciences Meeting including the New Horizons Forum and Aerospace Exposition*, AIAA 2013-0412, Texas, USA.

Marec, J. 2000, 'Drag reduction: a major task for research', *European Drag Reduction Conference*, vol. 76, pp. 17-27.

Parker, K., and Sayers, A. T. 1999, 'The effect of longitudinal micro-striations and their profiles on the drag of flat plates', *Journal of Mechanical Engineering Science*, vol. 213, no. 8, pp. 775-785.

Rienstra, S., and Hirschberg, A. 2001, 'An introduction to acoustics', *Report IWDE*, Eindhoven University of Technology.

Urzynicok, F. 2003, 'Separation control by flow-induced oscillations of a resonator', *Ph.D. Thesis*, University of Berlin.

Vukoslavcevic, P., Wallace, J., and Balint, J. L. 1992, 'Viscous drag reduction using streamwise-aligned riblets', *AIAA Journal*, vol. 30, no. 4, pp. 1119-1122.

Walsh, M. J. 1983, 'Riblets as a viscous drag reduction technique', *AIAA Journal*, vol. 21, no. 4, pp. 485-486.

# Chapter 2

# Literature Review

In this chapter, some of the key studies, conducted over the last century, into the flow behaviour of a self-excited Helmholtz resonator and turbulent boundary layer control will be presented. The cited papers are by no means exhaustive and merely provide a glimpse of the vast areas of research related to the present study. An overview of the flow-excited Helmholtz resonator will be presented in Section 2.1, with an emphasis on the primary flow characteristics within the resonator and downstream of its orifice. Following this, the characteristics of coherent structures and the energy production mechanisms within a turbulent boundary layer will be reviewed in Section 2.2. Subsequently, in Section 2.3, a semi-historical review of some of the successful strategies that have been used to reduce the instabilities within the turbulent boundary layer is presented. Finally, the chapter concludes with a summary of the literature review and the objectives of this research in Section 2.4.

### 2.1 Flow-excited Helmholtz resonator

A Helmholtz resonator is a type of side branch resonator for suppressing pure tones of constant frequency. As shown in Figure 2.1, it consists of a cavity, with a fixed volume of compressible fluid, coupled with the environment through a short neck or opening (Von Helmholtz 1896; Kinsler et al. 1999). The spring effect of the flow within the cavity allows the volume of the air in the cavity to compress and expand (Alster 1972; Tang and Sirignano 1973; Ronneberger 1980; Walker and Charwat 1982). A number of studies have been undertaken to acoustically excite two- and three-dimensional Helmholtz resonators (Hersh and Walker 1977; Cummings 1986; Tam et al 2008; Zhang et al. 2013). However, the number of published works on flow excited resonators are rather limited (De Metz and Farabee 1977; Nelson et al. 1981; Flynn and Panton 1990). It has been demonstrated that flow excitation of the resonators occurs when the frequency of the instabilities within the shear layer over the orifice is near or equal to the resonance frequency of the resonator, $f_r$ (Elder et al. 1982; Khosropour and Millet 1990; Kook 1997).

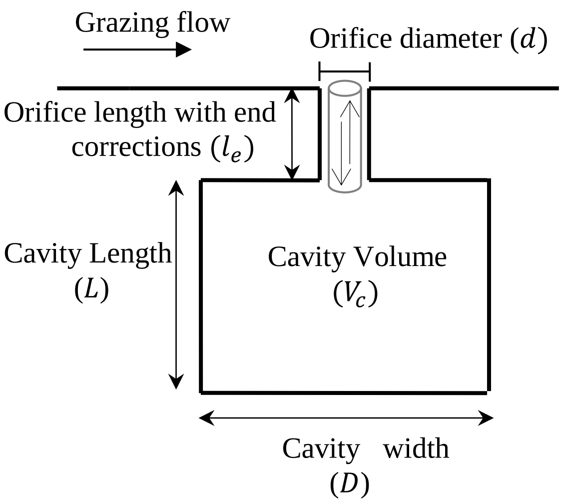


Figure 2.1: Schematic of a Helmholtz resonator.

Figure 2.2 shows one example of the flow behaviour over the resonator orifice in which the shear layer has a sheet-like motion until it reaches the mid-point of the orifice. Afterwards, it breaks down into quasi-periodic vortices which travel to the trailing edge of the orifice. Owing to the interaction of the vortices with the trailing edge, the produced pressure waves propagate back towards the leading edge of the orifice, which trigger the release of the next vortex. The pressure fluctuations inside the cavity are augmented when the frequency of these instabilities approaches the resonance frequency of the resonator. This process generates flow pulsation in the vicinity of the orifice to relieve the pressure inside the resonator. Therefore a flow-excited resonator can change the characteristics of the flow over the orifice. It should be stated that the acoustic performance of a Helmholtz resonator is also affected by the grazing flow. Tang and Sirignano (1973) developed a model based on the combined continuity and momentum equations for various resonators and showed that the energy absorption coefficient has a higher peak in the presence of mean flow. In other words, the real part of the acoustic impedance is amplified.

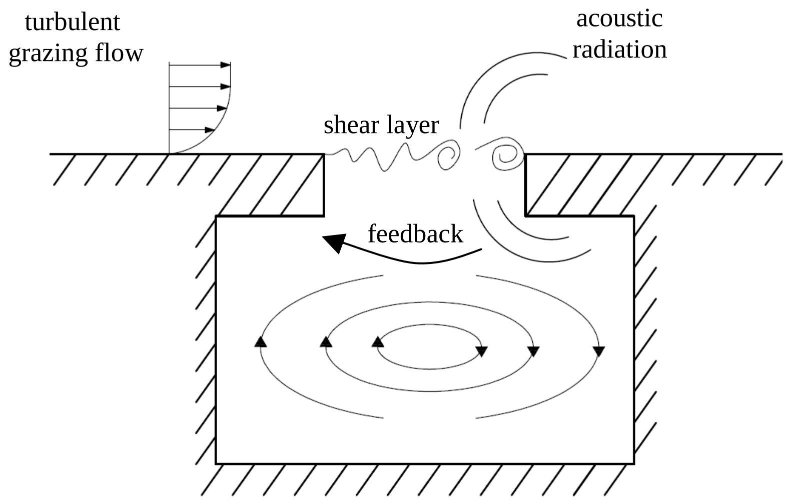


Figure 2.2: Flow behaviour inside and outside a cylindrical Helmholtz resonator with a turbulent boundary layer grazing flow.

The behaviour of the flow within a Helmholtz resonator can be described as a second-order mass-spring system using a mechanical analogy. In the mass-spring system, the mass is comprised of the mass of fluid ($m = \rho l_e S$) in the neck, and the compressibility of the fluid within the cavity acts as a spring (with stiffness, $K = \rho c^2 S^2 / V_c$), where $S$ is the cross-sectional area of the orifice, $\rho$ is the density of air, $c$ is the speed of sound, $V_c$ is the cavity volume and $l_e$ is the effective length of the orifice (Hémon et al. 2004). The effective length is comprised of the actual length of the orifice as well as a small parcel of air immediately adjacent, but external, to the orifice that is also displaced. The net effect is that the effective length of the orifice is increased, and thus leads to a reduction in the natural frequency of the resonator. Using lumped element analysis, the equation for the displacement of the flow in the orifice (Khosropour and Millet 1990; Meissner 2002) is

$$m\frac{d^2y}{dt^2} + R\frac{dy}{dt} + Ky = F_{ext} \tag{2.1}$$

where $t$ is time, $y$ is the displacement of the air in the orifice and $F_{ext}$ is the force exerted on the fluid inside the orifice. Due to the viscous effects of the flow and acoustic radiation at the orifice, the system is damped and, thus, acts as a mass-spring-damper with a damping constant of $R$.

Experimental investigations have shown that if the damping effect is ignored, a discrepancy of up to 30% between the measured and the calculated values of the displacement of the air within the neck is observed (Alster 1972; Kinsler et al. 1999). The damping has been modelled by Bies and Hansen (2009) as

$$R = \frac{\rho c}{S}\left[0.288k\delta \log\left[\frac{4S}{\pi\delta^2}\right] + \frac{Sk^2}{4\pi} + Ma\right] \tag{2.2}$$

where $\delta$ is the boundary layer thickness, $Ma$ is the Mach number of grazing flow, $k = \omega_a/c$ is the wavenumber, and $\omega_a = 2\pi f$ is the angular frequency. Therefore, assuming the air motion inside the resonator is harmonic, the displacement of the air in the orifice can be calculated as (Ma et al. 2009)

$$y(f) = \frac{F_{ext}(f)}{-4m\pi^2 f^2 + 2if\pi R + K} \tag{2.3}$$

where $f$ is the instability or driving frequency and $i$ is the imaginary number, $\sqrt{-1}$. As the driving frequency approaches the resonance frequency of the Helmholtz resonator, $f_r = f_n\sqrt{1-\zeta^2}$ (where $f_n = \sqrt{K/4m\pi^2}$ is the natural frequency of the system), the denominator of this expression approaches zero and, thus, the amplitude of displacement becomes very large. However, this simplified expression does not account for second order effects such as the resonator shape, the presence of a shear flow over the orifice or the acoustic impedance to which the resonator is coupled (Howard et al. 2000). It was demonstrated that the aforementioned formula for the resonance frequency is valid only when the length dimension is less than 1/16 of the wavelength of sound (Howard et al. 2000). Panton and Miller (1975) developed a more accurate expression for the calculation of the resonance frequency of a cylindrical Helmholtz resonator

$$f_r = \frac{c}{2\pi}\sqrt{\frac{S}{l_e V_c + 0.33L^2\, S}} \tag{2.4}$$

where $L$ is the cavity length. In the present study Equation (2.4) has been used to calculate the frequency of resonance.

### 2.1.1 Behaviour of the grazing flow over a Helmholtz resonator

Different patterns have been observed for propagation of the shear layer over the orifice of a Helmholtz resonator. Flow visualisation conducted by Baumeister and Rice (1975) showed that the grazing flow behaves in different manners during the inflow and outflow cycles. When the grazing flow travels into the orifice, the effective area of the orifice is reduced. As can be seen in Figure 2.3, during the inflow cycle, there exists a blockage region which is due to the momentum of the grazing flow. Furthermore, it was observed that in the outflow cycle the resistance of a Helmholtz resonator is reduced dramatically because of the emerging flow (Sun et al. 2002). However, the main drawback of this analysis is the omission of the pressure waves generated through interaction between the shear layer and the downstream edge of the orifice.

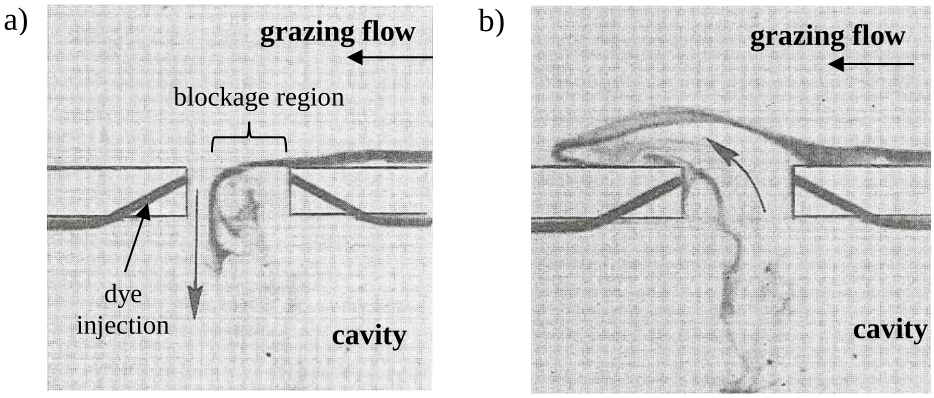


Figure 2.3: Flow behaviour in the vicinity of orifice, a) inflow, b) outflow (Baumeister & Rice 1975).

The flow rate and the direction of the grazing flow in the vicinity of a Helmholtz resonator have also been investigated by Rogers and Herb (1976). They suggested two different stream surfaces for low speed flow regimes passing over the orifice, or entering and leaving the orifice. It was observed that the ratio of the length to the diameter of the orifice and to the boundary layer thickness are two important parameters that characterise the flow behaviour in the vicinity of the orifice. As shown in Figure 2.4, for the inflow configuration, the grazing flow is separated from the upstream edge and for low flow rates most of the orifice volume can be filled by this separated region. Whereas during outflow, the increased cavity pressure forces the fluid out of the orifice by deflecting the grazing flow. This deflected flow induces drag in the grazing flow and then accelerates the flow at the downstream edge of the orifice. However, in their analysis the effects of viscous interaction of the shear layer with the downstream edge of the resonator orifice were ignored. The location of inflection points and slope of the shear layer at the separation point were also calculated by Michalke (1965) who determined a hyperbolic tangent velocity profile for the shear flow. It must be noted that the location of the separation point of the oncoming boundary layer is also related to the free stream velocity (Walker and Charwat 1983).

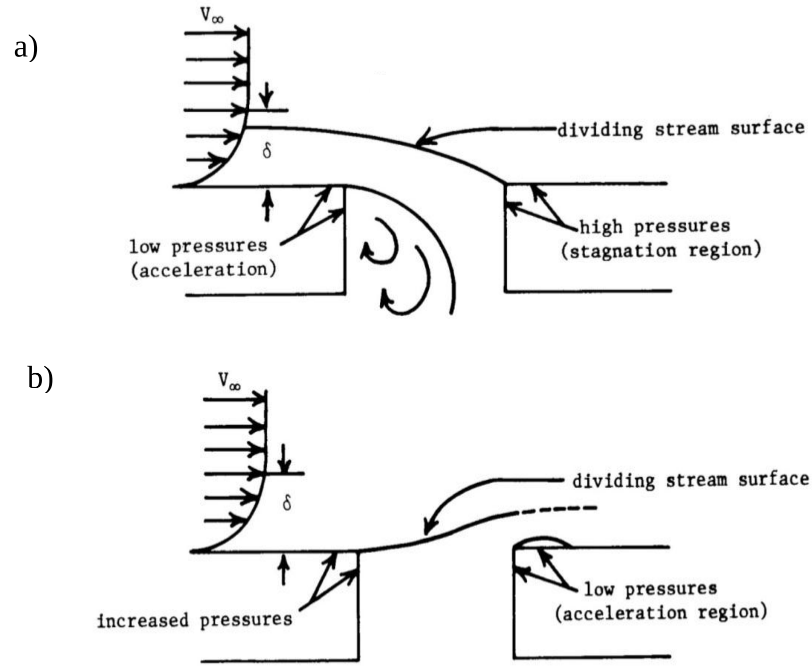


Figure 2.4: Configuration of the grazing flow over the orifice; a) inflow, b) outflow (Rogers & Herb 1976).

Nelson et al. (1981) used a Laser Doppler Velocimetry system in the neck of the resonator to observe the interaction between the grazing flow and the reciprocating flow driven by the pressure fluctuation within the resonator cavity. It was demonstrated that there exists a periodic shedding of the compact vortices from the upstream edge of the orifice to the downstream edge. As can be seen in Figure 2.5, the vortices grow in size as they travel towards the trailing edge of the resonator orifice. The speed of the vortex reaches its maximum magnitude close to the downstream edge of the orifice. The measurements revealed that the mean velocity of the vortex is approximately half of the free stream velocity. This observation was also confirmed by Mallick et al. (2003) who applied Re-Normalization Group methods (RNG) based on the $k - \varepsilon$ turbulence model. The vortices are stretched and leave the resonator in a direction tangential to the downstream wall surface. It should be noted that the phase lag between the vortical flow and acoustic volume flow, which comes from the vortex-edge interaction at the downstream edge of the orifice, was also determined as a function of the resonator cavity depth and free stream velocity (Bilanin and Covert 1973) and is given by

$$\varphi = \frac{3\pi}{2} - \frac{2\omega_r L}{U}. \tag{2.5}$$

where $U$ is mean free stream velocity, $\omega_r = 2\pi f_r$ and $L$ is the cavity depth.

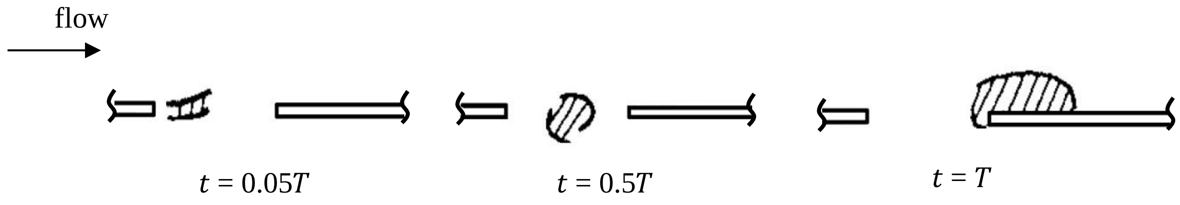


Figure 2.5: Position of vortex in vicinity of the orifice during one period (Nelson et al. 1981).

Toulorge et al. (2012) demonstrated that while the vortices convect across the orifice, their amplitude and size increase due to shear layer instability (Figure 2.6). They concluded that at low Mach numbers, the convection time for the vortices to reach the downstream edge is higher than the time for acoustic perturbation generated at the downstream edge to propagate to the upstream edge. However, the effects of the flow conditions such as flow speed and the turbulence intensity on the vortically induced flow field were not considered.

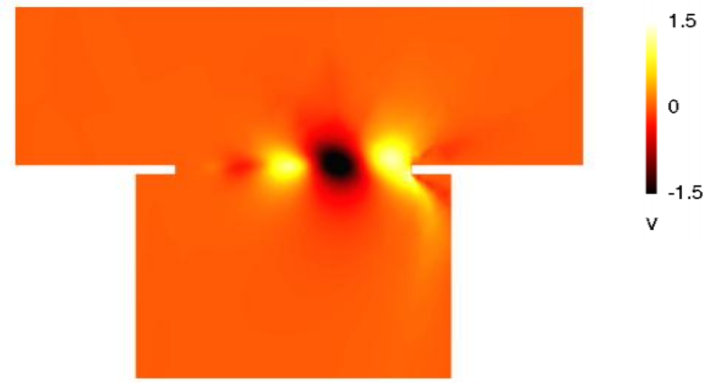


Figure 2.6: Snapshot of the vertical components of the velocity perturbation in the vicinity of the orifice (scale in m/s) (Toulorge et al. 2012).

For convenience, Nelson et al. (1983) assumed that the total flow field in the vicinity of the Helmholtz resonator consists of the vortical flow, which is associated with the vortices within the shear layer, and the potential flow which consists of the grazing flow and the acoustic field. The acoustic field is related to the fluctuating part of the potential flow, whilst the vortical flow and the mean potential flow generate the hydrodynamic flow. The mean and unsteady parts of the potential flow were predicted using models of the frequency response of the Helmholtz resonator. Therefore, the circulation strength of the rotational flow, assuming a constant convection velocity of the vortices within the shear layer, was calculated as

$$\Gamma = -\frac{1}{2} U^2 t \tag{2.6}$$

where $t$ is time. It was shown that the Coriolis force influences the vortical and the unsteady potential flows and is given as

$$\mathrm{F}_c = \rho(\Omega' \times v_t) \tag{2.7}$$

where $\Omega'$ is vorticity and $v_t$ is the local flow velocity. Due to imposition of the Coriolis force, the vortices, during the first stage of the vortex generation process near the leading edge of the opening, are rolled up. The energy balance showed that this force acts perpendicular to the potential flow field. In fact, the Coriolis force accelerates the vortices when the acoustic flow is directed into the resonator and decelerates them during the second half of the acoustic cycle. However, Nelson et al. (1983) did not consider the influence of the oncoming turbulent boundary layer on the flow behaviour over the orifice opening. Analysis by Bruggeman et al. (1991) further revealed that the vortex distribution within the shear layer is related to the ratio of the acoustic particle velocity to the grazing flow velocity, $u_a/U$. It was demonstrated that at low pulsation levels, $u_a/U \leq 10^{-3}$, the linear instability theory is valid. In the linear shear layer instability theory, derived from Rayleigh's equations, it was demonstrated that the velocity profile within the shear layer is related to the overall shear layer momentum thickness as (Rayleigh 1896),

$$u(y) = \frac{U}{2}\left(1 + \tanh\left(\frac{y}{2\theta}\right)\right), \tag{2.8}$$

where $\theta$ is the momentum thickness of the boundary layer and $y$ is wall-normal direction. By further increasing $u_a/U$ to $10^{-1}$, the shear layer rolled up into discrete vortices in the vicinity of the opening. It was also concluded that at high pulsation levels, $u_a/U > 10^{-3}$, the acoustic pulsation determines the path of the vortices and their convection velocities. The investigation was continued by Bruggeman et al. (1991) through analysis of the acoustic power generated by vortices within the shear layer of a closed side-branch resonator. It was assumed that the vortices were shed from the leading edge of the opening when the pressure inside the resonator was at its minimum. From this assumption, the power transfer from the vortices to the acoustic flow was represented as

$$\mathrm{P}_t = -\rho \int (\vec{\omega} \times \vec{v}_t).\, u_a \, dv. \tag{2.9}$$

This equation shows that the vortices, in the first half of the acoustic cycle, act like a sink for the acoustic energy. On the other hand, during the second half of the cycle, the discrete vortices generated the acoustic energy. It was concluded that when the generation of power is higher than its absorption, self-excitation is maintained. This investigation was continued by Meissner (2002) who applied a one-dimensional lumped-element model to calculate the driving force generated by discrete vortices. It was assumed that the instabilities within the shear layer have to be treated as a concentrated vortex and modelled as such. The model predicted that the amplitude of the maximum pressure fluctuations inside the cavity of the resonator is proportional to the square of the velocity of the grazing flow. However, the main concern with these analyses is associated with the effects of the three-dimensional turbulent structures within the boundary layer on the shear layer development.

The vortex sheet is another pattern of shear layer propagation over the orifice. Arunajatesan and Sinha (2005) analysed this kind of flow pattern by implementing a numerical study and predicted the aero-acoustic behaviour of the unstable shear flow when the resonant oscillations in pressure occur. Firstly, it was demonstrated that Reynolds-averaged Navier–Stokes (RANS) methods are too dissipative and direct numerical simulation is too computationally expensive to model the flow. Therefore, it was concluded that using high mesh resolution, the hybrid RANS/Large Eddy Simulation (LES) approach is the best model to characterise the flow. Spanwise vorticity contours, shown in Figure 2.7, reveal that the fluctuations within the shear layer are dominated by a large scale vortex in the vicinity of the orifice and its strength has a larger magnitude in the resonant conditions compared to the non-resonant cases. This was thought to be due to the fact that the resonance occurs at a higher flow speed compared with the non-resonant condition. They also found that the shear layer close to the upstream edge of the orifice has a flapping sheet-like character, while in the aft portion of the orifice changes to discrete vortices that interact with eddies within the boundary layer. Sheet-like motion of the shear layer was also observed by Ma et al. (2009) through PIV measurements and De Jong et al. (2012) who applied a Lattice Boltzmann method to predict the aero-acoustic behaviour of the shear layer.

(a)

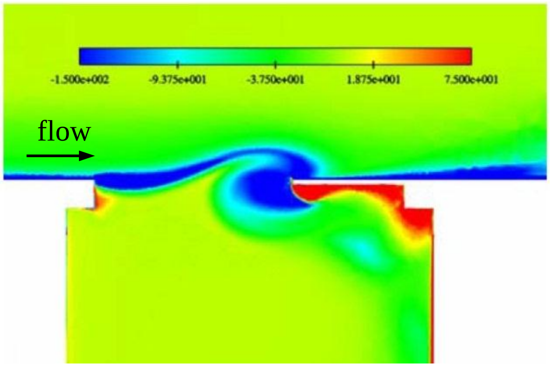


(b)

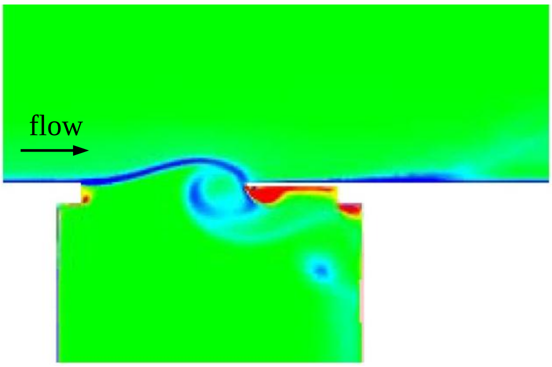


Figure 2.7: Instantaneous vorticity contours, a) non-resonant and b) resonant cases (Arunajatesan & Sinha 2005).

The vortex sheet pattern was also investigated by Dai et al. (2012) who analysed the shear layer over the orifice. They developed a two dimensional model which revealed that the characteristics of the shear layer are a function of the flow velocity normal to the grazing flow, $v$ , and the free stream velocity, $U$. It was observed that when $v/U$= 0.3 the sheet-like motion develops over the orifice; whilst with increasing flow velocity in the neck to up to $v/U$= 0.9, the rolling-up vortex sheet changes into a large vortex within the grazing flow. Howe (1981a), in his analytical work, proposed a linear model for the low Strouhal number instabilities in the vicinity of various apparatus and wall cavities. In his study, it was assumed that the surface upstream and downstream of the slot was extended indefinitely to have a zero deflection within the shear layer, except over the opening. Applying the Kutta condition at the upstream edge of the slot, the energy extracted from the grazing flow due to creation of the additional vortices was predicted. The model calculated the relationship between the streamwise slot diameter and the wavelength of the disturbances to generate the self-sustained oscillations such that $0.5\lambda < d < 1.1\lambda$. Interestingly the maximum amplitude of the disturbances was predicted when $d \approx 0.76\lambda$. The effects of the volume flux in the vicinity of the downstream edge of the slot were also considered by Howe (1981b). The investigations revealed that the lateral wavy motion of the shear layer and the vortex-edge interaction in the vicinity of the trailing edge of the orifice, generate the net volume flux across the slot. However, the main drawback of this analysis is neglection of the velocity fluctuations generated by the orifice edge in the spanwise direction which affect the motion of the shear layer over the orifice.

In conclusion, the flow quality and behaviour of the shear layer over the orifice of a Helmholtz resonator depend on the characteristics of the resonator, the oncoming flow and aero-acoustic coupling in the shear layer. In the literature four types of shear layer propagation over the orifice are suggested: 1) vortex sheet, 2) shear layer with a velocity profile, 3) discrete vortices and 4) distributed vortices. Identifying the flow behaviour within the shear layer over different resonator orifices is one of the objectives of this research.

### 2.1.2 Frequency and amplitude of the instabilities within the shear layer

To better understand the physical aspects of the flow behaviour in the vicinity of the self-excited resonators, it is necessary to evaluate the values of the frequency and amplitude of the instabilities within the shear layer. Early experiments were carried out by Rossiter and Britain (1964), who investigated the flow excited resonance and acoustic feedback of shallow cavities with grazing flow at sub- and transonic Mach numbers. It was observed that the flow excitation is primarily due to the shear layer motion, which occurs close to the trailing edge of the orifice, and the propagation of acoustic disturbances toward the leading edge. They found that the shear layer moves in a direction lateral to the grazing flow and its displacement is proportional to the wavenumber of the disturbances within the shear layer. Therefore, based on the phase lag between displacement of the shear layer and the pressure disturbances at the separation point, a semi-empirical relationship for the oscillation frequencies within the shear layer was determined as

$$St = \frac{fd}{U} = \frac{i - 3/8 - \varphi/2\pi}{Ma + 1/n} \qquad i = 1, 2, 3 \ldots \tag{2.10}$$

where $St$ represents the Strouhal number, $n$ is a coefficient based on the convection velocity of the vortices over the orifice and $\varphi$ is an experimentally-determined function of length-to-depth ratio of the cavity. Tam and Block (1978) also calculated the frequency of the instabilities at low freestream velocities ($Ma \leq 0.2$) and concluded that the acoustic field related to the transverse cavity mode is dominated by the acoustic feedback associated with the streamwise modes.

Linear instability theory has also been used by numerous researchers to model the shear layer of flow-excited cavities. However, the model employs considerable simplifications and is, therefore, not able to calculate accurate values for the frequency and amplitude of the oscillations within the shear layer. Therefore, some researchers developed a predictive model in the form of a feedback loop, called the "Feedback Loop Analysis" (FLA) (Cremer and Ising 1967; Mast and Pierce 1995; Kook and Mongeau 2002). In this model, it was assumed that the shear layer is coupled with the acoustic mode of the resonator and, therefore, the excitation is a superposition of an aerodynamic and acoustic flow which together form a closed feedback loop. The forward gain function represents the influence of the acoustic field on the instabilities within the shear layer $(\hat{q}_o/\hat{q}_r)_f$, whilst the backward gain function is the acoustic response of the resonator to the aerodynamic excitation$(\hat{q}_r/\hat{q}_o)_b$, where $(\hat{q}_r)$ is the complex acoustic volume velocity and $(\hat{q}_o)$ is the complex aerodynamic volume velocity. The frequency and the amplitude of the fluctuations were obtained from the total gain of the system which is represented as

$$\left(\frac{\hat{q}_r}{\hat{q}_o}\right)_b \left(\frac{\hat{q}_o}{\hat{q}_r}\right)_f = 1. \tag{2.11}$$

Modelling the flow field around organ pipes, which are excited by a narrow flow jet, was the first attempt to use FLA by Cremer and Ising (1967). In their work, using root locus plots, the backward gain function was calculated based on the electro-acoustic impedance analogy, given by

$$\left(\frac{\hat{q}_r}{\hat{q}_o}\right)_b = -\frac{\hat{Z}_c}{\hat{Z}_c + \hat{Z}_M}, \tag{2.12}$$

where $\hat{Z}_M$ is the acoustic impedance of the pipe opening and $\hat{Z}_c$ is the total input impedance of the pipe. Using linear shear layer instability theory for a narrow jet flow, Rayleigh (1896) solved the forward gain function by assuming spatially growing instabilities over the cavity. The frequency of the flow oscillation was obtained from the phase of the vortex sheet deflection at the downstream edge of the pipe and it was concluded that most of the volume flow in the vicinity of the pipe mouth occurs close to the downstream edge. This approach was followed by Bilanin and Covert (1973), who found that the amplitude of the vortical flow within the shear layer is related to the amplitude of the acoustic volume flow, which triggers the instabilities and determines the grazing flow velocity. They concluded that the amplitude of the instabilities is proportional to the square of the free stream velocity and the acoustic response does not have a significant impact on the flow field.

### 2.1.3 Pressure fluctuation within the cavity of a flow-excited resonator

The pressure fluctuations within the resonator cavity have significant effects on the structure of the grazing flow around the orifice. An early investigation conducted by Elder (1978), using the FLA approach, showed that the maximum value of the pressure fluctuation within the resonator occurs at the frequency of the fundamental acoustic mode of the resonator. The forward gain function for the turbulent flow case was then given by

$$\left(\frac{\hat{q}_r}{\hat{q}_o}\right)_f = -\frac{u}{\omega d} e^{j\left(\pi - \frac{\omega d}{u_c}\right)} \quad , \tag{2.13}$$

where $\omega$ is angular frequency, $u_c$ is the convection velocity of the vortices, $u$ is the streamwise velocity and $d$ is the orifice diameter. It was found that the maximum value of the pressure amplitude inside the resonator is not related to the free stream velocity. However, when the free stream velocities are much lower than those corresponding to the resonator resonance, the gain functions achieved by Elder cannot predict the pressure fluctuations well. Therefore, Mast and Pierce (1995) suggested using the describing function theory for modelling the behaviour of the flow-excited Helmholtz resonator system. They assumed that the shear layer consists of some discrete vortices which travel from the leading edge to the trailing edge of the orifice and found that the amplitude of the flow disturbance is proportional to the square of the mean flow velocity, similar to the observations by Bilanin and Covert (1973), and the resonator pressure fluctuations can, therefore, be calculated from

$$\hat{p}_{res} = -\frac{i\rho c^2}{\omega V_c}\hat{q}_r. \tag{2.14}$$

Use of the describing function theory to calculate the instantaneous pressure field was also followed by Kook (1997) who developed a new forward gain function based on the "vortex sound" concept. It was assumed that all vortices within the shear layer convect on a line and build up at a constant rate, in the form of a point vortex, before leaving the resonator at the same instant. Therefore, the phasor of excitation pressure was calculated as

$$\hat{p}_{ext} = \xi_p \rho U^2 \frac{u_c}{\omega d} e^{-iSt}, \tag{2.15}$$

where $\xi_p$ can vary between 0, for a fully diffused vortex, and 1, for a perfect line vortex. The calculated frequency and amplitude associated with the maximum peaks in the pressure oscillations inside the resonator matched well with the experimental results. It should be stated that in the present study the flow behaviour inside the resonator was modelled using Equation (2.15) for the external excitation pressure.

Nelson et al. (1981) performed an experiment to measure the pressure fluctuations within the cavity of a rectangular resonator excited by a grazing flow. It was observed that when the pressure fluctuations within the cavity reach their maximum positive value, the vortex is at the mid-point of the orifice. When the vortex reaches the trailing edge of the orifice, the cavity pressure returns to its negative peak value. The results showed that within a specific range of free stream velocities, the frequency of peak excitation is very close to the natural frequency of the resonator, similar to the observation of Kook et al. (2002).

The pressure fluctuations within a Helmholtz resonator are also related to the force induced by the vortices within the shear layer. This force was predicted by Ma et al. (2009), who developed a simplified momentum balance for the unsteady flow in the vicinity of the orifice. It was concluded that the force, which is responsible for exciting the resonator, is directly related to the orifice shape and cavity volume and has a constant value over a wide range of boundary layer thicknesses. However, the main disadvantage of this study is the limited Reynolds numbers and turbulence intensities of the grazing flow investigated using their model. The flow-acoustic coupling within the unstable shear layer over six flow-excited Helmholtz resonators at low subsonic Mach number was also analysed to understand the relationship between the velocity fluctuations within the shear layer and the pressure fluctuations inside the resonator (Massenzio et al. 2008). It was demonstrated that when strong excitation occurs, the power spectral density of the pressure inside the resonator, and the streamwise velocity fluctuations over the orifice have a fundamental peak around the resonance frequency of the resonator.

Inagaki et al. (2002) also derived a set of equations to characterise the pressure fluctuations within the resonator at low Mach numbers. The instantaneous pressure fields were analysed by applying the second order spatial difference scheme to solve the three dimensional incompressible Navier-stokes equations. Structured meshes were used in the vicinity of the orifice to calculate the effects of the grazing flow on the pressure fluctuations inside the cavity. It was mentioned that the number of elements in the vicinity of the orifice should be selected such that the minimum grid spacing was $5 \times 10^{-3} d$. The results indicated that high amplitude pressure oscillation occurs within a specific range of free stream velocities such that strong pressure fluctuation occurs when $U = 14$m/s (Figure 2.8a), whereas by increasing the free stream velocity to 18m/s the pressure amplitude decreases considerably (Figure 2.9b). The computational data also showed that for fluid-resonant oscillations, the frequency of the pressure fluctuations within the cavity are locked at the resonance frequency of the resonator. When the coupling between the vortex shedding and the resonance frequency of the resonator is weak, the amplitude of the pressure fluctuations within the resonator is decreased. The main drawback of this analysis is that all calculations were conducted with a laminar boundary layer flow regime, whereas in the experiments it was turbulent. This causes an under prediction of the pressure amplitude for a given free stream velocity and use of even finer meshes did not modify the results. This was confirmed by Urzynicok (2003) who also observed that with increased thickness of the upstream turbulent boundary layer at the edge of orifice, the amplitudes of the induced pressure oscillations also increased.

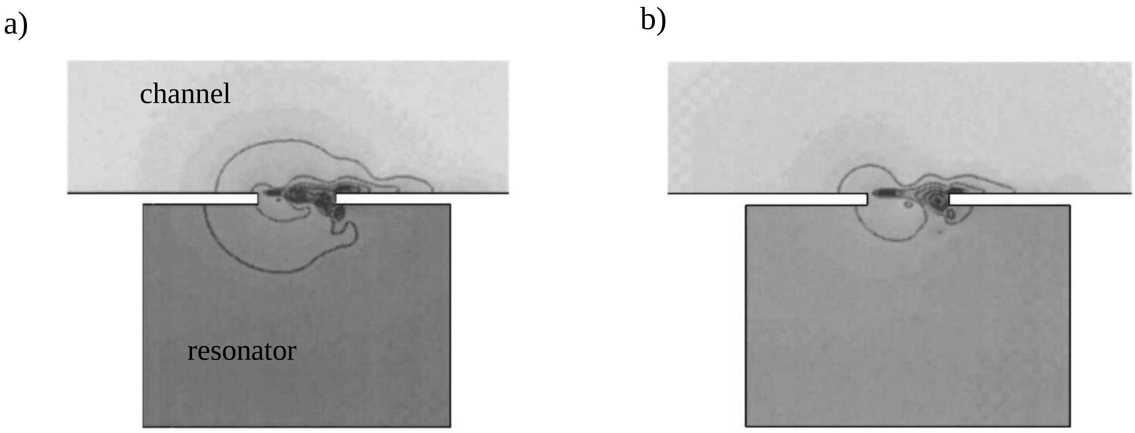


Figure 2.8: Root-mean-square of non-dimensional pressure fluctuations, where white corresponds to zero and black to 0.5; a) $U = 14$m/s and b) $U = 18$m/s (Inagaki et al. 2002).

The pressure fluctuations within the resonator cavity were also analysed using three dimensional simulations of aero-acoustic behaviour of the grazing flow around an inclined Helmholtz resonator placed in a duct (Georges et al. 2009). A structured mesh with 1.5 to 2.5 million elements, with a time step of $t = 1/10f_r$, was applied to characterise the flow structures in the vicinity of the resonator. Firstly, it was observed that in the LES model the hexahedral mesh reduces the numerical dissipation. However, using a tetra mesh the fluctuation parameters within the turbulent flow results in the turbulent energy decay not being accurately predicted. In order to capture impact on the pressure fluctuations due to the viscous interaction of the vortices with the resonator walls, the mesh within the resonator was of high density. It should be noted that the viscous effects of the side walls of the duct that the resonator was attached to were also ignored by applying slip boundary conditions on the walls. This was done primarily to reduce the number of elements in the near wall region since it was anticipated that the wall boundary layer would generate additional noise. The influence of subgrid scale (SGS) in the LES model has also been discussed and it was concluded that the WALE SGS model is appropriate to reduce the numerical dissipation in the aero-acoustic simulations. It was demonstrated that the use of increasingly fine meshes in the computational domain simply impacts the amplitude of the pressure fluctuations within the resonator and does not change the predicted frequency of the fluctuations. The results showed that when the instability frequency within the shear layer is close to the natural frequency of the resonator, the high pressure pulsations amplify the instabilities within the grazing flow in the vicinity of the resonator. It was demonstrated that the predicted resonance frequency observed in the LES results is slightly higher than the theoretical calculation, by up to 8%. The reason for this mismatch was thought to be due to the fact that the vortical flow structures penetrate the cavity and decrease the effective area of the resonator. As can also be seen in Figure 2.9, the pressure fluctuations within the resonator change the behaviour of the vortices over the orifice, such that increasing the pressure within the resonator cavity disrupts the sheet-like motion of the vortices and results in the earlier creation of discrete vortex structures.

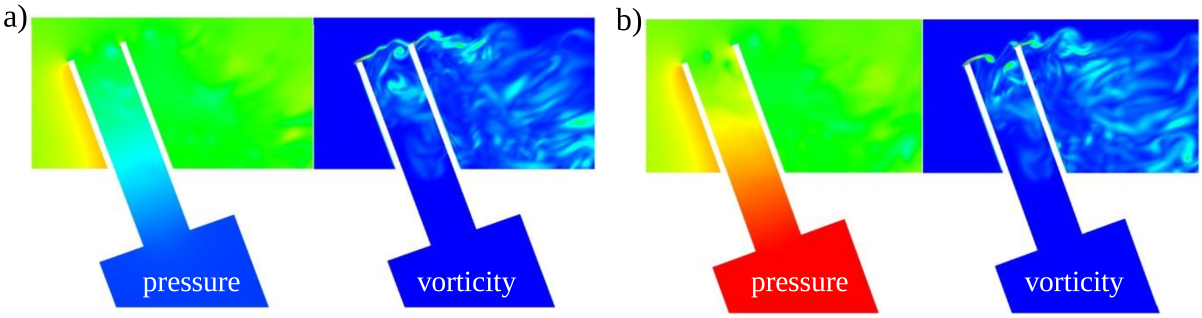


Figure 2.9**:** The pressure fluctuations and the related vorticity field in a resonance cycle: a) minimum pressure and b) maximum pressure within the resonator (Georges et al. 2009).

Hence, from the review of the literature in this section, it can be concluded that the pressure fluctuations within a resonator which is excited by a grazing flow can change the flow behaviour around the resonator. However, in the available literature an appropriate approach which can predict the response of a resonator excited by a turbulent boundary layer grazing flow is very scarce. In the present work, an analytical model and experimental measurements have been implemented to analyse the amplitude and frequency of the pressure fluctuations inside flow-excited Helmholtz resonators.

### 2.1.4 Effects of characteristics of the Helmholtz resonator on flow behaviour

In the literature, flow-excited cavities and resonators have often not been differentiated from each other. However, significant differences exist between a flow-excited Helmholtz resonator and the vast majority of the arrangements tested in previous studies. For example, the fundamental difference between the Helmholtz resonator and shallow cavities, $L/D \leq 1$, lies in the direction of the feedback disturbances (Sarohia1975; Colonius et al. 1999; Rowley et al. 2002; Sipp 2012). In the case of the flow-excited Helmholtz resonator, the feedback disturbance of the resonator volume is perpendicular to the shear layer. On the other hand, in shallow cavities, the feedback disturbances travel in a direction parallel to the plane of the shear layer. Moreover, the effects of the resonator orifice distinguish this configuration from other open or closed cavities. There is also a significant difference between the Helmholtz resonator and a deep cavity. The ratio of cavity volume to the orifice area in a Helmholtz resonator is greater than that of a deep cavity and, thus, it is possible to generate much lower frequencies compared to those attainable with a deep cavity (Rockwell and Naudascher 1979; Gharib and Roshko 1987; Chaterllier et al. 2004; Faure et al. 2007; Lee et al. 2010).

The effects of cavity dimensions on the sound pressure fields within the resonator were investigated by Selamet and Radvich (1997), who developed a one dimensional analytical solution for the flow inside the resonator. As can be seen in Figure 2.10, for a small value of resonator cavity depth-to-diameter ratio, $L/D \leq 0.1$, radial propagation of sound waves was predicted inside the cavity volume. On the other hand, as the $L/D$ ratio is increased to unity, multidimensional wave propagation occurs within the resonator. However, their model ignored the compressibility effects of the fluid within the cavity, which moves the flow inside the neck. The important role of the cavity depth in excitation was also observed by Panton (1990) who demonstrated that when the cavity depth to boundary layer thickness ratio is less than unity both velocity and pressure fluctuations within the resonator are reduced.

Orifice geometry also has a significant impact on the flow behaviour in the vicinity of the resonator. To investigate this effect, thirteen resonators with different orifice sizes, ranging from $0.02 < d/\delta < 0.4$, have been tested by Panton (1990). The pressure fluctuations within the resonators were measured by surface mounted microphones placed on the wall surface inside the cavity of the resonators. The results showed that, when the orifice diameter to boundary layer thickness ratio is less than 0.15 the oscillations occur far from the Helmholtz frequency. The reason is that the pressure fluctuations generated within the cavity have very small values and, in this case, the resonator is excited by the ambient acoustic noise. Moreover, when $d \leq 100\, \upsilon/u_\tau$, the viscous effects of the orifice reduce the growth of vortices within the shear layer.

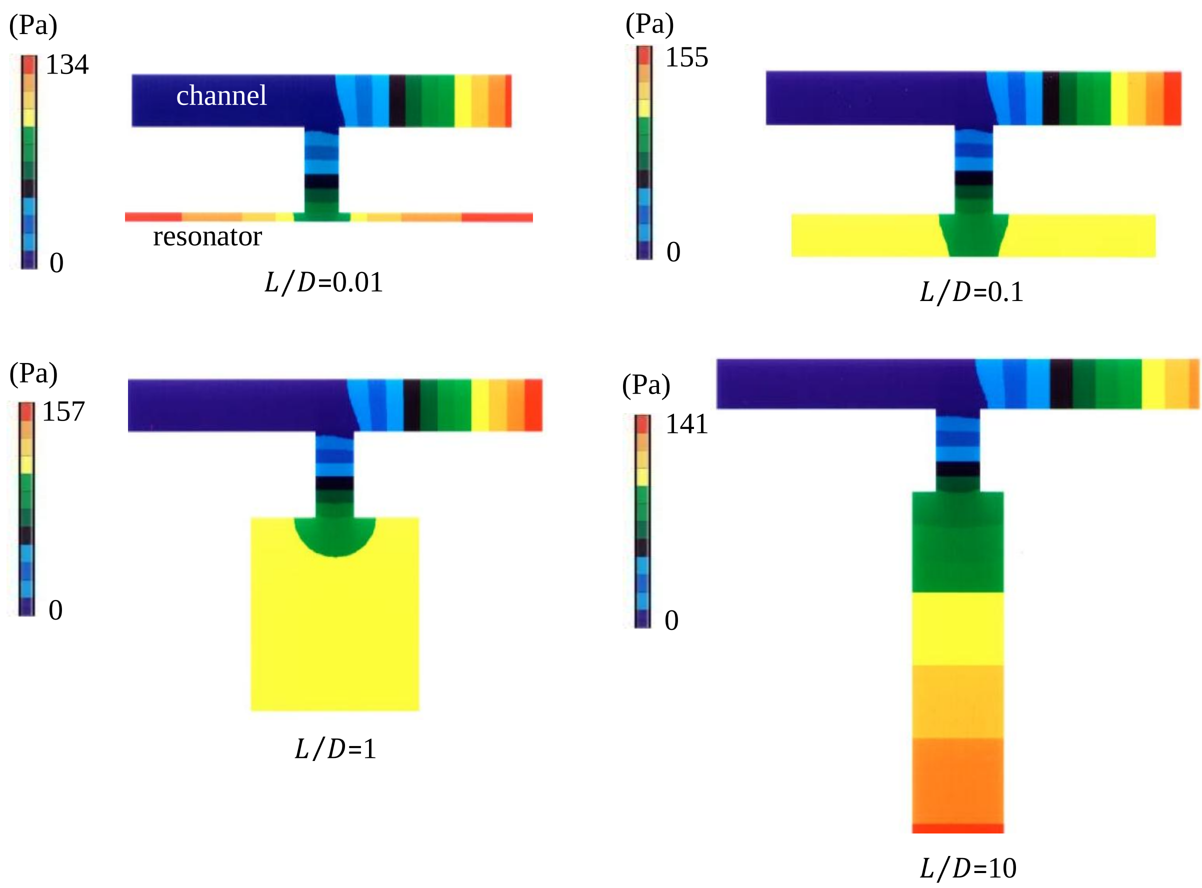


Figure 2.10: Pressure contour within the resonators with different cavity depth to diameter ratios (Selamet & Radvich 1997).

The effect of the orifice diameter was also investigated by Panton and Miller (1975). They tested nine different Helmholtz resonators on the fuselage of a glider to excite the resonators with a turbulent boundary layer. It was concluded that when the orifice diameter is approximately half the diameter of the eddies within the turbulent boundary layer, the vortices within the shear layer impose a frequency close to the resonant frequency of the resonator. PIV data obtained by Ma et al. (2009) also revealed that by increasing the ratio of the orifice diameter to the boundary layer thickness from 0.1 to 10, the convection velocity of the vortices within the shear layer is reduced by up to $0.2U$, whereas the net unsteady circulation of vortices does not change considerably. This is due to the fact that vortices within the inner region of a thick boundary layer have lower speeds compared to a thin boundary layer.

As can be seen in Figure 2.11(a), different orifice shapes were also tested by Panton (1990) and it was found that when the orifice is a slot aligned with the flow direction, the magnitude of oscillating pressure inside the cavity is decreased significantly in comparison with the circular orifice. The orifice wall shape was also changed such that the orifices were formed by rounded sidewalls or a circular reamer cutting at 45$^{o}$ angle (Figure 2.11b). The results showed that the maximum value of the pressure fluctuations that occurs within these resonators is higher than for the resonator with a circular orifice. It was proposed that this configuration of sidewalls aids the motion of inflow and outflow and results in a significant increase in the flow fluctuations within the resonator cavity. However, the pressure pulsations inside a resonator with a rounded upstream edge of the orifice are reduced, primarily because of the increasing acoustic flow near the sharp edges (Bruggeman et al. 1991).

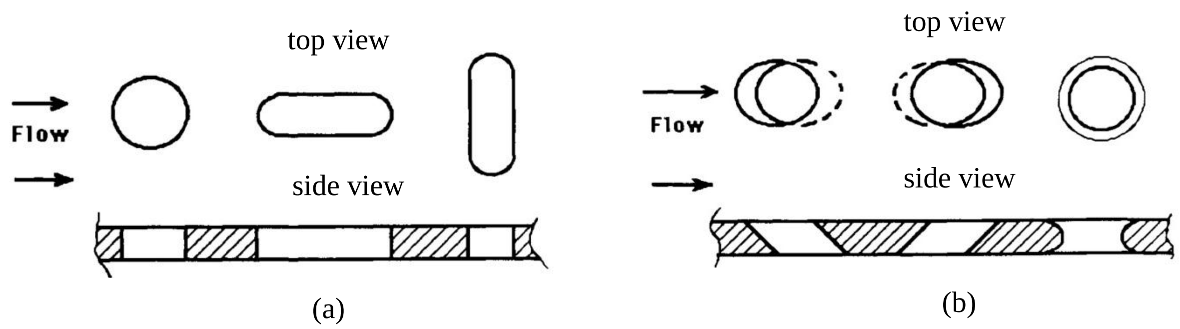


Figure 2.11: Different orifice geometry (Panton 1990).

A two dimensional study of the characteristics of the flow, in the vicinity of the orifice, by Toulorge et al. (2012) proved that the frequency of the instabilities within the shear layer are also decreased by the rounding of the upstream edge. It was found that the edge increases the convection time of the vortices as they become larger. Therefore the vortices are less localised and their interaction with the orifice edge has less impact. The resonance frequency of the resonator is also reduced as the neck offset from the centre of the cavity is increased (Selamet and Ji 2000).

Flow simulations and experimental measurements conducted by Dequand et al. (2003) also indicated that the characteristics of the shear layer are strongly coupled with the upstream edge of the orifice. Four different upstream edge configurations were studied. As can be seen in Figure 2.12, the vortex paths within the shear layers over the orifices with chamfered upstream edges (a & c) indicated close proximity of the vortex with the edge, whilst the sharp edges (b & d) caused the vortices to enter deeply into the neck and pass close to the downstream edge. Urzynicok (2001) also observed that when the orifice has an inclined upstream edge, the displacement of the shear layer is increased and the creation of discrete vortices occurs much earlier.

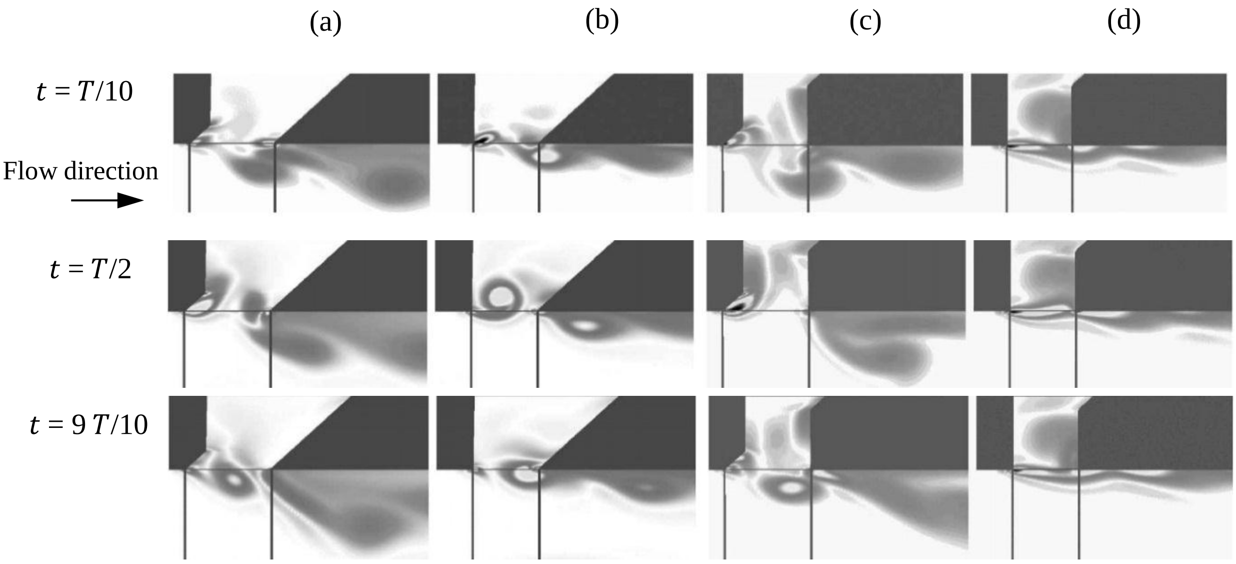


Figure 2.12 Vortex path within the shear layer over four different orifices (Dequand et al. 2003).

The orifice length to boundary layer thickness ratio also has significant effects on the flow behaviour within the resonator; such that when this ratio approaches unity, the maximum peak of pressure fluctuations is also reduced significantly, by up to 40 dB (Amandolese et al. 2004). The influence of the orifice length on the amplitude of the shear instabilities were also analysed by Toulorge et al. (2012), who observed that the travel time of the vortices is proportional to the orifice length, such that with increasing orifice length the frequency of the instabilities within the shear layer is reduced.

The characteristics of the grazing flow downstream of two or more Helmholtz resonators, placed close together, are different from the flow behaviour around a single resonator. Flynn and Panton (1989) investigated the pressure fluctuations within adjacent resonators that are excited by a turbulent boundary layer, with a thickness of $1/3d$ (Figure 2.13). It was observed that when the distance between each resonator equals the boundary layer thickness, flow interaction leads to an increase in the amplitude and frequency of the maximum pressure fluctuations, by a factor of 12% and 1%, respectively. Moreover, in a row of resonators, the interior resonators generate higher amplitude and frequency pressure fluctuations compared with the end resonators. This results in the energetic fluid within the cavity being ejected to the grazing flow and can be used favourably for separation control applications (Urzynicok 2003).

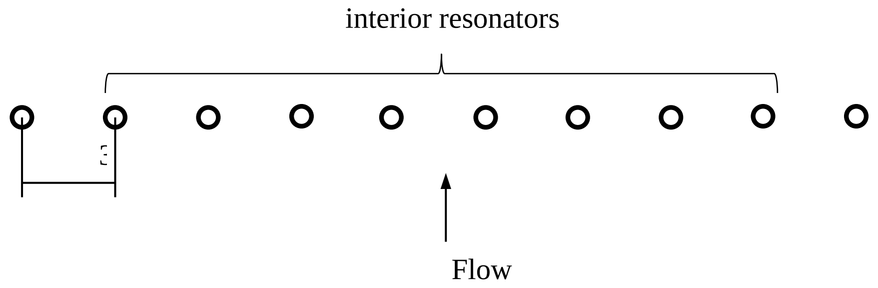


Figure 2.13: Plan view of adjacent resonators (Flynn and Panton 1989).

As a consequence, the geometry of the cavity, the ratio of diameter to depth, and the orifice shape have a direct impact on the flow oscillations inside and outside of the Helmholtz resonators. In the present work parametric studies have also been conducted to gain insight into the effects of the resonator characteristics on the resulting dynamics.

## 2.2 Turbulent boundary layer

In order to find an efficient means to control the turbulent boundary layer, a comprehensive understanding of the physics of turbulent production within the boundary layer is required. There is still some doubt that exists as to the exact cause of self-sustaining mechanisms of wall turbulence, however, it is generally accepted that turbulent boundary layers consist of "coherent structures". These coherent structures are constituted by low-momentum fluid, often resembling streamwise vortices (Cantwell 1981; Gad-el-Hak 2000; Stanislas et al. 2011) as shown in Figure 2.14. Earlier studies by Kline et al. (1967) demonstrated the presence of high- and low-speed regions within the turbulent boundary layer, simply referred to as "*streaks*". The exact origin of these structures is still unknown but the dimensions of the streaks are universally characterised by a time scale, $t^+ = \left(\frac{\nu}{u_\tau^2}\right)$, and a length scale, $l^+ = \left(\frac{\nu}{u_\tau}\right)$. Here, ν is the kinematic viscosity and $u_\tau$ is the friction velocity of the flow.

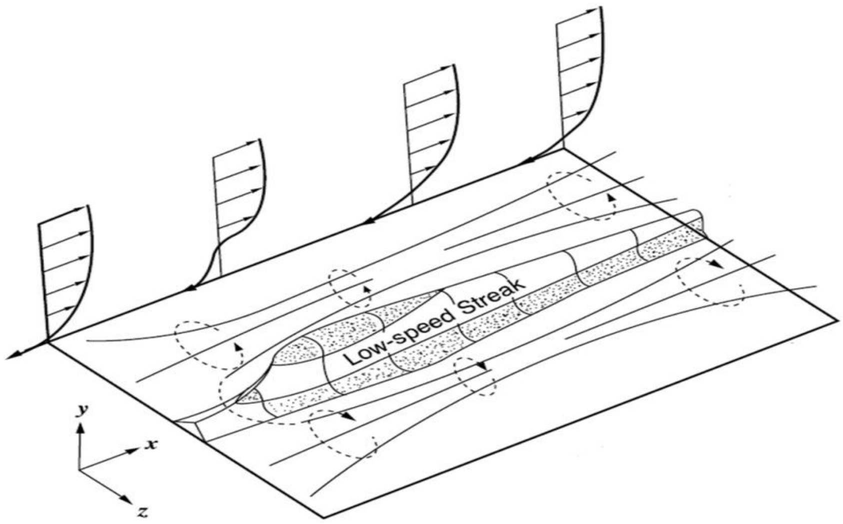


Figure 2.14: Near-wall streaky structure in turbulent wall-bounded flows (Gad-el-Hak 2000).

Visualisations of the turbulent boundary layer flow using the hydrogen bubble technique revealed that these streaky structures persisted up to $50l^+$ in the wall normal direction, with a spanwise spacing of $Z^+ = 80l^+$ to $100l^+$ (Smith and Metzler 1983; Chernyshenko and Baig 2005) . The low-speed streaks are typically $1000\ l^+$ in length, 10 $l^+$ to 20 $l^+$wide and have an almost constant propagation speed of $u_{cs} = 10\ u_\tau$ to 13 $u_\tau$ in the near-wall zone of 10 $l^+ <$ $Y^+ < 30\ l^+$ ( $Y^+$is the distance from the wall times the length scale) (Zhou et al., 1999).

The streamwise vortices are also responsible for the development of inflectional velocity profiles within the boundary layer. The vortices can pump the fluid into and away from the surface, resulting in the production of turbulent kinetic energy (Robinson 1991; Ganapathisubramani et al. 2006). There are numerous experimental investigations that characterise these vortex structures. Adrian et al. (2000) demonstrated using PIV that the streamwise vortices are the legs of a hairpin vortex structure, with an angle of approximately 45° to the surface. As shown in Figure 2.15, the vortices collect the low-momentum fluid, causing the appearance of the low-speed streaks, and lift it within the near wall region. It has been observed that the in-rush motion of the high-speed flow into the surface is directly linked to the lifting up process of the low-speed fluid, which is followed by bursting of the low-speed streaks (Hinze 1975; Jeong et al. 1997). In the first step of a bursting event, the low-speed streaks initially elongate and meander through the flow and then they rise above the surface to $Y^+ \approx 15\ l^+$, which has a higher speed, and accelerates the low-speed fluid from the decelerated wall-bounded region. Therefore, the streaks oscillate such that the wavelengths of oscillation reach up to $\lambda^+ \approx 150\ l^+$to $250\ l^+$. The oscillation is amplified within the buffer layer, such that the low-speed fluid ejects into the outer region of the turbulent boundary layer, with an average bursting frequency of ${f_b}^+ = 0.0035/\ t^+$ (Blackwelder and Haritonidis 1983; Lu and Willmarth 1973; Schoppa and Hussain 2002). This is followed by a sweep event, resulting in the downwash of high-speed fluid from the outer regions of the boundary layer towards the surface, leading to an increase in skin friction (Kravchencko et al., 1993; Orlandi and Jiménez, 1993). The induced sweep event generates the perturbation for the next oncoming vortices and the bursting cycle is repeated. These turbulent events of sweep and injection have been characterised by Blackwelder and Kaplan (1976), who applied a variable interval time averaging (VITA) technique to detect the changes in turbulence structures. The details of this technique will be presented in Chapter 6.

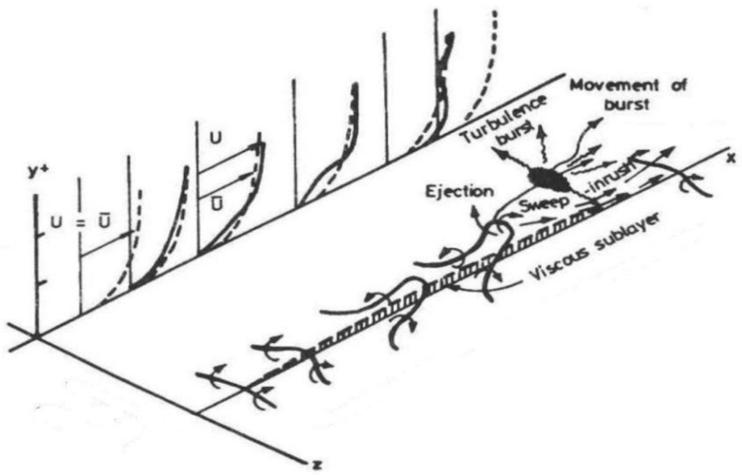


Figure 2.15: A cyclic process of turbulence generation within a turbulent boundary layer (Hinze 1975).

To assess alternative turbulent boundary-layer control methods, it is of great importance to understand the self-sustaining mechanism of wall turbulence. Therefore, the general principles of flow behaviour within the turbulent boundary layer were addressed in this section. A detailed examination of some successful flow control techniques will be presented in the following section.

### 2.3 Turbulent boundary layer control

There are several ways to suppress the instabilities that result from these turbulent events. An up-to-date summary of the mechanisms responsible for viscous drag reduction will be presented in the following section, and the advantages and limitations of various methods are also discussed.

#### 2.3.1 Riblets

Small longitudinal micro-grooves, aligned over a smooth surface in the streamwise direction, have been investigated and considered as a successful passive technique to reduce the turbulent energy (Hooshmand et al. 1983; Bacher and Smith 1985; Lee and Lee 2001; Peet et al. 2008). Such micro-grooves, or riblets, act as longitudinal fences that inhibit the quasi-streamwise vortices in the hairpin legs, causing the bursting events to weaken, with a reduction in the strength of the sweep cycles within the near wall region (Choi 1993; Tardu et al. 1993; Bechert et al. 1997). Lee and Choi (2008) through PIV measurements indicated that the riblets increase the spanwise spacing of the low-speed streaks, resulting in manipulation of longitudinal vortices and a reduction in the streamwise velocity fluctuations within the logarithmic region of the boundary layer (Figure 2.16). It was also observed that because of the spanwise vortices, with ring- or omega-shaped structures generated by riblet peaks, the eddy motion in the near wall region decreases and the mean velocity profiles above the riblet surface would be fuller than the velocity profile over the smooth surface.

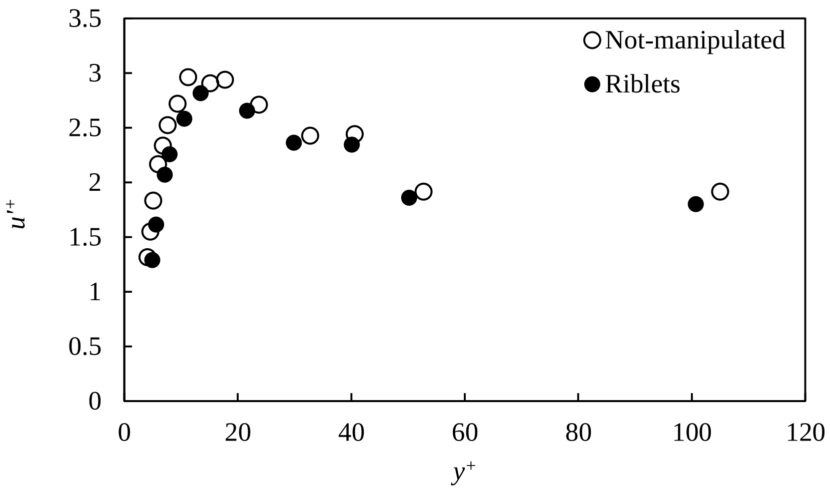


Figure 2.16: Streamwise velocity fluctuations (Lee & Choi 2008).

Attenuation of instabilities within a turbulent boundary layer is directly related to the riblet spacing, such that velocity fluctuations are attenuated when the riblets are wide-spread and the opposite is observed for densely-packed riblets (Koeltzsch et al. 2002). In order to achieve the maximum skin drag reduction, considerable efforts were made to develop an ideal riblet shape. Various riblet geometries including rectangular, triangular, trapezoidal and semicircular cross-sections were studied and it was illustrated that symmetric V-shaped grooves, such as those illustrated in Figure 2.17, are the optimum shape for the riblets. The length of the riblets is as the size of the viscous sublayer and reveals enormous consistency with regards to the degree of viscous drag reduction (Walsh and Weinstein 1978; Parker and Sayers 1999).

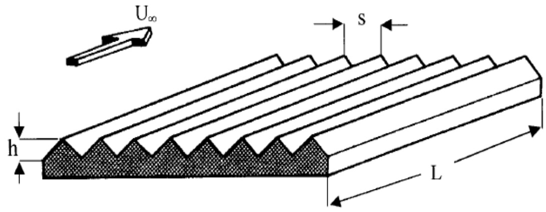


Figure 2.17: Schematic of riblets (Choi 1993).

It was demonstrated that the skin friction reduction is a function of the height $(h)$ and spacing $(s)$ of the grooves. If the riblet height equals its spacing and is around $15l^+$, a maximum drag reduction of 8% would be achieved (Walsh 1983). Another experiment conducted by El-samni et al. (2007), who tested a wide range of riblets with different spacing, indicated that maximum skin friction drag reduction could be obtained with a spacing of $18l^+$. García-Mayoral and Jiménez (2011), by implementing direct numerical simulations of flow within ribbed channels, claimed that if the non-dimensional groove area $(A^+)$ is around 10, the maximum drag reduction could be as much as 9%. However, for $s^+ > 30$, the riblets increase the instabilities within the boundary layer because the turbulent eddies have time to stay inside the riblet valleys, resulting in increased interaction of the high-speed flow with the wetted surface and increased viscous drag. Owing to boundary layer separation, riblets can also increase the turbulence events when their yaw angle is greater than 30 degrees (Choi 1989; Choi 1993). Therefore, finding the optimal size of the riblets for drag reduction purposes and also the manufacture and maintenance of these structures in real applications, such as an aircraft, are the issues for the widespread use of this method.

### 2.3.2 Blowing and suction of the turbulent boundary layer

The interaction of various types of active control with the coherent structures has also been investigated in earlier studies. One such method is wall suction, which delays the onset of turbulence or the transition process (Gad-el-Hak 2000). This technique has been known to reduce drag on the surface by dramatically increasing the boundary layer stability. The rule of thumb is that wall suction withdraws a small amount of fluid in the near-wall region which decreases the boundary layer thickness, and thus increases the critical Reynolds number which is related to the boundary layer thickness. It should be emphasised that the suction mechanism for turbulent boundary layer control is slightly different from the suction method for transition (or laminar) boundary layer control. When suction is applied on laminar boundary layers, inflection points in the velocity profile are decreased. In this laminar method, which is called "*asymptotic suction*", the asymptotic velocity profile generated by suction holes or slots, is more stable; therefore, transition onset is delayed (Blackwelder 1998). On the other hand, such uniform suction in the turbulent boundary layer has unwanted effects such that the viscous drag is increased by relatively small amounts of suction. In this case, the momentum thickness gradient does not change significantly due to the applied suction and the skin friction is increased (Gad-el-Hak 2000). Therefore, another appropriate alternative technique, known as "*selective suction*", was suggested to control the instabilities within a turbulent boundary layer (Jacobson and Reynolds 1998; Kerho et al. 2002). The location of suction and injection holes were changed to find an optimum arrangement to reduce the instabilities within the boundary layer (Kozlov et al. 1999). It was observed that when suction is applied between the high- and low-speed regions, the sweep events are accelerated; whilst, when the suction is applied under high speed streaks the instabilities are enhanced. It has also been demonstrated that blowing under high speed streaks allows the adjacent low speed streaks to expand so the skin friction drag is decreased (Choi and Kim 1994; Carlson and Lumley 1996; Rebbeck and Choi 2006). Therefore, in order to achieve a damping effect, a small amount of suction and injection are applied under the low and high speed streaks respectively, as illustrated in Figure 2.18. Since the exact positions of the low and high speed streaks are not predictable, special trips were used to produce these structures artificially and also small suction holes were implemented to generate artificial bursts upstream of the suction slot (Gad-el-Hak and Hussain 1986).

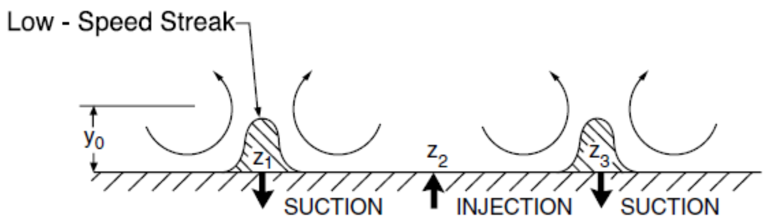


Figure 2.18: Selective suction underneath a low speed flow (Gad-el-Hak and Blackwelder 1989).

The selective suction method imposes counter rotating vortices into the near wall region and reduces the velocity differences between the low and high speed streaks and, thereby, suppresses the turbulent events. As can be seen in Figure 2.19, using this method, velocity fluctuations within the logarithmic region may be reduced by up to 10% (Segawa et al. 2007). The advantage of this method is a reduced mass flow requirement compared to uniform continuous suction, such that the optimum value of the suction coefficient to eliminate low speed streaks is $C_q$ = 0.0006 to 0.0015 which is almost 2 to 5 times lower than those applied in uniform suction methods (Myose and Blackwelder 1995).

However, most investigations have been performed in low turbulence intensity conditions to find the locations of the high and low speed streaks. Since viscous scales in the turbulent region are very small, small scale actuators are the ideal solution for the selective suction technique. Therefore, micro-electromechanical systems (MEMS) were suggested for active turbulence control (Rathnasingham and Breuer, 2003). This actuator acts like a synthetic jet to weaken the low speed streaks and results in an approximate reduction in the streamwise velocity fluctuations of up to 30% (Rathnasingham and Breuer, 2003). Although practical use of MEMS is not easy due to the manufacturing constraints, the concept has received much attention over the past few years. For example, using the velocity-vorticity equations, the effects of a MEMS actuator on the lifting up process of low speed streaks was investigated and it was concluded that three dimensional instabilities in the turbulent region on a flat plate are attenuated significantly (Lockerby et al. 2005).

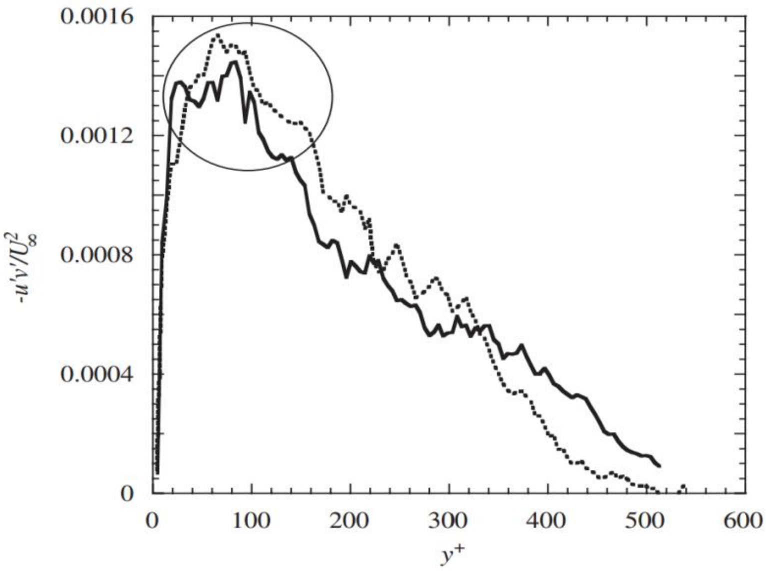


Figure 2.19: Reynolds stress with control (solid line) and without control (dotted line) within the turbulent boundary layer (Segawa et al. 2007).

Manipulation of the hairpin structures within the boundary layer has also been investigated as another way to suppress the turbulence generation. Through direct numerical simulation (DNS) of channel flow, Choi and Kim (1994) claimed that the sweep events could be suppressed by a combination of in-phase $u$-velocity and out-of-phase $v$-velocity in the near wall region and reported a 25% drag reduction. This investigation was followed by Kang et al. (2008) who manipulated the hairpin structures by a jet placed outside the turbulent boundary layer (Figure 2.20a). The jet flow destroys the head of the hairpin structures and through the downwash of high-speed fluid toward the surface, sweep is prevented. It must be noted that using this method results in significant reductions in sweep intensity which last up to $x^+ = xu_\tau/\upsilon$ = 90 as shown in Figure 2.20(b) (Rebbeck and Choi 2006).

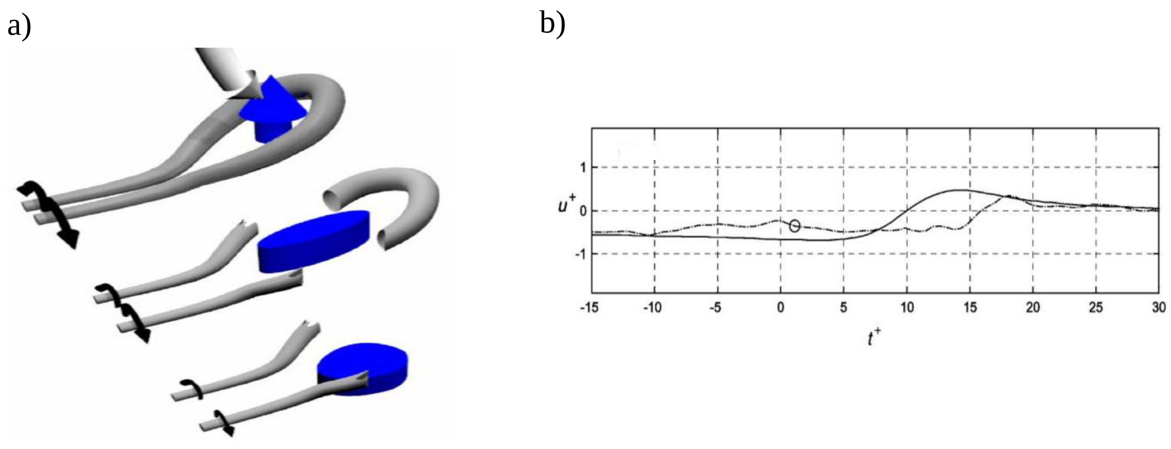


Figure 2.20: Opposition control technique; a) Schematic of the direct intervention of the hairpin head (Kang et al. 2008); b) Modifications made to the sweep events at $y^{+}$=15 and $x^{+}$=90 downstream of actuator (Rebbeck and Choi 2006).

### 2.3.3 Travelling waves

Modern techniques have been extensively focused on the local control of individual streamwise vortices. Introducing streamwise vorticity using a spanwise excitation, in the form of a travelling wave, is one way to suppress the near-wall flow instabilities within the turbulent boundary layer (Jung et al. 1992; Henoch and Stace 1995; Itoh et al. 2006). The wave is induced by a spanwise force (Figure 2.21) within the viscous sublayer, so that the maximum amplitude occurs at the surface, and decays exponentially with respect to the penetration depth. It was proposed that flush mounted electrodes (an array of tiles) and sub-surface magnets can provide the unsteady force, directly affecting the turbulent events in the turbulent boundary layer (Nosenchuck et al. 1995). This oscillatory excitation changes the near-wall streaky structure so that the low speed fluid forms wide ribbons and the near-wall streak spacing is altered. This results in twisted low speed streaks that are more organised and the high speed streaks are eliminated (Dhanak and Si, 1999; Du and Karniadakis 2000). It is widely believed that the artificially generated vortices produced by a travelling wave are responsible for collecting and spreading the low speed streaks in the near wall regions. Therefore, an appropriate spanwise wave generates the streamwise vortices which span across many pairs of streaks and reorganise the turbulent boundary layer structures, leading to skin friction drag reductions (Du et al. 2002; Pang and Choi, 2004). The waves must be in a suitable range of forcing period and amplitude to be capable of skin-friction reduction. It was reported that if the penetration depths exceed the viscous sublayer thickness, the friction could be increased (Berger et al. 2000).

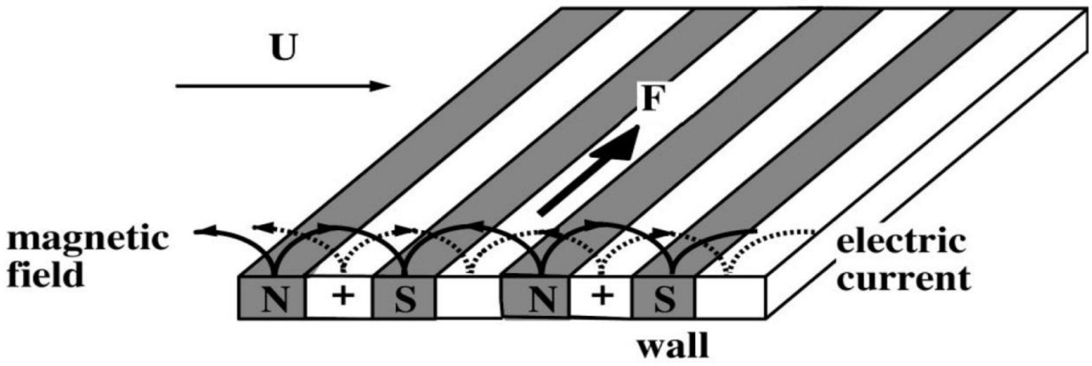


Figure 2.21: Schematic of an arrangement for the travelling wave method and creation of a Lorentz force along the spanwise direction (Berger et al. 2000).

New and interesting studies of spanwise travelling waves in a turbulent channel flow have been conducted using DBD plasma actuators to generate a spanwise travelling wave (Jukes et al. 2006; Whalley and Choi 2011). The plasma actuators can create wall jets within the viscous and buffer layers of the turbulent boundary layer. This process alters the streamwise vortices and generates a negative spanwise vorticity to suppress the near wall velocity gradients. As can be seen in Figure 2.22(a), the probability density function (PDF) of the instantaneous streamwise velocities with plasma actuation applied indicates positive skewing and narrowing compared with the uncontrolled case, reflecting an increase in skewness and kurtosis. Figure 2.22(b) further reveals that the intensity and duration of sweep events are reduced by up to 10% and 50%, respectively, which results in a 45% drag reduction downstream of the plasma actuators. Although there is a limitation to increase the Reynolds number because of the limited authority of the DBD plasma actuators, it was claimed that this technique is very simple with fast actuation and does not require any moving parts or complicated design (Whalley 2011).

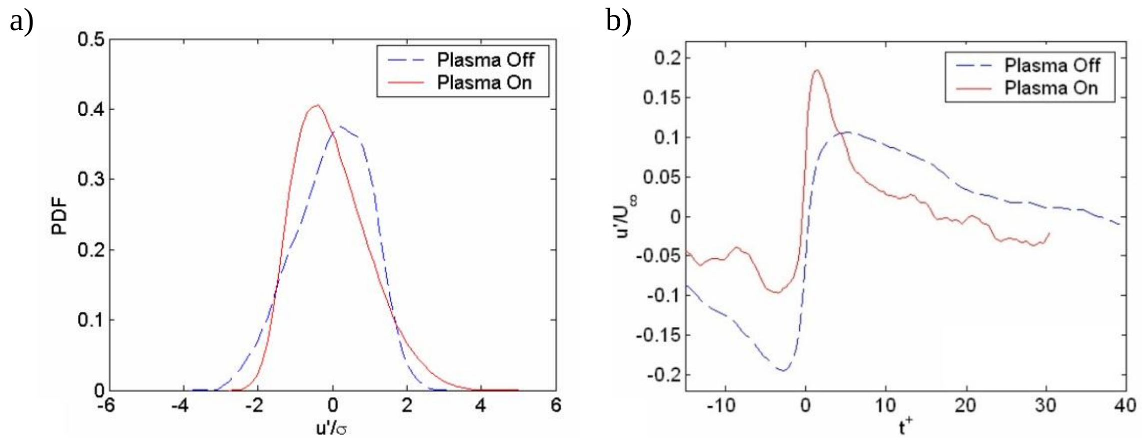


Figure 2.22: Modification of turbulent boundary layer using plasma actuators; a) probability density function of $\boldsymbol{u}$-component velocity fluctuations and b) variable interval time averaging of sweep events at $\boldsymbol{y}^{+}$=30 (Jukes et al. 2006).

**2.3.4 Wall oscillation**

It has also been demonstrated that the interaction between longitudinal vortices and the streaky structures in the turbulent boundary layer near wall region can be modified using spanwise wall motions (Choi 2002; Viotti et al. 2009). The basic mechanism of drag reduction in this technique is the enhancement of spanwise vorticity and simultaneous weakening of the quasi-streamwise vortices, leading to suppression of turbulence production mechanisms. It is important to note that the induced force using spanwise wall oscillation (Figure 2.23), is the same as the force created by the spanwise travelling waves when the wave has an infinite wavelength. The force pumps up the logarithmic part of the velocity profile and results in increased viscous sublayer thickness. It was observed that when the surface is oscillated with a period of $T^{+} = T_{\mathrm{osc}} u_{\tau}{}^{2}/v = 100$, the velocity fluctuations could be reduced by up to 40% (Jung et al. 1992). Drag reduction using this technique is a result of the attenuation of the formation of turbulent events, such that the quasi-streamwise vortices are shifted in the spanwise direction. This consequently causes the original streaky structure in the near wall region to break down, leading to a reduction in the sweep events (Laadhari 1994).

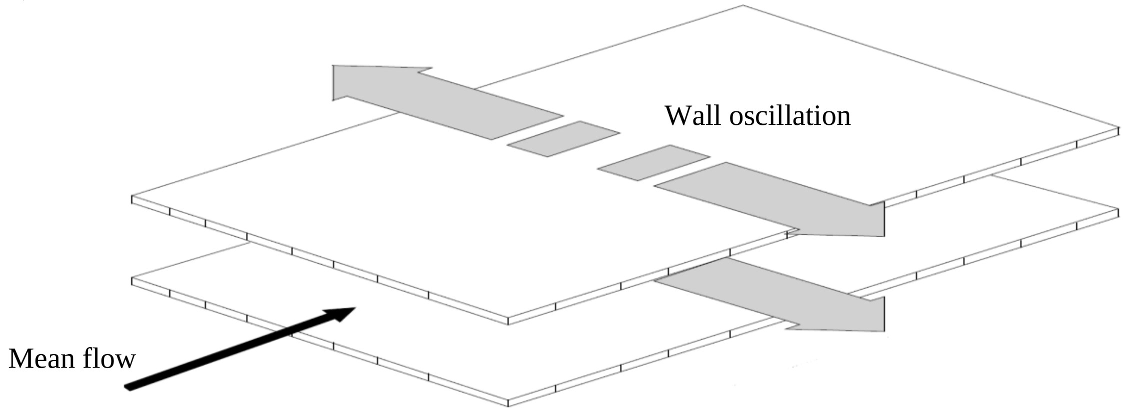


Figure 2.23: Schematic illustration of wall oscillation technique used for turbulent boundary layer control (Ricco and Quadrio 2008).

The wall oscillation mechanism moves the vortices to a different position relative to the high and low speed streaks. Therefore, the streamwise vortices pump up the high speed fluid rather than the low speed streaks and splash the low speed streaks into the high speed ones at the surface. This process thereby disrupts the burst-sweep cycles. From a fundamental point of view, using this mechanism, a thin Stokes layer is created which could stabilise the streaks in the near wall region. Experimental investigation shows that this periodic layer is twisted in the near wall region and creates the negative spanwise vorticity at the edge of the viscous sublayer (Choi and Graham 1998). These vortices reduce the stretching of longitudinal vortices, leading to a weakening in the near wall sweep events by up to 30%. Choi and Clayton (2001) also applied a sinusoidal oscillation force over a flat plate with oscillation frequencies from 1Hz to 7Hz and peak-to-peak amplitudes of up to 70mm then measured the changes within the turbulent boundary layer. As can be seen in Figure 2.24(a), the streamwise velocity fluctuations are reduced by increasing the frequency of the wall oscillations. Moreover, it was demonstrated that the turbulent energy within the logarithmic region of the boundary layer is reduced at low frequencies and results in the transfer of energy from the larger eddies to the smaller eddies, as shown in Figure 2.24(b). This reduction in the production of large scale structures demonstrates the suppression of turbulent events within the boundary layer (Schoppa and Hussain 1998). However, the optimum induced force and the speed of wall movement depend on the free stream velocity.

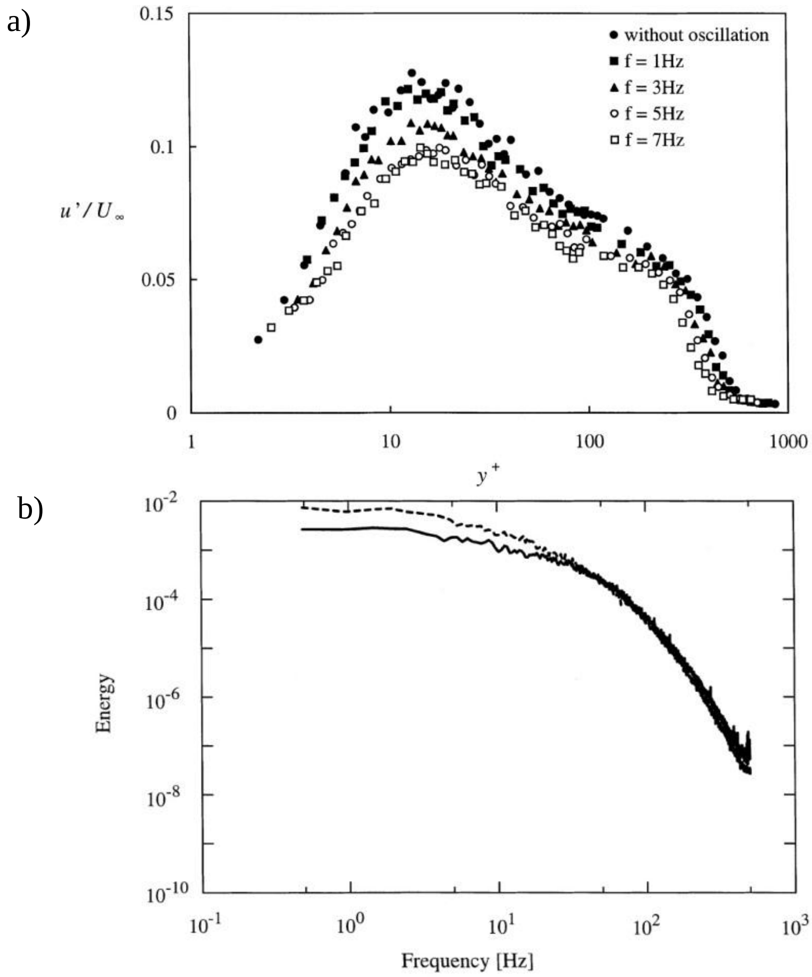


Figure 2.24: a) Normalised streamwise velocity fluctuations within the boundary layer for different frequencies of wall oscillation; b) energy spectra for streamwise velocity fluctuations, (solid line) with wall oscillation; (dashed line) without wall oscillation (Choi and Clayton 2001).

### 2.3.5 Other techniques

Adding minute quantities of polymers or string-like surfactants (Virk 1975), using compliant coatings (Choi et al. 1997), Micro-bubbles (Merkle and Deutsch, 1989), and Large-Eddy-Break-Up devices (LEBU) (Savill and Mumford, 1988; Badyopadhyay, 1986) are some other alternative methods to control the turbulent boundary layer. It is still rather early to decide which of the described techniques is the most appropriate one and can be used in the majority of applications. There is room for optimisation and development, based on the target engineering applications.

## 2.4 Conclusion of literature and research objectives

Various techniques for reducing drag within the turbulent boundary layer were reviewed in this chapter. It has been recognised that the aforementioned approaches for suppression of turbulent events still need further research prior to their implementation in real applications. For example, the inherent energy consumption associated with the selective suction technique is an undesirable side effect of this method, as is the problem of accurately targeting the high- and low-speed streaks within a boundary layer. The travelling wave and wall oscillation methods are very hard to implement in practice. Compared to the active methods, the disadvantages of riblets are rather low amount of drag reduction which they can achieve for an optimized configuration and manufacture of these structures. Therefore, the question remains regarding which control mechanism has minimal side effects, suitable performance, and simplicity of use in various conditions. In the present research, the Helmholtz resonator is used as a possible alternative for attenuation of three-dimensional instabilities within the turbulent boundary layer. The Helmholtz resonator is very simple in construction, and can be manufactured and implemented with relative ease. Moreover, the energy required for excitation of the resonator comes from the grazing flow. These features separate it from the previously investigated flow control devices that, in general, are difficult to implement.

The literature review presented in this chapter also showed that there is a lack of knowledge about the characteristics of the grazing flow downstream of the resonator and its effect on the structure of the turbulent boundary layer. In this study determining the near wall flow characteristics around the orifice and further downstream is considered a novel and worthwhile endeavour to explore the potential of the flow-excited Helmholtz resonator to attenuate instabilities within a turbulent boundary layer. The previous studies outlined in the Introduction section demonstrate that the optimal design of the Helmholtz resonator for attenuation of the instabilities within the turbulent boundary layer is also unknown. Although the appropriate configuration of the Helmholtz resonator to generate self-excitation conditions must be determined, it is of prime importance to understand the extent of the resonator effect on the boundary layer parameters. Hence identifying the optimal parameters of the resonator that have the potential to improve the stability of the turbulent boundary layer is another task in this research.

Therefore, in the present thesis, a novel approach for turbulent boundary layer control has been presented, based on the flow-excited Helmholtz resonator as the flow control device. The method has been developed and tested within the turbulent boundary layer and the effectiveness of the technology has been evaluated and compared with other published work.

**References**

Adrian, R. J., Meinhart, C. D., and Tomkins, C. D. 2000, 'Vortex organisation in the outer region of the turbulent boundary layer', *Journal of Fluid Mechanics*, vol. 422, pp. 1–54.

Amandolese, X., Hemon, P., and Regardin, C. 2004, 'An experimental study of the acoustic oscillations by flows over cavities', *Journal of Vibration and Acoustics*, vol. 126, no. 2, pp. 190-195.

Alster, M. 1972, 'Improved calculation of resonant frequencies of Helmholtz resonators', *Journal of Sound and Vibration*, vol. 24, no. 1, pp. 63-85.

Arunajatesan, S., and Sinha, N. 2005, 'Modelling Approach for Reducing Helmholtz Resonance in Submarine Structures', *11th AIAA/CEAS Aeroacoustics Conference*, California, USA.

Bandyopadhyay, P. 1986, 'Review—Mean flow in turbulent boundary layers disturbed to alter skin friction', *Journal of Fluids Engineering*, vol. 108, no. 2, pp. 127-140.

Baumeister, K. J., and Rice, E. J 1975, 'Visual study of the effect of grazing flow on the oscillatory flow in a resonator orifice', NASA TM x-3288, vol. 1.

Bechert, D., Bruse, M., Hage, W., Van Der Hoeven, J., and Hoppe, G. 1997, 'Experiments on drag-reducing surfaces and their optimization with an adjustable geometry', *Journal of Fluid Mechanics*, vol. 338, no. 5, pp. 59-87.

Berger, T. W., Kim, J., Lee, C., and Lim, J. 2000, 'Turbulent boundary layer control utilizing the Lorentz force', *Physics of Fluids*, vol. 12, pp. 631-649.

Bies, D. A., and Hansen, C. H. 2009, *Engineering Noise Control*, Spon Press/Taylor & Francis.

Bilanin, A. J., and Covert, E. E. 1973, 'Estimation of possible excitation frequencies for shallow rectangular cavities', *AIAA Journal*, vol. 11, pp. 347-351.

Blackwelder, R. F., and Kaplan, R. E. 1976, 'On the wall structure of the turbulent boundary layer', *Journal of Fluid Mechanics*, vol. 76, pp. 89–112.

Blackwelder, R and Haritonidis, J. 1983, 'Scaling of the bursting frequency in turbulent boundary layers', *Journal of Fluid Mechanics*, vol. 132, no. 1, pp. 87-103.

Blackwelder, R. 1998, 'Some notes on drag reduction in the near-wall region', *Flow Control:fundamental and practices, eds. M. Gad-el-Hak, A. Pollard*, pp. 155-198.

Bruggeman, J., Hirschberg, A., Van Dongen, M., Wijnands, A., and Gorter, J. 1991, 'Self-sustained aero-acoustic pulsations in gas transport systems: experimental study of the influence of closed side branches', *Journal of Sound and Vibration*, vol. 150, no. 3, pp. 371-393.

Cantwell, B., J. 1981, 'Organized motion in turbulent flow', *Annual Review Fluid Mechanics*, vol. 13, pp. 457–515.

Carlson, H. A., and Lumley, J. L. 1996, 'Active control in the turbulent wall layer of a minimal flow unit', *Journal of Fluid Mechanics*, vol. 329, no. 1, pp. 341-371.

Chatellier, L., Laumonier, J., and Gervais, Y. 2004, 'Theoretical and experimental investigations of low Mach number turbulent cavity flows', *Experiments in Fluids*, vol. 36, no. 5, pp. 728-740.

Choi, K. 1989, 'Near-wall structure of a turbulent boundary layer with riblets', *Journal of Fluid Mechanics*, vol. 208, pp. 417-458.

Choi, K. S. 2002, 'Near-wall structure of turbulent boundary layer with spanwise-wall oscillation', *Physics of Fluids*, vol. 14, no. 7, pp. 2530-2542.

Choi, H., and Kim, J. 1994, 'Active turbulence control for drag reduction in wall-bounded flows', *Journal of Fluid Mechanics*, vol. 262, pp. 75-110.

Choi, K. S., and Graham, M. 1998, 'Drag reduction of turbulent pipe flows by circular-wall oscillation', *Physics of Fluids*, vol. 10, pp. 7-9.

Choi, K., and Clayton, B., R. 2001, 'The mechanism of turbulent drag reduction with wall oscillation', *International Journal of Heat and Fluid Flow*, vol. 22, no. 1, pp. 1-9.

Choi, H., Moin, P., and Kim, J. 1993, 'Direct numerical simulation of turbulent flow over riblets', *Journal of Fluid Mechanics*, vol. 255, no. 1, pp. 503-539.

Choi, K.-S., Yang, X., Clayton, B. R., Glover, E., Atlar, M., Semenov, B. N., and Kulik, V. 1997, 'Turbulent drag reduction using compliant surfaces', *Proceedings of the Royal Society A: Mathematical, Physical and Engineering Sciences*, vol. 453, pp. 2229–2240.

Colonius, T., Basu, A. J., and Rowley, C. W. 1999, ‘Numerical investigation of the flow past a cavity’, *5th AIAA/CEAS Aeroacoustics Conference*, Paper No. AIAA 99-1912, Greater Seattle, Washington.

Cremer, L and Ising, H. 1967, 'Die selbsterregten schwingungen von orgelpfeifen', *Acustica*, vol. 19, no. 3, pp. 143-153.

Cummings, A. 1987, 'The response of a resonator under a turbulent boundary layer to a high amplitude non-harmonic sound field', *Journal of Sound and Vibration*, vol. 115, no. 2, pp. 321-328.

Dai, X., Jing, X., and Sun, X. 2012, 'Discrete vortex model of a Helmholtz resonator subjected to high-intensity sound and grazing flow', *Journal of the Acoustical Society of America*, vol. 132, no. 5, pp. 2988-2996.

de Jong, A., Bijl, H., Hazir, A., and Wiedemann, J. 2012, 'Aeroacoustic simulation of slender partially covered cavities using a Lattice Boltzmann method', *Journal of Sound and Vibration*, vol 323, no 7, pp. 1687-1703.

De Metz, F. C., and Farabee, T. M. 1977 'Laminar and turbulent shear flow induced cavity resonance', *AIAA paper*, AIAA 77- 1293, New York, USA.

Dequand, S., Hulshoff, S., Kuijk, H. V., Willems, J., and Hirschberg, A. 2003, 'Helmholtz-like resonator self-sustained oscillations, Part 2: Detailed flow measurements and numerical simulations', *AIAA Journal*, vol. 41, no. 3, pp. 416-423.

Dhanak, M., and Si, C. 1999, 'On reduction of turbulent wall friction through spanwise wall oscillations', *Journal of Fluid Mechanics*, vol. 383, pp. 175-195.

Du, Y., and Karniadakis, G. E. 2000, 'Suppressing wall turbulence by means of a transverse traveling wave', *Science*, vol. 288, no. 5469, pp. 1230-1234.

Du, Y., Symeonidis, V., and Karniadakis, G. 2002, 'Drag reduction in wall-bounded turbulence via a transverse travelling wave', *Journal of Fluid Mechanics*, vol. 457, pp. 1-34.

Elder, S. 1978, 'Self-excited depth-mode resonance for a wall-mounted cavity in turbulent flow', *Journal of the Acoustical Society of America*, vol. 64, pp. 877-890.

El-Samni, O., Chun, H. H., and Yoon, H. S. 2007, 'Drag reduction of turbulent flow over thin rectangular riblets', *International Journal of Engineering Science*, vol. 45, no. 2, pp. 436-454.

Elder, S., Farabee, T., and DeMetz, F. 1982, 'Mechanisms of flow-excited cavity tones at low Mach number', *Journal of the Acoustical Society of America*, vol. 72, pp. 532-549.

Faure, T. M., Adrianos, P., Lusseyran, F., and Pastur, L. 2007, 'Visualizations of the flow inside an open cavity at medium range Reynolds numbers', *Experiments in Fluids*, vol. 42, no. 2, pp. 169-184.

Flynn, K. P., and Panton, R. L. 1990, 'The interaction of Helmholtz resonators in a row when excited by a turbulent boundary layer', *Journal of the Acoustical Society of America*, vol. 87, no. 4, pp. 1482-1488.

Gad-el-Hak, M. 2000, *Flow control: passive, active, and reactive flow management*, Cambridge University Press, London.

Gad-el-Hak, M., and Hussain, A. K. M. F. 1986, 'Coherent structures in a turbulent boundary layer. Part 1: Generation of ‘artificial’ bursts', *Physics of Fluids*, vol. 29, no. 7, pp. 2124-2139.

Ganapathisubramani, B., Longmire, E.K. and Marusic, I. 2006, 'Experimental investigation of vortex properties in a turbulent boundary layer', *Physics of Fluids*, vol. 18, no. 5, pp. 1-14.

García-Mayoral, R., and Jiménez, J. 2011, 'Drag reduction by riblets', *Philosophical Transactions of the Royal Society A: Mathematical, Physical and Engineering Sciences*, vol. 369, pp. 1412-1427.

Georges, L., Winckelmans, G., Caro, S., and Geuzaine, P. 2009, 'Aeroacoustic simulation of the flow in a Helmholtz resonator', *Computational Fluid Dynamics*, DOI: 10.1007/978-3-540-92779-2 129, pp. 819-824.

Gharib, M., and Roshko, A. 1987, 'The effect of flow oscillations on cavity drag', *Journal of Fluid Mechanics*, vol. 177, pp. 501-530.

Hémon, P., Santi, F., and Amandolèse, X. 2004, 'On the pressure oscillations inside a deep cavity excited by a grazing airflow', *European Journal of Mechanics-B/Fluids*, vol. 23, no. 4, pp. 617- 632.

Hersh, A.S., and Walker, B. 1977, 'Fluid mechanical model of the Helmholtz resonator', *Final Report, Hersh Acoustical Engineering*, Chatsworth, CA.

Henoch, C., and Stace, J. 1995, 'Experimental investigation of a salt water turbulent boundary layer modified by an applied streamwise magnetohydrodynamic body force', *Physics of Fluids*, vol. 7, pp. 1371-1383.

Hinze, J. O. 1975, *Turbulence*, 2nd ed, McGraw-Hill, New York.

Hooshmand, D., Youngs, R., Wallace, J., and Balint, J. 1983, 'An experimental study of changes in the structure of a turbulent boundary layer due to surface geometry changes', *AIAA 21st Aerospace Sciences Meeting*, AIAA-83-0230, Nevada, USA.

Howard, C. Q., Cazzolato, B. S., and Hansen, C. H. 2000, 'Exhaust stack silencer design using finite element analysis', *Noise Control Engineering Journal*, vol. 48, no. 4, pp. 113-120.

Howe, M. 1981a, 'Influence of mean shear on unsteady aperture flow, with application to acoustical diffraction and self-sustained cavity oscillations', *Journal of Fluid Mechanics*, vol. 109, pp. 125-146.

Howe, M. 1981b, 'On the theory of unsteady shearing flow over a slot', *Philosophical Transactions of the Royal Society of London. Series A, Mathematical and Physical Sciences*, vol. 303, pp. 151-180.

Inagaki, M., Murata, O., Kondoh, T., and Abe, K. 2002, 'Numerical prediction of fluid-resonant oscillation at low Mach number', *AIAA Journal*, vol. 40, no. 9, pp. 1823-1829.

Itoh, M., Tamano, S., Yokota, K., and Tanigichi, S. 2006, 'Drag reduction in a turbulent boundary layer on a flexible sheet undergoing a spanwise travelling wave motion', *Journal of Turbulence*, vol. 7, pp. 1–17.

Jacobson, S. A., and Reynolds, W. C. 1998, 'Active control of streamwise vortices and streaks in boundary layers', *Journal of Fluid Mechanics*, vol. 360, no. 1, pp. 179-211.

Jeong, J., Hussain, F., Schoppa, W. and Kim, J. 1997, 'Coherent structures near the wall in a turbulent channel flow', *Journal of Fluid Mechanics*, vol. 332, pp. 185-214.

Jung, W., Mangiavacchi, N., and Akhavan, R. 1992, 'Suppression of turbulence in wall-bounded flows by high-frequency spanwise oscillations', *Physics of Fluids*, vol. 4, no. 8, pp. 1605-1607.

Jiménez, J., and Pinelli, A. 1999, 'The autonomous cycle of near-wall turbulence'. *Journal of Fluid Mechanics*, vol. 389, pp. 335–359.

Jukes, T. N., Choi, K. S., Johnson, G. A., and Scott, S. J. 2006, 'Turbulent drag reduction by surface plasma through spanwise flow oscillation', *3rd AIAA Flow Control Conference*, Paper No. AIAA-2006-3693, California, USA.

Jung, W., Mangiavacchi, N., and Akhavan, R. 1992, 'Suppression of turbulence in wall-bounded flows by high-frequency spanwise oscillations', *Physics of Fluids*, vol. 4, no. 8, pp. 1605-1607.

Kang, Y. D., Choi, K. S., and Chun, H. H. 2008, 'Direct intervention of hairpin structures for turbulent boundary-layer control', *Physics of Fluids*, vol. 20, no. 10, pp. 1-13.

Kerho, M. 2002, 'Active reduction of skin friction drag using low-speed streak control', *40th AIAA Aerospace Sciences*, *AIAA paper*, AIAA 2002-0271, Nevada, USA.

Khosropour, R., and Millet, P. 1990, 'Excitation of a Helmholtz resonator by an air jet', *Journal of the Acoustical Society of America*, vol. 88, pp. 1211-1221.

Kinsler, L. E., Frey, A. R., Coppens, A. B., and Sanders, J. V. 1999, *Fundamentals of Acoustics*, 4th Edition, ISBN 0-471-84789-5, Wiley-VCH.

Kline, S. J., Reynolds, W. C., Schraub, F. A., and Runstadler, P. W. 1967, 'The structure of turbulent boundary layers', *Journal of Fluid Mechanics*, vol. 30, pp. 741–773.

Koeltzsch, K., Dinkelacker, A., and Grundmann, R. 2002, 'Flow over convergent and divergent wall riblets', *Experiments in Fluids*, vol. 33, no. 2, pp. 346-350.

Kook, H. 1997, 'Prediction and control of the interior pressure fluctuations in a flow-excited Helmholtz resonator', Ph. D. thesis, Purdue University.

Kook, H., Mongeau, L., and Franchek, M. 2002, 'Active control of pressure fluctuations due to flow over Helmholtz resonators', *Journal of Sound and Vibration*, vol. 255, no. 1, pp. 61-76.

Kozlov, V., Bippes, H., Bakchinov, A., and Katasonov, M. 1999, 'Control of boundary layer transition at high free stream torbulence by localized suction ', *IUTAM Symposium on Mechanics of Passive and Active Flow Control*, vol. 53, pp. 159-164.

Kravchencko, A. G., Choi, H., and Moin, P. 1993, 'On the relation of near-wall streamwise vortices to wall skin friction in turbulent boundary layers', *Physics of Fluids*, vol 5, pp. 3307–3309.

Laadhari, F., Skandaji, L., and Morel, R. 1994, 'Turbulence reduction in a boundary layer by a local spanwise oscillating surface', *Physics of Fluids*, vol. 6, pp. 3218-3220.

Lee, S. J., and Choi, Y. S. 2008, 'Decrement of spanwise vortices by a drag-reducing riblet surface', *Journal of Turbulence*, vol. 9, no. 23, pp. 1–15.

Lee, S. J., and Lee, S. H. 2001, 'Flow field analysis of a turbulent boundary layer over a riblet surface', *Experiments in Fluids*, vol. 30, no. 2, pp. 153-166.

Lee, S. B., Seena, A., and Sung, H. J. 2010, 'Self-sustained oscillations of turbulent flow in an open cavity', *Journal of Aircraft*, vol. 47, no. 3, pp. 820-834.

Lockerby, D. A., Carpenter, P. W., and Davies, C. 2005, 'Control of sublayer streaks using microjet actuators', *AIAA Journal*, vol. 43, no. 9, pp. 1878-1886.

Lu, S., and Willmarth, W. 1973, 'Measurements of the structure of the Reynolds stress in a turbulent boundary layer', *Journal of Fluid Mechanics*, vol. 60, no. 3, pp. 481-511.

Mallick, S., Shock, R., and Yakhot, V. 2003, 'Numerical simulation of the excitation of a Helmholtz resonator by a grazing flow', *Journal of the Acoustical Society of America*, vol. 114, no. 4, pp. 1833-1840.

Ma, R., Slaboch, P. E., and Morris, S. C. 2009, 'Fluid mechanics of the flow-excited Helmholtz resonator', *Journal of Fluid Mechanics*, vol. 623, pp. 1-26.

Mast, T. D., and Pierce, A. D. 1995, 'Describing-function theory for flow excitation of resonators', *Journal of the Acoustical Society of America*, vol. 97, no. 1, pp. 163-172.

Massenzio, M., Biaise, A., and Lesueur, C. 2008, 'Mechanisms of self-sustained oscillations induced by a flow over a cavity', *Journal of Vibration and Acoustics*, vol. 130, no. 5, pp. 1-8.

Meissner, M. 2002, 'Excitation of Helmholtz resonator by grazing air flow', *Journal of Sound and Vibration*, vol. 256, no. 2, pp. 382–388.

Merkle, C., and Deutsch, S. 1989, 'Drag reduction in liquid boundary layers by gas injection. In: Viscous drag Reduction in Boundary layers', *AIAA paper*, AIAA-91-12688 02-34, Washington, USA

Myose, R. Y., and Blackwelder, R. F. 1995, 'Control of streamwise vortices using selective suction', *AIAA Journal*, vol. 33, no. 6, pp. 1076-1080.

Nelson, P. A., Halliwell, N. A., and Doak, P. E. 1981, 'Fluid dynamics of a flow excited resonance, Part I: Experiment', *Journal of Sound and Vibration*, vol. 78, no. 1, pp. 15-38.

Nelson, P., Halliwell, N., and Doak, P. 1983, 'Fluid dynamics of a flow excited resonance, Part II: Flow acoustic interaction', *Journal of Sound and Vibration*, vol. 91, no. 3, pp. 375-402.

Nishikawa, A. 2011, 'Aeroacoustic Source Strength Measurement of Helmholtz Resonator', *Honors Thesis*, University of Central Arkansas.

Nosenchuck, D., Brown, G., Culver, H., Eng, T., and Huang, I. 1995, 'Spatial and temporal characteristics of boundary layers controlled with the Lorentz force', *12th Australasian Fluid Mechanics Conference*, Sydney, Australia.

Orlandi, P., and Jiménez, J. 1993, 'On the generation of turbulent wall friction', *Physics of Fluids*, vol. 6, pp. 634–641.

Pang, J., and Choi, K. S 2004, 'Turbulent drag reduction by Lorentz force oscillation', *Physics of Fluids*, vol. 16, p. 35-38

Parker, K., and Sayers, A. T. 1999, 'The effect of longitudinal microstriations and their profiles on the drag of flat plates', *Proceedings of the Institution of Mechanical Engineers, Part C: Journal of Mechanical Engineering Science*, vol. 213, no. 8, pp. 775-785.

Panton, R. 1990, 'Effect of orifice geometry on Helmholtz resonator excitation by grazing flow', *AIAA Journal*, vol. 28, pp. 60-65.

Panton, R. L., and Miller, J. M. 1975, 'Excitation of a Helmholtz resonator by a turbulent boundary layer', *Journal of the Acoustical Society of America*, vol. 58, no. 4, pp. 800-806.

Peet, Y., Sagaut, P. and Charron, Y. 2008, 'Turbulent drag reduction using sinusoidal riblets with triangular cross-section', *38th AIAA Fluid Dynamics Conference and Exhibit, AIAA paper*, AIAA-2008-3745, Washington, USA.

Rathnasingham, R., and Breuer, K. 2003, 'Active control of turbulent boundary layers', *Journal of Fluid Mechanics*, vol. 495, pp. 209–233.

Rayleigh, B.J.W.S. 1896, *The theory of sound*, Macmillan, London.

Rebbeck, H., and Choi, K. S. 2006, 'A wind-tunnel experiment on real-time opposition control of turbulence', *Physics of Fluids*, vol. 18, no. 3, pp. 1-13.

Robinson, S. K. 1991, 'Coherent motions in the turbulent boundary layer', *Annual Review of Fluid Mechanics*, vol. 23, pp. 601–639.

Rockwell, D. and Naudascher, E. 1979 'Self-sustained oscillations of impinging free shear layers', *Annual Review of Fluid Mechanics*, vol. 11, no. 1, pp. 67-94.

Rogers, T. 1976, 'Effect of grazing flow on steady-state resistance of isolated square-edged orifices', *Final Report Hersh Acoustical Engineering*, Chatsworth, CA.

Ronneberger, D. 1980, 'The dynamics of shearing flow over a cavity—a visual study related to the acoustic impedance of small orifices', *Journal of Sound and Vibration*, vol. 71, no. 4, pp. 565-581.

Rossiter, J., and Britain, G. 1964, 'Wind tunnel experiments on the flow over rectangular cavities at subsonic and transonic speeds', Technical report 64037, RAE.

Rowley, C. W., Colonius, T., and Basu, A. J. 2002, 'On self-sustained oscillations in two-dimensional compressible flow over rectangular cavities', *Journal of Fluid Mechanics*, vol. 455, pp. 315-346.

Sarohia, V. 1975, 'Experimental and analytical investigation of oscillations in flows over cavities', *Ph.D. thesis*, California Institute of Technology.

Savill, A., and Mumford, J. 1988, 'Manipulation of turbulent boundary layers by outer-layer devices: Skin-friction and flow-visualization results', *Journal of Fluid Mechanics*, vol. 191, pp. 389-418

Schoppa, W., and Hussain, F. 2002, 'Coherent structure generation in near-wall turbulence', *Journal of Fluid Mechanics*, vol. 453, pp. 57-108.

Segawa, T., Mizunuma, H., Murakami, K., Li, F. C., and Yoshida, H. 2007, 'Turbulent drag reduction by means of alternating suction and blowing jets', *Fluid Dynamics Research*, vol. 39, no. 7, pp. 552-568.

Selamet, A., and Ji, Z. 2000, 'Circular asymmetric Helmholtz resonators', *Journal of the Acoustical Society of America*, vol. 107, no. 5, pp. 2360-2369

Selamet, A., Radavich, P., Dickey, N., and Novak, J. 1997, 'Circular concentric Helmholtz resonators', *Journal of the Acoustical Society of America*, vol. 101, no. 1, pp. 41-51.

Sipp, D 2012, 'Open-loop control of cavity oscillations with harmonic forcings', *Journal of Fluid Mechanics*, vol. 708, pp. 439-468.

Smith, C. R., and Metzler, S. P. 1983, 'The characteristics of low-speed streaks in the near-wall region of a turbulent boundary layer', *Journal of Fluid Mechanics*, vol. 129, pp. 27–54.

Stanislas, M., Jimenez, J. and Marusic, I. 2011 'Progress in Wall Turbulence: Understanding and Modeling', Springer.

Sun, X., Jing, X., Zhang, H., and Shi, Y. 2002 'Effect of grazing–bias flow interaction on acoustic impedance of perforated plates', *Journal of Sound and Vibration*, vol. 254, no. 3, pp. 557-573.

Tam, C. K., Ju, H., and Walker, B. E. 2008, 'Numerical simulation of a slit resonator in a grazing flow under acoustic excitation', *Journal of Sound and Vibration*, vol. 313, no. 3, pp. 449-471.

Tam, C. K. W., and Block, P. 1978, 'On the tones and pressure oscillations induced by flow over rectangular cavities', *Journal of Fluid Mechanics*, vol. 89, no. 2, pp. 373-399.

Tang, P. K., and Sirignano, W. A. 1973, 'Theory of a generalized Helmholtz resonator', *Journal of Sound and Vibration*, vol. 26, no. 2, pp. 247-262.

Tardu, S., Truong, T., and Tanguay, B. 1993, 'Bursting and structure of the turbulence in an internal flow manipulated by riblets', *Applied Scientific Research*, vol. 50, no. 3, pp. 189-213.

Toulorge, T., De Roeck, W., Denayer, H., and Desmet, W. 2012, 'Computational aeroacoustic characterization of different orifice geometries under grazing flow conditions'. *In Proceedings of the International Conference on Noise and Vibration Engineering (ISMA 2012)*, Leuven, Belgium, pp. 617-632.

Urzynicok, F. 2003, 'Separation control by flow-induced oscillations of a resonator', *Ph.D. Thesis*, University of Berlin.

Viotti, C., Quadrio, M., and Luchini, P. 2009, 'Streamwise oscillation of spanwise velocity at the wall of a channel for turbulent drag reduction', *Physics of Fluids*, vol. 21, pp. 1-9.

Von Helmholtz, H. 1896, *Theory of air oscillations in tubes with open ends*, Leipzig: W. Engelmann.

Virk, P. 1975, 'Drag reduction fundamentals'. *AIChE Journal*, vol. 21, pp. 625–656.

Walker, B., and Charwat, A. 1982, 'Correlation of the effects of grazing flow on the impedance of Helmholtz resonators', *Journal of the Acoustical Society of America*, vol. 72, pp. 550-555.

Walsh, M. J. 1983 'Riblets as a viscous drag reduction technique', *AIAA Journal*, vol. 21, no. 4, pp. 485-486.

Walsh, M., and Weinstein, L. 1978, 'Drag and heat transfer on surfaces with small longitudinal fins', *11th Fluid and Plasma Dynamics Conference,* Washington, USA.

Whalley, R. D. 2011, 'Turbulent boundary-layer control with DBD plasma actuators using spanwise travelling-wave technique', Ph.D. thesis, University of Nottingham.

Whalley, R. D., and Choi, K. S. 2011, 'Turbulent boundary-layer control with spanwise travelling waves', *13th European Turbulence Conference*, vol. 318, pp. 1-7.

Zhang, Q., and Bodony, D. J. 2013 'Impedance Prediction of Three-Dimensional Honeycomb Liners with Laminar/Turbulent Boundary Layers using DNS', *19th AIAA/CEAS Aeroacoustics Conference,* Berline, Germany.

Zhou, J., Adrian, R. J., Balachander, S. and Kendall, T. 1999 'Mechanisms for generating coherent packets of hairpin vortices in channel flow', *Journal of Fluid Mechanics*, vol. 387, pp. 353–396.

# Chapter 3

# Pressure field within the flow-excited Helmholtz resonator

This chapter has been submitted for publication as

Ghanadi, F., Arjomandi, M., Cazzolato, B. S., and Zander, A. C. 2013, 'Analysis of the pressure fluctuations induced by grazing flow over a Helmholtz resonator', submitted to *Jounral of Fluids and Structures*.

An understanding of the flow behaviour inside the flow-excited Helmholtz resonator is an essential requirement in the process of identifying the mechanisms for the manipulation of the flow through the resonator. This chapter presents a model for calculating the amplitude and frequency of the pressure fluctuations inside a Helmholtz resonator that is excited by a grazing turbulent boundary layer. The model is based on a momentum balance between the external driving pressure and the internal cavity pressure.

The results obtained from the developed model showed that certain geometries of the resonator are susceptible to self-excitation. The possibility of excitation occurring reduces with the reduction of the orifice width. Conversely, the resonator with a small neck is a better choice for a generation in large pressure fluctuations inside the resonator. The parametric study also showed that when the cavity volume increases, the energy exchange between the air flow inside the cavity and the grazing flow decreases, which reduces the possibility of excitation occurring. The potential benefit of the model presented is the capability to gain insight into the effects of the resonator characteristics on the flow behaviour in the vicinity of the resonator.

With further evidence for the flow behaviour within the resonator, the three dimensional flow within the resonator cavity and orifice is analysed in the following chapter.

# Statement of Authorship

| | |
|---|---|
| Title of Paper | Analysis of the pressure fluctuations induced by grazing flow over a Helmholtz resonator |
| Publication Status | O Published, O Accepted for Publication, ⦿ Submitted for Publication, O Publication style |
| Publication Details | Journal of Fluids and Structures |

## Author Contributions

By signing the Statement of Authorship, each author certifies that their stated contribution to the publication is accurate and that permission is granted for the publication to be included in the candidate's thesis.

| | | | |
|---|---|---|---|
| Name of Principal Author (Candidate) | Farzin Ghanadi | | |
| Contribution to the Paper | Performed analytical work, interpreted data, wrote manuscript and acted as corresponding author. | | |
| Signature | | Date | 19.09.14 |

| | | | |
|---|---|---|---|
| Name of Co-Author | Maziar Arjomandi | | |
| Contribution to the Paper | Supervised development of work, helped in data interpretation and manuscript evaluation. | | |
| Signature | | Date | 19.09.14 |

| | | | |
|---|---|---|---|
| Name of Co-Author | Benjamin Cazzolato | | |
| Contribution to the Paper | Supervised the research and contributed in academic discussion and manuscript review | | |
| Signature | | Date | 19/9/14. |

| | | | |
|---|---|---|---|
| Name of Co-Author | Anthony Zander | | |
| Contribution to the Paper | Supervised the research and contributed in academic discussion and manuscript review | | |
| Signature | | Date | 19/9/14 |

# Analysis of the pressure fluctuations induced by grazing flow over a Helmholtz resonator


## Abstract

Grazing flow over a Helmholtz resonator is a source of pressure fluctuations within its cavity. The flow excitation phenomenon is assumed to be associated with both external pressure fluctuations within the turbulent boundary layer of the grazing flow and the acoustic response of the resonator cavity. In this paper an analytical model has been developed to enable prediction of the amplitude and frequency of the pressure fluctuations within a flow-excited Helmholtz resonator. The model employs a simplified momentum balance equation between the interior and exterior of the resonator. The formulation combines the incompressible and fully developed flow within the resonator neck and compressible flow inside the cavity. For the purpose of validation, results obtained from the model have been compared with experimental values obtained by Ghanadi et al. (2014). It was demonstrated that the analysis provides an accurate representation of the phase and amplitude of the resonator pressure fluctuations. A sensitivity study has been undertaken by changing the main geometrical parameters of the resonator and characteristics of the incoming turbulent boundary layer. The results show that increasing the ratio of the orifice diameter to the momentum thickness from 1 to 40, results in a significant increase in the maximum pressure PSD within the resonator cavity, from 11dB to 32dB. Conversely, when the orifice length is greater than the momentum thickness, pressure fluctuations within the resonator cavity are reduced. It was also demonstrated that increasing Reynolds number amplifies the flow fluctuations within the resonators and if high pressure fluctuations are to be generated then the ratio of the depth to the diameter of the cavity must be in specific range. These investigations assist in identifying the optimal parameters to generate ideal pressure fluctuations within the Helmholtz resonator for the purpose of flow control in the vicinity of the resonator.


## Nomenclature

| | |
|---|---|
| $A$ | = cross-section area of the orifice (mm$^2$) |
| $c$ | = speed of sound (m/s) |
| $d$ | = orifice diameter (mm) |
| $D$ | = cavity diameter (mm) |
| $f$ | = frequency (Hz) |
| $F_{ext}$ | = force exerted on the fluid inside the orifice (N) |
| $f_n$ | = natural frequency of the resonator (Hz) |
| $f_r$ | = resonance frequency of the resonator (Hz) |

| | |
|---|---|
| $i$ | = imaginary component |
| $m$ | = resonator mode number |
| $n$ | = non-negative integers |
| $k$ | = wavenumber |
| $K_r$ | = spring constant |
| $L$ | = cavity depth (mm) |
| $l_e$ | = effective length of the orifice (mm) |
| $M_n$ | = mass of fluid (kg) |
| $M_c$ | = mass of fluid in the cavity (kg) |
| $Ma$ | = Mach number |
| $k_c$ | = compliance of the resonator |
| $p_m$ | = mean value pressure in the cavity (Pa) |
| $P_t$ | = excitation pressure (Pa) |
| $P_f$ | = resonator pressure fluctuations (Pa) |
| $Q$ | = volumetric flow rate ($m^3$/s) |
| $r$ | = radial coordinate |
| $R$ | = orifice radius (mm) |
| $R_d$ | = damping constant |
| $t$ | = time (s) |
| $U$ | = mean free stream velocity (m/s) |
| $u$ | = flow velocity (m/s) |
| $U_c$ | = convection velocity of the vortices (m/s) |
| $V_c$ | = cavity volume ($mm^3$) |
| $x$ | = indicates the x-direction (streamwise) (m) |
| $y$ | = indicated the y-direction (wall-normal direction) (m) |
| $z$ | = indicates the z-direction (spanwise direction) (m) |

**Symbols**

| | |
|---|---|
| $\Gamma$ | = circulation ($m^2$/s) |
| $\zeta$ | = damping ratio |
| $\omega$ | = angular frequency (rad/s) |
| $\Omega$ | = vorticity (1/s) |
| $\rho$ | = density of air (kg/$m^3$) |
| $\alpha$ | = phase lag between the vortical flow and acoustic volume flow (rad) |
| $\upsilon$ | = kinematic viscosity ($m^2$/s) |
| $\mu$ | = dynamic viscosity (kg/m.s) |
| $\delta$ | = boundary layer thickness (mm) |

**Superscripts**

| | |
|---|---|
| $()'$ | = denotes the fluctuating part of () |
| $()^*$ | = denotes non-dimensional of () |
| $\widehat{()}$ | = denotes Fourier transform of () |

**Prefixes**

| | |
|---|---|
| $J_0(x)$ | = Bessel function of the first kind |
| $\mathrm{ber}(x)$ | = real part of the Kelvin function |
| $\mathrm{bei}(x)$ | = imaginary part of the Kelvin function |

## 1. Introduction

Grazing flow past a Helmholtz resonator results in flow oscillation within the resonator cavity which is a common phenomenon in many applications such as an automobile with an open sunroof or window, aircraft landing gear and pipelines with closed side branches (Rossiter and Britain 1964; Ricot et al. 2001; Malmary and Carbonne 2001; Crouse et al. 2006). Under certain condition kinematic energy can efficiently transfer between the boundary layer and the flow field inside the flow-excited resonator. There is an immense body of literature about the acoustic impedance of the flow-excited resonator (Lee and Ih 2002; Kooijman et al. 2008) and flow fluctuations within a Helmholtz resonator excited by an external pressure field like loudspeakers (Hersh and Walker 1977; Cummings 1987; Tam et al. 2014; Zhang et al. 2014). However, the information accessible in publically available literature on an appropriate model which can predict response of a resonator excited by a turbulent boundary layer grazing flow is very scarce. It must be noted that in the literature, there are significant differences between a flow-excited Helmholtz resonator and the majority of the arrangements in a large number of the previous studies, like T-junction pipes (Martínez-Lera et al. 2009; Karlsson and Abom 2010), perforated plates with porous backing (Dickey and Selamet 1996; Kirby and Cummings 1998), deep and shallow cavities (Sarohia 1975; Colonius et al. 1999; Rowley et al. 2002; Sipp 2012). The important difference between the Helmholtz resonator and the configuration involving shallow cavities, $D/L \geq 1$, is in the direction of feedback disturbances. In the case of the flow-excited Helmholtz resonator the feedback disturbance of the resonator volume is perpendicular to the shear layer, whilst in the shallow cavities the feedback disturbances necessarily travel in a direction parallel to the plane of the shear layer. Moreover, the effects of the resonator orifice distinguish this configuration from other open or closed cavities. There is also a significant difference between the Helmholtz resonator and a deep cavity. The ratio of cavity volume to the orifice area in a Helmholtz resonator is greater than a deep cavity and thus it is possible to generate much lower frequencies as compared to those attainable with a deep cavity (Rockwell and Naudascher 1978; Gharib and Roshko 1987; Chaterllier et al. 2004; Faure et al. 2007; Lee et al. 2010). This paper presents a detailed model of a flow-excited Helmholtz resonator to investigate pressure fluctuations within and external to the cavity and the results provide an insight into the effects of the resonator geometry and incoming flow conditions on the flow behaviour within the resonator. The motivation of this work is explore the effects of self-excited Helmholtz resonators on turbulent boundary layer grazing flows for the purpose of drag reduction.

As illustrated in Figure 1, the Helmholtz resonator is formed by a cavity with a fixed volume of compressible fluid connected to the surrounding through a single small opening (Von Helmholtz 1896; Kinsler et al. 1999).

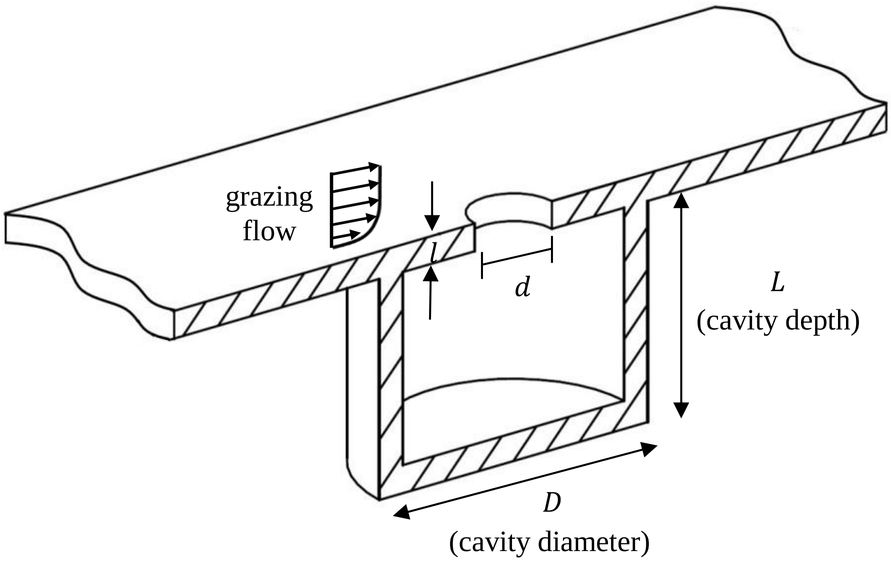


**Figure 1:** Schematic of a cross-section of the Helmholtz resonator

The behaviour of a Helmholtz resonator can be described by a second-order mass spring system or, equivalently, with a capacitor, resistor and an inductor (Alster 1972; Tang and Sirignano 1973; Ronneberger 1980; Walker and Charwat 1982). In this mass spring system, the mass comprises the mass of fluid in the orifice whereas compressibility of the fluid in the cavity acts as a spring. Using lumped element analysis, the following equation can be used for the displacement of the air in the orifice (Meissner 2002),

$$M_n \frac{d^2y}{dt^2} + R_d \frac{dy}{dt} + K_r y = F_{ext} \tag{1}$$

where $t$ is time, $y$ is the displacement of the flow within the orifice in cross-stream direction, $F_{ext}$ is the force exerted on the fluid inside the orifice, $M_n = \rho l_e A$ is effective mass of the air within the orifice and, $K_r = \rho c^2 A^2/V$ is the spring constant associated with the compressibility of the air inside the cavity. The cross-sectional area of the orifice is $A$, $\rho$ is the density of air, $c$ is the speed of the sound, $V$ is cavity volume and $l_e$ is the effective length of the orifice. The effective length is comprised of the actual length of the orifice as well as a small parcel of air immediately adjacent but external to the orifice that is also displaced. The net effect of this is that the effective length of the orifice is increased and thus leads to a reduction of the natural frequency of the resonator. The parameter $R_d$ in Equation (1) is the damping constant and represents a loss in the system which comes from viscosity of flow within the orifice and radiated pressure at the orifice. Assuming the air motion inside the resonator is harmonic, the displacement of the air in the orifice can be calculated as (Ma et al. 2009),

$$y(f) = \frac{F_{ext}(f)}{-4M_n\pi^2f^2 + 2if\pi R_d + K_r} \ . \tag{3}$$

where $f$ is the instability or driving frequency. As the frequency in Equation (3) approaches the resonance frequency of the Helmholtz resonator, $f_r = f_n\sqrt{1-\zeta^2}$ (where $f_n = \sqrt{K_r/4M_n\pi^2}$ is the natural frequency of the system), the dominator of this expression approaches zero and thus the amplitude of displacement becomes very large. It was observed that the resonance frequency could increase with an increase in free stream velocity (Anderson 1977; Peat et al. 2003). The reason of this behaviour is associated with either pressure changes within the cavity which changes the density, or mass reduction because the grazing flow is removing mass phase-locked to the mass in the orifice. However, when the length dimension is more than 1/16 of the wavelength of sound the aforementioned formula is not valid, thus a more accurate expression for the calculation of the resonance frequency of a cylindrical Helmholtz resonator was developed by Panton and Miller (1975) and Howard et al. (2000) as

$$f_r = \frac{c}{2\pi}\sqrt{\frac{S}{l_eV_c + 0.33L^2\,S}} \ . \tag{4}$$

where c is the speed of sound, $L$ is the cavity depth, $S$ the cross-section area of the orifice, $l_e$ is the effective length of the orifice and $V_c$ is the cavity volume. In this paper Equation (4) has been used to calculate the resonance frequency. When the frequency of flow fluctuations over the orifice is near the resonance frequency of the resonator, it is excited (Elder et al. 1982; Khosropour and Millet 1990; Kook 1997). Depending on the losses, a small external pressure fluctuation can produce a relatively large magnitude velocity fluctuation within the orifice, which is accompanied by a large pressure fluctuation inside the cavity. When the wall boundary layer of the grazing flow reaches the upstream edge of the resonator orifice, different patterns can occur for propagation of the shear layer over the orifice which is related to the geometry of the orifice and incoming flow conditions (Baumeister and Rice 1975;

Panton 1990; Sun et al. 2002). In the literature, different types of shear layer propagation over the orifice have been suggested, for example; vortex sheet, discrete vortices and distributed vortices (Bilanin and Covert 1973; Howe 1981; Toulorge et al. 2012; Dai et al. 2012; De Jong et al. 2012). Interaction of the shear layer with the downstream edge of the orifice generates an acoustic pulse which propagates back to the incoming flow and produces a series of periodically shed vortices, which is a non-linear saturation mechanism with a limit cycle and finite amplitude. The amplitude of the cycle depends strongly on the shape of the upstream edge of the orifice such that for sharp thin edges, the ratio of acoustic pulsation velocity to the free stream velocity within the shear layer is less than 0.1, whilst for rounded thick edges the ratio is more than 0.5 (Bruggeman 1991; Dequand 2003; Tonon 2011; Kooijmana et al. 2008). When the Strouhal number of the vortices, $\mathrm{St} = fd/U_c$, is of order of unity the maximum of pulsation amplitude occurs. Nelson et al. (1993) and Kook (1997) demonstrated that the circulation strength of the vortices at the upstream edge is only a function of the free stream flow velocity, and the net circulation is related to the orifice geometry and the convection velocity of the discrete vortices, $\mathrm{d}\Gamma_{\mathrm{net}} = U_\infty^2 d/2U_c$, where d is the orifice diameter and $\mathrm{U_c}$ is the convection velocity of the vortices.

Prediction of the resonator pressure oscillations has been extensively studied both experimentally and analytically. Implementing vortex sound theory, the hydrodynamic force of the vortex shedding was analysed by using two forward and backward functions which illustrate oscillatory flow in the orifice and its effect (Kook et al. 2002; Mast and Pierce 1995). It was suggested that grazing flow over the orifice is a superposition of an aerodynamic and an acoustic flow and each of them can be expressed by a gain function of a feedback loop. The analysis of this feedback loop provides the peak amplitude and frequency of the pressure oscillations. The Helmholtz resonator has also been used for flow separation control in two different test cases of a diffuser and a wing (Urzynicok and Fernholz 2002), where it was observed that the vortices ejected from the orifice can shift the momentum in the near-wall region, and therefore reattach the downstream flow.

More recent research has seen numerical investigations of flow-excited Helmholtz resonators. For example Inagaki et al. (2002) derived equations to numerically predict the flow oscillations over a Helmholtz resonator at low Mach number. They predicted the frequency of pressure fluctuations within the flow over a resonator orifice with high aspect ratio at low Mach number using compressible Navier-Stokes equations. It was concluded that the pressure fluctuations have a frequency very close to the resonance frequency of resonator over a wide range of flow velocities. Mallick et al. (2003) later applied a modified lattice–Boltzmann equation to calculate the pressure spectrum within the grazing flow over a self-excited Helmholtz resonator. Using a full turbulent model they demonstrated that to achieve a good match of their results with experimental work of Nelson et al. (1981) some of the model parameters required scaling. For example if the velocity of the grazing flow is multiplied by 0.7, the predicted amplitude of the pressure fluctuations inside the cavity is very close to the experimental data. The justification for reason of this scaling was that the effects of the boundary layer thickness alter the convection velocity of the vortex within the shear layer as it passes over the orifice. A recent experimental attempt to explore the flow characteristics in and outside the resonator has also been carried out by Ma et al. (2009), who tested a self-excited Helmholtz resonator with various free stream velocities. They concluded that the magnitude of the external force induced by the grazing flow has almost constant value in a wide range of boundary layer thicknesses. The aforementioned studies of the flow-excited Helmholtz resonators are by no means exhaustive, they merely provide a flavour of the vast areas of research in this field.

The objective of this paper is to derive an analytical model of flow over a Helmholtz resonator. The sensitivity of the turbulent boundary layer to the resonator geometry is also investigated. In the first step of the derivation of the analytical model, a volume flow rate and an axial flow velocity inside the orifice using a fully developed pipe flow with known pressure gradient was calculated. Then using a simplified Navier-Stokes equation a relationship between the pressure inside the cavity and the pressure fluctuations within the turbulent boundary layer was derived. The effects of turbulence intensity, turbulent boundary layer thickness and free stream velocity were analysed as well as the influence of resonator geometry. The remainder of the paper is organized as follows. The equations relating to the pressure fluctuations are described in §2. In §3 results of the proposed model are compared with previously published data to validate the theory, followed by a discussion of the effects of flow conditions and geometry of the resonator on pressure fields. In the last section the conclusions and a summary of this study are presented.

## 2. Theoretical analysis

Flow characteristics within an orifice with a given pressure gradient can be modelled by a one-dimensional unsteady solution (Rathnasingham and Breuer 1997). It was concluded that an unsteady cavity pressure developed an unsteady orifice flow in the direction perpendicular to the grazing flow such that the velocity of the grazing flow could be modelled using the unsteady Bernoulli equation for inviscid flow in streamline coordinates. Kook (1997) and Ma et al. (2009), also using the Euler momentum equation, developed an analytical model to calculate the pressure fluctuations within the resonator. However, their model is not appropriate for resonators with long orifices because the viscid interaction of the shear layer with cavity flow is ignored. Another approach has been implemented by Crook et al. (1999), who investigated a quasi-steady Poiseuille equation for modelling flow in the orifice of a synthetic jet. They were able to predict the magnitude of the maximum flow velocity over the orifice and concluded that viscous effects associated with the small orifice size have an important role when calculating the flow behaviour through the orifice. In this paper, flow within the orifice was modelled in cylindrical coordinates and it was assumed that incompressible fully-developed flow exists within the neck. Thus the momentum equation can be written as

$$\frac{\partial u_y}{\partial t} = -\frac{p_{t-}p_f}{l_e} + \frac{\nu}{r}\frac{\partial u_y}{\partial r} + \nu\frac{\partial^2 u_y}{\partial r^2}, \tag{5}$$

where $u_y$ is the velocity component inside the orifice which is perpendicular to the grazing flow , $r$ is radial coordinate, $p_t$ is the pressure within the grazing flow, $p_f$ is the pressure of the cavity flow, which is comprised of the force response of vortex shedding over the orifice, and the incoming and outgoing acoustic waves, and $\nu$ is the kinematic viscosity. The pressure gradient through the orifice is $(p_f - p_t)/l_e = K_0 e^{i\omega t}$, where $\omega$ is the frequency of the pressure fluctuation and $K_0$ is a constant, hence the Navier-Stokes equation can be modified to

$$\frac{\partial^2 u_y}{\partial r^2} + \frac{1}{r}\frac{\partial u_y}{\partial r} - \frac{1}{\nu}\frac{\partial u_y}{\partial t} = -K_0 e^{i\omega t} \ . \tag{6}$$

Assuming the velocity to be harmonic, $u_y = U_y e^{i\omega t}$, therefore the amplitude of that in the orifice ($U_y$) can be solved as (Womersley 1955)

$$U_y = \frac{K_0}{i\rho\omega}\left\{1 - \frac{J_0\left(ir\sqrt{\frac{\omega}{\nu}i}\right)}{J_0\left(iR\sqrt{\frac{\omega}{\nu}i}\right)}\right\} , \tag{7}$$

where $R$ is orifice radius and $J_0$ is the Bessel function of order zero and $i^2 = -1$. Bessel functions with complex components can be defined as Kelvin functions,

$$J_0(i\sqrt{i}x) = \mathrm{ber}(x) + i\mathrm{bei}(x), \tag{8}$$

where $\mathrm{ber}(x)$ and $\mathrm{bei}(x)$ are the real and imaginary parts respectively of the Kelvin function and can be expressed as,

$$\mathrm{ber}(x) = \sum_{n=0}^{\infty} \left(\frac{x}{2}\right)^{4n} \frac{(-1)^n}{(2n!)^2} \ , \qquad \mathrm{bei}(x) = \sum_{n=0}^{\infty} \left(\frac{x}{2}\right)^{4n+2} \frac{(-1)^n}{((2n+1)!)^2} \ . \tag{9}$$

Therefore the instantaneous unsteady flow velocity can be expressed as

$$u_y(r,t) = -\frac{K_0 i}{\rho\omega}\left[1 - \frac{\mathrm{ber}\left(\sqrt{\frac{R^2\omega}{\nu}}\frac{r}{R}\right) + i\mathrm{bei}\left(\sqrt{\frac{R^2\omega}{\nu}}\frac{r}{R}\right)}{\mathrm{ber}\left(\sqrt{\frac{R^2\omega}{\nu}}\right) + i\mathrm{bei}\left(\sqrt{\frac{R^2\omega}{\nu}}\right)}\right] e^{i\omega t} \ . \tag{10}$$

On the other hand the volumetric flow rate, $Q = 2\pi \int_0^R u_y r dr$, can be estimated via the velocity inside the orifice and therefore

$$Q = \frac{\pi i}{8\rho\omega}\int_0^R \left[1 - \frac{\mathrm{ber}\left(\sqrt{\frac{R^2\omega}{\nu}}\frac{r}{R}\right) + i\mathrm{bei}\left(\sqrt{\frac{R^2\omega}{\nu}}\frac{r}{R}\right)}{\mathrm{ber}\left(\sqrt{\frac{R^2\omega}{\nu}}\right) + i\mathrm{bei}\left(\sqrt{\frac{R^2\omega}{\nu}}\right)}\right] r dr \ . \tag{11}$$

The pressure oscillations within and outside the resonator cause pressure fluctuations within the orifice, and this pressure difference between the pressure inside the boundary layer and the Helmholtz resonator cavity generates an excitation in the grazing flow. If integrating the momentum balance through the orifice across the orifice cross section yields

$$\int_0^R \frac{\partial u_y}{\partial t} 2\pi r dr = -\int_0^R \frac{\partial p}{\partial y}\ 2\pi r\, dr + \int_0^R \left(\frac{\nu}{r}\frac{\partial u_y}{\partial r} + \nu\frac{\partial^2 u_y}{\partial r^2}\right) 2\pi r dr \ , \tag{12}$$

where $y$ is perpendicular to grazing flow and $p$ is flow pressure. The left hand side of Equation (12) is the time derivative of the volumetric flow rate and the second term on the right hand side is the wall shear stress. In order to solve the pressure gradient given by the first right hand side term in Equation (12), the thermodynamic behaviour of flow inside the resonator must be defined. As mentioned previously, viscous dissipation is not negligible in the present model, however it has been assumed that heat exchange between the grazing flow and the air cavity is negligible. Hence the relationship between the fluctuating components of pressure and density and their mean values can be related using the equation of state for an ideal gas. Therefore, the volumetric flow rate which exits the cavity at any specific instant can be calculated by

$$Q = \frac{1}{\rho}\frac{dM_c}{dt} = -\frac{V_c}{p_m}\frac{dp_f}{dt}\,, \tag{13}$$

where $M_c$ is the mass of fluid in the cavity, $V_c$ is cavity volume and $p_m$ is the mean value pressure in the cavity. The minus sign is due to the flow direction. In Equation (13) it was assumed that the density fluctuation is small relative to the equilibrium density. Hence the simplified momentum equation can be written as

$$-\frac{V_c}{p_m}\frac{d^2p_f}{dt^2} = -\frac{p_t - p_f}{l_e}\pi R^2 + \frac{\mu V_c}{p_m}\frac{\int_0^R\left[1 - \frac{\mathrm{ber}\left(\sqrt{\frac{R^2\omega}{\nu}}\frac{r}{R}\right) + i\mathrm{bei}\left(\sqrt{\frac{R^2\omega}{\nu}}\frac{r}{R}\right)}{\mathrm{ber}\left(\sqrt{\frac{R^2\omega}{\nu}}\right) + i\mathrm{bei}\left(\sqrt{\frac{R^2\omega}{\nu}}\right)}\right]rdr}{\left[\frac{\mathrm{ber}'\left(\sqrt{\frac{R^2\omega}{\nu}}\frac{r}{R}\right) + i\mathrm{bei}'\left(\sqrt{\frac{R^2\omega}{\nu}}\frac{r}{R}\right)}{\mathrm{ber}\left(\sqrt{\frac{R^2\omega}{\nu}}\right) + i\mathrm{bei}\left(\sqrt{\frac{R^2\omega}{\nu}}\right)}\right]}\frac{dp_f}{dt}\,, \tag{14}$$

where $\mu$ is air dynamic viscosity, $\mathrm{ber}'$ and $\mathrm{bei}'$ are derivatives of Kelvin functions and expressed by

$$\begin{aligned}\mathrm{ber}'(x) &= \sum_{n=0}^{\infty}\left(\frac{x}{2}\right)^{4n+3}\frac{(-1)^{n+1}}{\big((2n+1)!\,(2n+2)!\big)^2}\,,\\ \mathrm{bei}'(x) &= \sum_{n=0}^{\infty}\left(\frac{x}{2}\right)^{4n+1}\frac{(-1)^{n}}{((2n)!\,(2n+1)!)^2}\,.\end{aligned} \tag{15}$$

In order to solve Equation (14), the external pressure, $p_t$, is required. As illustrated in Figure 2, to calculate the pressure within the shear layer it is assumed that the grazing flow in the proposed control surface over the orifice is in Cartesian co-ordinate system.

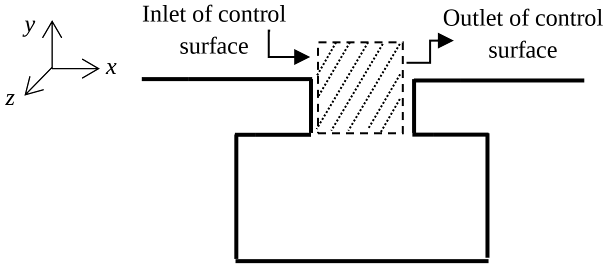


Figure 2: A schematic of control surface and co-ordinate system for analytical solution

The vortices which are shed over the orifice impose an external force on the air flow inside the resonator cavity. Therefore, the pressure fluctuations within the turbulent boundary layer over the orifice can be calculated by dividing this force by the orifice cross-sectional area. Kook et al. (2002) assumed that vorticity shedding occurs along a specific line from the leading edge to the downstream edge of the orifice and calculated the phasor of the external pressure as

$$\hat{p}_t = \rho U^2 \frac{U_c}{\pi d f}\, e^{-i\left(\frac{\pi d f}{U_c}\right)}, \tag{16}$$

Recall that Equation (14) was formulated based on the external pressure within the turbulent boundary layer which is $\hat{p}_t \exp(i2\pi f t)$. In the literature various correlations have been proposed to calculated the convection velocity of the vortices. For example, Nelson et al. (1981) by using flow visualisation observed that the vortex convection velocity is approximately half of the free stream velocity. Applying Laser Doppler anemometry showed that the convection velocity is less than 0.4 of the free stream velocity (Graf and Durgin 1993). It must be noted that the vortices within a thick turbulent boundary layer convect more slowly than those within a thin boundary layer, thus the convection velocity of the vortices is a function of the boundary layer thickness and the free stream velocity. Ma et al. (2009) stated that the convection velocity in a specific location within the turbulent boundary layer can be obtained by applying 1/7 power law velocity profile, $U_c = \frac{U}{2}\left(\frac{0.05\, d}{\delta}\right)^{1/7}$. However, using the boundary layer thickness is not convenient in the equation proposed by Ma et al. (2009) because this quantity cannot be determined accurately. Therefore other researchers (Kooijman et al. 2008; Nakiboglu et al. 2011) proposed the momentum thickness, $\theta$, as a measure for the boundary layer thickness to calculate the convention velocity,

$$U_c = \frac{4U}{10}\left(\frac{d}{\theta}\right)^{1/5} \tag{17}$$

In this study the boundary layer assumed to be turbulent and, hence associated correlations for boundary layer thickness are applied in this model. As a result, by combining Equations (14) & (16), the pressure fluctuations within the boundary layer and within the resonator cavity are calculated. In the following two sections the model verification and analysis of the effects of resonator geometry and grazing flow condition will be described.

## 3. Validation of the model

In order to validate the accuracy of the presented model, the results were compared with the experimental values obtained by Ghanadi et al. (2014). As presented in Table 1, for the validation purposes the resonators investigated in this paper were selected to be identical to those ones used in Ghanadi et al.'s (2014) experiment. In order to compare the resonance frequency of the resonators with the published data, the frequency associated with the peak value of the difference between the power spectral density (PSD) of the pressure oscillation inside the grazing flow, which generates the external unsteady force, and the pressure fluctuation within the cavity was evaluated. The PSD values have been obtained using a Hanning window with $2^7$ FFT points and a 50% overlap for averaging. As demonstrated in Figure 3 the calculated resonance frequency of HR2 is very close to the experimental data, less than 6% difference. As can be seen in Table 1 the calculated resonance frequency of each resonator is well matched with the experimental value.

Table1. Characteristics of the different resonators and the resonance frequency of each resonator measured by Ghanadi et al. (2014) and calculated through presented model. In all cases the cavity diameter is 25mm and cavity depth is 100mm.

| | Dimensions (mm) | | Resonance frequency, $f_r$ (Hz) | |
|---|---|---|---|---|
| Helmholtz resonator designation | $l$ | $d$ | Ghanadi et al (2014) | Present model |
| HR1 | 5 | 20 | 712 | 708 |
| HR2 | 5 | 5 | 398 | 418 |
| HR3 | 2 | 10 | 605 | 624 |
| HR4 | 15 | 10 | 550 | 578 |

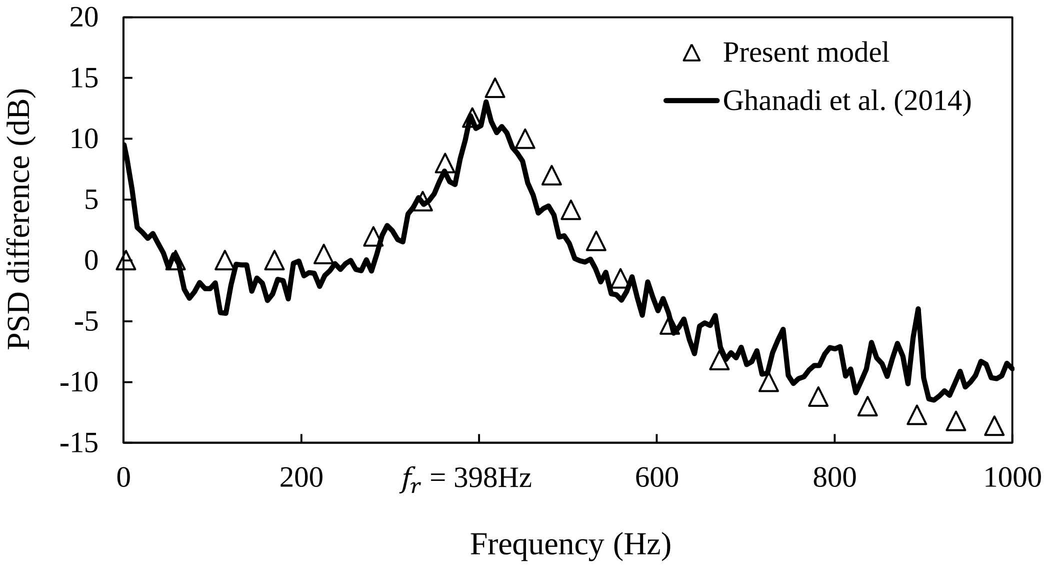


Figure 3: PSD difference between the pressure fluctuations inside HR2 and the instantaneous pressure within the grazing flow when $\mathrm{Re}_\theta = 2770$.

The pressure PSD difference for other resonators have also been calculated and compared with the experimental values. As shown in Figure 4, near the resonance frequency, $0.5 < f/f_r < 1.5$, amplitude of the calculated pressure response for each resonator are very close to the experimental data. However, there is a mismatch between the results when the $f/f_r < 0.3$ which is due to radiation impedance of the resonator into the coupled channel which was not considered in the developed model. The qualitative and quantitative agreement between the developed model and experimental data are favourable and thus this model has sufficient accuracy to be used to study the sensitivity of the flow behaviour for various conditions.

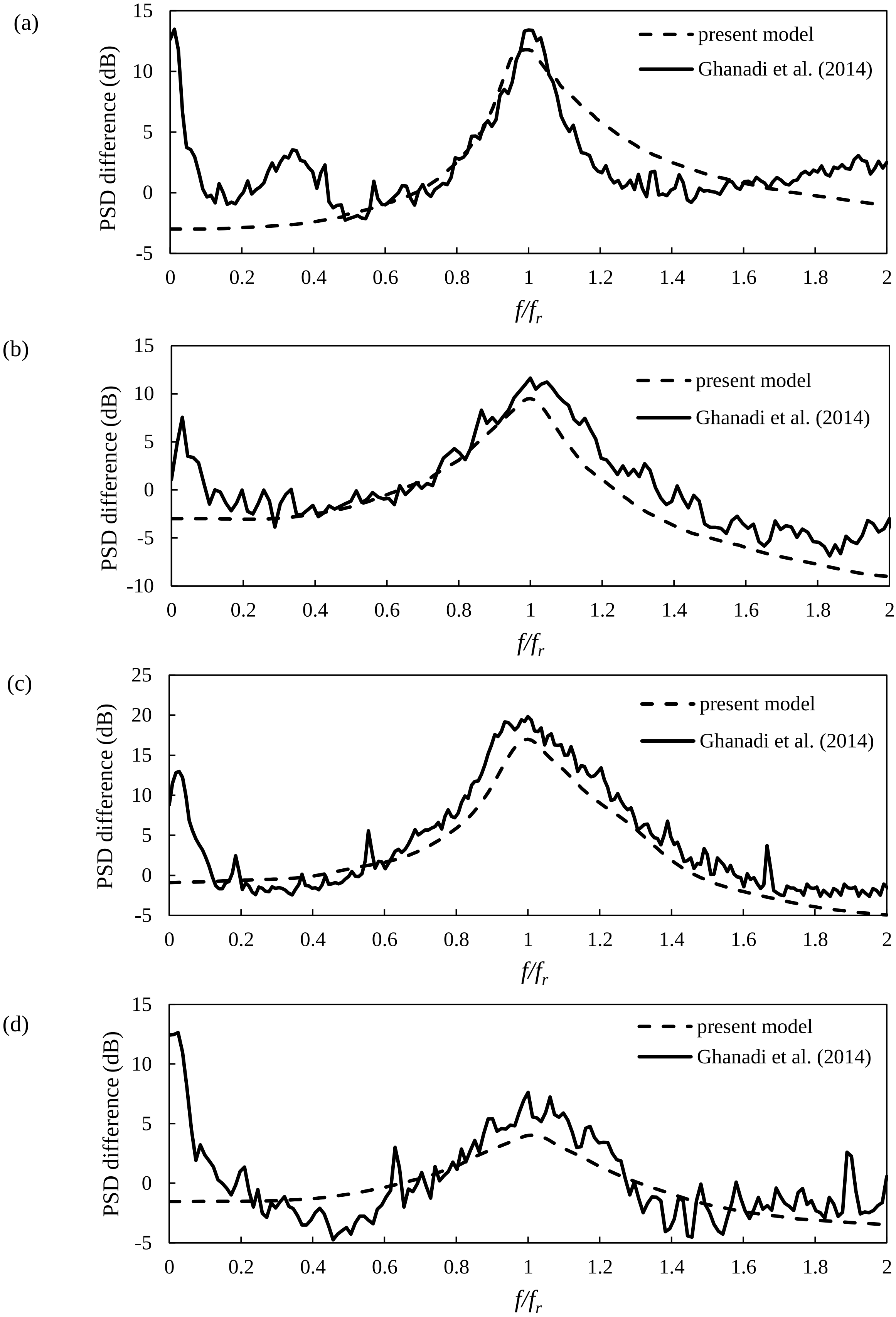


Figure 4: The PSD difference of the pressure fluctuations within the incoming flow and inside the resonator cavity at $Re_{\theta}$ =1680: (a) HR1, (b) HR2, (c) HR3 and (d) HR4.

## 4. Discussion

By use of the developed analytical method described in the present study, the effects of changing the characteristics of the Helmholtz resonator on the flow behaviour within the cavity and over the orifice have been investigated. It must be noted that, changing the incoming flow conditions also affects flow pulsation in the vicinity of the resonator orifice, thus the parametric study has been conducted for different Reynolds numbers.

### 4.1 Effects of the orifice geometry

Considering firstly the influence of the orifice diameter, a wide range of the diameter values, $6 < d/\theta < 60$, have been investigated when the orifice length and cavity dimensions were fixed. As shown in Figure 5, the amplitude of the pressure fluctuations inside the resonator cavity is proportional to the orifice diameter, so that by increasing the cross-sectional area of the orifice the maximum value of the pressure within the cavity around the resonance frequency of the resonator is increased. As illustrated in the figure, increasing the Reynolds number results in amplification of the pressure fluctuations inside the resonator. This increase is not linear for $\mathrm{Re}_\theta < 2700$, such that when the diameter is increased from $d/\theta$ = 0.1 to 60 the maximum value of PSD difference is increased by up to 20dB. Increasing the orifice area eventually changes the resonator to an open cavity, which is very sensitive to the incoming flow conditions, and thus the grazing flow significantly affects the air flow within the cavity. However, the results show that when the orifice diameter is decreased to the thickness of the inner boundary layer, $d/\theta < 0.7$, the maximum value of the PSD difference of the instantaneous pressure is reduced up to 9dB

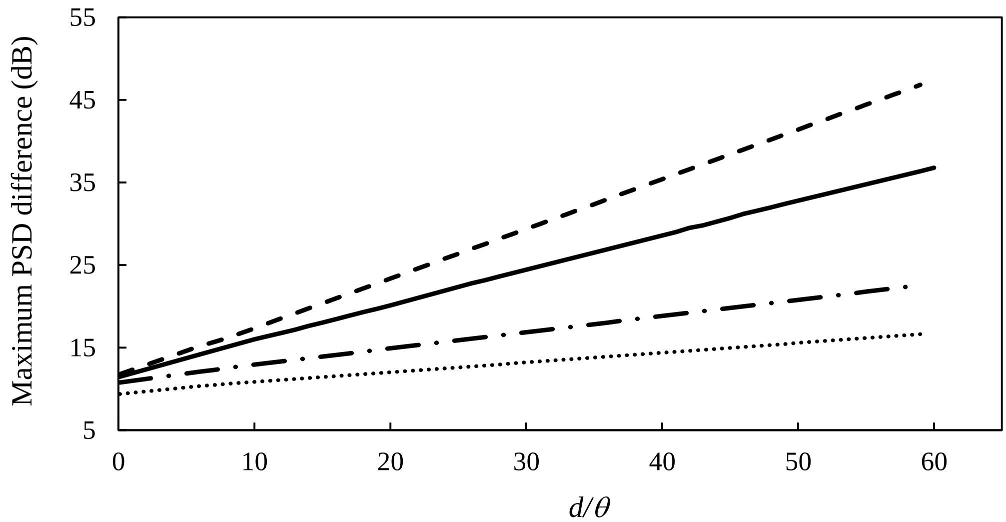


Figure 5: The maximum PSD difference of the pressure fluctuation within incoming turbulent boundary layer and inside the resonator with different orifice diameter, when $l/L$ = 0.05, $L/D$ = 4; (········) $\mathrm{Re}_\theta$= 1000, (— · —) $\mathrm{Re}_\theta$= 1700, (———) $\mathrm{Re}_\theta$= 2000 and (— — —) $\mathrm{Re}_\theta$= 2800.

The effects of varying the orifice length on the pressure fluctuations within the Helmholtz resonator have also been analysed when the cavity dimensions and the orifice diameter were fixed. As can be seen in Figure 6, the resonator with a long orifice length, $l/\theta > 14$, has the lowest peak value in the pressure amplitude inside the cavity, less than 8dB. It is due to higher viscous losses within the long neck, which results in the significant reduction in the pressure fluctuations within the resonator cavity. However, when the orifice length is close to the thickness of the inner layer of the turbulent boundary layer, the pressure fluctuations are increased by up to 32dB at $Re_{\theta}$= 2800. The results also show that increasing Reynolds number has significant effects on the pressure fluctuations only when $l/\theta < 7$.

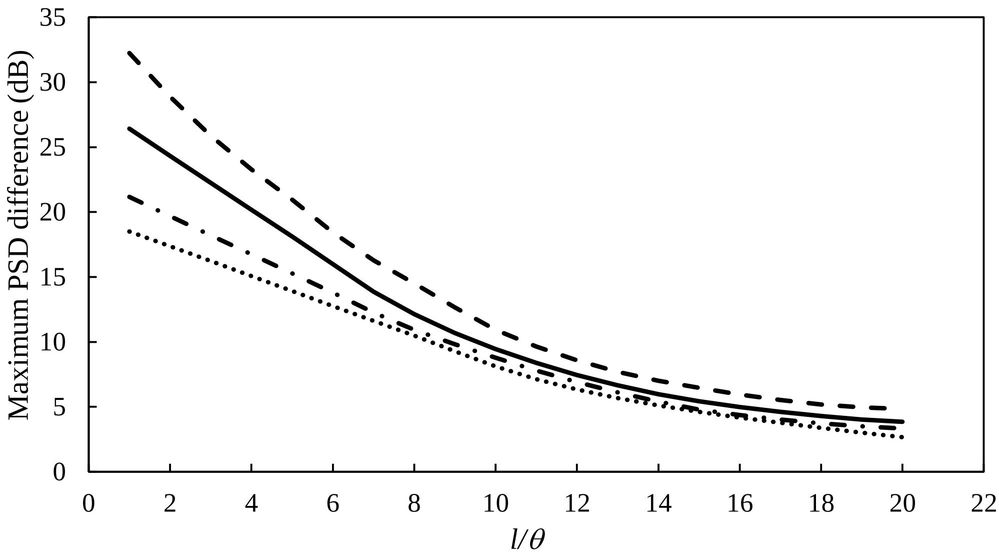


Figure 6: The effects of the orifice length on the amplitude of the PSD difference of the pressure fluctuation within incoming turbulent boundary layer and inside the resonator cavity, when $d/D$ = 0.4, $L/D$ = 4; (·······) $Re_{\theta}$= 1000, (— · —) $Re_{\theta}$= 1700, (——) $Re_{\theta}$= 2000 and (— — —) $Re_{\theta}$= 2800.

### 4.2 Effects of the cavity geometry

The cavity dimensions, as well as the orifice geometry, can affect the pressure fluctuations inside the resonator. In most previous studies the volume of the cavity was considered as a single parameter. However, in the present paper the diameter and length of the cavity were investigated separately to understand the effects of each on the excitation conditions. It can be seen from the results presented in Figure 7, for a given orifice geometry flow suction in the cavity amplifies with increasing the cavity diameter such that for $D \approx d$ there is a dramatic pressure oscillation within the cavity. The reason of this flow behaviour is due to this fact that when the cavity diameter is near to the orifice diameter the Helmholtz resonator changes to an open cavity in which the grazing flow can affect the flow behaviour significantly. Additionally, as shown in the figure, as the Reynolds number increases from $\mathrm{Re}_\theta$= 1000 to $\mathrm{Re}_\theta$= 2800 the energy exchange between the grazing flow and the cavity flow is increased. It must be also noted that changing the cavity diameter in the low Reynolds number $\mathrm{Re}_\theta < 2000$ has a more pronounced effects on the pressure fluctuations such that with increasing the cavity diameter from $D/d$ = 1 to 5, at $\mathrm{Re}_\theta$= 1000, the maximum PSD difference is reduced by up to 5dB.

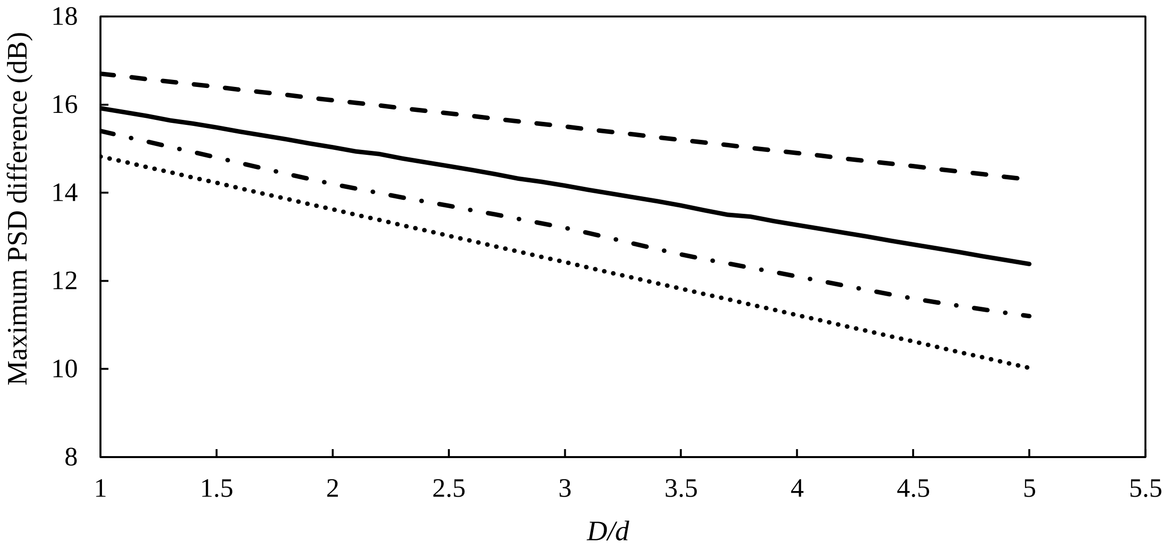


Figure 7: Effects of cavity diameter on the PSD pressure difference when $l/d$ = 2, $l/L$ = 0.1; (········) $\mathrm{Re}_\theta$= 1000, (– · –) $\mathrm{Re}_\theta$= 1700, (——) $\mathrm{Re}_\theta$= 2000 and (– – –) $\mathrm{Re}_\theta$= 2800.

The sensitivity of the pressure fluctuations to the cavity depth also examined when all other parameters of the resonator remained fixed. As shown in Figure 8, when the aspect ratio of the cavity is reduced from $L/D$ = 3.5 to 0.2, the maximum pressure fluctuations decrease by up to 9dB. However, the pressure oscillations inside the resonator have the highest peak values over a specific range of cavity depth, 3.5< $L/D$ < 4.5. Therefore, it can be mentioned that the grazing flow cannot significantly change the characteristics of the flow within the resonator when $L/D > 5$, or $L/D < 1$. The results also demonstrate that increasing the Reynolds number amplifies the pressure fluctuations within the resonator for the all cavity lengths.

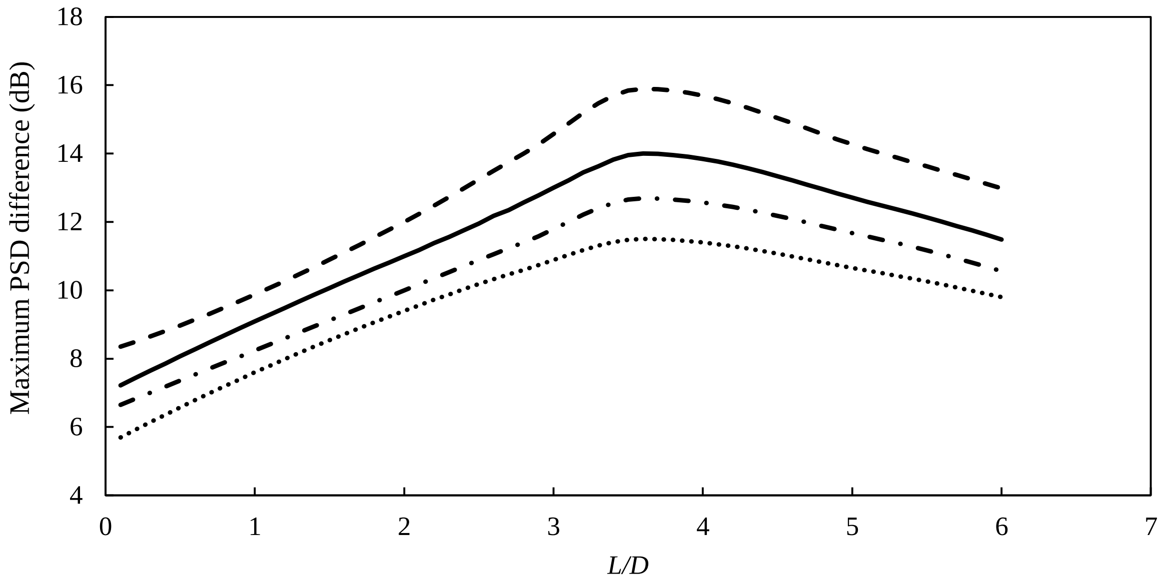


Figure 8: PSD difference between pressure fluctuations internal and external to the Helmholtz resonator for various cavity lengths when $l/d$ = 0.5, $d/D$ = 0.4; (········) $Re_\theta$= 1000, (— · — ) $Re_\theta$= 1700, (——— ) $Re_\theta$= 2000 and (— — —) $Re_\theta$= 2800.

## 5. Summary and conclusion

The excitation of Helmholtz resonators arising from the interaction of a turbulent boundary layer occurs in many practical applications, and can be detrimental to a system's function if the pressure fluctuations are sufficiently high. This study describes the flow behaviour within a Helmholtz resonator which is excited by a shear layer over its orifice. To this end, this paper presents a method for predicting the pressure inside a Helmholtz resonator with a grazing flow as a function of the resonator geometry. A theoretical model based on combination of the vortex sheet and discrete vortex models was developed and both the inflow and outflow were considered in the system. The results prove that the derived theory successfully captures the coupled dynamics arising from the interaction of the turbulent boundary layer with the Helmholtz resonator. For the validation purposes, the results were compared to the data available in the literature and it was shown that the model can accurately predict the amplitude of pressure fluctuations inside the cavity. Moreover, it was observed that the maximum pressure fluctuation occurred at a frequency close to the resonance frequency of the resonator which means that the resonator was self-excited.

The developed model showed that the pressure amplitudes inside the resonator are strongly affected by resonator shape and therefore certain geometries are susceptible to self-excitation. A sensitivity study on the orifice geometry showed that the possibility of excitation occurring reduces with the reduction of the orifice diameter. However, when the cross section area of the orifice increases, the resonator behaves similar to an open cavity and grazing flow induces high pressure fluctuations. The parametric study of the resonator also showed that when the orifice length equals the inner layer of the turbulent boundary layer, $l \approx 0.1\theta$, the pressure fluctuations are significantly increased. It was hypothesised that, for the resonator with a short orifice, the flow velocity is reduced, which results in a reduction of the convection velocity of vortices and thereby increasing the chance of their penetration into the cavity. However, resonators with a long orifice, $l/\theta > 10$, experienced reduced pressure fluctuations within the resonator which is due to longer skin friction or increased velocity inside the orifice. It was also concluded that to generate significant PSD pressure differences, the cavity diameter must be equal to the orifice diameter and the energy exchange between the air flow inside the cavity and the grazing flow decreases when $L/D > 5$, which reduces the likelihood of excitation occurring. It must be also noted that increasing the Reynolds number amplifies the magnitude of the instantaneous pressure within the resonators.

A considerable benefit of the model presented, besides its predictive capacity, was the capability to gain insight into the effects of the resonator characteristics on the resulting dynamics. The summary of the findings may also apply for passive synthetic jets to understand the flow behaviour within theses kind of actuators. This is very useful to find the best mechanism to create a strong pulsejet without any power input for the purpose of boundary layer control.

## References


Alster, M 1972, 'Improved calculation of resonant frequencies of Helmholtz resonators', *Journal of Sound and Vibration*, vol. 24, no. 1, pp. 63-85.

Anderson, J 1977, 'The effect of an air flow on a single side branch Helmholtz resonator in a circular duct', *Journal of Sound and Vibration*, vol. 52, no. 3, pp. 423-431.

Baumeister, KJ & Rice, EJ 1975, 'Visual study of the effect of grazing flow on the oscillatory flow in a resonator orifice', *National Aeronautics and Space Administration report (NASA TM-X3288),* Washington, USA.

Bilanin, AJ & Covert, EE 1973, 'Estimation of possible excitation frequencies for shallow rectangular cavities', *AIAA Journal*, vol. 11, no. 3, pp. 347-351.

Bruggeman, J, Hirschberg, A, Van Dongen, M, Wijnands, A & Gorter, J 1991, 'Self-sustained aero-acoustic pulsations in gas transport systems: Experimental study of the influence of closed side branches', *Journal of Sound and Vibration*, vol. 150, no. 3, pp. 371-393.

Chatellier, L, Laumonier, J & Gervais, Y 2004, 'Theoretical and experimental investigations of low Mach number turbulent cavity flows', *Experiments in Fluids*, vol. 36, no. 5, pp. 728-740.

Colonius, T, Basu, AJ & Rowley, CW 1999, 'Numerical investigation of the flow past a cavity', *AIAA Paper 99-1912*, 5th AIAA/CEAS Aeroacoustics Conference, Washington, USA.

Crook, A, Sadri, AM & Wood, NJ 1999, 'The development and implementation of synthetic jets for the control of separated flow', *AIAA1999-0449*, 37th Aerospace Sciences Meeting and Exhibit, Reno, USA.

Crouse, B, Senthooran, S, Freed, D, Balasubramanian, G, Gleason, M, Puskarz, M, Lew, P & Mongeau, L 2006, 'Experimental and numerical investigation of a flow induced cavity resonance with application to automobile buffeting', *AIAA paper 2006-2494*, 27th AIAA Aeroacoustics Conference, Massachusetts, USA.

Cummings, A 1987, 'The response of a resonator under a turbulent boundary layer to a high amplitude non-harmonic sound field', *Journal of Sound and Vibration*, vol. 115, no. 2, pp. 321-328.

Dai, X, Jing, X & Sun, X 2012 'Discrete vortex model of a Helmholtz resonator subjected to high-intensity sound and grazing flow', *Journal of the Acoustical Society of America*, vol. 132, no 5, pp. 2988-2996.

De Jong, A, Bijl, H, Hazir, A & Wiedemann, J 2012, 'Aeroacoustic simulation of slender partially covered cavities using a Lattice Boltzmann Method', *Journal of Sound and Vibration*, vol. 332, no 7, pp. 1687-1703.

Dequand, S, Luo, X, Willems, J & Hirschberg, A 2003, 'Helmholtz-like resonator self-sustained oscillations, Part 1: Acoustical measurements and analytical models', *AIAA Journal*, vol. 41, no. 3, pp. 408-415.

Dickey, N & Selamet, A 1996 'Helmholtz resonators: One-dimensional limit for small cavity length-to-diameter ratios', *Journal of sound and vibration*, vol. 195, no. 3, pp. 512-517.

Elder, S, Farabee, T & DeMetz, F 1982, 'Mechanisms of flow-excited cavity tones at low Mach number', *Journal of the Acoustical Society of America*, vol. 72, p. 532-549.

Faure, TM, Adrianos, P, Lusseyran, F & Pastur, L 2007, 'Visualizations of the flow inside an open cavity at medium range Reynolds numbers', *Experiments in Fluids*, vol. 42, no. 2, pp. 169-184.

Gharib, M & Roshko, A 1987, 'The effect of flow oscillations on cavity drag', *Journal of Fluid Mechanics*, vol. 177, pp. 501-530.

Graf, HR & Durgin, WW 1993, 'Measurement of the nonsteady flow field in the opening of a resonating cavity excited by grazing flow', *Journal of Fluids and Structures*, vol. 7, no. 4, pp. 387-400.

Hersh, AS & Walker, B 1977, 'Fluid mechanical model of the Helmholtz resonator', *National Aeronautics and Space Administratio report*, Washington, USA.

Howard, CQ, Cazzolato, BS & Hansen, CH 2000, 'Exhaust stack silencer design using finite element analysis', *Noise Control Engineering Journal*, vol. 48, no. 4, pp.113-120.

Howard, CQ & Craig, RA 2012, 'Acoustic performance of three orifice geometries of side-branches in a duct with flowing gas', *Proceedings of Acoustics 2012*, Western Australia, Australia, 21-23 November, Paper 80.

Howe, M 1981, 'Influence of mean shear on unsteady aperture flow, with application to acoustical diffraction and self-sustained cavity oscillations', *Journal of Fluid Mechanics*, vol. 109, pp. 125-146.

Inagaki, M, Murata, O, Kondoh, T & Abe, K 2002, 'Numerical prediction of fluid-resonant oscillation at low Mach number', *AIAA Journal*, vol. 40, no. 9, pp. 1823-1829.

Karlsson, M & Åbom, M 2010, 'Aeroacoustics of T-junctions: An experimental investigation', *Journal of Sound and Vibration*, vol. 329, no. 10, pp. 1793-1808.

Khosropour, R & Millet, P 1990, 'Excitation of a Helmholtz resonator by an air jet', *Journal of the Acoustical Society of America*, vol. 88, no. 3, pp.1211-1221.

Kinsler, LE, Frey, AR, Coppens, AB & Sanders, JV 1999, *Fundamentals of Acoustics, 4th Edition, pp. 560. ISBN 0-471-84789-5. Wiley-VCH, December 1999.*

Kook, H 1997, 'Prediction and control of the interior pressure fluctuations in a flow-excited Helmholtz resonator', *Ph.D. Thesis*, Purdue University.

Kook, H, Mongeau, L & Franchek, M 2002, 'Active control of pressure fluctuations due to flow over Helmholtz resonators', *Journal of Sound and Vibration*, vol. 255, no. 1, pp. 61-76.

Kooijmana, G , Hirschberga, A & Golliard, J 2008, 'Acoustical response of orifices under grazing flow: Effect of boundary layer profile and edge geometry', *Journal of Sound and Vibration*, vol. 315, no. 4, pp. 849–874.

Kirby, R & Cummings, A 1998, 'The impedance of perforated plates subjected to grazing gas flow and backed by porous media ', *Journal of Sound and Vibration*, vol. 217, no 4, pp. 619-636.

Kooijmana, G , Hirschberga, A & Golliard, J 2008, 'Acoustical response of orifices under grazing flow: Effect of boundary layer profile and edge geometry', *Journal of Sound and Vibration*, vol. 315, no. 4, pp. 849–874.

Lee, SB, Seena, A & Sung, HJ 2010, 'Self-sustained oscillations of turbulent flow in an open cavity', *Journal of Aircraft*, vol. 47, no. 3, pp. 820-834.

Lee, SH & Ih, JG 2003, 'Empirical model of the acoustic impedance of a circular orifice in grazing mean flow', *Journal of the Acoustical Society of America*, vol. 114, no. 1, pp. 98-113.

Ma, R, Slaboch, PE & Morris, SC 2009, 'Fluid mechanics of the flow-excited Helmholtz resonator', *Journal of Fluid Mechanics*, vol. 623, pp. 1-26.

Malmary, C & Carbonne, S 2001, 'Acoustic impedance measurement with grazing flow', A*IAA-2001-2193*, 7th AIAA/CEAS Aeroacoustics Conference, Maastricht, Netherlands.

Martinez-Lera, P, Schram, C, Föller, S, Kaess, R & Polifke, W 2009, 'Identification of the aeroacoustic response of a low Mach number flow through a T-joint', *Journal of the Acoustical Society of America*, vol. 126, no. 2, pp. 582-586.

Mallick, S, Shock, R & Yakhot, V 2003, 'Numerical simulation of the excitation of a Helmholtz resonator by a grazing flow', *Journal of the Acoustical Society of America*, vol. 114, pp. 1833-1840.

Mast, TD & Pierce, AD 1995, 'Describing-function theory for flow excitation of resonators', *Journal of the Acoustical Society of America*, vol. 97, pp. 163-172.

Nakiboğlu, G, Belfroid, S, Golliard, J & Hirschberg, A 2011, 'On the whistling of corrugated pipes: effect of pipe length and flow profile', *Journal of Fluid Mechanics*, vol 672, pp. 78-108.

Nelson, PA, Halliwell, NA & Doak, PE 1981, 'Fluid dynamics of a flow excited resonance, part I: Experiment', *Journal of Sound and Vibration*, vol. 78, no. 1, pp. 15-38.

Panton, R 1990, 'Effect of orifice geometry on Helmholtz resonator excitation by grazing flow', *AIAA Journal*, vol. 28, pp. 60-65.

Panton, RL & Miller, JM 1975, 'Excitation of a Helmholtz resonator by a turbulent boundary layer', *Journal of the Acoustical Society of America*, vol. 58, no. 4, pp. 800-806.

Peat, KS, Ih, JG & Lee, SH 2003, 'The acoustic impedance of a circular orifice in grazing mean flow: Comparison with theory', *Journal of the Acoustical Society of America*, vol. 114, no. 6, pp. 3076-3086.

Rathnasingham, R & Breuer, K 1997, 'Coupled fluid-structural characteristics of actuators for flow control', *AIAA Journal*, vol. 35, no. 5, pp. 832-837.

Ricot, D, Marie, S, Sagaut, P & Bailly, C 2009 'Lattice Boltzmann method with selective viscosity filter'. *Journal of Computational Physics*, vol. 228, no. 12, pp. 4478–4490.

Rockwell, D & Naudascher, E 1978, 'Review-self-sustaining oscillations of flow past cavities', *ASME Transactions Journal of Fluids Engineering*, vol. 100, pp. 152-165.

Ronneberger, D 1980, 'The dynamics of shearing flow over a cavity: A visual study related to the acoustic impedance of small orifices', *Journal of Sound and Vibration*, vol. 71, no. 4, pp. 565-581.

Rossiter, J & Britain, G 1964, 'Wind tunnel experiments on the flow over rectangular cavities at subsonic and transonic speeds'.Technical report 64037, RAE.

Rowley, CW, Colonius, T & Basu, AJ 2002, 'On self-sustained oscillations in two-dimensional compressible flow over rectangular cavities', *Journal of Fluid Mechanics*, vol. 455, pp. 315-346.

Sarohia, V 1975, 'Experimental and analytical investigation of oscillations in flows over cavities', *Ph.D Thesis*, California Institute of Technology.

Sipp, D 2012, 'Open-loop control of cavity oscillations with harmonic forcings', *Journal of Fluid Mechanics*, vol. 708, pp. 439-468

Sun, X, Jing, X, Zhang, H, & Shi, Y 2002, 'Effect of grazing–bias flow interaction on acoustic impedance of perforated plates', *Journal of Sound and Vibration*, vol. 254, no. 3, pp. 557-573.

Tam, CKW, Pastouchenko, NN, Jones, MG & Watson, WR 2014, 'Experimental validation of numerical simulations for an acoustic liner in grazing flow: Self-noise and added drag', *Journal of Sound Vibration,* vol. 333, no. 13, pp. 2831-2854.

Tang, PK & Sirignano, WA 1973, 'Theory of a generalized Helmholtz resonator', *Journal of Sound and Vibration*, vol. 26, no. 2, pp. 247-262.

Tonon, D, Landry, B, Belfroid, S, Willems, J, Hofmans, G & Hirschberg, A 2010, 'Whistling of a pipe system with multiple side branches: Comparison with corrugated pipes', *Journal of Sound and Vibration*, vol. 329, no. 8, pp. 1007-1024.

Toulorge, T 2012, 'Efficient Runge-Kutta discontinuous Galerkin Methods applied to aeroacoustics', *Ph.D. Thesis,* University of Leuven.

Urzynicok, F & Fernholz, H 2002, 'Flow-induced acoustic resonators for separation control', *AIAA Journal*, vol. 2819, pp 1-9.

Von Helmholtz, H 1896, 'Theorie der Luftschwingungen in Röhren mit offenen Enden', W. Engelmann.

Walker, B. and Charwat, A 1982, 'Correlation of the effects of grazing flow on the impedance of Helmholtz resonators', *Journal of the Acoustical Society of America*, vol. 72, pp. 550-555.

Womersley, J 1955, 'Method for the calculation of velocity, rate of flow and viscous drag in arteries when the pressure gradient is known', *The Journal of Physiology*, vol. 127, no. 3, pp. 553-563.

Zhang, Q & Bodony, DJ 2014, 'Direct numerical simulation and analytical modeling of locally reacting, single degree of freedom acoustic liners with turbulent grazing flow', *AIAA Paper* 2014-3354, 20th AIAA/CEAS Aeroacoustic Conference, Georgia, USA.

# Chapter 4

# Flow behaviour on a Helmholtz resonator excited by grazing flow

This chapter has been published as

Ghanadi, F., Arjomandi, M., Cazzolato, B. S., and Zander, A. C. 2013 'Numerical simulation of grazing flow over a self-excited Helmholtz resonator', *Engineering Letters*, vol. 21, no 3, pp. 137-142.

and

Ghanadi, F., Arjomandi, M., Cazzolato, B. S., and Zander, A. C. 2014, 'Understanding of the flow behaviour on a Helmholtz resonator excited by grazing flow', *International Journal of Computational Fluid Dynamics,* published online (DOI: 10.1080/10618562.2014.922681).

This chapter reports on the investigations of the self-sustained oscillations of the grazing flow in the vicinity of the resonator orifice using Large Eddy Simulation of the flow over a Helmholtz resonator. The results comprise the material presented in two journal papers.

The first paper, entitled "Numerical Simulation of Grazing Flow over a Self-excited Helmholtz Resonator" shows the mean values of the convection velocity of the vortices within the shear layer and the sound pressure levels associated with acoustic response of the resonator. The numerical results were compared in great detail to published experimental data, and demonstrate a high level of validation.

The second paper, entitled “Understanding of the flow behaviour on a Helmholtz resonator excited by grazing flow”, reports further analysis of the flow behaviour within the flow-excited Helmholtz resonator and both time dependent pressures and velocity fluctuations were simulated. The cross-stream component of the velocity fluctuations over the orifice exit was also computed and it was concluded that the maximum value of the suction and injection occurs when the flow excitation occurs.

With further investigation of the effects of flow-excited resonator on the grazing flow, the properties of the boundary layer downstream of the resonator are analysed in the next chapter.

# Statement of Authorship

| | |
|---|---|
| Title of Paper | Understanding of the flow behaviour on a Helmholtz resonator excited by grazing flow |
| Publication Status | ⦿ Published, O Accepted for Publication, O Submitted for Publication, O Publication style |
| Publication Details | Ghanadi, F., Arjomandi, M., Cazzolato, B. S., and Zander, A. C. 2014, 'Understanding of the flow behaviour on a Helmholtz resonator excited by grazing flow', International Journal of Computational Fluid Dynamics, published online (DOI: 10.1080/10618562.2014.922681). |

## Author Contributions

By signing the Statement of Authorship, each author certifies that their stated contribution to the publication is accurate and that permission is granted for the publication to be included in the candidate's thesis.

| | | | |
|---|---|---|---|
| Name of Principal Author (Candidate) | Farzin Ghanadi | | |
| Contribution to the Paper | Performed numerical work, interpreted data, wrote manuscript and acted as corresponding author. | | |
| Signature | | Date | 19.09.14 |

| | | | |
|---|---|---|---|
| Name of Co-Author | Maziar Arjomandi | | |
| Contribution to the Paper | Supervised development of work, helped in data interpretation and manuscript evaluation. | | |
| Signature | | Date | 19.09.14 |

| | | | |
|---|---|---|---|
| Name of Co-Author | Benjamin Cazzolato | | |
| Contribution to the Paper | Supervised the research and contributed in academic discussion and manuscript review | | |
| Signature | | Date | 19/9/14 |

| | | | |
|---|---|---|---|
| Name of Co-Author | Anthony Zander | | |
| Contribution to the Paper | Supervised the research and contributed in academic discussion and manuscript review | | |
| Signature | | Date | 19/9/14 |

Ghanadi, F., Arjomandi, M., Cazzolato, B. & Zander, A.. (2014) Understanding of the flow behaviour on a Helmholtz resonator excited by grazing flow.
*International Journal of Computational Fluid Dynamics, v. 28(5), pp. 219-231*

# Statement of Authorship

| | |
|---|---|
| Title of Paper | Numerical simulation of grazing flow over a self-excited Helmholtz resonator |
| Publication Status | ⦿ Published, O Accepted for Publication, O Submitted for Publication, O Publication style |
| Publication Details | Ghanadi, F., Arjomandi, M., Cazzolato, B. S., and Zander, A. C. 2013, 'Numerical simulation of grazing flow over a self-excited Helmholtz resonator', Engineering Letters, vol. 21, no 3, pp. 137-142. |

## Author Contributions

By signing the Statement of Authorship, each author certifies that their stated contribution to the publication is accurate and that permission is granted for the publication to be included in the candidate's thesis.

| | | | |
|---|---|---|---|
| Name of Principal Author (Candidate) | Farzin Ghanadi | | |
| Contribution to the Paper | Performed numerical work, interpreted data, wrote manuscript and acted as corresponding author. | | |
| Signature | | Date | 19.09.14 |

| | | | |
|---|---|---|---|
| Name of Co-Author | Maziar Arjomandi | | |
| Contribution to the Paper | Supervised development of work, helped in data interpretation and manuscript evaluation. | | |
| Signature | | Date | 19.09.14 |

| | | | |
|---|---|---|---|
| Name of Co-Author | Benjamin Cazzolato | | |
| Contribution to the Paper | Supervised the research and contributed in academic discussion and manuscript review | | |
| Signature | | Date | 19/9/14. |

| | | | |
|---|---|---|---|
| Name of Co-Author | Anthony Zander | | |
| Contribution to the Paper | Supervised the research and contributed in academic discussion and manuscript review | | |
| Signature | | Date | 19/9/14 |

# Numerical Simulation of Grazing Flow over a Self-excited Helmholtz Resonator

F. Ghanadi, M. Arjomandi, A. C. Zander and B. S. Cazzolato

*Abstract*— **Self-sustained oscillations of the grazing flow along the orifice of a Helmholtz resonator were considered numerically. These fluctuations are driven by hydrodynamic instabilities inside the shear layer and the resonant acoustical field. Quantitative prediction of this process requires accurate calculations of grazing flow characteristics over the three dimensional resonator. In this paper flow excitation phenomenon assumed to be associated with external pressure fluctuations within the turbulent boundary layer of grazing flow and acoustic response of the cavity. To this end a Large Eddy Simulation (LES) of the three dimensional shear flow over the orifice carried out at a low Mach number to allow predictions of the amplitude and frequency of the pressure and velocity fluctuations. For validation propose, for pressure fluctuations inside the cavity, a good quantitative agreement with published data was obtained. Therefore the simulations provide an ability to predict the resonating frequency, pressure and velocity field for different inlet conditions.**

*Index Terms*—**Helmholtz resonator, large eddy simulation, pressure fluctuations, self- excitation**

## I. Introduction

A resonator exposed to an external flow field can produce a flow excited resonance over a specific range of flow conditions. This process is common phenomenon in many engineering applications such as flow over open sunroof or window of an automobile, aircraft landing gear and pipelines with closed side branches. All of these systems can produce high amplitude pressure fluctuations at different Mach number. There is immense body of literature about velocity and pressure fluctuations within the Helmholtz resonator which was excited by external force. Most of these studies carried out experimentally using loudspeakers to apply external force to excite air flow inside the cavity. Moreover an appropriate quantitative explanation of self excitation phenomena requires extremely accurate prediction of shear flow properties, compressibility and flow inlet effects, etc. The motivation of the current study was derived from the excitation of a resonator caused by grazing flow to predict the flow characteristics in and outside the resonator. This paper presents a model to simulate a flow-excited resonator to investigate pressure and velocity fluctuations in and outside of the cavity. This simulation can provide an accurate quantitative description for capability of a Helmholtz resonator to reduce instinct disturbances within the turbulent boundary layer.

The Helmholtz resonator as an alternative type of side branch resonator is formed by a cavity with a fix volume of compressible flow connected to the surrounding through a single small opening [1, 2]. As can be seen in Fig. 1, a schematic of the Helmholtz resonator and the behaviour of a Helmholtz resonator can be described by a second-order mass spring or, equivalently, with a capacitor and an inductor. In this mass spring system, the mass comprises of the mass of fluid in the neck whereas compressibility of the fluid in the cavity acts as a spring. Owing to viscous effects of flow and acoustic radiation at the orifice, the mass spring system has also damping parameter which in calculations typically be considered.

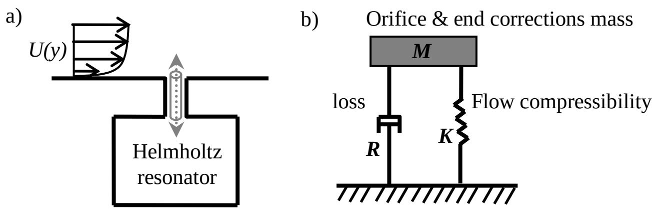


Fig. 1. a) Schematic of a Helmholtz resonator b) Mass-spring analogy

The quasi-periodic vortex shedding by an incompressible low Mach number grazing flow past the orifice and excitation of acoustic resonances in the cavity can produce intense energy exchange. When the frequency of the flow oscillations is far from that of natural frequency of the resonator, the two processes are weakly coupled. When the frequency of flow fluctuations over the orifice is near the natural frequency of the resonator, it is excited and then a small pressure fluctuation can produce a relatively large magnitude velocity fluctuation around the neck, which is accompanied by large pressure fluctuations inside the cavity. When wall boundary layer of grazing flow reaches the upstream edge of the orifice, it suddenly separates resulting in the formation of vortices, which, in turn, form a shear layer in this area. As a result, excitation is associated with the periodical shedding of these compact vortices from a separation edge of the resonator mouth to the downstream edge, and consequently an intense energy exchange occurs between the driving flow oscillations and the fluid inside the

F. Ghanadi is with the School of Mechanical Engineering, University of Adelaide, SA 5005, Australia (corresponding author to provide phone: (+61 8) 83136385; e-mail: farzin.ghanadi@adelaide.edu.au).

M. Arjomandi is with the School of Mechanical Engineering, University of Adelaide, SA 5005, Australia (email: maziar.arjomandi@adelaide.edu.au)

A. C. Zander is with the School of Mechanical Engineering, University of Adelaide, SA 5005, Australia (email: benjamin.cazzolato@adelaide.edu.au)

B. S. C Cazzolato is with the School of Mechanical Engineering, University of Adelaide, SA 5005, Australia (email: anthony.zander@adelaide.edu.au)



(Advance online publication: 19 August 2013)

resonator [3]. Therefore, to predict self excitation condition of a Helmholtz resonator, it is very important to determine the natural frequency of such a resonator. In general using lumped element analysis, the following expression can be used for the calculation of the natural frequency of the resonator.

$$f_r = \frac{c}{2\pi}\sqrt{\frac{S}{l_e V}} \qquad (1)$$

where $c$ is the speed of sound, $S$ and $V$ are the cavity volume and the cross sectional area of the orifice respectively. Orifice flow, of course, cannot fluctuate separated from grazing flow. The quasi-periodic vortex shedding by an incompressible low mach number grazing flow past the orifice and excitation of acoustic resonances in the cavity can produce intense energy exchange. When the frequency of the flow oscillations is far from that of natural frequency of the resonator, the two processes are weakly coupled. When the frequency of flow fluctuations over the orifice is near the natural frequency of the resonator, it is excited and then a small pressure fluctuation can produce a relatively large magnitude velocity fluctuation around the neck, which is accompanied by large pressure fluctuations inside the cavity. When wall boundary layer of grazing flow reaches the upstream edge of the orifice, it suddenly separates resulting in the formation of vortices, which, in turn, form a shear layer in this area. On of the earliest experimental investigation for flow excited resonance carried out by Rossiter (1964) who examined shallow cavities at subsonic and transonic flow regimes. It was demonstrated that the convection of discrete vortices within grazing flow over the resonator opening generates the frequency spectrum of the sound. A semi-empirical correlation was suggested to predict the frequency of natural hydrodynamic instability of low Mach number ($0.4 \le M \le 1.2$) grazing flow over the opening as

$$\frac{fl}{U} = \frac{n-\alpha}{Ma + 1/k}, \qquad (2)$$

in which $n$ is the mode number ($n$ =1, 2, 3,….), $Ma$ is Mach number and $\alpha$ and $k$ are constant values

Prediction of the resonator pressure oscillations has been extensively studied both experimentally and analytically. The hydrodynamic force of this vortex shedding is also analysed by describing two forward and backward functions which illustrate oscillatory flow in the orifice and its effect or by implementing vortex sound theory. [4, 5]. The Helmholtz resonator has also been used for flow separation control in two different test cases of a diffuser and a wing [6]. They observed that the vortices ejected from the orifice can shift the momentum in the near-wall region, and therefore reattach the downstream flow. The most recent researchers numerically investigate to the subject of flow-excited Helmholtz resonator. For example Inagaki et al. [7] who derived new equations to predict numerically the flow oscillations over a Helmholtz resonator at low Mach number. They predicted frequency of pressure fluctuations within flow over a resonator orifice with high aspect ratio at low Mach number using compressible Navier-stokes equations. It was concluded that the pressure fluctuations have frequency very close to the natural frequency of resonator in a wide range of velocity. Mallick et al. [8] later applied a modified lattice– Boltzmann equation to calculate the pressure fluctuations spectrum within the grazing flow-excited over a Helmholtz resonator. Using $k-\varepsilon$ RNG turbulent model they demonstrated that to validate their results with Nelson et al. [3] experimental work some parameters required scaling. For example if velocity of grazing flow multiple by 0.7 predicted pressure fluctuation inside the cavity is very close to the experimental data. The reason of this scaling was described as the effects of boundary layer thickness on convection velocity of the vortex within the shear layer over the orifice. A recent experimental attempt to explore flow characteristics in and outside the resonator also carried out by Ma et al. [9] who tested a self-excited Helmholtz resonator with various free stream velocity. They concluded that the magnitude of external force which induced by grazing flow is in a specific range over a large variety of free stream speed and boundary layer thickness.

The objective of this paper is to simulate the effects of a self-excited Helmholtz resonator on the turbulent grazing flow. The simulations were performed in a wide range of Reynolds numbers and turbulent intensity to analyse the inlet flow properties on excitation condition. The outline of the remainder of the paper is as followed. The next sections are organized as follows. Necessity of using LES model and the basic equations related to that are described in §2. In §3 results of the proposed model are compared with experimental published data to validate the model. Then the effects of flow conditions on pressure and velocity fields are discussed. In the last section conclusions and summary of this study are presented.

## II. NUMERICAL SET UP AND PROCEDURE

In order to calculate the fluctuation parameters of shear flow over the orifice and flow field inside the resonator a sophisticated modelling tool is required to simulate adequately the three dimensional complex flow. The primary requirement of this model is that it must handle the complex geometries with high order of accuracy. The model also must have a very low dissipation part to predict the fluctuations accurately in shear flow over the orifice and acoustic field. It has been shown that Reynolds-averaged Navier-Stokes (RANS) methods have been typically are too dissipative and then the models under-predict velocity and pressure fluctuations in the flow field [10, 11]. The accuracy of simulations strongly depends on the spatial and temporal resolution employed. RANS models were not considered suitable since cannot resolve the time dependant parameters within the grazing flow. These methods are adequate for steady flows, or, unsteady flows with very weak non-resonant coupling. It has been observed that these models are inadequate for highly unsteady flow and involve strong vortex acoustic coupling and resonance like phenomena [12]. This is the main reason why the RANS method was useless for the flow calculations for Helmholtz resonator. Among turbulence models Large Eddy Simulation (LES) as an unsteady simulation can accurately simulate the characteristics of the flow in the presence of acoustic field [13]. LES is also capable of handling the flows for which

RANS models work and also for flows involving strong vortex-acoustic coupling, including resonating pressure disturbances. LES represents a three dimensional and time dependant solution of the Navier-Stokes equations. This kind of simulation is a method intermediate between the Direct Numerical Simulation (DNS) and Reynolds-average solutions.

In this paper LES was used as an invaluable tool for capturing the fluctuations which come from coherent structures in the turbulent boundary layer and perturbations which within separation flow within the resonator opening. This model, using “sub-grid” scale for the small-scale structures, can accurately predict flow fluctuations in the wall bounded regions [14]. LES model separates the small and large scale structures by using filtering and resolves the large scale motion so that the large scale structures are computed explicitly. On the other hand, this method, can model the small scale motion accurately [15]. Therefore, pressure fluctuations in acoustic feedback field can be modelled with adequate accuracy using this technique. Moreover, an appropriate prediction for the velocity perturbations generated by the grazing flow passing over the resonator can be calculated. On the following the detail of the numerical method and its governing equations are presented.

### A. Governing Equations

Owing to compressibility of the air flow inside the cavity the filtered compressible Navier–Stokes equations for a Newtonian fluid were used. To simplify the equations a mass-weighted change of variable defined as

$$\tilde{\phi} = \frac{\overline{\rho\phi}}{\bar{\rho}} \tag{3}$$

where $\bar{\rho}$ a space-filtered variable. Therefore, conversation and Navier-Sockes equations are then given by

$$\frac{\partial\bar{\rho}}{\partial t} + \frac{\partial(\bar{\rho}\tilde{u}_i)}{\partial x_i} = 0 \tag{4}$$

$$\frac{\partial(\bar{\rho}\tilde{u}_i)}{\partial t} + \frac{\partial(\bar{\rho}\tilde{u}_i\tilde{u}j)}{\partial x_j} + \frac{\partial}{\partial x_i} - \frac{\partial(\tilde{\delta}_{ij})}{\partial x_j} =$$
$$-\frac{\partial}{\partial x_j}\Bigg[\underbrace{\bar{\rho}(u_i\tilde{u}_j - \tilde{u}_i\tilde{u}j)}_{\tau_{ij}}\Bigg] + \frac{\partial}{\partial x_j}(\bar{\sigma}_{ij} - \tilde{\delta}_{ij}) \tag{5}$$

where $\bar{\sigma}_{ij}$ is the filtered stress tensor and $\tilde{\delta}_{ij}$ the computable stress tensor. The filtered Navier-Stokes equations govern the evolution of the large scales of motion. The effect of the small structures comes out through a subgrid scale stress term ( $\tau_{ij}$ ) which is given by

$$\tau_{ij} - \frac{1}{3}\tau_{kk}\delta_{ij} = 2\nu_t\bar{S}_{ij} \tag{6}$$

where $\delta_{ij}$ is Kronecker delta and $\bar{S}_{ij}$ is the deformation tensor of the subgrid field,

$$\bar{S}_{ij} = \left(\frac{\partial\bar{u}_i}{\partial x_j} + \frac{\partial\bar{u}_j}{\partial x_i}\right) \tag{7}$$

The most popular subgrid model is the Smagorinsky model, but this model is of order $O(1)$ and is just related to the strain rate of the turbulent structure. In this project the *Wale* subgrid model has been used which can accurately predict flow behaviour of the subgrid viscosity at the wall in zero pressure gradient incompressible boundary layer, and is of order $O(3)$ [16],

$$\nu_t = (C_w\Delta x)^2 \frac{(S_{ij}^d S_{ij}^d)^{3/2}}{(S_{ij}S_{ij})^{5/2} + (S_{ij}^d S_{ij}^d)^{5/2}}, \tag{8}$$

where $C_w$ is 0.5 and

$$S_{ij}^d = \frac{1}{2}\left(\left(\frac{\partial\bar{u}_i}{\partial x_j}\right)^2 + \left(\frac{\partial\bar{u}_j}{\partial x_i}\right)^2\right) - \frac{1}{3}\delta_{ij}\left(\frac{\partial\bar{u}_k}{\partial x_k}\right)^2, \tag{9}$$

In next section the characteristics of the simulations which include study of the effects of the mesh grid and of the nature of the inflow condition are described.

### B. Simulation Characteristics

The geometry studied here corresponds to that examined experimentally and analytically by Ma et al. [9]. The cavity is 59 cm long with square cross section of 50 cm× 50 cm. The 12.5 cm× 12.5 cm orifice is cut from a 0.16 cm thick plate. Various free stream velocity settings, corresponding to resonant and non-resonant conditions were studied by Ma et al. [9]. The free stream speed was in the range of 10-30 m/s with a boundary layer thickness of 0.5 cm to 2 cm at the orifice upstream lip. Moreover, as part of their experimental work, microphone measurements yielding pressure fluctuations inside the cavity. Therefore to validate the model it is necessary to simulate the resonator under these inlet flow conditions and calculate the pressure fluctuations within the cavity. In Ma et al. studies there were not any hot-wire measurements to evaluate the velocity profile inside the shear layer over the orifice. In the present paper mean velocity profile and velocity fluctuations within the grazing flow were calculated. Since in LES only small turbulence structures are modelled and the large and energy carrying are computed, requires high grid resolution in near wall region in streamwise and crosswise Wagner et al. [17]. Therefore, in the first part of this task a development of accurate physical geometries with a suitable mesh for the computational domain is required. As illustrated in Fig. 2, in order to capture the behaviour of the near-wall flow, a sufficiently fine mesh has been used in the present work. An accumulated mesh structure has been utilized in the region near the resonator orifice to ensure that there are at least a few cells in the buffer layer of the turbulent boundary layer. Using this kind of grid allows a fine mesh within the turbulent boundary layer and fits the plate shape very well. In order to calculate the characteristics of flow in outer region the number of grid points (Cells) should be proportional to $(Re)^{0.4}$ and in viscous region this is increased to $(Re)^{1.8}$. Although these cell sizes result in fairly fine meshes, in comparison with DNS method this approach allows to reduce the computational costs. A computational mesh containing 2.5 million cells (1 million vertices).

In order to evaluate near-wall fluctuations the $(Y)^{+}$ parameter should less than 1, which in this project for all case studies this non-dimensional parameter was around 0.2.

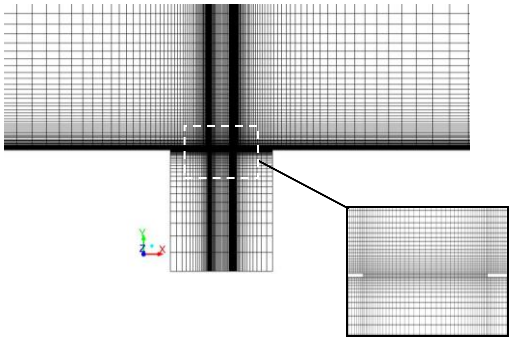

Fig 2. Volumetric mesh in the orifice of the resonator. The resolution is highest in this region.

The highest resolution needs to be applied over the surface to capture the characteristics of the boundary layer. In order to analyse the sensitivity of the results to the domain size

TABLE I
DOMAIN SIZES TESTED FOR SENSITIVITY

| Case | Channel volume (m^3) | Total number of nodes |
|---|---|---|
| 1 | 2.4 | 1,253,871 |
| *2* | 4.6 | 2,542,756 |
| *3* | 7.4 | 4,705,748 |

three domain sizes equal (Cases 1, 2, 3) from the trailing edge were tested.

The results of the three runs with the same boundary conditions and surface grid parameters were compared. Mesh quality assessment was performed using definition of Maximum y+ for the cases.

## III. RESULTS AND DISCUSSION

Based on equation (1) the Helmholtz resonator frequency was determined to be 45 Hz. The primary non-dimensional parameter of interest was defined based on free stream velocity; $U^{*} = U / Lf_r$ .where $U$ is free stream velocity. The inlet velocity was varied from 5 to 30 m/s with turbulent intensity of 0.3 % and boundary layer thickness over the orifice was found to be 2 cm or, $\delta / L = 0.16$ . By use of the turbulence model and boundary conditions described above, velocity and pressure distributions inside and over the resonator were calculated.

### *A. Pressure fluctuations*

The resonator pressure fluctuations within the flow excited Helmholtz resonator are explained in this section. In order to show the results in terms of frequency, another variable based on natural frequency of the resonator was defined; $f^{*} = f / f_r$ . where $f$ is the natural hydrodynamic instability frequency. Fig. 3 shows the calculated sound pressure level (SPL) as a function of $f^{*}$ when $U^{*} = 3$. It can be seen that one mode was dominant and it is just very close to the resonance frequency of the Helmholtz resonator.

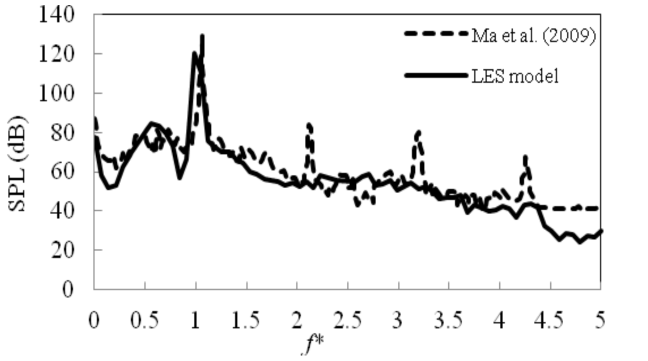


Fig 3. Sound pressure level of the resonator at different inlet flow velocity

Therefore it seems that just in specific range of free stream velocity the strong pick happen and out of this span there is no clear sign of resonance. It can be see that in the figure, in the number of mesh and domain size cannot affect on the results. The model also calculated the pressure fluctuations inside the resonator and it was examined the ability of the LES to match the frequency and amplitude of the fluctuations which have been described in the literature. The pressure fluctuations in the literature were normalized by integrating the spectral densities in the region of peak resonance which is given by

$$p^{*}_{res} = \frac{\sqrt{\int_{0.8 f_p}^{1.2 f_p} G_{pp}(f) df}}{0.5 \rho U^{2}}, \tag{10}$$

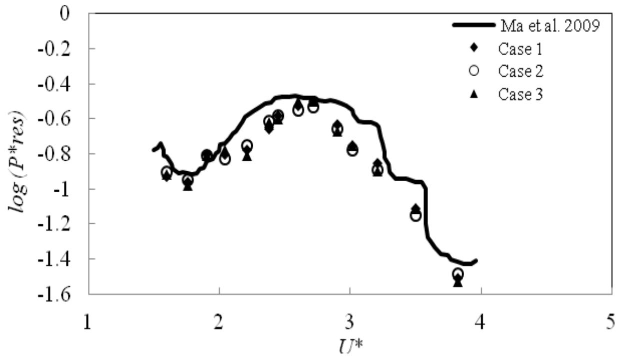


Fig 4. The resonator pressure amplitude for various free stream velocities

### *B. Velocity fluctuations*

The mean and fluctuation flow velocity was determined using the LES model over the resonator opening. In order to develop the determine behaviour of the shear flow over the orifice length, velocity profiles was calculated within the shear layer from leading edge to trailing edge. in first step the mean velocity profiles at the tips and middle points of the orifice was considered. As shown in the Fig. 5, the shear layer thickness at the three stations ( $x = -6.25\,cm, x = 0$ and $x = 6.25\,cm$ are corresponding to the upstream edge, midpoint, and the downstream edge of the resonator opening, respectively) are $\delta = 1.25\,cm, \delta = 2.4\,cm$ and $\delta = 3.3\,cm$ .

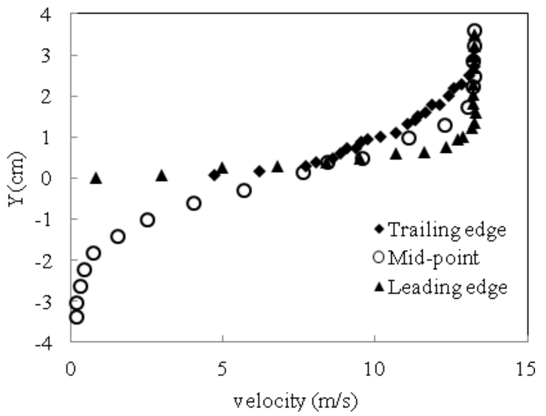


Fig 5. Mean velocity profiles, in resonator opening at three stations

The velocity of vortices inside the shear layer plays an important role to generate high pressure fluctuations within the resonator and exchange energy between boundary layer and cavity flow. Vortices in a thick turbulent boundary layer convect slower compared to a thin boundary layer. In the literature flow visualizations reported that this speed is a function of the boundary layer thickness and free stream velocity [4, 18]. Therefore the convection velocity is given by

$$U_c = \frac{U}{2}\left(\frac{0.05\,d}{\delta}\right)^{1/7} \tag{11}$$

Using the mean velocity profiles convection velocity of the vortex within the shear layer was found. As can be seen in the Fig 6. in the mid point at the middle of orifice height velocity of the flow is around 7 m/s. Considering turbulent boundary layer thickness in this area was about 1.5 cm, the convection velocity using Equation (11) is around $0.5U$ which is match with simulation result.

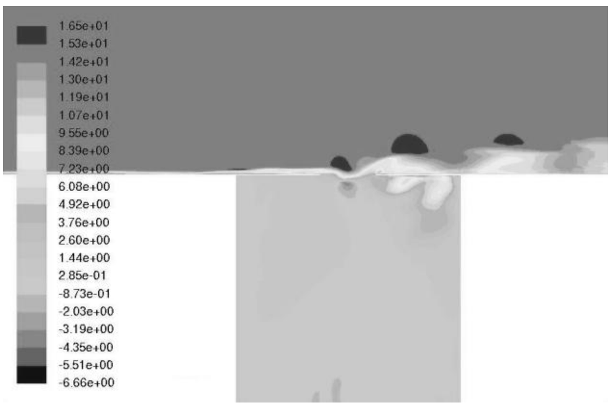


Fig 6. stream-wise velocity contour over the resonator

## IV. Conclusions

Owing to difficulties and time constraints of experimental tests, CFD investigations have been conducted to find the various parameters affecting the Helmholtz resonator performance. To this end the three-dimensional boundary layer within a channel with a grazing flow-excited Helmholtz resonator were simulated and time dependent pressures and velocity fluctuation were calculated. Since the RANS models cannot accurately model the fluctuation parameters of the turbulent flows the LES model was utilized which its dissipation part has minimum effects on sub-gird scales. The resonance characteristics of the resonator were described using LES for three different mesh cases.

The calculated sound pressure level of acoustic response of the resonator was compared with experimental results and concluded that in specific free stream speed the strong excitation of the resonator happen. Characteristics of inlet flow states were changed to evaluate their effects on excitation condition. It was observed that when $U^* = 3$ frequency of instabilities was very close to the natural frequency of the resonator and then high pressure amplitude can be achieved (around 111 dB). It was also concluded from time series of pressure fluctuations inside the cavity that around this inlet flow velocity, maximum pressure takes place within the resonator and by increasing the Reynolds number the pressure dramatically dropped. It was also shown that increasing mesh numbers and domain sizes cannot affects the results so much.

In the next step to check capability of the model to calculate velocity fluctuations over the orifice, velocity distribution for a wide range of Reynolds numbers was tested. Mean velocity profile over the whole distance of the resonator orifice showed that the computed convection velocity of the vortices inside the shear layer was very close to the experimental observations. Pressure fluctuations in vertical direction were also calculated that to find the maximum amplitude of the shear flow velocity perpendicular to the shear flow. This value can help us to find the energy exchange between air flow inside the resonator and shear flow over the orifice.

## REFERENEC


[1] L. E. Kinsler, *et al.*, "Fundamentals of acoustics," *Fundamentals of Acoustics, 4th Edition, by Lawrence E. Kinsler, Austin R. Frey, Alan B. Coppens, James V. Sanders, pp. 560. ISBN 0-471-84789-5. Wiley-VCH, December 1999.*, vol. 1, 1999.

[2] H. Von Helmholtz, *'Theorie der Luftschwingungen in Röhren mit offenen Enden'*: W. Engelmann, 1896.

[3] P. A. Nelson, *et al.*, "Fluid dynamics of a flow excited resonance, part I: Experiment," *Journal of Sound and Vibration,* vol. 78, pp. 15-38, 1981.

[4] H. Kook, *et al.*, "Active control of pressure fluctuations due to flow over Helmholtz resonators," *Journal of Sound and Vibration,* vol. 255, pp. 61-76, 2002.

[5] T. D. Mast and A. D. Pierce, "Describing-function theory for flow excitation of resonators," *The Journal of the Acoustical Society of America,* vol. 97, p. 163, 1995.

[6] F. Urzynicok and H. Fernholz, "Flow-induced acoustic resonators for separation control," in *AIAA* 2002.

[7] M. Inagaki, *et al.*, "Numerical prediction of fluid-resonant oscillation at low Mach number," *AIAA journal,* vol. 40, pp. 1823-1829, 2002.

[8] S. Mallick, *et al.*, "Numerical simulation of the excitation of a Helmholtz resonator by a grazing flow," *The Journal of the Acoustical Society of America,* vol. 114, p. 1833, 2003.

[9] R. Ma, *et al.*, "Fluid mechanics of the flow-excited Helmholtz resonator," *Journal of Fluid Mechanics,* vol. 623, p. 1, 2009.
[10] N. Sinha, *et al.*, "High Fidelity Simulation Of Weapons Bay Aeroacoustics Attenuation Using Active Flow Control," in *Paper No. AIAA-2000-1968, 6th AIAA/CEAS Aeroacoustics Conference, Lahaina, Hawaii*, 2000.
[11] L. Georges, *et al.*, "Aeroacoustic simulation of the flow in a Helmholtz resonator," *Computational Fluid Dynamics 2006,* pp. 819-824, 2009.
[12] S. Arunajatesan and S. Menon, "Towards hybrid LES-RANS computations of cavity flowfields," *AIAA paper,* vol. 401, 2000.
[13] P. Moin, "Large eddy simulation of incompressible turbulent channel flow," 1978.
[14] P. Schlatter, "Large-eddy simulation of transition and turbulence in wall-bounded shear flow," *Swiss Federal Institute of Technology, Zurich,* 2005.
[15] J. Blazek, *Computational fluid dynamics: principles and applications* vol. 2: Elsevier Science, 2005.
[16] F. Nicoud and F. Ducros, "Subgrid-scale stress modelling based on the square of the velocity gradient tensor," *Flow, Turbulence and Combustion,* vol. 62, pp. 183-200, 1999.
[17] C. A. Wagner, *et al.*, *Large-eddy simulation for acoustics* vol. 20: Cambridge Univ Pr, 2007.
[18] S. Elder, *et al.*, "Mechanisms of flow-excited cavity tones at low Mach number," *The Journal of the Acoustical Society of America,* vol. 72, p. 532, 1982.

# Chapter 5

# Interaction of a flow-excited Helmholtz resonator with a grazing turbulent boundary layer

This chapter has been published as

Ghanadi, F., Arjomandi, M., Cazzolato, B. S., and Zander, A. C. 2014, ' Interaction of a flow-excited Helmholtz resonator with a grazing turbulent boundary layer', *Experimental Thermal and Fluid Science,* vol. 58, pp. 80-92.

and submitted as

Ghanadi, F., Arjomandi, M., Cazzolato, B. S., and Zander, A. C. 2014, 'Analysis of the turbulent boundary layer in the vicinity of a self-excited cylindrical Helmholtz resonator', submitted to *Journal of Turbulence*.

This chapter presents the detailed fluid dynamic and acoustic analyses of the flow within the flow-excited resonator through a full experimental investigation and by implementing a Large Eddy Simulation (LES). To assist in understanding the effect of the resonator on the flow structure, a sensitivity study was undertaken by changing the main geometrical parameters of the resonator. The results comprise the material presented in two journal papers.

The experimental results presented in the first paper, entitled “Interaction of a flow-excited Helmholtz resonator with a grazing turbulent boundary layer” demonstrate the potential of the flow-excited Helmholtz resonator to stabilize the turbulent boundary layer. The turbulence intensity and energy spectra of the velocity fluctuations within the turbulent boundary layer downstream of the resonators reveal that in a specific velocity range certain resonators have the potential to modify the flow instabilities within the turbulent boundary layer.

The numerical simulations undertaken in the second paper, entitled “Analysis of the turbulent boundary layer in the vicinity of a self-excited cylindrical Helmholtz resonator”, predict the flow features in the vicinity of the resonator orifice with potential to stabilize the grazing flow. The results show that a low value of the velocity pulsation penetrates the logarithmic region and suppress the instabilities within the boundary layer. Further explanations for weakening of the turbulence production using the resonator are reported in the following chapter.

# Statement of Authorship

| | |
|---|---|
| Title of Paper | Interaction of a flow-excited Helmholtz resonator with a grazing turbulent boundary layer |
| Publication Status | ⦿ Published, O Accepted for Publication, O Submitted for Publication, O Publication style |
| Publication Details | Ghanadi, F., Arjomandi, M., Cazzolato, B. S., and Zander, A. C. 2014, ' Interaction of a flow-excited Helmholtz resonator with a grazing turbulent boundary layer', Experimental Thermal and Fluid Science, vol. 58, pp. 80-92. |

## Author Contributions

By signing the Statement of Authorship, each author certifies that their stated contribution to the publication is accurate and that permission is granted for the publication to be included in the candidate's thesis.

| | | | |
|---|---|---|---|
| Name of Principal Author (Candidate) | Farzin Ghanadi | | |
| Contribution to the Paper | Performed experimental work, interpreted data, wrote manuscript and acted as corresponding author. | | |
| Signature | | Date | 19.09.14 |

| | | | |
|---|---|---|---|
| Name of Co-Author | Maziar Arjomandi | | |
| Contribution to the Paper | Supervised development of work, helped in data interpretation and manuscript evaluation. | | |
| Signature | | Date | 19.09.14 |

| | | | |
|---|---|---|---|
| Name of Co-Author | Benjamin Cazzolato | | |
| Contribution to the Paper | Supervised the research and contributed in academic discussion and manuscript review | | |
| Signature | | Date | 19/9/14. |

| | | | |
|---|---|---|---|
| Name of Co-Author | Anthony Zander | | |
| Contribution to the Paper | Supervised the research and contributed in academic discussion and manuscript review | | |
| Signature | | Date | 19/9/14 |

Ghanadi, F., Arjomandi, M., Cazzolato, B. & Zander, A.. (2014) Interaction of a flow-excited Helmholtz resonator with a grazing turbulent boundary layer.
*Experimental thermal and fluid science, v. 58(October), pp. 80-92*

# Statement of Authorship

| | |
|---|---|
| Title of Paper | Analysis of turbulent boundary layer in the vicinity of a self-excited cylindrical Helmholtz resonator |
| Publication Status | O Published, O Accepted for Publication, ⦿ Submitted for Publication, O Publication style |
| Publication Details | Journal of Turbulence |

## Author Contributions

By signing the Statement of Authorship, each author certifies that their stated contribution to the publication is accurate and that permission is granted for the publication to be included in the candidate's thesis.

| | | | |
|---|---|---|---|
| Name of Principal Author (Candidate) | Farzin Ghanadi | | |
| Contribution to the Paper | Performed numerical work, interpreted data, wrote manuscript and acted as corresponding author. | | |
| Signature | | Date | 19.09.14 |

| | | | |
|---|---|---|---|
| Name of Co-Author | Maziar Arjomandi | | |
| Contribution to the Paper | Supervised development of work, helped in data interpretation and manuscript evaluation. | | |
| Signature | | Date | 19.09.14 |

| | | | |
|---|---|---|---|
| Name of Co-Author | Benjamin Cazzolato | | |
| Contribution to the Paper | Supervised the research and contributed in academic discussion and manuscript review | | |
| Signature | | Date | 19/9/14 |

| | | | |
|---|---|---|---|
| Name of Co-Author | Anthony Zander | | |
| Contribution to the Paper | Supervised the research and contributed in academic discussion and manuscript review | | |
| Signature | | Date | 19/9/14 |

# Analysis of the turbulent boundary layer in the vicinity of a self-excited cylindrical Helmholtz resonator

Farzin Ghanadi*, Maziar Arjomandi, Benjamin S. Cazzolato, Anthony C. Zander

University of Adelaide, School of mechanical Engineering, SA 5005, Australia

## Abstract

This study investigates the changes in the structure of a turbulent boundary layer downstream of a flow-excited Helmholtz resonator. To this end a fully developed turbulent boundary layer over a resonator mounted flush with a flat plate was simulated by implementing a Large Eddy Simulation (LES). To assist in understanding the effect of the resonator on the flow structure, a sensitivity study was undertaken by changing the main geometrical parameters of the resonator. The results demonstrated that when the boundary layer thickness equals the orifice length, the cross-stream component of velocity fluctuations penetrates the boundary layer, resulting in a reduction of the turbulence intensity by up to 12%. Therefore, it is concluded that a Helmholtz resonator has the potential to reduce the instabilities within the boundary layer. These investigations also assist in identifying the optimal parameters to delay turbulence events within the grazing flow using Helmholtz resonators.

**Keywords:** turbulent boundary layer, flow-excited Helmholtz resonator, turbulence intensity, LES model.

## Nomenclature

| | |
|---|---|
| $c_f$ | = friction coefficient |
| $d$ | = orifice diameter (mm) |
| $c$ | = speed of sound (m/s) |
| $f_L$ | = arbitrary flow variable |
| $f_r$ | = resonance frequency of the resonator (Hz) |
| $H$ | = Shape factor |
| $l$ | = length of the orifice (mm) |
| $l_e$ | = effective length of the orifice (mm) |
| $L$ | = cavity depth (mm) |
| $N$ | = number of grid points |
| $S$ | = cross-section area of the orifice (mm$^2$) |
| $V_c$ | = cavity volume (mm$^3$) |

* Corresponding author. Email: farzin.ghanadi@adelaide.edu.au

| | |
|---|---|
| $p$ | = static pressure of the flow (Pa) |
| $\mathrm{Re}_\tau$ | = Reynolds number based on friction velocity |
| $\mathrm{Re}_x$ | = Reynolds number based on the streamwise length |
| $\mathrm{Re}_\theta$ | = Reynolds number based on momentum thickness |
| $t$ | = time (s) |
| $T$ | = total time over which turbulence statistics are collected (s) |
| $Tu$ | = turbulence level |
| $u$ | = air velocity (m/s) |
| $u_\tau$ | = friction velocity (m/s) |
| $U$ | = free stream velocity (m/s) |
| $u'^{+}$, rms | = non-dimensional averaged turbulence intensity |
| $w$ | = flow velocity perpendicular to the grazing flow (m/s) |
| $Y^+$ | = non-dimensional wall distance to the first grid point |

**Symbols**

| | |
|---|---|
| $\delta_{ij}$ | = Kronecker delta |
| $\nu_t$ | = eddy viscosity ($m^2$/s) |
| $\delta$ | = boundary layer thickness (mm) |
| $\tau$ | = sub-grid scale stress tensor ($N/m^2$) |
| $\tau_v$ | = viscous stresses ($N/m^2$) |
| $\rho$ | = air density ($kg/m^3$) |
| $\nu$ | = kinematic viscosity ($m^2$/s) |
| $\theta$ | = momentum thickness (mm) |

**Symbols**

| | |
|---|---|
| $+$ | = time scale $\left(\frac{\nu}{u_\tau^2}\right)$ or length scale $\left(\frac{\nu}{u_\tau}\right)$ |

## 1. Introduction

Flow past a Helmholtz resonator results in pressure fluctuations and self-sustained oscillations of the flow within the resonator. This type of flow behaviour has been analysed due to its wide contribution to the fundamental understanding of flow control, as well as its diverse industrial applications (Rossiter 1964; Rockwell & Naudascher 1978; Dequand et al. 2003; Ghanadi et al. 2013b). A number of numerical studies have been undertaken to simulate the acoustic excitation of 3D and 2D Helmholtz resonators (Amandolese et al. 2004; Tam et al. 2010; Zhang et al. 2012). For example, grazing-incidence sound waves at different sound pressure levels (SPL) have been used to excite a resonator in the presence of a low Mach number grazing flow (Roche et al. 2010; Tam et al. 2014). It was observed that at low SPLs, the presence of the flow over the orifice increases the resistance of the resonator. With increased SPL the structure of the vortices within the shear layer over the orifice is also altered and dissipated more quickly. Using direct numerical simulations (DNS), Zhang et al.

(2011; 2014) also analysed the velocity and pressure fluctuations within a Helmholtz resonator in the presences of a grazing flow and acoustic field. It was concluded that when the grazing flow is laminar the fluctuations within the resonator cavity are limited, while the turbulent boundary layer produces more interactions. Moreover, it was found that at low Mach number grazing flow the shed vortices within the shear layer can penetrate into the higher regions of the boundary layer. It must be noted that when the resonator is excited only by the grazing flow, the flow features become more complicated, and the amount of published work on flow-excited resonators is very limited. Many researchers have also investigated flow oscillation in shallow and deep cavities, however, it is very important to note the difference between the flow behaviour in the vicinity Helmholtz resonators and open cavities. For the flow-excited Helmholtz resonator, the feedback disturbance of the resonator volume is perpendicular to the shear layer, whilst in shallow cavities, $D/L \geq 1$, the disturbances necessarily travel in a direction parallel to the plane of the shear layer (Colonius et al. 1999; Rowley et al. 2002; Sipp 2012). There is also a significant difference between the Helmholtz resonator and a deep cavity. The ratio of cavity volume to cavity orifice area in a Helmholtz resonator is greater than a deep cavity and thus it is possible to generate much lower frequencies compared to those attainable with a deep cavity (Rockwell & Naudascher 1978).

Depending on the application, the self-sustained oscillation of flow by a Helmholtz resonator may be desirable, for example in sound generation using musical instruments. These oscillations may also have undesirable effects, for instance high amplitude pressure fluctuations inside the car cabin with an open window (Bruggeman et al. 1991; Crouse et al. 2006). In most engineering applications the flow oscillations are undesirable, thus an immense body of previous studies focused on active or passive methods for suppression of the unwanted excitation (Kook 1997; Shaw 1998; Ma et al. 2009). In contrast, exploration of the potential of a flow-excited Helmholtz resonator to change the turbulence events downstream of the resonator has received very little attention (Lockerby 2001; Ghanadi et al. 2013a). In this novel approach, the resonator is used as a device capable of stabilising or amplifying the instabilities within the incoming boundary layer. Owing to the simplicity of the structure and installation of a Helmholtz resonator, this passive device has significant potential to be used as a flow control device. In this paper the flow fluctuations inside four different resonators and their effect on the structure of the downstream turbulent boundary layer are investigated. The results provide an insight into the ability of Helmholtz resonators to stabilise turbulent events in a boundary layer.

At low Mach numbers, flow-excited resonance occurs when one of the instability frequencies within the shear layer is close to the resonance frequency of the Helmholtz resonator (Meissner 2002; Ma et al. 2009). In general, the self-sustained oscillations in a Helmholtz resonator are generated as a result of the formation of a feedback loop incorporating the following series of events. The vortical perturbations within the shear layer are convected from the leading edge to the trailing edge of the orifice, which results in an increase in the pressure disturbances inside the cavity. The interaction of the vortices with the trailing edge of the orifice generates acoustic pulses which, in turn, triggers the instabilities near the upstream edge and thus new fluctuations are initiated (Kooijman 2007; Holmberg 2010). Around the orifice of the flow-excited Helmholtz resonator small pressure fluctuations generate large magnitude velocity distributions, which in turn increase the pressure fluctuations within the cavity (Hemon et al. 2004).

The self-sustained oscillations in a Helmholtz resonator have been analysed by applying several methods. For example using a simple lumped model, in which the mass and compressibility of the fluid within the neck and cavity, the viscous effects of the flow and acoustic radiation in the vicinity of the orifice are modelled by a mass-spring damper system (Alster 1972; Meissner 2002). Using the compressible Navier-Stokes equations Inagaki et al. (2002) developed a method to predict the frequency of the pressure fluctuations within the shear layer and inside the cavity at low Mach number. It was demonstrated that when the coupling between the vortex shedding and the resonance frequency of the resonator is weak the amplitude of the pressure fluctuations within the resonator is decreased.

The oscillating motion of the flow in the vicinity of the orifice has also been analysed by Hardin & Mason (1977) and Kook et al. (2002) who demonstrated that the boundary layer suddenly separates at the leading edge, resulting in the formation of discrete vortices which grow and are then convected over the orifice. Other studies have found that the flow has a sheet-like motion until it reaches the middle point of the orifice and then breaks into vortical perturbations which convect to the downstream edge (Tam & Block 1978; Howe 1981; Massenzio et al. 2004). Nelson et al. (1981) using Laser Doppler Velocimetry observed that the excitation of a Helmholtz resonator is directly related to the periodic convection of the vortices within the shear layer. The forcing of these vortices was also investigated by Ma et al. (2009) who tested a self-excited Helmholtz resonator for various grazing flow speeds. It was observed that there are no significant changes in the force over a wide range of free stream flow speeds. Using an analytical approach it was also proposed that the velocity field within the shear layer can be described by a superposition of a purely rotational and a potential flow (Nelson et al. 1983). The hydrodynamic flow comes from mean potential and rotational flow, whereas the acoustic field is related to the transient potential flow. This superposition of the aerodynamic and acoustic flows was also used in the feedback loop analysis and the describing function theory to calculate the force of vortex shedding over the orifice (Kook et al. 2002; Mast & Pierce 1995). A detailed description of the coupling between vortex shedding and acoustic resonance over the orifice of a Helmholtz resonator has also been modelled using a CFD solver based on the Lattice Boltzmann Method (LBM) (Ricot et al. 2001). It was shown that eddy viscosity damping is an important parameter affecting the pressure and velocity fluctuations inside the resonator. They demonstrated that the residual background noise has significant effects on the fluctuations inside the cavity and thus models with a low dissipative parameter can simulate the characteristics of the flow accurately.

The influence of inflow conditions on the resonance response has also been investigated by De Jong et al. (2012) who implemented LBM to predict the flow behaviour around a resonator. It was concluded that the fluctuations within the boundary layer have a significant impact on the resonance amplitude, such that when incoming flow is steady an over-prediction occurs. The effects of boundary layer thickness on the convection velocity of vortices over the orifice diameter were also investigated by using Re-Normalization Group methods (RNG) based on the $k - \varepsilon$ turbulence approximation (Mallick et al. 2003). It was concluded that the free stream velocity must be multiplied by a factor of 0.7 to achieve the same convection velocity of the vortices within the shear layer as investigated by Nelson et al. (1981). The importance of the resonator characteristics in the excitation phenomenon was investigated by Panton (1990) who examined three orifices with different orifice shapes. It was found that when the orifice is a slot aligned with the flow direction, the magnitude of the oscillating pressure inside the cavity is decreased significantly in comparison with a circular orifice. Panton & Miller (1975) also showed that strong flow excitation occurs when the orifice diameter is approximately half the diameter of the eddies within the turbulent boundary layer.

In the present study the pressure and velocity fluctuations inside the cavity and in the vicinity of the orifice have been investigated using an LES model with a low dissipative parameter. The ratio of the orifice diameter to the boundary layer thickness has been selected to be in the range of 0.25 to 2, and the unsteady grazing flow has a low turbulence intensity of 0.5%. The purpose of the present research is to (1) investigate the flow features around a flow-excited resonator and (2) to explore the potential of the resonator to affect the instabilities within the turbulent boundary layer. In the next section the governing equations of the proposed model and the simulation procedure are described. In §3 & §4 the characteristics of the grazing flow in the vicinity of the resonator are presented and then in the final section the results are discussed.

## 2. Method of investigation

The flow around a Helmholtz resonator can be modelled as a complex mixing, via strong vortex-acoustic-coupling, of the shear layer over the orifice with the air flow inside the cavity and the multi-scale turbulent boundary layer downstream of the resonator. To simulate the flow behaviour inside and outside of the resonator, as well as capture the turbulent mixing effects in the vicinity of the orifice, an unsteady 3D approach is required. Various turbulence models using unsteady Reynolds-averaged Navier-Stokes (URANS) equations have been proposed to simulate the aeroacoustic behaviour of the flow within the resonators and it was shown that these models, due to their dissipative parameter, are very sensitive to the turbulent viscosity and under-predict the pressure and velocity fluctuations (Candler 1996; Sinha et al. 2000). Using DNS to solve all characteristics of the flow is the most accurate option, however it requires an intensive computational resource (Zhang and Bodony 2014). Three dimensional large-eddy simulation (LES) represents an alternative to DNS, in which small sub-grid scales (SGS) structures are modelled and the large scale ones are resolved through application of a filtering procedure (Moin & Kim 1982; Schlatter 2005). This filtering reduces the computational complexity, such that the high frequencies are removed from the solutions, but their effects on the resolved scales are still taken into account (Georges et al. 2009). This procedure is suitable to model the radiated field induced by the orifice edges, which is directly related to the concentration of the coherent structures within the turbulent boundary layer. Therefore, this unsteady model can capture instabilities within the grazing flow and achieve a strong vortex-acoustic coupling. Therefore in the present study the simulations were carried out using the LES model to calculate the magnitude of the pressure and velocity fluctuations within the boundary layer and the shear layer in the vicinity of the orifice. The details of the numerical procedure and its governing equations are presented in the following section.

### 2.1 Parameters for the simulations

As shown in Figure 1, the resonator is located 1800mm downstream from the inlet surface of a channel. The boundary layer on the lower surface of the channel has been simulated such that there is a fully developed turbulent boundary layer in the vicinity of the resonator orifice. It is important to note that as the boundary layers over the upper and side walls of the channel have an unfavourable impact on the results, it was assumed that there is no friction over these surfaces. The inlet boundary of the flow velocity was set between 1 to 30m/s with a low turbulence level of $Tu \approx 0.5\%$. An atmospheric pressure boundary condition was applied at the outlet, which reduces flow distortion on the boundary as opposed to an outflow condition. To calculate the characteristics of the grazing flow, a spatial discretization method based on the cell-centred finite volume methodology was used in this work because of its low intrinsic numerical dissipation (Larchevêque et al. 2003). Moreover, the second order implicit non-iterative time-advancement scheme has been used for the time advancement.

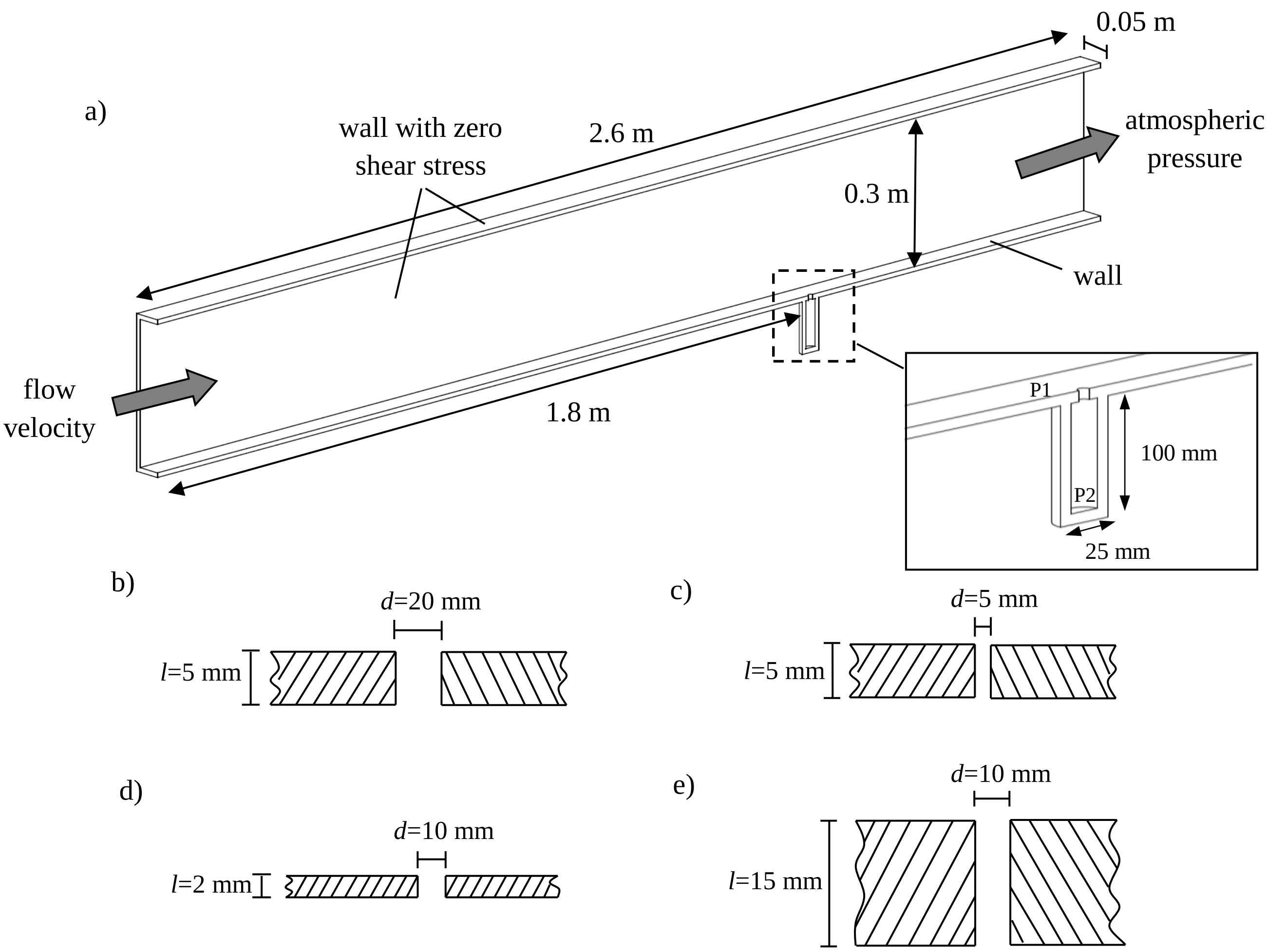


**Figure 1**:Cross-section showing dimensions for the CFD model, a) boundary conditions, cavity dimensions and two points (P1 & P2) for pressure calculations. The neck detail of the four cylindrical Helmholtz resonators (HR); b) HR1, c) HR2, d) HR3 and e) HR4.

The influence of the geometric characteristics of the resonator has been studied previously in an experiment carried out by the authors (Ghanadi et al. 2014) and it was shown that the maximum pressure fluctuations occur when the ratio of the cavity depth ($L$) to its diameter ($D$) is 4. The large amplitude pressure fluctuations induce a force on the shear flow to relieve the pressure inside the cavity. This process may change the structure of the turbulent boundary layer downstream of the resonator. Therefore, as presented in Figure 1, in this study four different cylindrical resonators with different orifice geometries have been modelled. The dimensions of the resonator were chosen such that the ratio of the orifice diameter ($d$) to the boundary layer thickness ($\delta$) is in the range of 0.2 to 2 and its resonance frequency in the range of 400Hz to 800Hz.

In general to accommodate the large length scales of turbulence in the grazing flow and to calculate the effects of the small structures of the turbulent flow, the domain size must be sufficiently large and the mesh scales must be small. Moreover, in LES the inner layer is modelled rather than resolved, thus a high mesh resolution must be utilized to ensure that the viscous dissipation of the kinematic energy is accurately captured. Therefore the first step to accurately model the flow around the resonator is development of a multi-grid mesh with linear transfinite interpolation for the mesh blocks to generate a fine mesh grid in the vicinity of the Helmholtz resonator. It must be noted that to ensure a homogenous mesh within the resonator cavity a hybrid mesh type has been generated in which a H-type mesh exists in the core of the cavity and an O-type mesh is used near the cavity walls. This assists in developing a mesh without a singularity at the origin and reduces the aspect ratio of the cells within the cavity. As suggested by Chapman (1979), in studies such as the present one, the number of grid points, N, in the computational domain is proportional to ${\mathrm{Re}_\mathrm{x}}^{2/5}$ (where $\mathrm{Re}_\mathrm{x} = \mathrm{Ux}/\nu$) and should be increased such that in the near wall region the number of grid points is proportional to ${\mathrm{Re}_\mathrm{x}}^{9/5}$. However, as demonstrated by Choi and Moin (2012), this number should be further increased to ${\mathrm{Re}_\mathrm{x}}^{13/7}$ for accurate estimation of boundary layer properties over wide range of Reynolds numbers. As illustrated in Figure 2, the structured fine meshes were used throughout the domain to fit the geometry and support a high amount of skewness and stretching without affecting the results. This kind of mesh keeps the first few layers as uniform as possible, as required to capture the longitudinal vortices within the boundary layer. For all case studies there were at least 3 cells in the viscous sublayer and the dimensionless wall distance, $Y^+$, was less than 0.4, which indicates that the mesh is capable of capturing the near wall fluctuations. The grid spacing in streamwise, spanwise and wall-normal directions, expressed in wall units, are $\Delta x^+ = 84$ to 160, $\Delta y^+= 15$ to 21 and $\Delta z^+= 37$ to 58, respectively. To establish the mesh-independent solution, three cases with a total number of nodes of $1.5 \times 10^6$ to $4.8 \times 10^6$ were generated and the results compared with the experimental findings obtained by Ghanadi et al. (2014). The sensitivity of the solution to the pressure fluctuations within the resonator cavity, and the mean and fluctuating velocity profiles upstream of the resonators demonstrated that meshes with $2.5 \times 10^6$ to $2.8 \times 10^6$ nodes are appropriate for the resonators studied here.

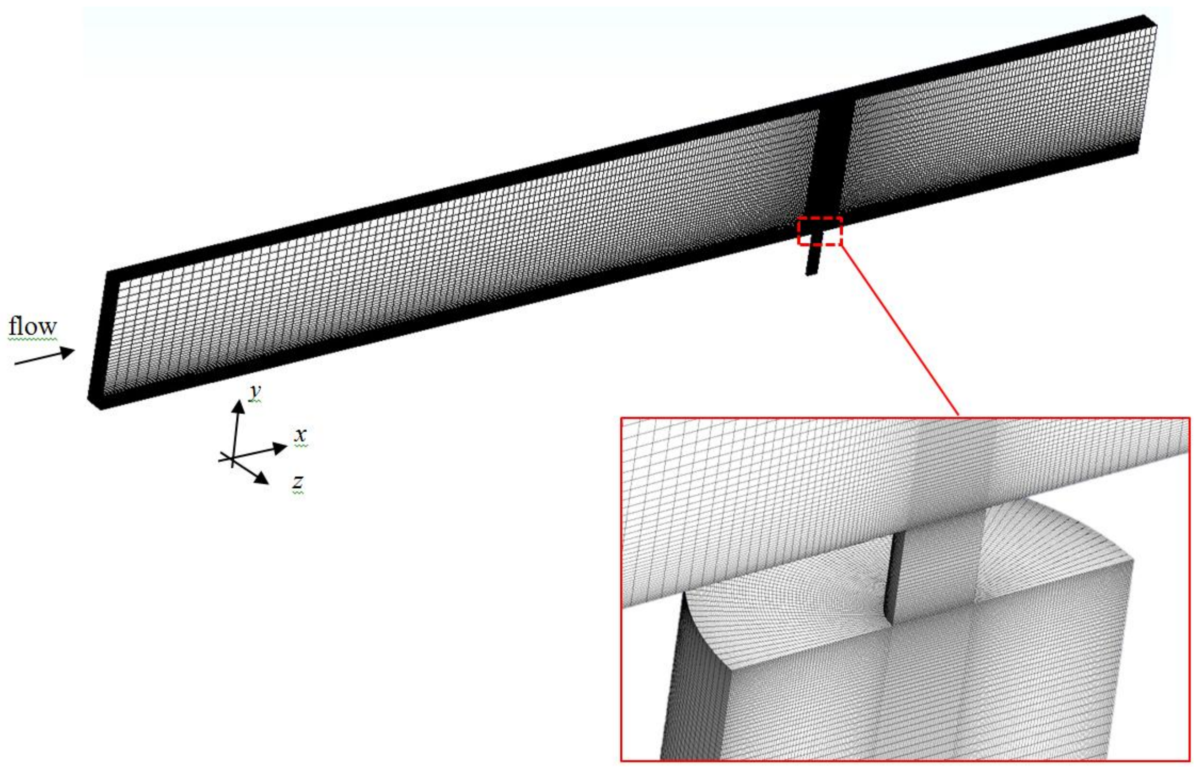


**Figure 2**: Volumetric fine mesh in the vicinity of the orifice of the resonator.

### 2.2 Computational model and governing equations

The simulations were carried out using the compressible Navier-Stokes equations to model the compressibility of the flow inside the cavity. In LES the conservation of mass and momentum equations are typically filtered with the related filter operator (Favre 1983) as

$$\tilde{f}_L = \frac{\overline{\rho f_L}}{\bar{\rho}}, \tag{1}$$

where $f_L$ is any flow variable, for example the velocity in all three directions, and $\rho$ is the flow density. The bar denotes the filtered variables and the ~ operator corresponds to a change of variables. Therefore, the filtered momentum and mass conservation equations yield (Vreman 1995)

$$\frac{\partial \bar{\rho}}{\partial t} + \nabla.(\bar{\rho}\tilde{u}) = 0, \tag{2}$$

$$\frac{\partial(\bar{\rho}\tilde{u})}{\partial t} + \nabla.(\bar{\rho}\tilde{u}\tilde{u}) + \nabla.\bar{p} - \nabla.\tilde{\tau}_v = -\nabla.\tau + \nabla.(\bar{\tau}_v - \tilde{\tau}_v), \tag{3}$$

where $u$ is the flow velocity, $\tau_v$ is the viscous stress, and $\tau$ is the sub-grid scale stress. The term $\tau$ represents their effects based on an eddy viscosity assumption as

$$\tau_{ij} - \tfrac{1}{3}\tau_{kk}\delta_{ij} = 2\mu_t\overline{S}_{ij}, \tag{4}$$

where

$$\overline{S}_{ij} = \tfrac{1}{2}\left(\frac{\partial \overline{u}_i}{\partial x_j} + \frac{\partial \overline{u}_j}{\partial x_i}\right), \tag{5}$$

and $\overline{S}_{ij}$ is the deformation tensor of the sub-grid field. There are several models available to calculate the eddy viscosity, $\nu_t$; for example in the Smagorinsky model this parameter is simply calculated through local strain rate (Addad et al. 2003; Chai & Mahesh 2012). However, one of the more accurate models commonly used to calculate $\nu_t$ is the WALE (Wall Adapting Local Eddy-viscosity) sub-grid model. This model is based on the square of the velocity gradient tensor, and accounts for the effects of both the strain and the rotation rate of the smallest resolved turbulent fluctuations and no explicit filtering is needed (Toda et al. 2010). Unlike Smagorinsky's, this model is sensitive to both the strain and rotation rate of the small turbulent structures. In the present study the WALE model was used to calculate the eddy viscosity as (Nicoud & Ducros 1999)

$$\nu_t = \left(\frac{1}{2} \times \Delta x\right)^2 \frac{\left(S_{ij}^d S_{ij}^d\right)^{\frac{3}{2}}}{\left(\bar{S}_{ij}\bar{S}_{ij}\right)^{\frac{5}{2}} + \left(S_{ij}^d S_{ij}^d\right)^{\frac{5}{4}}}, \tag{6}$$

where

$$S_{ij}^d = \frac{1}{2}\left(\left(\frac{\partial \overline{u}_i}{\partial x_j}\right)^2 + \left(\frac{\partial \overline{u}_j}{\partial x_i}\right)^2\right) - \frac{1}{3}\delta_{ij}\left(\frac{\partial \overline{u}_k}{\partial x_k}\right)^2, \tag{7}$$

and the $d$ superscript represents the deviatoric part and $\delta_{ij}$ is the Kronecker delta. For completeness, the characteristics of the incoming flow and boundary conditions will be described in the next section and the mesh grid resolution effects in the near wall regions are also discussed.

### 3. Validation of the numerical model

In a flow-excited Helmholtz resonator, resonance occurs when the frequency of the pressure fluctuations within the resonator is very close to the natural frequency of the resonator. Therefore, the calculation of the pressure fluctuations in the presence of grazing flow is the first important step in the present study. In the experiments conducted by Ghanadi et al. (2014), the upstream pressure fluctuations were measured using a single microphone located upstream of the resonator orifice. For comparison, the pressure fluctuations have also been calculated at one fixed location of P1($y \approx 0, z = z_1$ , t) upstream of the resonator. For the purpose of validation the calculated pressure fluctuations within the incoming turbulent boundary layer were compared with the DNS solution obtained by Jimenez et al. (2010). As shown in Figure 3 the simulation results were found to agree well with experimental data throughout the boundary layer thickness.

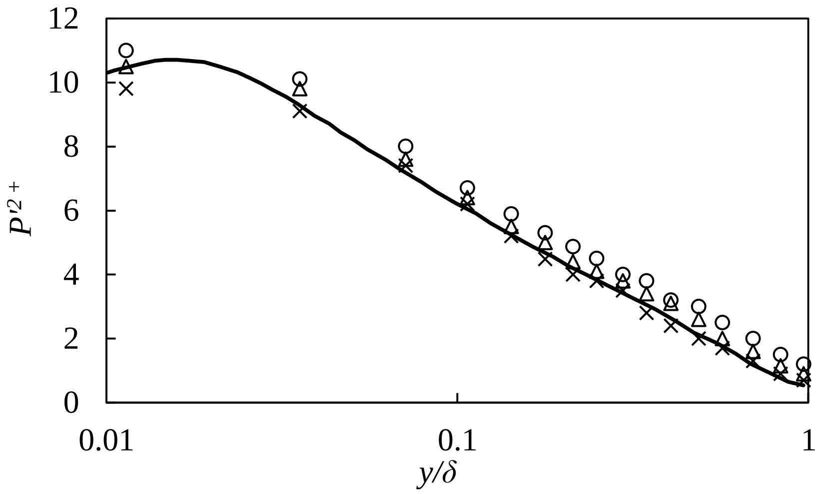


**Figure 3:** Profiles of the pressure fluctuation intensities; DNS results obtained by Jimenez et al. (2010) (solid line), $Re_\theta$=1824 (cross) $Re_\theta$= 2944 (triangle) $Re_\theta$=4163 (circle).

The difference between the instantaneous pressure within the incoming turbulent boundary layer (P1 in Figure (1a)) and that inside the resonators (P2), has been calculated at three different flow speeds and compared against previous experimental data (Ghanadi et al. 2014). The Power Spectral Density (PSD) of the pressure difference between P1 and P2 has been calculated and compared with experimental results when $U$=23m/s. The PSD was obtained using a Hanning window with $2^7$ FFT points and a 50% overlap for averaging. As shown in Figure 4(a), the frequency and magnitude of the calculated pressure response for HR1 are very close to the experimental data. However, for an unknown reason there is a small peak in the pressure response at 380Hz which the CFD results do not predict. The PSD difference of the pressure fluctuations for HR2 and HR4 are also in relatively good agreement with the experimental results over the range of frequencies examined (Figure 4(b & d)). It must be noted that, as shown in Figure 4(c), the maximum PSD value for HR3 occurs at a slightly higher frequency compared with the experimental results. The source of this mismatch is thought to be due to both the input impedance of the resonator as well as the radiation impedance of the resonator into the coupled channel not being adequately captured in the LES model.

The resonance frequency in both the experimental and numerical data is associated with the maximum peaks in the pressure response. In Table 1 the calculated resonance frequencies are presented and compared with the experimental data and expected values obtained using the empirical formula (Panton & Miller 1975; Howard et al. 2005)

$$f_r = \frac{c}{2\pi}\sqrt{\frac{S}{l_e V_c + 0.33L^2\,S}}, \tag{8}$$

where $c$ is the speed of sound, $l_e$ is the effective length of the orifice, $L$ is the cavity depth, $S$ the cross-section area of the orifice and $V_c$ is the cavity volume. It was demonstrated that the resonance frequencies calculated using the LES model are relatively close (less than 2.5% difference) to the experimental values, and are much closer than the values estimated using Equation (8), which differ to the experiments by up to 16%.

**Table 1:** Characteristics of the resonators and predicted, and experimentally measured resonance frequencies. $L/D$=4 in all cases.

| | Resonator parameters | | $f_r$ (Hz) | | |
|---|---|---|---|---|---|
| Helmholtz resonator designation | $l/D$ (non-dimensional orifice length) | $d/D$ (non-dimensional orifice diameter) | CFD | Exp. | Empirical |
| HR1 | 0.2 | 0.8 | 722 | 712 | 748 |
| HR2 | 0.2 | 0.2 | 414 | 402 | 338 |
| HR3 | 0.08 | 0.4 | 619 | 605 | 592 |
| HR4 | 0.6 | 0.4 | 561 | 550 | 498 |

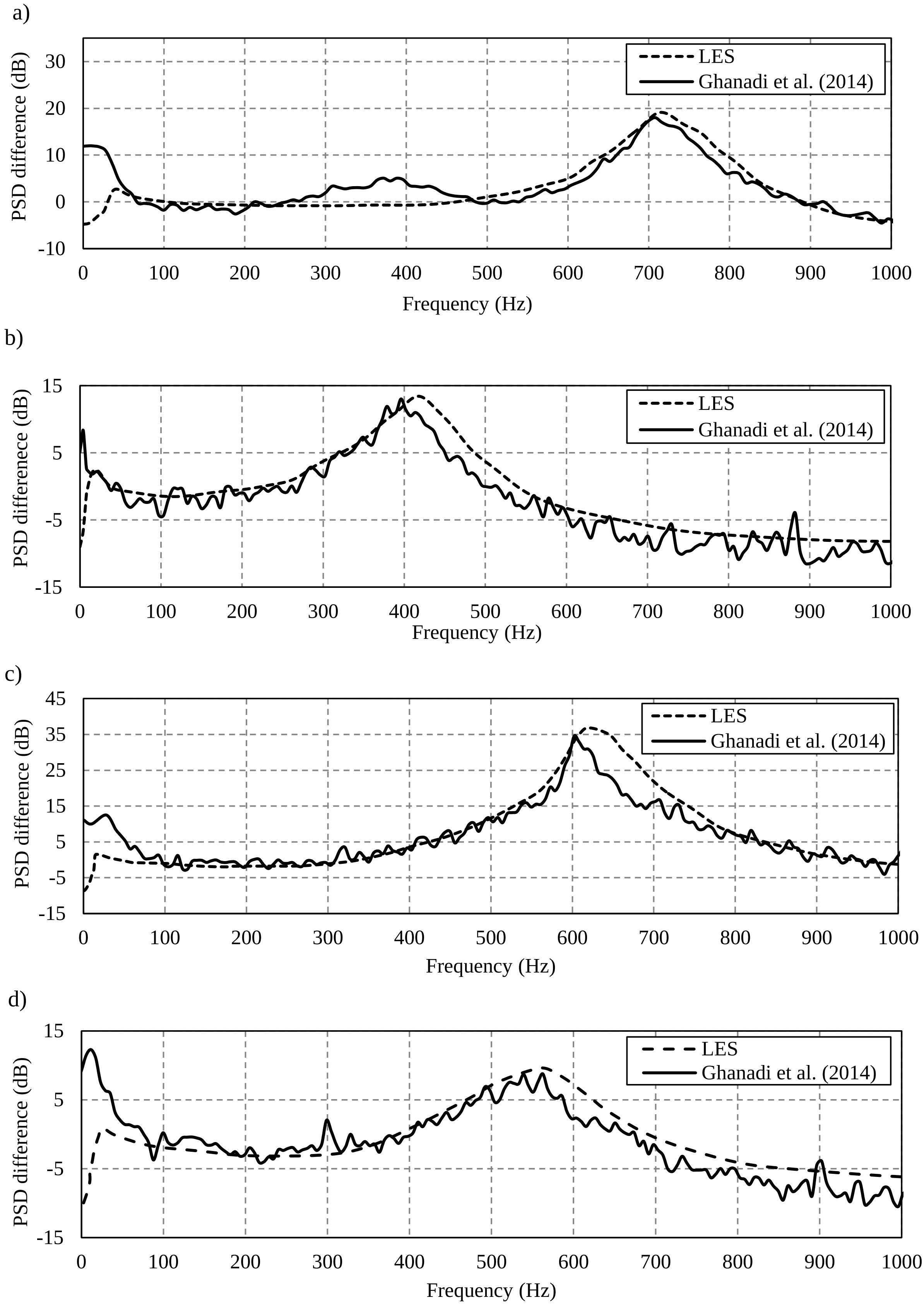


**Figure 4:** PSD of the difference between PSD of the pressure fluctuations within the incoming turbulent boundary layer and inside the cavity of the resonator at $Re_\theta$= 2944; a) HR1, b) HR2, c) HR3, d) HR4.

To verify that the turbulent boundary layer over the resonators is fully developed, the streamwise mean velocity and turbulence intensity were calculated and compared against published data. There are a number of experimental and numerical studies focusing on the flow properties across entire zero pressure wall turbulent boundary layer (Moin & Kim 1982; Klewicki et al. 2009; Sillero et al. 2013). The results obtained by Marusic & Kunkel (2003) have been chosen for validation purposes in this paper because their formulation can describe the properties of the turbulent boundary layer with a high degree of accuracy over a large range of Reynolds numbers. Figure 5 shows the characteristics of the turbulent boundary layer upstream of the orifice. There is relatively good agreement between the simulation results and the published data for mean velocity within all the regions (Figure 5(a)). As shown in Figure 5(b) there is a mismatch of up to 10% between the data for turbulence intensity within the viscous region, due to the energy dissipation of the model for subgrid scales. This level of discrepancy is considered acceptable for prediction of the turbulence intensity (Inoue 2012). Table 2, presents the dimension of the box for the boundary layer simulation at different momentum thickness Reynolds numbers, $\mathrm{Re}_\theta = U\theta/\nu$.

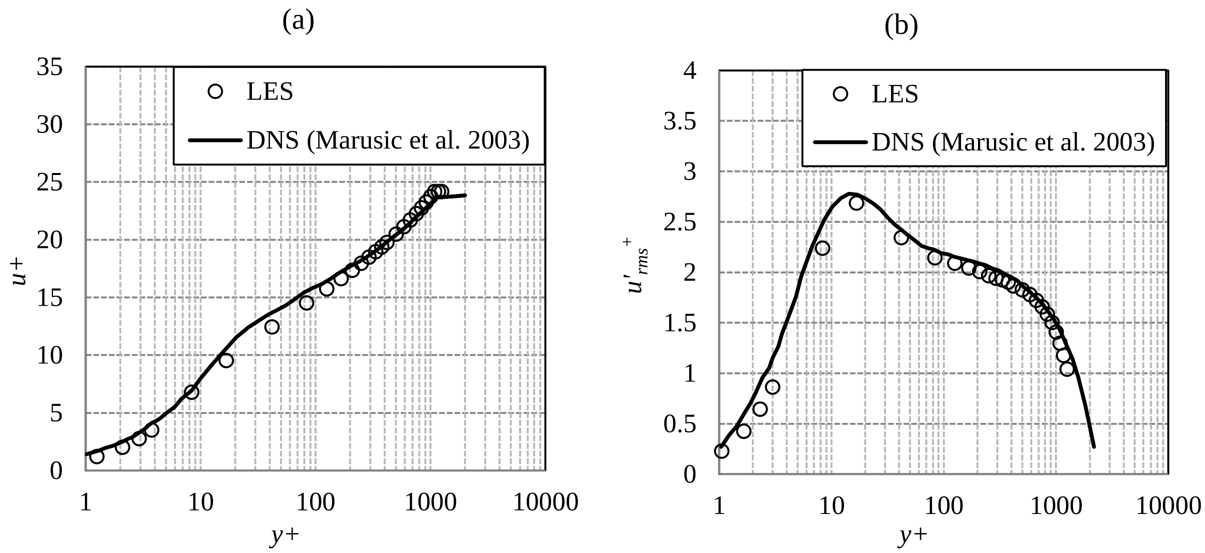


**Figure 5:** Streamwise velocity profiles within the turbulent boundary layer upstream of the resonator a) mean velocity; b) turbulence intensity.

Other parameters can also be compared with the data available in the literature to verify the simulation results. For example, the shape factor $H \approx \delta^*/\theta$ and the local skin-friction coefficient $C_f \approx 0.058 Re_x^{-1/5}$ of the incoming turbulent boundary layer have been selected to compare with LES results obtained by Eitel-Amor et al. (2014). The error bars presented in Figure 6 demonstrate that the simulation can accurately calculate the boundary layer parameters.

**Table 2.** Characteristics of incoming turbulent boundary layer. $L_x$, $L_y$, and $L_z$ are the box dimensions along the three axes. $N_x$, $N_y$, and $N_z$ are the collocation points. $T$ is the total time over which turbulence statistics are collected.

| $U^+$ | $\mathrm{Re}_\theta$ | $\{L_x, L_y, L_z\}/\theta$ | $N_x, N_y, N_z$ | $Tu_\tau/\delta$ |
|---|---|---|---|---|
| 20 | 1168-1824 | 467×18×29 | 383×70×73 | 19.6 |
| 21 | 1808-2944 | 421×16×26 | 387×74×74 | 18.7 |
| 23 | 2300-4163 | 402×14×23 | 394×76×78 | 15.8 |

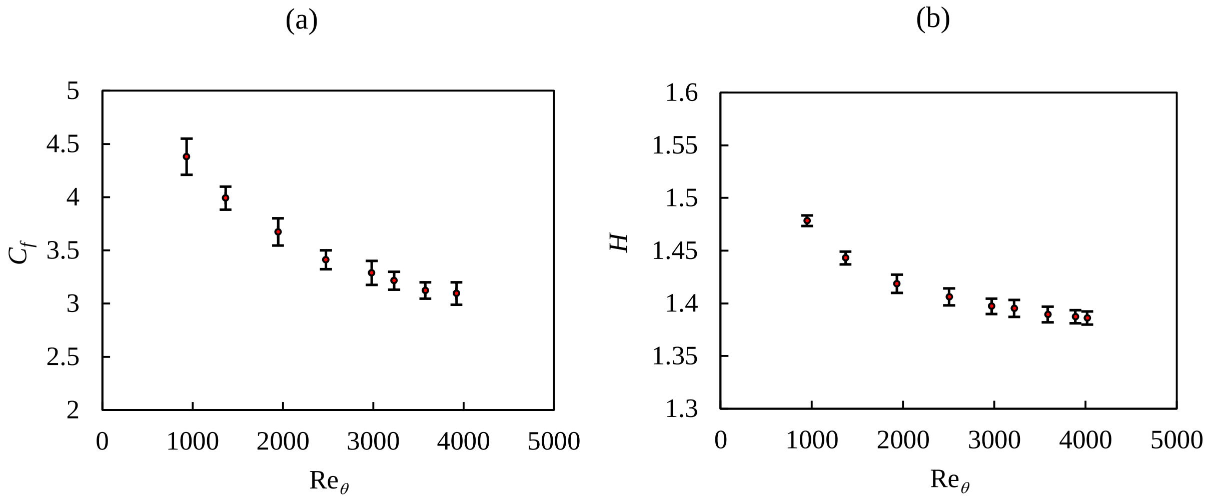


Figure 6: Turbulent boundary layer parameters; (a) skin friction and (b) shape factor.

## 4. Pressure fluctuations in the presence of grazing flow

The pressure fluctuations inside each of the resonators were calculated over a range of free stream velocities. At resonance the large magnitude of the pressure within the cavity forces the shear layer out of the orifice. This process changes the characteristics of the boundary layer in the vicinity of the resonator. Therefore, in the present study the effects of the resonator on the grazing flow were considered when the high-amplitude pressure fluctuations inside the resonator occur. In the present study the velocities were varied between 16 to 28m/s because in the experiment carried out by Ghanadi et al. (2014) it was observed that there are no significant pressure fluctuations when $U < 16$ m/s due to weak instabilities within the grazing flow. In order to understand the effects of the boundary layer on the flow behaviour inside the cavity, in the results presented in this paper the resonator dimensions have been normalized by boundary layer thickness. As can be seen in Figure 7(a), when the orifice diameter is close to the boundary layer thickness, $\delta/d$ =1, the frequency of the maximum pressure fluctuations calculated by LES occurs very close to the experimentally measured resonance frequency of the resonator (≈ 712 Hz). Further increasing $\delta/d$ decreases the value of the maximum pressure fluctuations inside HR2 (Figure 7b). It is hypothesised that in the case of HR2 the large eddies within the thick turbulent boundary layer cannot easily penetrate the cavity. Moreover, with increasing $\mathrm{Re}_\tau$ the convection velocity of the vortices within the shear layer is increased (Kooijman et al. 2008; Nakiboglu et al. 2011), which in turn reduces the interaction of the cavity flow with the vortices. Figure 7(c) shows that the pressure variation inside the resonator is very sensitive to the orifice length. When the orifice length is approximately 10% of the boundary layer thickness the maximum amplitude in the pressure PSD occurs very close to the resonance frequency. By comparing the results presented in Figure 7(c) and Figure 7(d) it was demonstrated that the maximum magnitude of the PSD pressure difference drops by almost 22 dB as the ratio of boundary layer thickness to the orifice length, $\delta/l$, approaches unity. It is hypothesized that this is due to the viscous effects along the long orifice ($l \approx \delta$) which act as an effective damping parameter, reducing the pressure fluctuations inside the resonator.

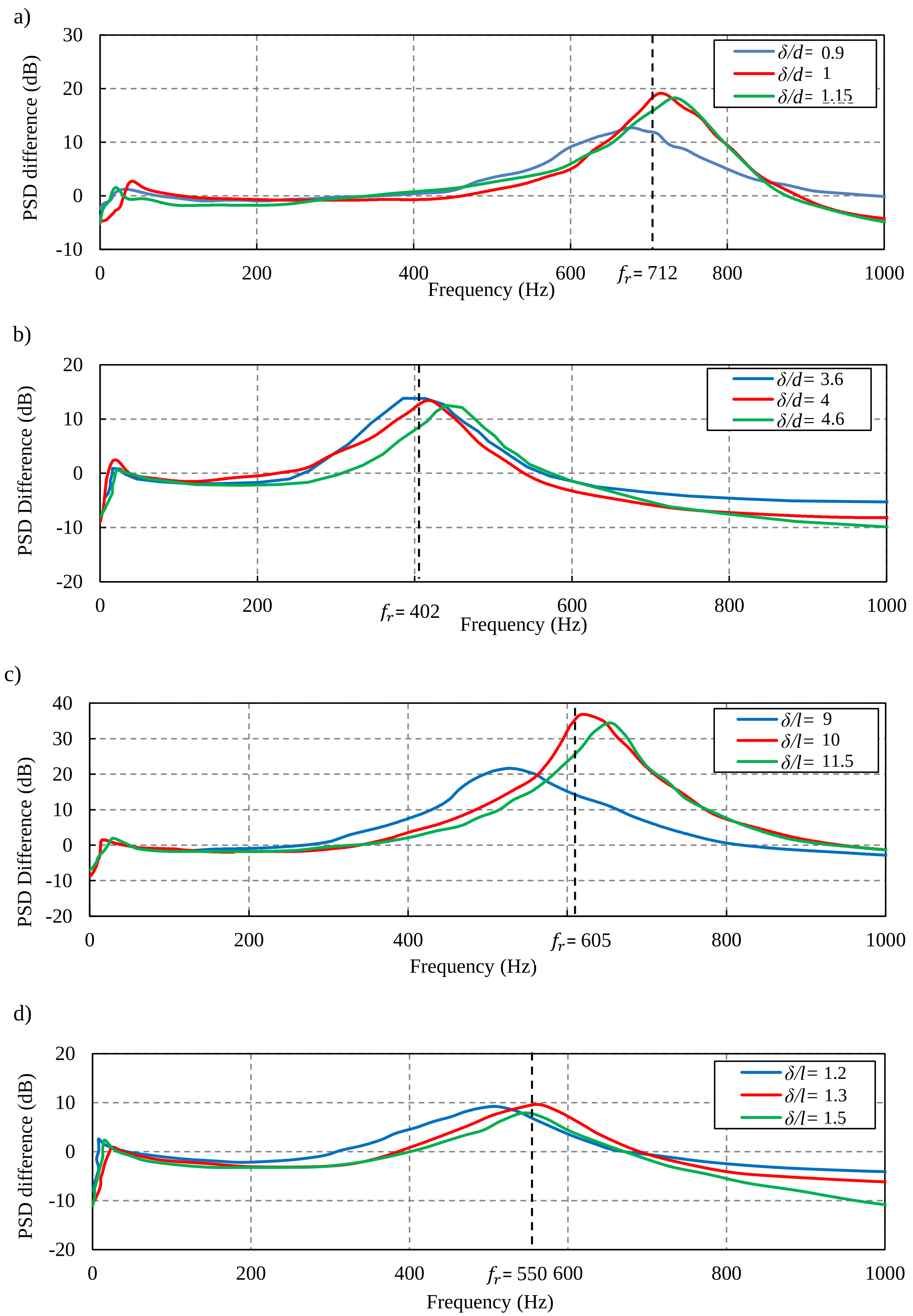


**Figure 7:** Amplitude and frequency of the PSD pressure difference between inside the resonators and incoming flow for different $\delta/l$ ratio; a) HR1, b) HR2, c) HR3, d) HR4. The value of the resonance frequency of each resonator is indicated on each graph by the dashed line.

## 5. Characteristics of the turbulent boundary layer around the orifice

In this section the grazing flow behaviour in the vicinity of the resonator orifice is analysed. Initially the unexcited turbulent boundary layer upstream of the orifice has been characterized and then the effects of the resonator on the turbulent boundary layer have been investigated. As shown in Figure 8, Point 1 was chosen to be sufficiently far upstream of the orifice to calculate the characteristics of the unaffected boundary layer. The local influence of the resonator on the turbulent boundary layer has been analysed at the location of Point 2. The characteristics of the boundary layer at Points 3 and 4 show the durability of the resonator impact on the grazing flow. Also shown in Figure 8 are ten equally spaced locations (S1 to S10) where the velocity fluctuations within the shear layer over the orifice were calculated to analyse the grazing flow behaviour in the vicinity of the resonator opening.

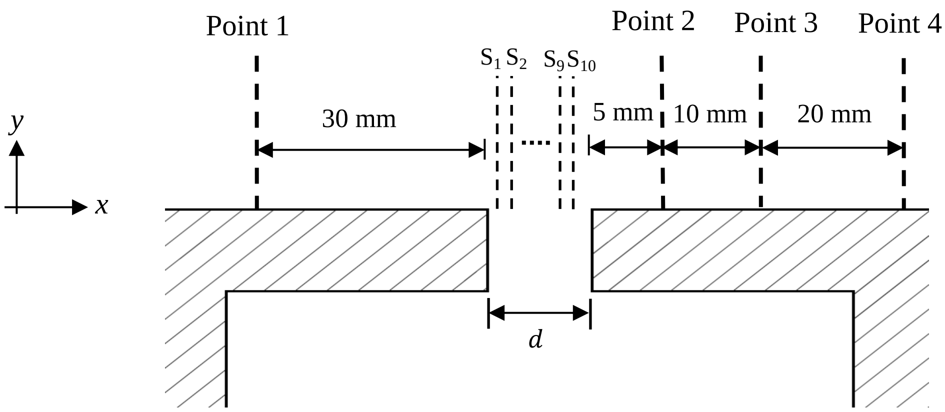


**Figure 8:** Upstream and downstream positions for calculations.

The Helmholtz resonator can act to stabilise or destabilise the turbulent boundary layer. To investigate the extent of this effect, the streamwise averaged turbulence intensity, ${u'_{rms}}^+$, downstream of each resonator has been compared with the turbulence intensity of an unexcited turbulent boundary layer at P1 for three different velocities (Figure 9). At $Re_\theta = 1824$ the resonator with the greatest orifice diameter, HR1, amplifies the velocity fluctuations within the boundary layer in the region $50 < y^+ < 200$. This destabilization is due to the strong interaction between the vortices within the shear layer and the cavity flow. This leads to generation of a fast jet in the vicinity of the orifice, which results in amplification of the instabilities. As shown in Figure 9, the effect of HR1 is not local and extends at least to Point 4, a distance of approximately 2d downstream of the resonator. At a higher flow velocity of $Re_\theta = 2944$, the location of the amplified turbulence intensity downstream of HR1, at all points, is shifted away from the surface to $80 < y^+ < 400$. High pressure fluctuations within HR1 lead to greater flow injection, which in turn increases the turbulence intensity downstream of the orifice. The amplification of the velocity fluctuations downstream of HR1, also occurs at $Re_\theta = 4163$, although the amplitude is decreased by 5% compared to $Re_\theta = 2944$. It must be noted that the peak value of the instabilities is also shifted closer to the fully turbulent region at $y^+ = 273$.

Figure 9 also shows that at $Re_\theta = 1824$, HR2 reduces the velocity fluctuations within the logarithmic region of the turbulent boundary layer, $11 < y^+ < 650$, by up to 16% at Point 3. At $Re_\theta = 1824$, the boundary layer thickness over HR2 is approximately 4 times the orifice diameter, which results in a diminishing of the effects of the grazing flow on the pressure increase inside the cavity. As noted before, at $Re_\theta = 2944$ the pressure fluctuations inside HR2 are the same as for $Re_\theta = 1824$, however the higher free stream velocity increases the interaction of vortices with the orifice edges and thus the boundary layer is more unstable. At a higher flow velocity of $Re_\theta = 4163$, as investigated in the previous experiments by the authors (Ghanadi et al. 2014), downstream of HR2, at Point 2, a jump in the turbulence intensity occurs over a small section of the boundary layer $75 < y^+ < 125$.

There is a slight reduction in the turbulence intensity of up to 8% downstream of HR3 at Point 3 in the region $20 < y^+ < 50$ when $Re_\theta$ =1824. It must be noted that the maximum value of the PSD of the pressure fluctuations inside HR3 were higher than HR1, however the ratio of the orifice diameter to the boundary layer thickness is smaller. Interestingly, the turbulence intensity is increased by 9% far from the downstream edge of the orifice. It was observed that the maximum pressure fluctuations inside HR3 occur at $Re_\theta$ =2944, which leads to increased flow injection in the vicinity of the orifice and thus the turbulence intensity at Point 3 is increased by a maximum of 20% at $20 < y^+ < 90$. By comparing the turbulence intensity at $Re_\theta = 2944$ with the results for $Re_\theta = 4163$, it was found that the magnitude of the velocity fluctuations within the logarithmic region downstream of HR3 are decreased by up to 10% at the higher flow speed. It was hypothesized that the flow suction area over the orifice is more than the flow injection area which assists the stabilization process.

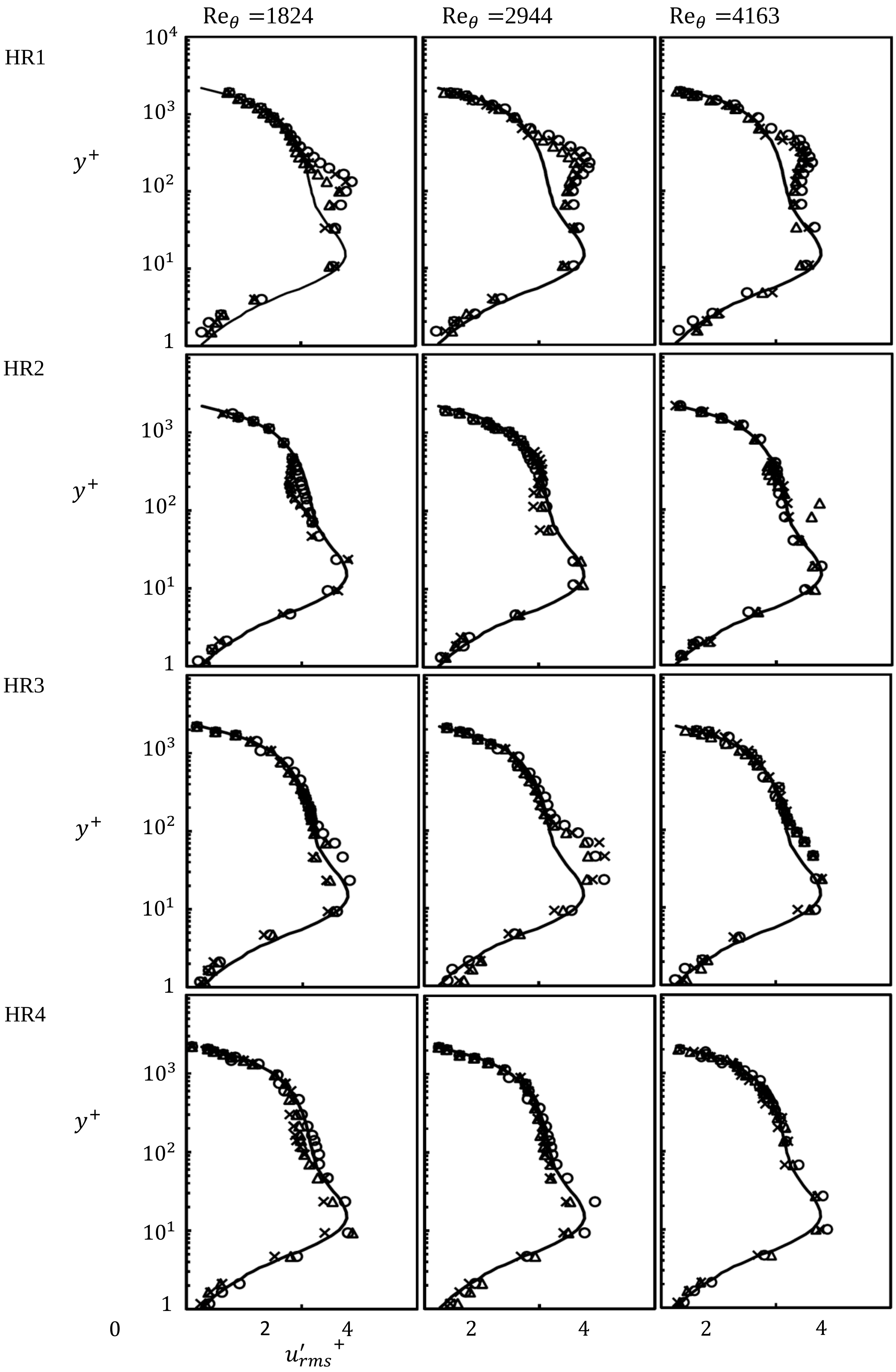


**Figure 9:** Turbulence intensity profiles within the boundary layer downstream of the resonators; Point 2 (triangle), Point 3 (cross), Point 4 (circle) and unexcited turbulent boundary layer (line).

Up to $y^{+} = 200$ the velocity fluctuations in the vicinity of the orifice of HR4 are decreased by a maximum of 12% when $\mathrm{Re}_{\theta}$ =1824 at Points 2 and 3. It seems that because of the long orifice length, the pressure fluctuations inside HR4 cannot significantly change the structure of the turbulent boundary layer in the near wall region. This flow behaviour is due to the damping effect of the longest neck investigated so that at Point 4 slight pressure fluctuations within the resonator have minimal effects on the structure of the boundary layer. The increased boundary layer thickness over HR4 at the higher Reynolds number of $\mathrm{Re}_{\theta}$ =2944 causes greater flow injection and thus the stabilization effect of this resonator is slightly decreased at Points 3 and 4. As stated before, the maximum peak value of the pressure fluctuations inside HR4 was decreased by 20% at $\mathrm{Re}_{\theta} = 4163$, relative to the corresponding value for $\mathrm{Re}_{\theta} = 2944$ and thus the flow is more stable at least to Point 4.

One common feature of drag reducing flows is a reduction by 10% to 30% in the streamwise turbulence intensities in the viscous and logarithmic regions (Laadhari et al. 1994; Choi and Clayton 2001; Jukes et al. 2006; Lee et al. 2008). In the present study the results associated with HR2 and HR4 at $\mathrm{Re}_{\theta}$ =1824 and $\mathrm{Re}_{\theta}$ =2944 present a decrease in the turbulence production, which is in agreement with other drag reduction techniques. It must be noted that downwash of quasi-longitudinal vortices which brings the high momentum fluid towards the surface (sweep) is also responsible for an increase in the skin-friction drag (Rebbeck and Choi 2001; Jukes 2007). However a detailed discussion of sweep changes is beyond the scope of this paper, and will be addressed in future investigations.

It should be noted that the effects of a flow-excited Helmholtz resonator on the instabilities within the boundary layer can be compared with the changes in turbulent structures made by other mechanisms, such as riblets or wall oscillation. In these drag reduction mechanisms artificial vortices disrupt the turbulence production cycle and result in a reduction in the sweep intensity and duration. As can be seen in Figure 10, the turbulence intensity downstream of HR4, at $\mathrm{Re}_{\theta}$ =2944, has a similar trend to the data for riblets and oscillating wall methods (Choi and Clayton 2001; Lee and Choi 2008). As marked in the plot, the maximum reduction of instabilities occurs within the viscous sub-layer and logarithmic regions $9 < y^{+} < 130$.

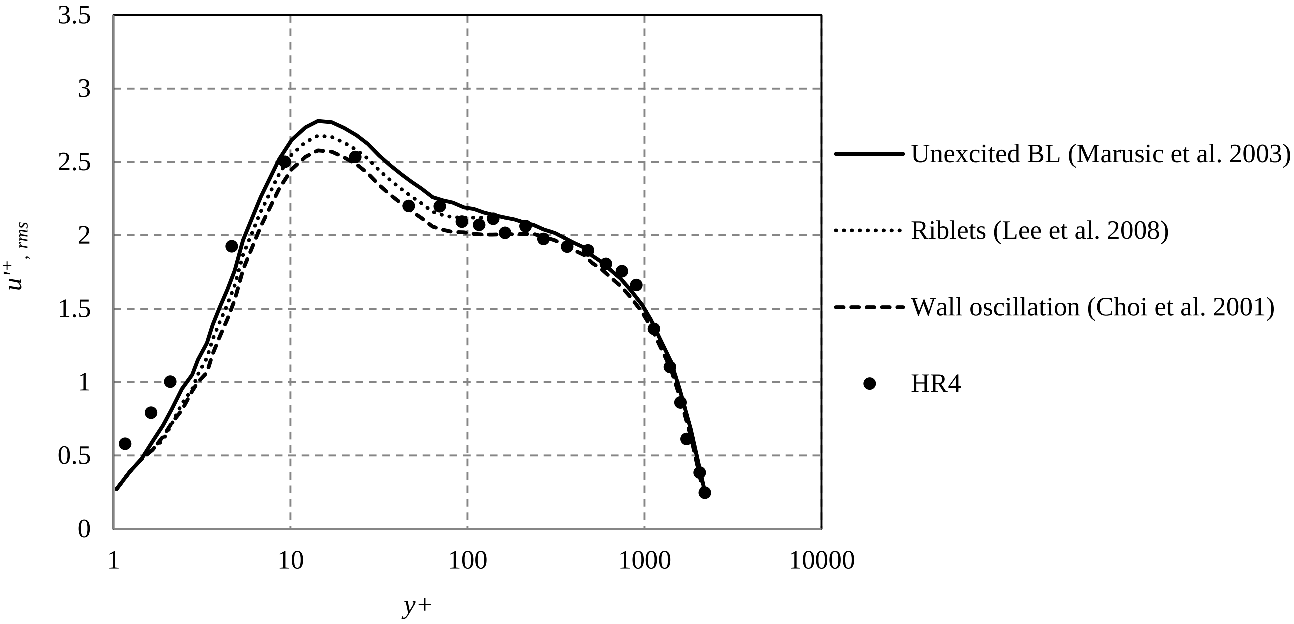


**Figure 10:** Near-wall profiles of the turbulence intensity for the current study compared to riblets (Lee & Choi 2008) and wall oscillation (Choi & Clayton 2001).

This reduction in turbulence intensities can also be seen in the energy spectra of the velocity fluctuations throughout the aforementioned regions. The energy spectra of the streamwise velocity at one spatial position in the logarithmic region of the boundary layer ($y^+$=35) downstream of the orifice of HR4 were compared with unexcited data. As shown in Figure 11, the turbulence energy has decreased at low frequencies, $f < 80$ Hz, while the energy at higher frequencies is increased. This shifted energy is due to the fact that the large eddies in the near wall region downstream of HR4 transfer their energy to the small structures, thereby reducing the energy at low frequencies. Choi and Clayton (2001) observed the same trend in the energy spectra of the eddies within the logarithmic region of the boundary layer when excited by the wall oscillation technique. Therefore, it was concluded that a Helmholtz resonator can be used as a passive device to stabilize the fluctuations within the boundary layer and suppress the turbulence production. Post-processing of the presented numerical data has demonstrated that the Helmholtz resonator can change the skewness, kurtosis and PDF (Probability density function) profiles. The effects of the vortices generated by the Helmholtz resonator on the instabilities and the intensity and duration of the sweep events are the subject of further work.

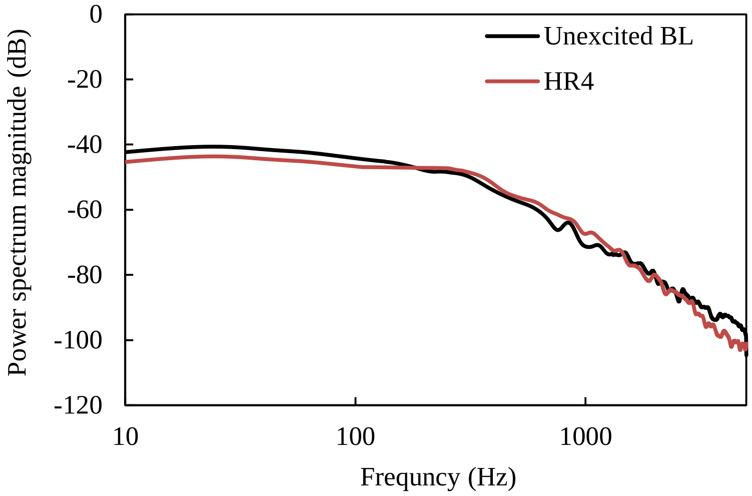


**Figure 11:** Energy spectra of streamwise velocity fluctuations at $y^{+}$= 35 downstream of HR4 at $\mathrm{Re}_{\theta}$ $= 2944$.

## 1. Characteristics of the shear layer

The flow patterns in the vicinity of each resonator have been investigated in order to understand the effects of the flow pulsation on improving the flow instabilities. The $y$ component of the instantaneous velocity, $w$, during one period, $T = 1/f_r$, has been presented via contour and vector plots. As discussed, HR1 increases the streamwise velocity fluctuations within the logarithmic region of the boundary layer whilst the flow is more stable downstream of HR4. Therefore, comparison of the flow pulsation over the orifice of these two resonators can provide an insight into the effects of the flow suction/injection on the stability of the grazing flow. The vector forms were chosen to investigate the different flow behaviour around these two resonators (Figure 12). As shown in Figure 12(a-d), for resonator HR1 the flow injection area is greater than the area where the flow suction occurs. It can also be seen that the maximum flow injection and suction occurs very close to the trailing edge of the orifice. This flow behaviour causes high turbulence production within the logarithmic region downstream of HR1 at $\mathrm{Re}_{\theta} = 2944$. It should also be noted that there is little fluctuation within the grazing flow in the first quarter of the orifice. The velocity vectors for HR4 at $\mathrm{Re}_{\theta}$ =4163 reveal that the flow suction area is more than the flow injection area, which results in suppression of the instabilities (Figure 12 e-h). It was seen that in the first half of the period, $T/4 < t < T/2$, the maximum value of the flow suction is slightly increased with time and moves toward the trailing edge. As discussed previously, downstream of HR4 at $\mathrm{Re}_{\theta}$ =4163 there is a slight reduction in the instabilities within the turbulent boundary layer, which is thought to be associated with this flow behaviour. It should be noted that the frequency and amplitude of the fluctuations within the shear layer over HR1 are greater than those for HR4. This demonstrates that the stabilisation and amplification of the instabilities within the boundary layer are related to the frequency and magnitude of the velocity pulsations generated by the resonators. Comparison of the pulsation frequencies and the frequency of sweep or ejection events is the subject of further work.

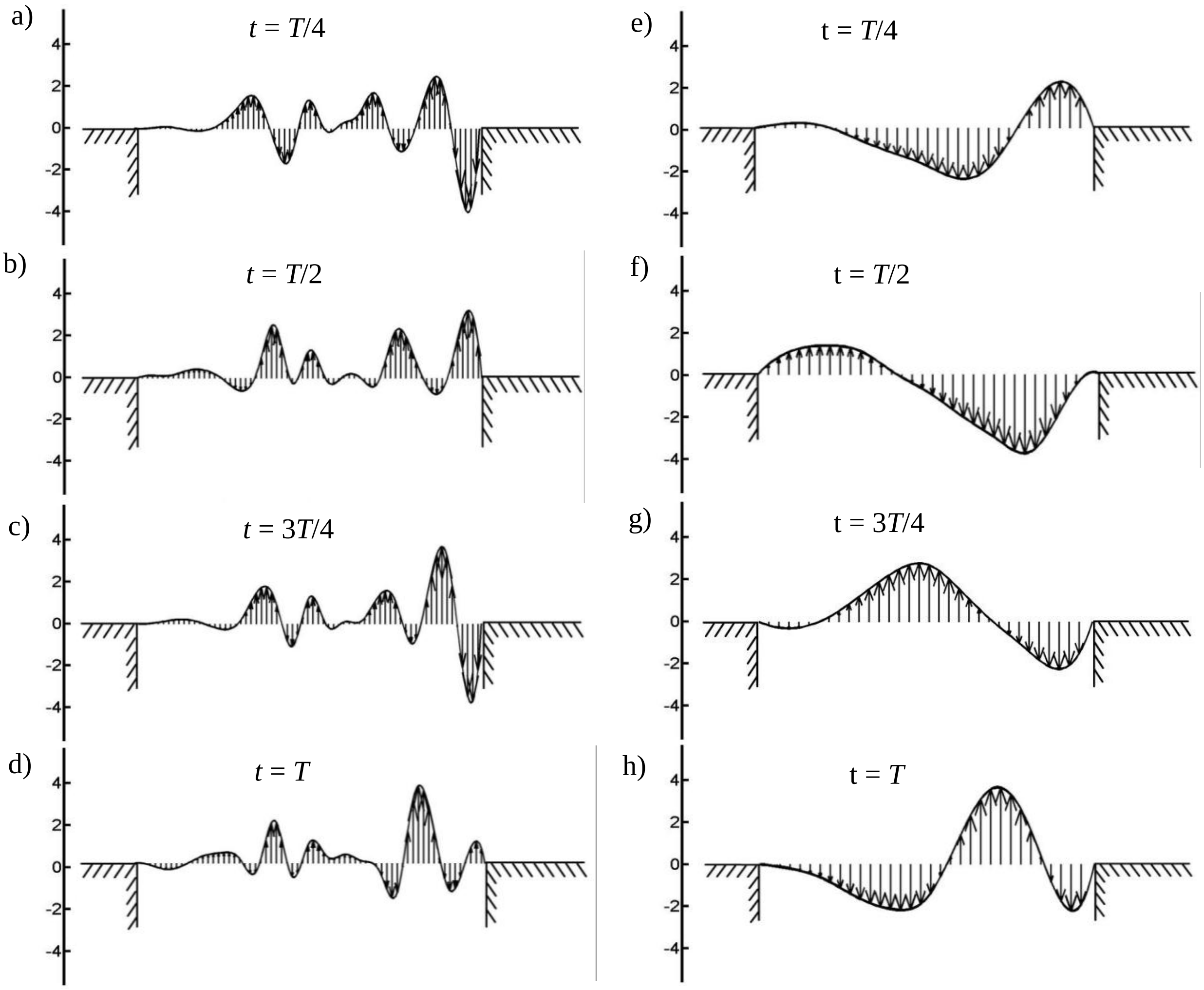


**Figure 12:** $y$ component of the instantaneous velocity, $w$, over the orifice exit: (a-d) HR1 at $\mathrm{Re}_\theta$= 2944 and (e-h) HR4 at $\mathrm{Re}_\theta$= 4163 (scale unit is in m/s).

Extending the discussion to the remaining two resonators, HR2 at $\mathrm{Re}_\theta = 1824$ can stabilize, and HR3 at $\mathrm{Re}_\theta = 4163$ can destabilize, the instabilities within the downstream flow, respectively. Therefore HR2 and HR3 have been selected to show the contours of the y component of the velocity fluctuations in the vicinity of the orifice. The results provide an insight into the effects of shed vortices within the shear layer and the logarithmic region of the boundary layer in modification of the instabilities. Figure 13 (a-e) shows a low magnitude in the vertical velocity fluctuations over the orifice of HR2, with a maximum value of 0.5m/s. As marked in Figure 13(b), the maximum value of $w$ occurs very close to the leading edge of the orifice. It can be seen that in Figure 13(b-d), with progressing time, the location of maximum velocity fluctuations moves toward the middle of the orifice, whilst its value is reduced. Figure 13(c) also shows that when $t = T/2$ the velocity fluctuations which have low magnitude (up to 0.5m/s) penetrate the logarithmic region of the boundary layer downstream of the orifice. The penetration area at $t = 3T/4$ is also extended up to $2d$ from the trailing edge of the orifice (marked in Figure 13(d)). This process is one reason for stabilisation of the turbulence production within the grazing flow downstream of the resonator. However, the grazing flow behaviour in the vicinity of the orifice of HR3 is completely different (Figure 13(f-j)). At $\mathrm{Re}_{\theta} = 4163$ the velocity fluctuations are increased at all locations from the leading edge to the trailing edge. As marked in Figure 13(h), when $t = T/2$ there are two areas of maximum velocity fluctuations, which move inside and outside the resonator separately, and increase the production of large-scale structures in the vicinity of the trailing edge of the orifice. This flow behaviour causes the augmentation of instabilities which occur downstream of HR3.

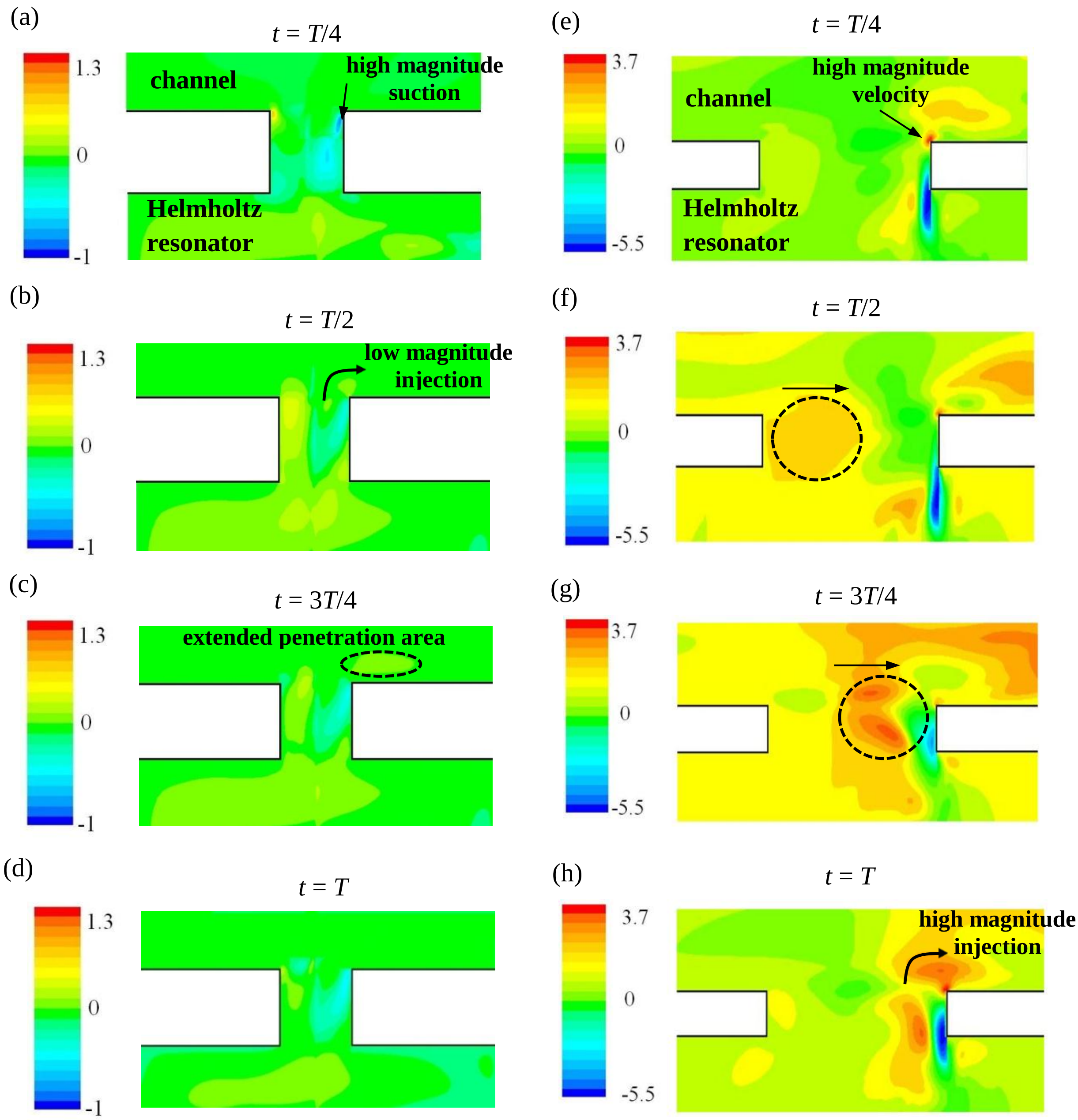


**Figure 13:** $y$ component of the instantaneous velocity over the orifice exit: (a-e) HR2 at $Re_\theta$= 1824 and (f-j) HR3 at $Re_\theta$ =4163 (scale unit is in m/s).

## 2. Summary and conclusion

In this study the fully-developed turbulent grazing flow over four cylindrical flow-excited Helmholtz resonators has been analysed using an LES model. The calculations provide insight into how the resonators change the turbulence structures of the boundary layer. The numerical simulations were undertaken to predict the time-dependent pressure distributions inside the resonators and the velocity fluctuations within the shear layer and downstream of the resonators. In the previous experimental investigations carried out by the authors (Ghanadi et al. 2014), it was observed that there is almost no excitation of the pressure field when $\mathrm{Re}_\theta = 1824$ and the greatest pressure fluctuations inside the resonator occur for $L/D > 3.5$. Therefore in the present paper, all investigations have been for $1800 < \mathrm{Re}_\theta < 4200$ and $L/D = 4$.

Initially a comprehensive validation of the numerical results has been conducted. To this end the PSD of the pressure fluctuations inside the resonators were compared against previously published experimental data. The calculated frequency and amplitude of the maximum pressure fluctuations within the resonator were very close to the experimental data, such that a maximum difference of 15% was observed between the values. The velocity field within the boundary layer upstream of the orifice of the resonators has also been compared with previously published results. The streamwise velocity calculations indicated that the incoming grazing flow is a fully developed turbulent boundary layer with zero pressure gradient.

To understand the pressure distribution within the resonators, the pressure difference between the internal and external pressure fluctuations for three different flow velocities has been calculated. It was shown that when the turbulent boundary layer thickness is close to the orifice diameter the maximum value of the PSD of the pressure fluctuations occurs. In fact, when $\delta \approx d$ eddies can easily penetrate the cavity and increase the pressure magnitude of the cavity flow. It was also observed that when the ratio of the boundary layer thickness to the orifice diameter, $\delta/d$, is around 4, the maximum value of the PSD pressure difference between the resonator interior and the incoming flow decreases by up to 8 dB. The orifice length also has a significant effect on the pressure distribution within the resonator. The vortices within the shear layer over the orifice with the shortest length of those investigated, 2mm, easily penetrate the cavity and thus increase the pressure inside the resonator such that the amplitude of the maximum PSD pressure difference reaches 35 dB. With increased orifice length, $\delta/l \approx 1$, the vortices within the grazing flow cannot induce significant force on the cavity flow such that the amplitude of the PSD pressure is decreased by up to 22dB.

The effects of the resonator on the instabilities within the boundary layer downstream of the resonator were also investigated by calculating the r.m.s. value of the turbulence intensity. The results indicated that there is a considerable increase (a maximum of 24%) in the turbulence intensity within the near wall region downstream of the resonator with $d \approx \delta$.

Moreover, the y component of the velocity fluctuations over this resonator also revealed that the frequency of flow injection over the orifice is more than for the other resonators. The instabilities downstream of the resonator with minimum orifice length, $l/\delta \approx 0.1$, were also amplified by a maximum of 20%. It should be noted that the maximum values of the pressure fluctuations for both of these resonators are greater than the other two resonators. In addition, the maximum flow injection over the orifice of these resonators, HR1 and HR3, also occurs very close to the trailing edge of the orifice, which leads to an increase in the turbulence intensity of the downstream flow. The results also indicated that a reduction in the orifice diameter, from $d/D$ = 0.8 to 0.2, causes a significant decrease in the velocity fluctuations, such that at $Re_\theta$ = 1824 the minimum velocity fluctuations, ${u'_{rms}}^{+} \approx 1.75$, within the logarithmic and fully developed regions occurs downstream of the resonator with the smallest orifice diameter, $d \approx 0.25\,\delta$.

The contour plots of the velocity fluctuations normal to the grazing flow indicated that the low value of the velocity pulsation, up to 0.5m/s, penetrates the logarithmic region and generates semi-longitudinal vorticity, which suppresses the instabilities within the boundary layer. The reduction of the turbulence intensity at all of the free stream velocities investigated also occurs over the logarithmic region downstream of the resonator with $l \approx \delta$. The vector plot of the $y$ component (normal to the flow) of the velocity fluctuations over this resonator revealed that the area of the flow suction is greater than the flow injection area, which results in suppression of the instabilities. The energy spectra of the eddies also showed that the energy contained in the large eddies is reduced in the near wall region downstream of the resonator with the longest orifice, HR4. The energy transferred from the large-scale to small-scale turbulence eddies suppresses the instabilities within the boundary layer.

It is recommended that when the orifice length is equal to the boundary layer thickness and the orifice diameter is almost approximately half of the boundary layer thickness, the resonator can be used as a flow control device. The presented analyses indicate the potential of the flow-excited Helmholtz resonator to delay the turbulence events within the boundary layer and further investigations in this area are the subject of future work.

**References**

Addad, Y, Laurence, D, Talotte, C & Jacob, M 2003, 'Large eddy simulation of a forward–backward facing step for acoustic source identification', *International Journal of Heat and Fluid Flow*, vol. 24, no. 4, pp. 562-571.

Alster, M 1972, 'Improved calculation of resonant frequencies of Helmholtz resonators', *Journal of Sound and Vibration*, vol. 24, no. 1, pp. 63-85.

Amandolese, X, Hemon, P & Regardin, C 2004, 'An experimental study of the acoustic oscillations by flows over cavities', *Journal of Vibration and Acoustics*, vol. 126, no. 2, pp. 190-195.

Bruggeman, J, Hirschberg, A, Van Dongen, M, Wijnands, A & Gorter, J 1991, 'Self-sustained aero-acoustic pulsations in gas transport systems: experimental study of the influence of closed side branches', *Journal of Sound and Vibration*, vol. 150, no. 3, pp. 371-393.

Candler, GEW 1996, 'Comparison of Baldwin-Lomax turbulence models for two-dimensional open cavity computations', *AIAA Journal*, vol. 34, no. 3, pp. 629-631.

Chai, X & Mahesh, K 2012, 'Dynamic k-equation model for large eddy simulation of compressible flows', *Journal of Fluid Mechanics*, vol 699, pp. 385-413.

Choi H & Moin P 2012, 'Grid-point requirements for large eddy simulation: Chapman's estimates revisited', *Physics of Fluids*, vol 24, no 1, pp. 0117021-0117025.

Choi, K & Clayton, BR, 2001, 'The mechanism of turbulent drag reduction with wall oscillation', *International Journal of Heat and Fluid Flow*, vol 22, no. 1, pp. 1-9.

Chapman, DR. 1979, 'Computational aerodynamics development and outlook', *AIAA Journal*. vol. 17, no.12, pp. 1293–1313.

Colonius, T, Basu, AJ & Rowley, CW 1999, 'Numerical investigation of the flow past a cavity', positions, *5th AIAA/CEAS Aeroacoustics Conference*, Washington, USA.

Crouse, B, Senthooran, S, Freed, D, Balasubramanian, G, Gleason, M, Puskarz, M, Lew, P & Mongeau, L 2006, 'Experimental and numerical investigation of a flow induced cavity resonance with application to automobile buffeting', *27th AIAA Aeroacoustics Conference*, Massachusetts, USA.

De Jong, A, Bijl, H, Hazir, A & Wiedemann, J 2012, 'Aeroacoustic simulation of slender partially covered cavities using a Lattice Boltzmann method', *Journal of Sound and Vibration*, vol. 332, no 7, pp. 1687-1703.

Dequand, S, Luo, X, Willems, J & Hirschberg, A 2003, 'Helmholtz-like resonator self-sustained oscillations, Part 1: Acoustical measurements and analytical models', *AIAA Journal*, vol. 41, no. 3, pp. 408-415.

Favre, A 1983, 'Turbulence: Space-time statistical properties and behavior in supersonic flows', *Physics of Fluids*, vol. 26, pp. 2851-2863.

Georges, L, Winckelmans, G, Caro, S & Geuzaine, P 2006, 'Aeroacoustic simulation of the flow in a Helmholtz resonator', *4th International Conference on Computational Fluid Dynamic*, pp. 819-824, Ghent, Belgium.

Ghanadi, F, Arjomandi, M, Cazzolato, BS & Zander, AC 2013 (a), 'Numerical simulation of grazing flow over a self-excited Helmholtz resonator', *Engineering Letters*, vol. 21, no. 3, pp. 137-142.

Ghanadi, F, Arjomandi, M, Cazzolato, BS & Zander, AC 2013 (b), 'Velocity fluctuations within the turbulent flow over a flow-excited helmholtz resonator', *The 2013 International Conference on Mechanical and Materials Engineering*, Stockholm, Sweden.

Ghanadi, F, Arjomandi, M, Cazzolato, BS & Zander, AC 2014, 'Interaction of a flow-excited Helmholtz resonator with a grazing turbulent boundary layer', *Experimental Thermal and Fluid Science,* vol. 58, pp. 80-92.

Hardin, JC & Mason, JP 1977, 'Broadband noise generation by a vortex model of cavity flow', *AIAA Journal,* vol. 15, no. 5, pp. 632-637.

Hémon, P, Santi, F & Amandolèse, X 2004, 'On the pressure oscillations inside a deep cavity excited by a grazing airflow', *European Journal of Mechanics-B/Fluids*, vol. 23, no. 4, pp. 617-632.

Henderson, J., Badcock, K. and Richards, B. 2000, 'Subsonic and transonic transitional cavity flows', *6th AIAA/CEAS Aeroacoustics Conference*, Hawaii, USA.

Holmberg, A 2010, 'Experimental determination of aeracoustic sources in low Mach number internal flows', *Licentiate Thesis,* KTH, Sweden.

Howe, M 1981, 'Influence of mean shear on unsteady aperture flow, with application to acoustical diffraction and self-sustained cavity oscillations', *Journal of Fluid Mechanics,* vol. 109, pp. 125-146.

Inagaki, M, Murata, O, Kondoh, T & Abe, K 2002, 'Numerical prediction of fluid-resonant oscillation at low Mach number', *AIAA Journal*, vol. 40, no. 9, pp. 1823-1829.

Inoue, M 2012, 'Large-eddy simulation of the flat-plate turbulent boundary layer at high Reynolds numbers', *Ph.D. thesis*, California Institute of Technology.

Jimenez, J, Hoyas, S, Simens, MP & Mizuno, Y 2010, 'Turbulent boundary layers and channels at moderate Reynolds numbers', *Journal of Fluid Mechanics*. vol. 657, pp. 335-360.

Jukes, TN 2007, 'Turbulent drag reduction using surface plasma', *Ph.D. thesis*, University of Nottingham.

Jukes, TN, Choi, KS, Johnson, GA and Scott, SJ 2006, 'Turbulent drag reduction by surface plasma through spanwise flow oscillation', *3rd AIAA Flow Contorl Conference, Paper No. AIAA-2006-3693*, California, USA.

Klewicki, JC, Fife, P & Wei, T 2009, 'On the logarithmic mean profile', *Journal of Fluid Mechanics*. Vol 638, pp. 73–93.

Kooijman, G 2007, 'Acoustical response of shear layers', *Ph.D. T hesis*, Endhoven University of Technology.

Kooijmana, G , Hirschberga, A & Golliard, J 2008, 'Acoustical response of orifices under grazing flow: Effect of boundary layer profile and edge geometry', *Journal of Sound and Vibration*, vol. 315, no. 4, pp. 849‑874.

Kook, H 1997, 'Prediction and control of the interior pressure fluctuations in a flow-excited Helmholtz resonator', *Ph.D. Thesis*, Purdue University.

Kook, H, Mongeau, L & Franchek, M 2002, 'Active control of pressure fluctuations due to flow over Helmholtz resonators', *Journal of Sound and Vibration,* vol. 255, no. 1, pp. 61-76.

Laadhari, F, Skandaji, L and Morel, R 1994, 'Turbulence reduction in a boundary layer by a local spanwise oscillating surface', *Physics of Fluids*, vol. 6, no. 10, pp. 3218-3220.

Lee, SJ & Choi, YS 2008, 'Decrement of spanwise vortices by a drag-reducing riblet surface', *Journal of Turbulence*, vol. 9, no. 23, pp. 1-15.

Lockerby, D 2001, 'Numerical simulation of boundary-layer control using MEMS actuation', *Ph. D. Thesis*, The University of Warwick.

Ma, R, Slaboch, PE & Morris, SC 2009, 'Fluid mechanics of the flow-excited Helmholtz resonator', *Journal of Fluid Mechanics*, vol. 623, pp. 1-26.

Mallick, S, Shock, R & Yakhot, V 2003, 'Numerical simulation of the excitation of a Helmholtz resonator by a grazing flow', *Journal of the Acoustical Society of America*, vol. 114, no. 4, pp. 1833-1840.

Marusic, I & Kunkel, GJ 2003 'Streamwise turbulence intensity formulation for flat-plate boundary layers', *Physics of Fluids*, vol. 15, no. 8, pp. 2461-2464.

Massenzio, M, Biaise, A & Lesueur, C 2008, 'Mechanisms of self-sustained oscillations induced by a flow over a cavity', *Journal of Vibration and Acoustics*, vol. 130, no. 5, pp. 1-8.

Mast, TD & Pierce, AD 1995, 'Describing-function theory for flow excitation of resonators', *The Journal of the Acoustical Society of America*, vol. 97, no.1, pp. 163-172.

Meissner, M 2002, 'Excitation of Helmholtz resonator by grazing air flow', *Journal of Sound and Vibration*, vol. 256, no. 2, pp. 382-388.

Moin, P & Kim, J 1982, 'Numerical investigation of turbulent channel flow', *Journal of Fluid Mechanics*. vol. 118, pp. 341-377.

Nakiboglu, G, Belfroid, SPC, Golliard, J. & Hirschberg, A 2011, 'On the whistling of corrugated pipes: Effect of pipe length and flow profile', *Journal of Fluid Mechanics*, vol. 672, pp. 78-108.

Nelson, PA, Halliwell, NA & Doak, PE 1981, 'Fluid dynamics of a flow excited resonance, part I: Experiment', *Journal of Sound and Vibration*, vol. 78, no. 1, pp. 15-38.

Nelson, PA, Halliwell, NA & Doak, PE 1983, 'Fluid dynamics of a flow excited resonance, Part II: Flow acoustic interaction', *Journal of Sound and Vibration*, vol. 91, no. 3, pp. 375-402.

Nicoud, F & Ducros, F 1999, 'Subgrid-scale stress modelling based on the square of the velocity gradient tensor', *Flow, Turbulence and Combustion*, vol. 62, no. 3, pp. 183-200.

Panton, R 1990, 'Effect of orifice geometry on Helmholtz resonator excitation by grazing flow', *AIAA Journal*, vol. 28, pp. 60-65.

Panton, RL & Miller, JM 1975, 'Excitation of a Helmholtz resonator by a turbulent boundary layer', *Journal of the Acoustical Society of America*, vol. 58, no. 4, pp. 800-806.

Rebbeck, H and Choi, KS 2001, 'Opposition control of near-wall turbulence with a piston-type actuator', *Physics of Fluids*, vol. 13 no. 8, pp. 2142-2145.

Ricot, D, Maillard, DRV & Bailly, C 2001, 'Numerical simulation of the unsteady flow past a cavity and application to the sunroof buffeting'. *7th AIAA/CEAS Aeroacoustics Conference*, Maastricht, Netherlands.

Roche, JM, Vuillot, F, Leylekian, L, Delattre, G, Piot, E & Simon, F 2010, 'Presented Numerical and Experimental Study of Resonant Liners Aeroacoustic Absorption Under Grazing Flow', *AIAA paper* 2010-3767, 16th AIAA/CEAS Aeroacoustics Conference, Stockholm, Sweden.

Rockwell, D & Naudascher, E 1978, 'Review-self-sustaining oscillations of flow past cavities', *ASME Transactions Journal of Fluids Engineering*, vol. 100, pp. 152-165.

Rowley, CW, Colonius, T & Basu, AJ 2002, 'On self-sustained oscillations in two-dimensional compressible flow over rectangular cavities', *Journal of Fluid Mechanics*, vol. 455, pp. 315-346.

Schlatter, P 2005, 'Large-eddy simulation of transition and turbulence in wall-bounded shear flow', *PhD thesis*, Swiss Federal Institute of Technology, Zurich.

Shaw, L 1998, 'Active control for cavity acoustics', *AIAA paper*, vol. 2347, pp. 827-835.

Sinha, N, Arunajatesan, S & Ukeiley, L 2000, 'High fidelity simulation of weapons bay aeroacoustics attenuation asing active flow control', *6th AIAA/CEAS Aeroacoustics Conference, Paper No. AIAA-2000-1968, Lahaina, Hawaii*.

Sillero, J, Jiménez, J & Moser, RD 2013, 'One-point statistics for turbulent wall-bounded flows at Reynolds numbers up to δ+ ~ 2000', *Physics of Fluids*, vol 25, no 10, pp. 1-16.

Sipp, D 2012, 'Open-loop control of cavity oscillations with harmonic forcings', *Journal of Fluid Mechanics*, vol. 708, pp. 439-468

Tam, CKW, & Block, P 1978, 'On the tones and pressure oscillations induced by flow over rectangular cavities', *Journal of Fluid Mechanics*, vol. 89, no. 2, pp. 373-399.

Tam, CKW, Ju, H, Jones, MG, Watson, WR & Parrott, TL 2010, 'Computational and experimental study of resonators in three dimensions', *Journal of Sound and Vibration*, vol. 329, no. 24, pp 5164-5193.

Tam, CKW, Pastouchenko, NN, Jones, MG & Watson, WR 2014, 'Experimental validation of numerical simulations for an acoustic liner in grazing flow: self-noise and added drag', *Journal of Sound Vibration*, vol.333, no13, pp. 2831-2854.

Toda, HB, Cabrit, O, Balarac, G, Bose, S, Lee, J, Choi, H & Nicoud, F 2010, 'A subgrid-scale model based on singular values for LES in complex geometries', *Proceedings of the Summer Program (Center for Turbulence Research, NASA Ames/Stanford University, Stanford, CA, 2010)*, pp. 193-202.

Vreman, B 1995, 'Direct and large eddy simulation of the compressible turbulent mixing layer'. PhD. Thesis, Twente University.

White, FM 1991, 'Viscous fluid flow', McGraw-Hill Professional Publishing.

Zhang, Q & Bodony, DJ 2011, 'Numerical Simulation of Two-Dimensional Acoustic Liners with High Speed Grazing Flow', *AIAA Journal*, vol. 49, no. 2, pp. 365-382 .

Zhang, Q & Bodony, DJ 2012, 'Numerical investigation and modeling of acoustically-excited flow through a circular orifice backed by a hexagonal cavity, *Journal of Fluid Mechanics*, vol. 693, pp. 367-401.

Zhang, Q & Bodony, DJ 2014, 'Direct numerical simulation and analytical modeling of locally reacting, single degree of freedom acoustic liners with turbulent grazing flow', *AIAA Paper* 2014-3354, 20th AIAA/CEAS Aeroacoustic Conference, Atlanta, Georgia.

# Chapter 6

# Control of the Turbulent Boundary Layer by a Self-excited Helmholtz Resonator

This chapter has been submitted as

Ghanadi, F., Arjomandi, M., Cazzolato, B. S., and Zander, A. C. 2014, 'Control of turbulent boundary layer by a self-excited Helmholtz resonator', submitted to *Journal of Fluid Mechanics*.

To further confirm and support the hypothesis described in the previous chapters, a detailed analysis of the turbulent boundary layer in the vicinity of the resonator is explained in this chapter. An LES model and extensive experiments have been undertaken to investigate the structure of the manipulated turbulent boundary layer downstream of different cylindrical flow-excited Helmholtz resonators for a wide range of Reynolds numbers.

The results show that when the orifice diameter approximately equals the thickness of the inner layer of the boundary layer an energy transfer from the large eddies to the small eddies occurs, resulting in a slight suppression of the velocity fluctuations. A resonator with the orifice length approximately the same as the boundary layer thickness was found to reduce the duration and intensity of the sweep events, which reveals an attenuation of the turbulence energy production within the boundary layer.

The results presented in this chapter provide an insight into how the resonators can reduce the turbulence production in the boundary layer and also identifies the resonator parameters required to stabilise the boundary layer.

# Statement of Authorship

| | |
|---|---|
| Title of Paper | Control of the turbulent boundary layer by a self-excited Helmholtz resonator |
| Publication Status | O Published, O Accepted for Publication, ⊙ Submitted for Publication, O Publication style |
| Publication Details | Journal of Fluid Mechanics |

## Author Contributions

By signing the Statement of Authorship, each author certifies that their stated contribution to the publication is accurate and that permission is granted for the publication to be included in the candidate's thesis.

| | | | |
|---|---|---|---|
| Name of Principal Author (Candidate) | Farzin Ghanadi | | |
| Contribution to the Paper | Performed experimental and numerical work, interpreted data, wrote manuscript and acted as corresponding author. | | |
| Signature | | Date | 19.09.14 |

| | | | |
|---|---|---|---|
| Name of Co-Author | Maziar Arjomandi | | |
| Contribution to the Paper | Supervised development of work, helped in data interpretation and manuscript evaluation. | | |
| Signature | | Date | 19.09.14 |

| | | | |
|---|---|---|---|
| Name of Co-Author | Benjamin Cazzolato | | |
| Contribution to the Paper | Supervised the research and contributed in academic discussion and manuscript review | | |
| Signature | | Date | 19/9/14. |

| | | | |
|---|---|---|---|
| Name of Co-Author | Anthony Zander | | |
| Contribution to the Paper | Supervised the research and contributed in academic discussion and manuscript review | | |
| Signature | | Date | 19/9/14 |

# Control of the turbulent boundary layer by a self-excited Helmholtz resonator


## Abstract

An extensive study has been undertaken to attenuate the instabilities which naturally occur within a turbulent boundary layer, through application of a flow-excited Helmholtz resonator. A fully developed turbulent boundary layer over a Helmholtz resonator flush mounted with the surface of a flat plate was investigated for $800 < \mathrm{Re}_\tau < 2000$, and low turbulence intensity flow, $Tu \approx 0.5\%$. Quantitative numerical predictions of the three dimensional flow using Large Eddy Simulations (LES), along with experimental measurements using hotwire anemometry and microphones, have been conducted to provide a detailed analysis of the boundary layer in the vicinity of the resonator. For the purpose of identifying the effects of the Helmholtz resonator shape, the main geometrical parameters have been varied. The results showed that when the orifice diameter approximately equals the thickness of the inner layer of the boundary layer, $y^+ \approx 400$, the instantaneous velocity normal to the grazing flow penetrates the boundary layer resulting in a reduction of the turbulence intensity by up to 16% and energy transfer from large eddies to the small eddies within the logarithmic region. Up to an 8% reduction in the sweep duration and a 5% reduction in the sweep intensity have also been observed within the boundary layer downstream of the resonator for an orifice length approximately the same as the boundary layer thickness. The present study provides an insight into the effect of the Helmholtz resonator on the turbulence production and indicates the parameters of the resonator that result in a reduction of the instabilities.


## Nomenclature

| | |
|---|---|
| $c_f$ | = friction coefficient |
| $d$ | = orifice diameter (mm) |
| $D$ | = cavity diameter (mm); detector function |
| $c$ | = speed of sound (m/s) |
| $f$ | = frequency (Hz) |
| $f_r$ | = resonance frequency of the resonator (Hz) |
| $H$ | = shape factor |
| $l$ | = length of the orifice (mm) |
| $l_e$ | = effective length of the orifice (mm) |
| $L$ | = cavity depth (mm) |
| $S$ | = cross-section area of the orifice (mm$^2$) |
| $V_c$ | = cavity volume (mm$^3$) |

| | |
|---|---|
| $p_{\text{ref}}$ | = reference pressure (Pa) |
| $Re_\tau$ | = Reynolds number based on friction velocity |
| $Re_\theta$ | = Reynolds number based on momentum thickness |
| $t$ | = time (s) |
| $x$ | = indicates the x-direction (streamwise) (m) |
| $y$ | = indicates the y-direction (wall-normal direction) (m) |
| $z$ | = indicates the z-direction (spanwise direction) (m) |
| $T$ | = time period (s) |
| $T_w$ | = window length (s) |
| $T_{\text{av}}$ | = averaging window length (s) |
| $k$ | = VITA threshold |
| $Tu$ | = turbulence intensity |
| $u$ | = free stream component of the velocity (m/s) |
| $w$ | = cross-stream component of the velocity (m/s) |
| Var | = indicates variance |
| $B(\sigma)$ | = probability density function of $u$ |
| $u_\tau$ | = friction velocity (m/s) |
| $U$ | = mean free stream velocity (m/s) |
| ${u'_{\text{rms}}}^+$ | = non-dimensional averaged turbulence intensity |
| $Y^+$ | = non-dimensional wall distance to the first grid point |

**Symbols**

| | |
|---|---|
| $\sigma$ | = standard deviation |
| $\nu$ | = kinematic viscosity ($m^2$/s) |
| $\delta$ | = boundary layer thickness (mm) |
| $\theta$ | = momentum thickness (mm) |

## 1. Introduction

At resonance, strong pressure fluctuations within a Helmholtz resonator excited by a grazing flow eject the shear layer that develops over the orifice into the outer region of the boundary layer, which may result in a modification to the turbulent energy production. The study of flow oscillations over Helmholtz resonators has gained renewed interest due to its wide contribution to the fundamental understanding of flow control, as well as due to its diverse industrial applications (Rienstra and Hirschberg 2001; Hemon et al. 2004; Ghanadi et al. 2014a). Depending on the application, the self-sustained oscillation of flow around the Helmholtz resonator may be desirable; for example, for separation control or sound generation using musical instruments (Khosropour and Millet 1990; Urzynicok 2003). On the other hand, these oscillations may also have undesirable effects; for instance, gas fluctuations inside pipelines with closed side branches, the grazing flow over aircraft landing gear, and cabin pressure fluctuations inside a vehicle with an open window or sunroof (Bruggeman et al. 1991; Inagaki et al. 2002; Crouse et al. 2006). In most engineering applications, the flow oscillations are therefore deemed undesirable and thus a large amount of research focuses on active or passive methods for suppression of the unwanted excitations (Kook 1997; Shaw 1998; Alam et al. 2007; Ma et al. 2009). Conversely, the potential of a flow-excited Helmholtz resonator to induce changes in turbulence downstream of the resonator has received very little attention (De Metz et al. 1977; Flynn et al. 1990; Lockerby 2001; Ghanadi et al. 2014b). The motivation of this study is to provide further detailed information of the grazing flow downstream on the resonator for the purpose of boundary layer control.

The reduction of turbulence energy production by flow control techniques is of paramount importance in numerous applications. Significant savings in costs and power consumption in commercial airlines, enhanced mixing in combustion engines and heat transfer in heat exchangers, and increased speed of underwater vehicles, are some examples of the benefits of turbulent boundary layer control (Hefner 1988; Gad-el-Hak 2000; Kasagi et al. 2009). In a turbulent boundary layer the quasi-streamwise vortices collect the low-speed fluid (streaks) within the near wall region and pump them into (sweep) or away from (ejection) the surface, and are responsible for production of the turbulent kinetic energy within the boundary layer. Therefore, suppressing the vortices is an effective way to stabilize the boundary layer; for example, streamwise longitudinal micro-grooves over the surface of a plate retain the streamwise vortices, resulting in a reduction in the strength of the sweep cycles, turbulence intensity and skin-friction drag by up to 8% (Walsh, 1983; El-Samni et al. 2007; Lee & Choi 2008; García-Mayoral et al. 2011). Weakening the quasi-streamwise vortices through the addition of artificial vortices generated by spanwise wall oscillation has also been suggested by Jung et al. (1992) and Choi & Clayton (2001). In this method the quasi-streamwise vortices are shifted to a different position relative to the streaks, thereby disrupting the sweep and ejection cycles. It was observed that when wall surface is oscillated with a period of $T^{+}$=100 and speed of $w^{+}$=15, up to 45% reduction in the instabilities can be achieved (Laadhari et al. 1994; Dhanak & Si 1999; Viotti et al. 2009). Another interesting way to produce streamwise vortices is by using a travelling wave to restrict the vorticity field within the turbulent boundary layer (Berger et al 2000; Du et al. 2004). DBD plasma actuators can generate these travelling waves up to $y^{+}$=100, and reduce the turbulent energy production by up to 48% (Choi et al. 2011). Implementing a selective suction technique (Myose & Blackwelder 1995), Micro-Electro-Mechanical-Systems (MEMS) (Rathnasingham and Breuer, 2003), polymers or surfactants (Virk, 1975), micro-bubbles (Merkle and Deutsch, 1989), compliant coatings (Kramer, 1961), Large-Eddy-Break-Up devices (LEBU) (Savill & Mumford, 1988) are some other alternative ways to control the turbulent boundary layer. In the present study, attenuation of the turbulent energy production using a flow-excited Helmholtz resonator has been investigated. In this method the energy required for manipulation of the low momentum flow and associated streamwise vortices is extracted from the grazing flow and is returned to it almost entirely as periodic fluctuations. A Helmholtz resonator is a passive device and thus does not need an external energy source to be activated and due to the simplicity of its structure and installation it has extensive broad potential as a flow control device for skin friction reductions in real engineering systems.

Flow-excitation of a Helmholtz resonator occurs at low Mach numbers when one of the instability frequencies within the shear layer over the orifice is near or equal to the resonance frequency of the resonator (Elder et al. 1982; Flynn & Panton 1990; Khosropour & Millet 1990). In the literature, a distinction between flow-excited cavities and resonators is often not made, whereas the resonance frequencies of the resonators and the direction of disturbances within the shear layer over a flow-excited Helmholtz resonator are totally different from the majority of the arrangements in a large number of the previous studies (Rossiter 1964; Rockwell & Naudascher 1978; Charwat & Walker 1983; Colonius et al. 1999; Sipp 2012; Zhang et al. 2013). It has been shown that excitation of a Helmholtz resonator occurs when the power spectral density of the instantaneous pressure field within the cavity has a maximum peak very close to the resonance frequency of the resonator (Inagaki et al. 2002; Massenzio et al. 2008). By applying a feedback loop system, it was also demonstrated that at resonance the vortex shedding and the resonance frequency are strongly coupled (Mast & Pierce 1995; Kook et al. 2002). This coupling was modelled by Ricot et al. (2001), who applied a CFD solver based on the Lattice Boltzmann Method (LBM), and showed that the dissipative parameters and background noise in the numerical model caused significant errors in the prediction of the instantaneous properties of the flow in the vicinity of the resonator. In the previous studies, it was also demonstrated that the behaviour of the shear layer over the orifice of a Helmholtz resonator depends on the geometry of the resonator and the Reynolds number of the grazing flow; with both discrete vortices (Hardin & Mason 1977; Nelson et al. 1981a & b) and an unstable sheet-like motion observed (Chatellier et al. 2004, Tam & Block 1978; Howe, M 1981; Massenzio et al. 2004; Bilanin & Cover 1973). In the present study, the shear layer also develops as a combination of an unstable sheet and vortical structures. Interaction of the shear layer with the downstream edge of the orifice causes pressure waves to propagate back towards the incoming boundary layer and generate new fluctuations (Kooijman 2007; Holmberg 2010). The instabilities within the shear layer force the cavity flow and increase the amplitude and frequency of the pressure fluctuations (Amandolese et al. 2004; Meissner 2005; Ma et al. 2009).

The characteristics of the incoming flow significantly impact on the excitation of the resonator (Mallick et al. 2003). Panton & Miller (1975) showed that when the size of the eddies within the turbulent boundary layer is approximately twice the orifice diameter, they can impose an oscillation equal in frequency to the resonance frequency. The turbulence intensity of the incoming flow also has significant influence on the flow behaviour around the resonator, such that use of the steady-state assumption for the grazing flow causes an over-prediction in pressure spectra (De Jong et al. 2012). The sensitivity of the pressure fluctuations to the characteristics of the Helmholtz resonator has also been studied (Selamet et al. 1997; Georges et al. 2006). It was observed that a circular orifice generates greater pressure fluctuations within the resonator compared to a resonator with a slot-type orifice aligned with the flow direction (Panton 1990). The vortex path within the shear layer is also directly related to the profile of the leading edge of the orifice, such that sharp edges cause vortices to enter the neck and pass close to the downstream edge (Dequand et al. 2003). The previous discussion of investigations on flow-excited Helmholtz resonators is by no means exhaustive; it merely provides a flavour of the vast areas of research related to the present study.

The purpose of the present work is to assess the ability of a cylindrical flow-excited Helmholtz resonator to reduce the turbulent energy production within the boundary layer. Therefore, in the subsequent sections the characteristics of the studied Helmholtz resonators will be presented together with details of the simulation procedure and experimental method. This is followed by discussion of the flow fields within the resonator and downstream of the orifice to provide an insight into the capability of using a Helmholtz resonator for flow control.

## 2. Experimental procedure

The experiments were performed in a closed-return-type wind tunnel which can be operated at speeds of up to 30m/s with a low level of turbulence intensity, ranging between 0.3% to 0.7%. The rectangular test section is 2m long with a cross-section of 50cm × 50cm.

The walls of the test section were fixed at the leading edge and adjusted horizontally downstream to maintain zero streamwise pressure gradient along the working area. To measure the pressure gradient along the plate, pressure tappings were installed in the roof of the test section. Throughout the investigations the pressure variation along the working section was measured to be less than $\pm$0.5%. A horizontal 2m long flat plate was positioned inside the tunnel such that it spanned the whole width of the test section. The finite thickness of the flat plate leads to bluff body separation effects, therefore to minimize any possible flow separation a super-elliptical leading edge was attached to the flat plate. A 12.5cm long circulation flap was also mounted downstream of the plate to minimize any circulation developed over the plate and to ensure that the stagnation point is on the measurement side of the plate. The flap could also be adjusted as appropriate to balance the pressure gradient along the working section. As can been seen in Figure 1, the boundary layer examined in this study was tripped by a 3mm diameter wire placed near to the leading edge to assure a fully developed turbulent boundary layer over the surface. A cylindrical Helmholtz resonator with a fixed cavity diameter of 25mm was positioned underneath the flat plate and was set flush to the surface 35cm from the leading edge.

The pressure and velocity fluctuations were measured within the resonator and over the orifice. One microphone was installed upstream of the resonator orifice and another inside the cavity, set flush to the surface, in order to quantify the effects of the boundary layer on the instantaneous pressure fields within the resonator. The low sensitivity microphones $1/8''$ G.R.A.S type 46DD, were selected because of their small diameter, broad bandwidth and ability to measure high sound pressure levels. A hot-wire anemometer was also used over the orifice and downstream of the resonator to characterize the changes in turbulent structures. The streamwise velocity measurements were made with an IFA 300 CTA system, using a single platinum-plated tungsten wire of 5 μm in diameter and 1.25mm in length, which was operated in constant current mode at 0.2mA with an over-heat ratio of 1.8 and an operating temperature around 230°C. The probe has sufficient sensitivity to measure the velocity fluctuations with minimum thermal effects. The repeatability of each measurement was also verified and the data were sampled at 10kHz for 10 seconds to ensure suitable temporal resolution.

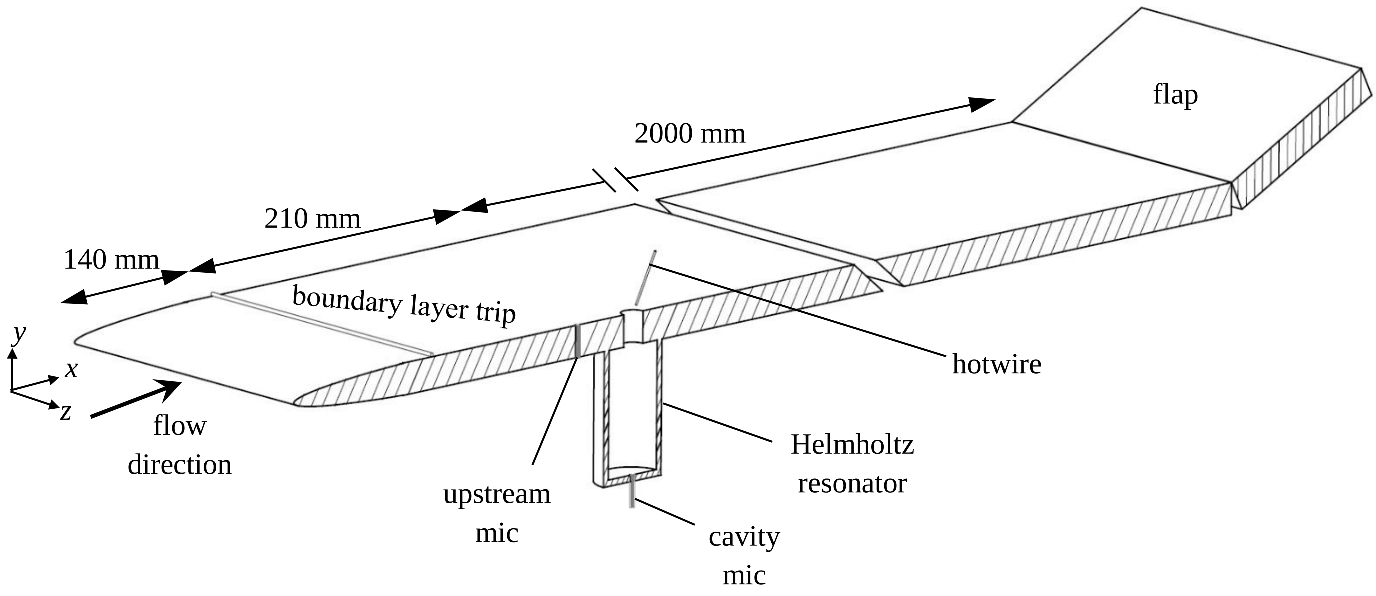


**Figure 1:** Schematic of a cross-section of the experimental arrangement.

### 3. Characteristics of the Helmholtz resonators

To investigate the sensitivity of the flow field to the resonator shape, different geometries have been previously studied by the authors (Ghanadi et al. 2014b), and the pressure fluctuations within the resonators for different orifice shapes and cavity volumes, $V_c$, were measured. As can be seen in Figure 2, four different circular orifices with sharp edges were selected, in which the ratio of the orifice diameter ($d$) to the boundary layer thickness ($\delta$) is in the range of 0.2 to 2. The cavity depth ($L$) to diameter ($D$) ratio was also changed and it was observed that the resonator was not excited when $L/D < 4$ (Ghanadi et al. 2014b).

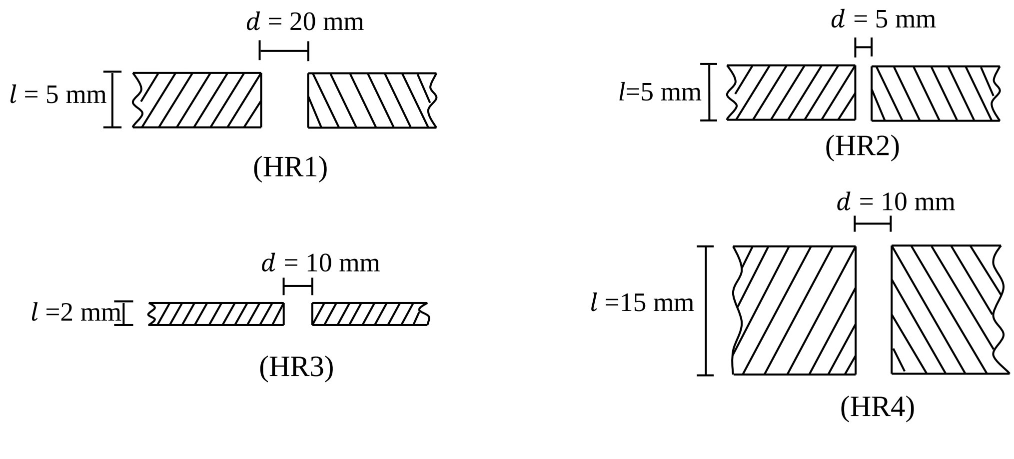


**Figure 2:** Cross-section through resonator centreline illustrating the four different orifice shapes investigated.

Table 1 shows the characteristics of the four different resonator geometries investigated. The dimensions of the resonator orifice presented in Figure 1 have been non-dimensionalised by the cavity diameter.

**Table 1:** Characteristics of the resonators and their resonance frequencies. The depth to diameter ratio of the cavity, $L/D$, was 4 in all cases.

| Helmholtz resonator designation | Resonator parameters: $l/D$ (non-dimensional orifice length) | Resonator parameters: $d/D$ (non-dimensional orifice diameter) | $f_r$ (Hz): LES | $f_r$ (Hz): Exp. | $f_r$ (Hz): Theory |
|---|---|---|---|---|---|
| HR1 | 0.2 | 0.8 | 722 | 712 | 748 |
| HR2 | 0.2 | 0.2 | 414 | 402 | 338 |
| HR3 | 0.08 | 0.4 | 619 | 605 | 592 |
| HR4 | 0.6 | 0.4 | 561 | 550 | 498 |

## 4. Numerical method

Owing to mixing of the vortices within the shear layer with the acoustic response from the downstream edge of the orifice, an unsteady 3D approach is required for simulation of this complex flow. The previous studies indicate an under-prediction of the velocity and pressure fluctuations which arise from the dissipative parameter in URANS and hybrid RANS-LES approaches, making them unfavourable models for this problem (Candler 1996; Sinha et al. 2000; Wagner et al. 2007). Use of direct numerical simulation (DNS) permits all turbulent scales to be characterized, however intensive computational resources are required, which is often impractical. In an LES model a filtering procedure is used whereby the flow structures within the near wall region, i.e., the sub-grid scales (SGS), are modelled and the large scales are solved (Georges et al. 2009). The filtering helps to remove high frequencies from the solutions, whilst their influences are resolved. Therefore a three dimensional LES which has a low numerical dissipation is an appropriate candidate to capture all turbulent structures for self-sustained oscillations with a reasonable computational cost. In the present study, LES has been used to predict the changes in the shear layer structures and the velocity fluctuations within the flow over the resonator.

In order to accurately model the effects of the cavity flow on the shear layer, the compressible Navier-Stokes equations have been considered in all of the simulations. The

Wall Adapting Local Eddy-viscosity (WALE) sub-grid model was also selected because of its accurate prediction of the strain and the rotation rate of the smallest resolved turbulent fluctuations (Nicoud & Ducros 1999; Toda et al. 2010). As suggested by Larchevêque et al. (2003), the cell-centred finite volume scheme was applied for spatial discretization to reduce the intrinsic numerical dissipation. The resonator is far enough from the inlet to have a fully developed turbulent boundary layer over the orifice and the inlet flow velocity is in the range of 1 to 30m/s with a low turbulence level, $Tu \approx 0.5\%$, corresponding to the values in the experiments carried out in the present study. An atmospheric pressure was selected as the outflow condition to reduce the distortion of the boundary layer. To ensure that near wall fluctuations within the turbulent flow are accurately captured, the first few cells in the near wall region must have a minimum skewness and stretching. Therefore, a structured mesh has been used to keep the cells as uniform as possible (Figure 3). The near-wall mesh sizes, expressed in wall units, are $\Delta x^+ = 110$ to 200, $\Delta y^+$= 13 to 19, and $\Delta z^+$= 120 to 230, such that at least three cells exist within the viscous region and the dimensionless wall distance, $Y^+$, at the wall is in the range of 0.3 to 0.5. It was concluded from investigation of the mesh dependency that 2.5 to 2.8 million cells are appropriate to simulate the flow around the Helmholtz resonator.

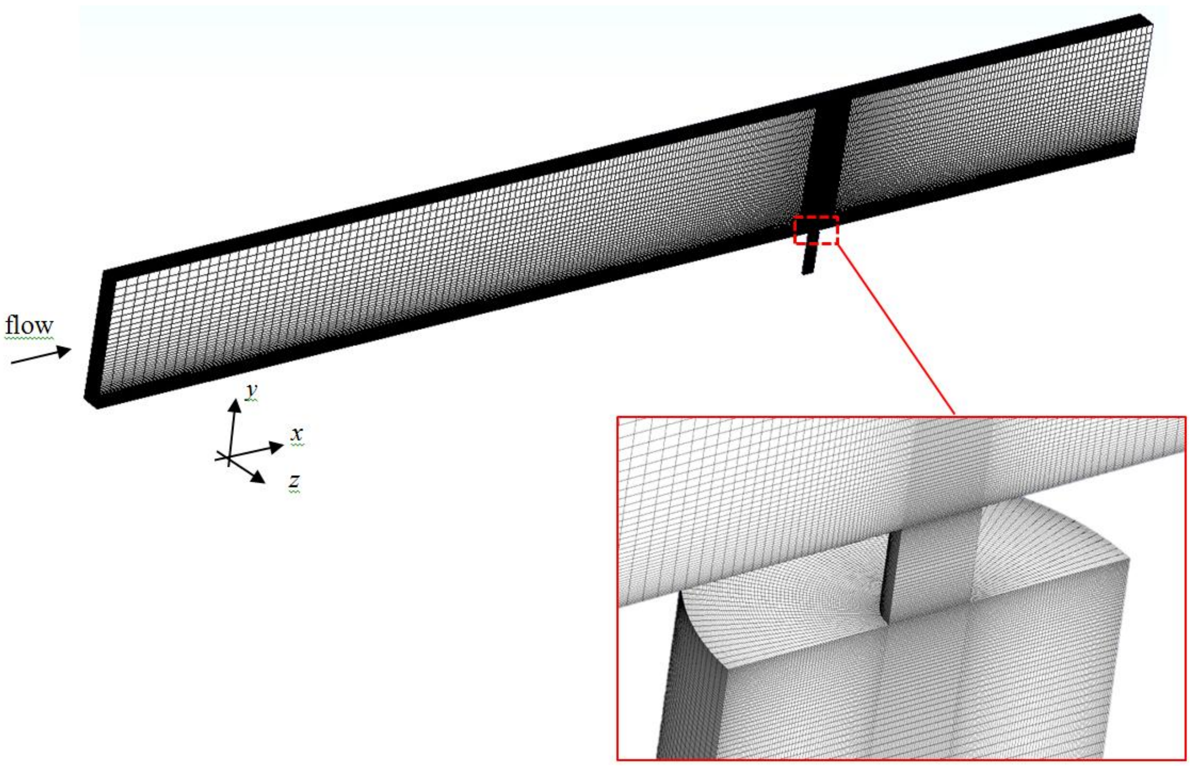


**Figure 3**: Structured mesh in the computational domain. The mesh around the Helmholtz resonator is shown in the inset.

## 5. Validation of the results

For the purpose of validation, the resonance frequency of each resonator was determined by numerical simulation as well as experiment and compared with the theoretical values obtained using the empirical formula (Panton & Miller 1975; Howard et al. 2000),

$$f_r = \frac{c}{2\pi}\sqrt{\frac{S}{l_e V_c + 0.33L^2\, S}} \tag{1}$$

where $c$ is the speed of sound, $S$ cross-section area of the orifice, $l_e$ is the effective orifice length and $L$ is the cavity depth. The resonance frequencies predicted using Equation (1) are shown in Table 1. As previously mentioned, the maximum pressure fluctuations within the cavity of a flow-excited Helmholtz resonator occur very close to the resonance frequency. Therefore, the power spectral density (PSD) of the instantaneous pressure difference between the incoming turbulent boundary layer and the cavity has been investigated. For example, as shown in Figure 4, for HR3 both the experimental and numerical results show that the frequencies associated with the maximum peaks in the pressure (600Hz $< f_r <$620Hz), are very close to the theoretical values predicted by Equation (1). At low frequencies, $f$ <50Hz, the simulation results and the experimental results diverge, which is believed to be due to only modelling the working section of the tunnel, however above 50Hz the predicted frequency and magnitude of the maximum pressure fluctuations are very close to the experimental data.

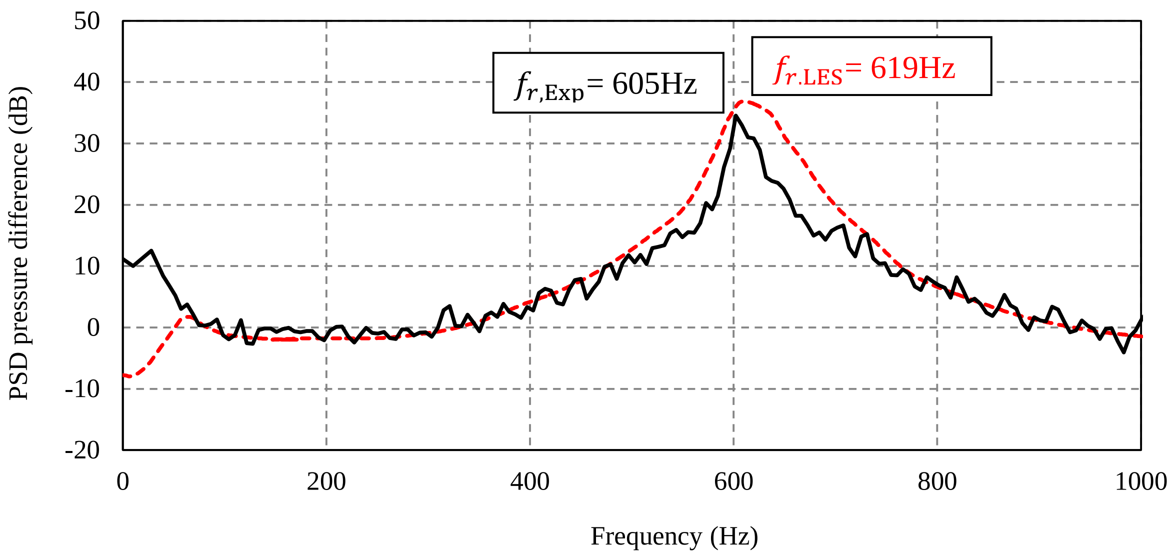


**Figure 4**: The PSD difference of the pressure fluctuations within the incoming turbulent boundary layer and inside the cavity of HR3 at $U$= 23m/s; LES calculation (red dashed line) and experimental data (solid line).

## 6. Characteristics of the turbulent boundary layer

The turbulent boundary layer upstream of the resonator was also characterized for validation purposes. Figure 5 shows the non-dimensional mean and fluctuating velocity profiles which are plotted against the results obtained by Marusic et al. (2003). The predicted and measured profiles in the logarithmic region are well matched (up to 6% difference) with published data, which verifies that the incoming turbulent boundary layer is fully developed with zero pressure gradient. The slight mismatch of up to 10% in the simulated fluctuating velocity profile within the viscous sub-layer is due to energy dissipation in the sub-grid scales of the LES and the radiation impedance of the resonator into the coupled channel.

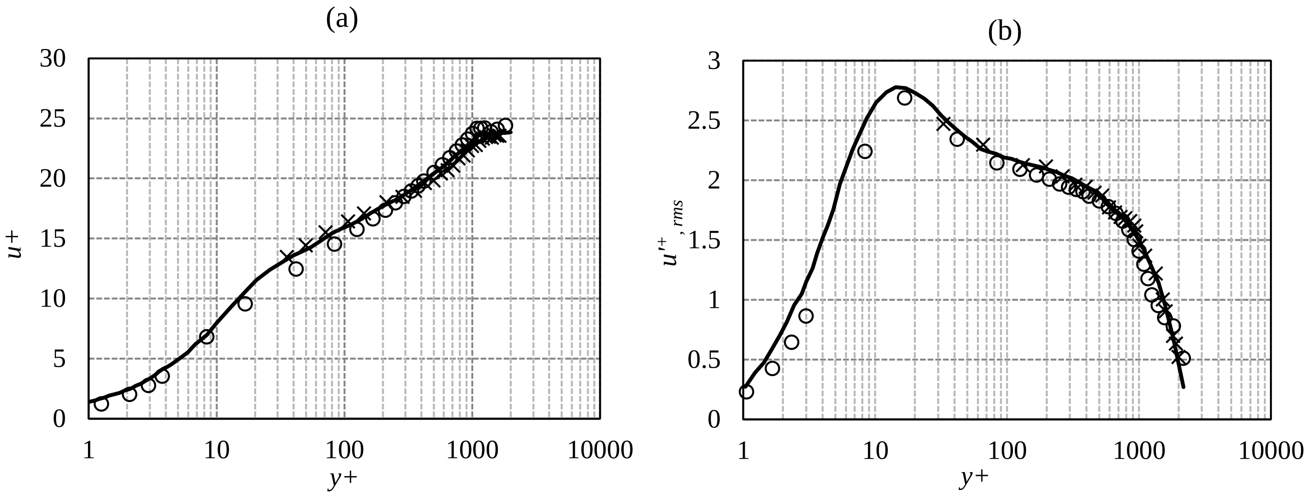


**Figure 5:** a) Mean velocity profile and b) turbulence intensity profiles within the incoming turbulent boundary layer; Numerical results (circle), experimental data (cross), results obtained by Marusic et al. (2003) (line).

It must be noted that in the experiments carried out by Ghanadi et al. (2014b), no significant pressure fluctuations were measured within the cavity below flow speeds of 16m/s which means that the resonator was not excited. Therefore, the flow fields have been investigated for three different free stream velocities; 16m/s, 21m/s and 28m/s. Table 2 presents the typical parameters of the turbulent boundary layer measured in this study and the theoretical values obtained by White (1991), which were calculated using the following parameters; the boundary layer thickness $\delta \approx 0.37\mathrm{Re}_x{}^{-1/5}x$, the friction velocity $U_\tau = U\left(C_f/2\right)^{0.5}$, the momentum thickness $\theta \approx 7\delta/72$ , the Reynolds number based on friction velocity $\mathrm{Re}_\tau = u_\tau\delta/\nu$, the momentum thickness Reynolds number $\mathrm{Re}_\theta = U\theta/\nu$, the local skin-friction coefficient $C_f \approx 0.058\mathrm{Re}_x{}^{-1/5}$ and the shape factor $H \approx \delta^*/\theta$. The experimental and numerical data compares favourably with the data from White (1991).

**Table 2.** Characteristics of the incoming turbulent boundary layer. Simulated (LES) and measured experimental data compared against White (1991) shown in shaded rows.

| $U$ (m/s) | | $\delta$ (mm) | $u_\tau$ (m/s) | $\theta$ (mm) | $\mathrm{Re}_\tau$ | $\mathrm{Re}_\theta$ | $c_f \times 10^3$ | $H$ |
|---|---|---|---|---|---|---|---|---|
| 16 | LES | 18 | 0.78 | 1.71 | 936 | 1824 | 4.1 | 1.38 |
| | Exp. | 17 | 0.77 | 1.58 | 873 | 1685 | 3.9 | 1.37 |
| | White (1991) | 21 | 0.68 | 1.95 | 890 | 1980 | 3.6 | 1.33 |
| 23 | LES | 20 | 1.1 | 1.92 | 1466 | 2944 | 3.88 | 1.36 |
| | Exp. | 19 | 0.9 | 1.81 | 1140 | 2775 | 3.6 | 1.34 |
| | White (1991) | 22 | 0.92 | 1.9 | 1450 | 2850 | 3.2 | 1.31 |
| 28 | LES | 23 | 1.2 | 2.23 | 1840 | 4163 | 3.75 | 1.33 |
| | Exp. | 21 | 1.12 | 2.1 | 1568 | 3920 | 3.5 | 1.32 |
| | White (1991) | 24 | 1.1 | 1.98 | 1785 | 3785 | 2.95 | 1.28 |

## 7. Effect of Helmholtz resonator on turbulence intensity and energy spectra

One common feature of drag reducing flows is a 10% to 30% reduction in the streamwise turbulence intensities in the viscous and logarithmic regions (Choi & Clayton 2001; Pang & Choi 2004; Lee & Choi 2008). Therefore, in the present study the streamwise averaged turbulence intensity, ${u'_{\mathrm{rms}}}^{+}$, downstream of each resonator was compared against the case with no resonator present. The results show the potential of the resonators to stabilise, as well as destabilise, the turbulent boundary layer (Figure 6). It was observed that the turbulence intensity downstream of HR1, which has the greatest orifice diameter of the resonators investigated, is increased by up to 24% at $\mathrm{Re}_\tau = 890$. This effect is reduced at increased free stream velocity, however the resonator still increases the instabilities within the logarithmic region. The results for HR2 show that the velocity fluctuations are also significantly reduced, by up to 16% at $\mathrm{Re}_\tau = 890$. Interestingly, increasing the velocity of the grazing flow changes the resonator to a device which amplifies the turbulence intensity, such that at $\mathrm{Re}_\tau = 1785$ the fluctuations are increased by up to 26% at $y^+$=100. Downstream of the resonator with the shortest orifice length of those investigated, HR3, the turbulence intensity at $\mathrm{Re}_\tau = 890$ is slightly decreased, however the resonator amplifies the instabilities within the boundary layer at higher flow velocities. It must be noted that pressure measurements conducted by Ghanadi et al. (2014b) demonstrated that the maximum pressure fluctuations occur within this resonator. Therefore, to relieve the cavity pressure a significant force has to be induced on the boundary layer which increases the instabilities. When the orifice diameter is almost equal to the boundary layer thickness, as in HR4, the turbulence intensity is reduced by up to 12% at $\mathrm{Re}_\tau = 890$. As mentioned previusly, when $\delta \approx l$ slight pressure fluctuations occur inside HR4, which result in a reduction in the turbulence intensity within the boundary layer (Ghanadi et al. 2014b). At higher flow velocities, the effect of HR4 on the velocity fluctuations is decreased so that at $\mathrm{Re}_\tau = 1785$ the turbulence intensity remains unaltered. A reduction in the turbulence intensities downstream of HR2 and HR4 shows that both resonators can stabilize the turbulent boundary layer. Therefore, in the following analysis attention has been focused on the alterations in the underlying turbulence structure caused by HR2 and HR4.

In most drag reducing flows the energy contained in large eddies within the turbulent boundary layer is reduced (Choi 1989; Jukes 2007). Therefore, changes in the characteristics of the boundary layer downstream of HR2 and HR4 have also been investigated via analysis of the energy contained in the boundary layer. To this end, a single spatial location within the logarithmic region, $y^+$=35, was selected at which the PSD of the measured $u$-component of the velocity fluctuations was calculated. As shown in Figure 7(a), downstream of HR2 at $\mathrm{Re}_\tau$ = 890 there is a reduction in energy throughout the majority of the frequency spectrum. This shows that the energy contained in both large and small eddies within the boundary layer is reduced. With further increase in the flow velocity to $\mathrm{Re}_\tau$ = 1450, the turbulence energy is decreased at low frequencies ($f <$ 100Hz), whilst the energy at higher frequencies is increased in comparison with the no-resonator case (Figure 7b). Therefore, HR2 causes the large eddies to transfer their energy to the small scales within the logarithmic region. Downstream of HR4 at $\mathrm{Re}_\tau$ = 890 the energy also transfers from large scales to small eddies ($f >$ 130Hz), whilst at $\mathrm{Re}_\tau$= 1450 the energy over the entire frequency range is largely unaltered (Figures 7c & d).

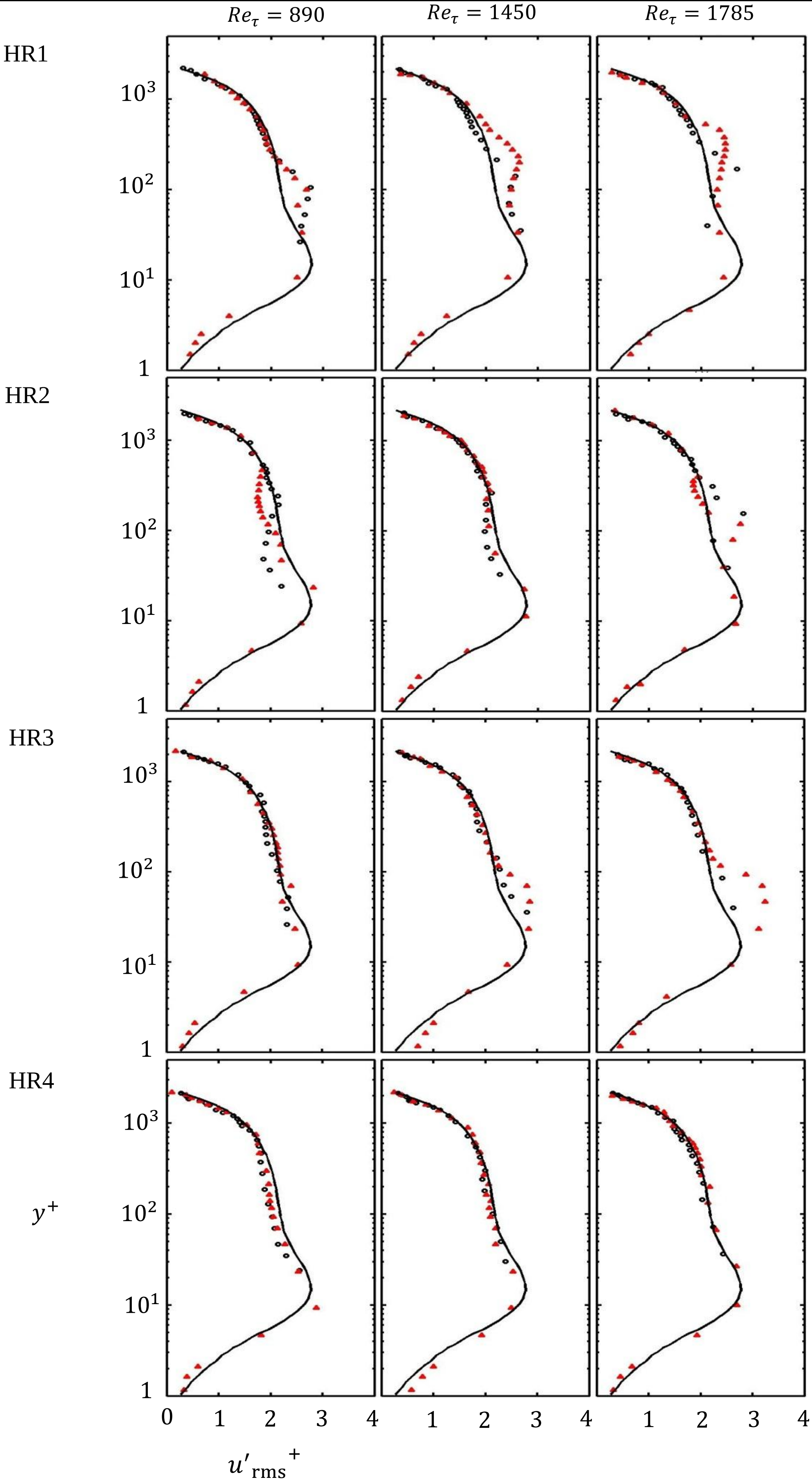


**Figure 6:** Turbulence intensity profiles within the boundary layer downstream of the resonators; (red triangle) numerical results, (black circle) experimental data, (line) results obtained by Marusic et al. (2003) for no resonator present.

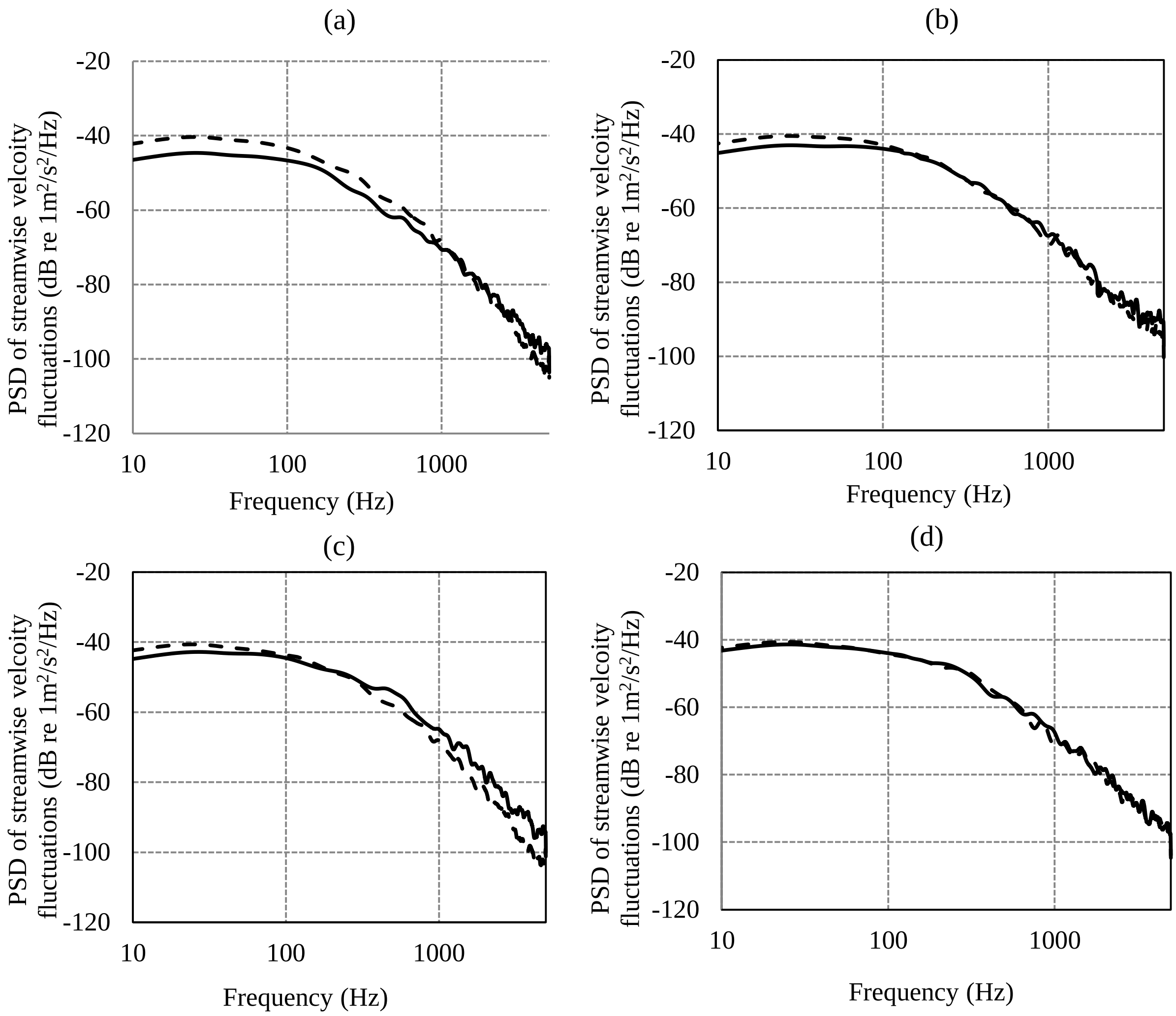


**Figure 7:** Energy contained in the boundary layer structure at $y^{+}$=35; (dashed line) without resonator, (solid line) with resonator: (a) HR2 at Re$_{\tau}$= 890, (b) HR2 at Re$_{\tau}$= 1450, (c) HR4 at Re$_{\tau}$= 890 and (d) HR4 at Re$_{\tau}$= 1450.

For the purpose of understanding the vortical structures within the downstream flow, the velocity fluctuations normal to the grazing flow in the vicinity of the orifice during one period, $T = 1/f_r$, were also investigated. To compare the flow field around the resonator, which can either increase or decrease the instabilities within the boundary layer, contours of the cross-stream component of the velocity fluctuations around HR2 and HR3 obtained from the numerical simulations were investigated. As marked in Figure 8(a), when $t = T/4$ the maximum flow suction, $w/U$ = -0.05m/s, occurs very close to the downstream edge of the orifice. Figure 8(b & c) show that, when $T/2 < t < 3/4T$ a velocity fluctuation with low magnitude, up to $w/U$ = 0.03m/s, is injected into the boundary layer and penetrates up to $2d$ further downstream from the edge of the orifice. This flow behaviour is thought to be associated with the reduction in turbulence intensity downstream of HR2 (Figure 8d). However, as marked in Figure 9(a), when $t = T/4$, the maximum value of cross-stream velocity fluctuations, $w/U$ = 0.13m/s, occurs at the trailing edge of the orifice of HR3. As time progresses, the velocity fluctuations travel over the orifice, whilst their value is increased (Figure 9b & c). As marked in Figure 9(d), when $t = T$ the high value of the velocity fluctuations, $w/U$= 0.1m/s, occurs in the vicinity of the trailing edge of the orifice which increases the production of streamwise velocity fluctuations within the downstream boundary layer.

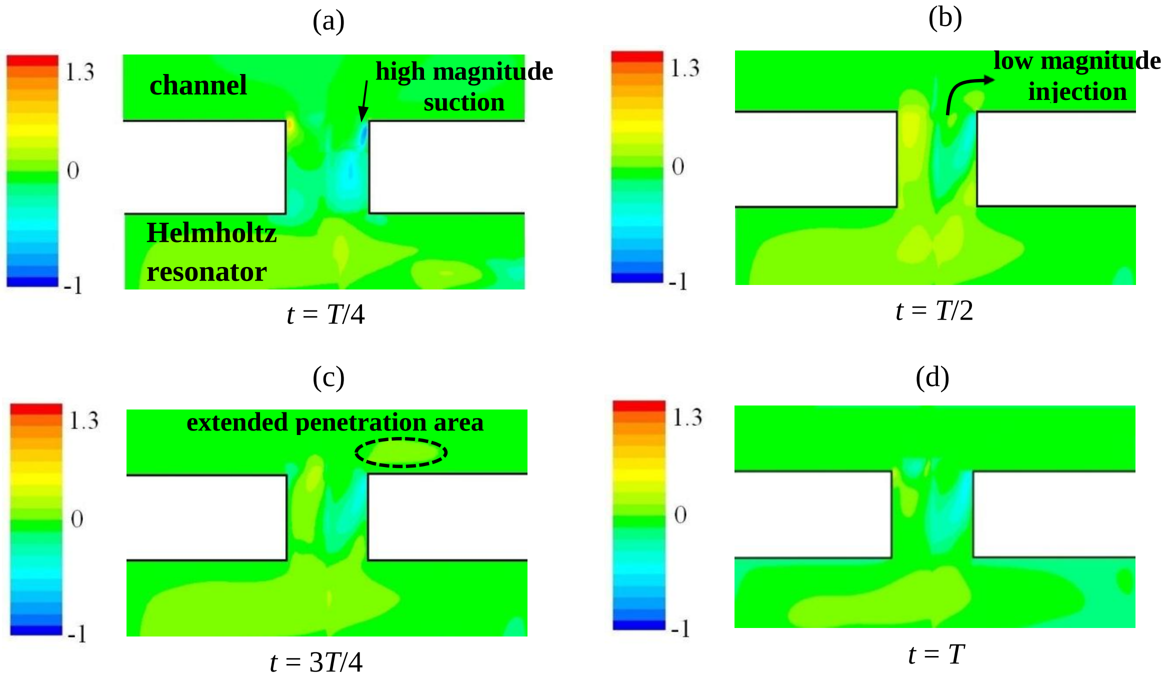


**Figure 8:** Contours of velocity fluctuations (in m/s) normal to the grazing flow in the vicinity of the orifice of HR2 at $Re_\tau$ =890 at various times in a period of the resonance frequency.

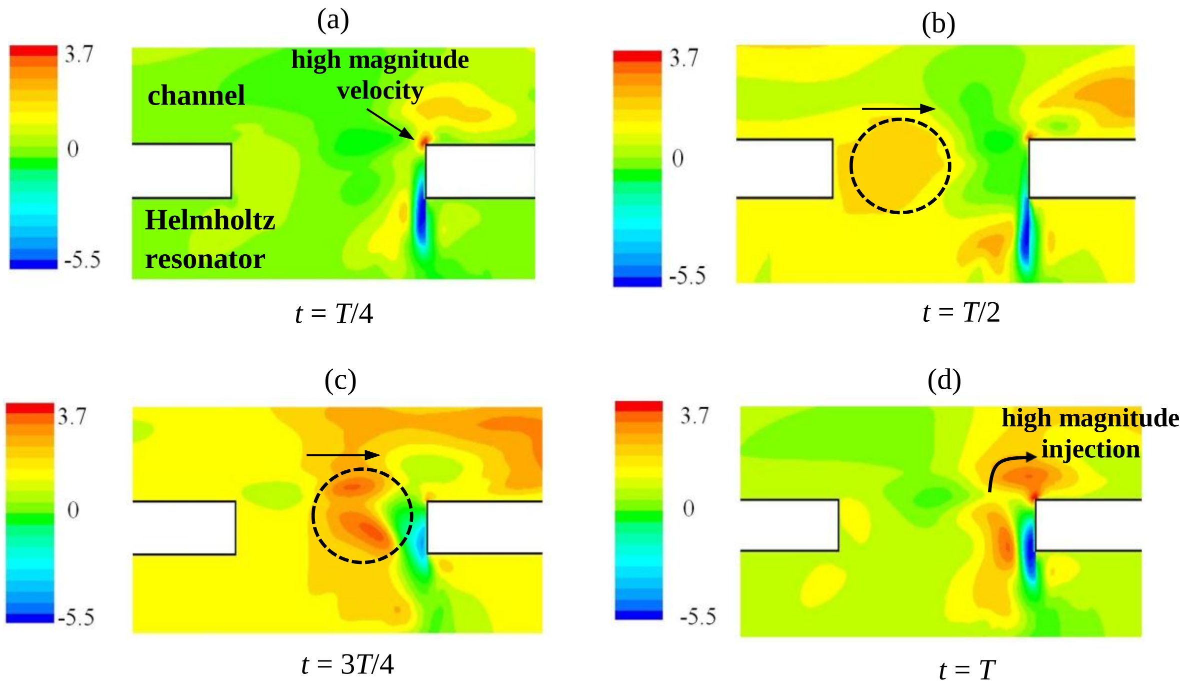


**Figure 9:** Contour of velocity fluctuations (in m/s) normal to the grazing flow in vicinity of the orifice of HR3 at $Re_\tau$ =1785 at various times in a period of the resonance frequency.

## 8. Modification of turbulent events by Helmholtz resonator

In the present study the variable interval time averaging (VITA) technique has been applied to detect the changes in turbulence structures over the entire Reynolds number range. This technique was first used by Blackwelder and Kaplan (1976) for studying the near-wall region of the turbulent boundary layer and it was successful in quantifying the turbulent events. This technique is based on the fact that during the sweep and ejection events the velocity changes rapidly. The VITA of the streamwise velocity fluctuations is defined by

$$\hat{u}\,(t, T_w) = \frac{1}{T_w}\int_{t-T_w/2}^{t+T_w/2} u(s)ds, \tag{2}$$

where $T_w$ is the interval used for the time averaging and must be of the order of the time scale of the turbulent events, which are typically of size ${T_w}^+ = T_w {u_\tau}^2/\nu = 10$. This small window moves through the signals, scans the fluctuating streamwise velocity signal, $u\,(s)$, and at each point the local variance of the signal is calculated as

$$\text{Var}\,(t, T_w) = \hat{u}^2(t, T_w) - [\hat{u}\,(t, T_w)]^2. \tag{3}$$

When the ratio of the variance across the window to the variance of the entire signal, $\text{Var}\,(t) = \lim_{t\to\infty} \int_0^t u^2(t)dt$, is larger than a threshold value, $k$, the sweep or ejection events are considered to occur. To differentiate the events a detection function, $\text{D}(t)$, has been defined as

$$\text{D}(t) = \begin{cases} 1 & \text{Var}\,(t, T_w) > k\text{Var}\,(t) \qquad \dfrac{du}{dt} > 0 \text{ (sweep event)} \\ 0 & \text{Var}\,(t, T_w) < k\text{Var}\,(t) \qquad \text{(no event)} \\ -1 & \text{Var}\,(t, T_w) > k\text{Var}\,(t) \qquad \dfrac{du}{dt} < 0 \text{ (ejection event)} \end{cases} \tag{4}$$

The frequency of the events is a strong function of the threshold value. In the present study the detector function, $k$, was set to 1.2. Figure 10 shows example values of the time series of the streamwise velocity fluctuations, the ratio of the variance across the window to the entire variance of the signal, and the detection function within the incoming boundary layer. It can be seen that one ejection and three sweep events have been detected. It must be noted that the majority of the turbulence energy is generated in burst-sweep cycles and hence they are responsible for instabilities within the boundary layer. Therefore, in the present study sweep events downstream of the resonators have been investigated.

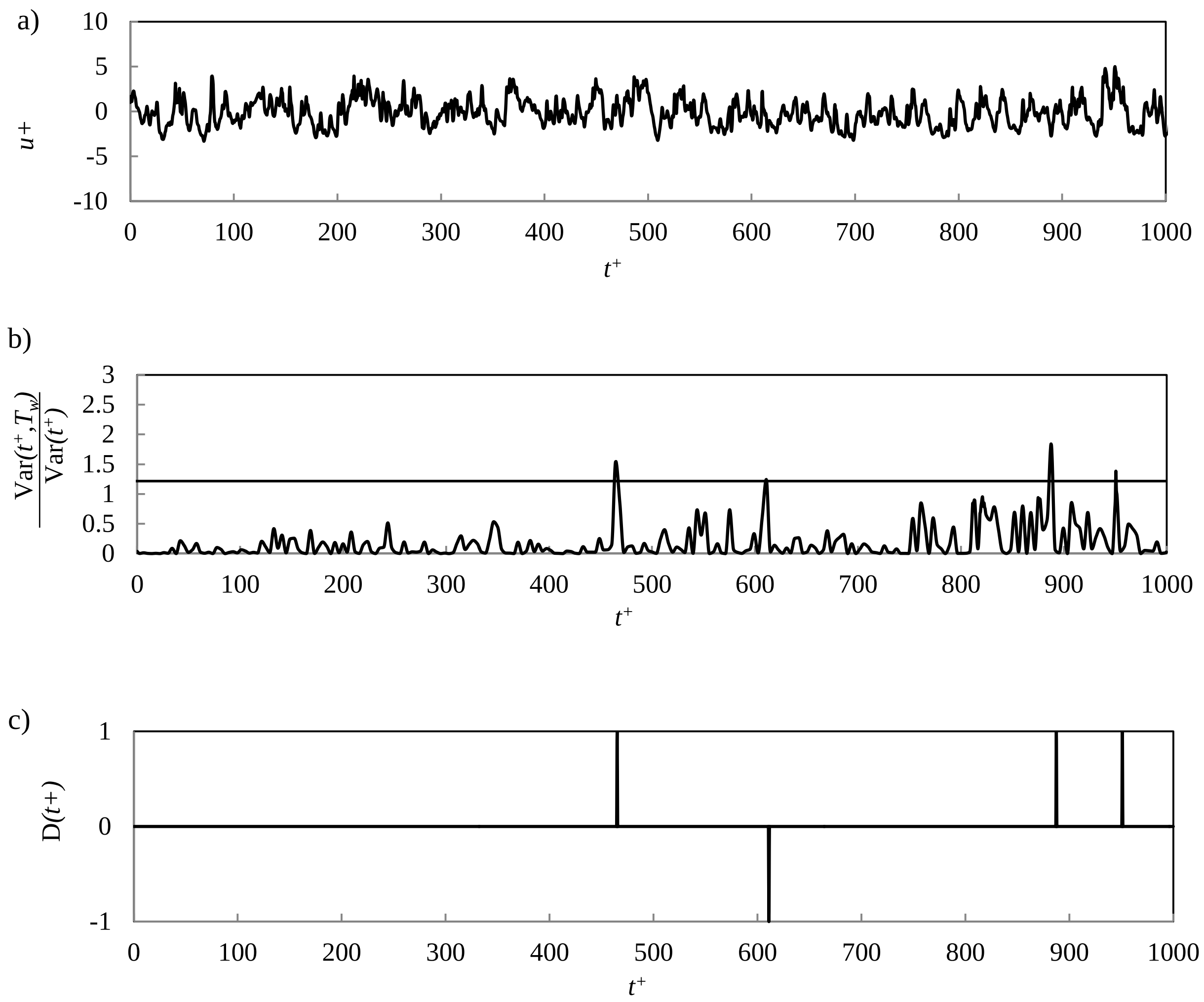


**Figure 10:** VITA detection of no-control turbulent boundary layer at $y^+ = 35$, a) streamwise velocity fluctuations, b) the ratio of the variance across the window to the entire variance of the signal, and c) the detection function.

The VITA events must be averaged to analyse the intensity and duration of each sweep event at different $y^+$positions. All events at each $y^+$ have been averaged within a small window with a size of $T_{\mathrm{av}}^+= -20$ to 20. The events are centred, such that $T_{\mathrm{av}}^+= 0$, at the maximum value of the velocity gradient. Figure (11a) reveals the multiple individual events over the small time window. It can also be seen from Figure 11b that the average of the VITA sweep events within the turbulent boundary layer is in good agreement with the published experimental results obtained by Whalley (2011).

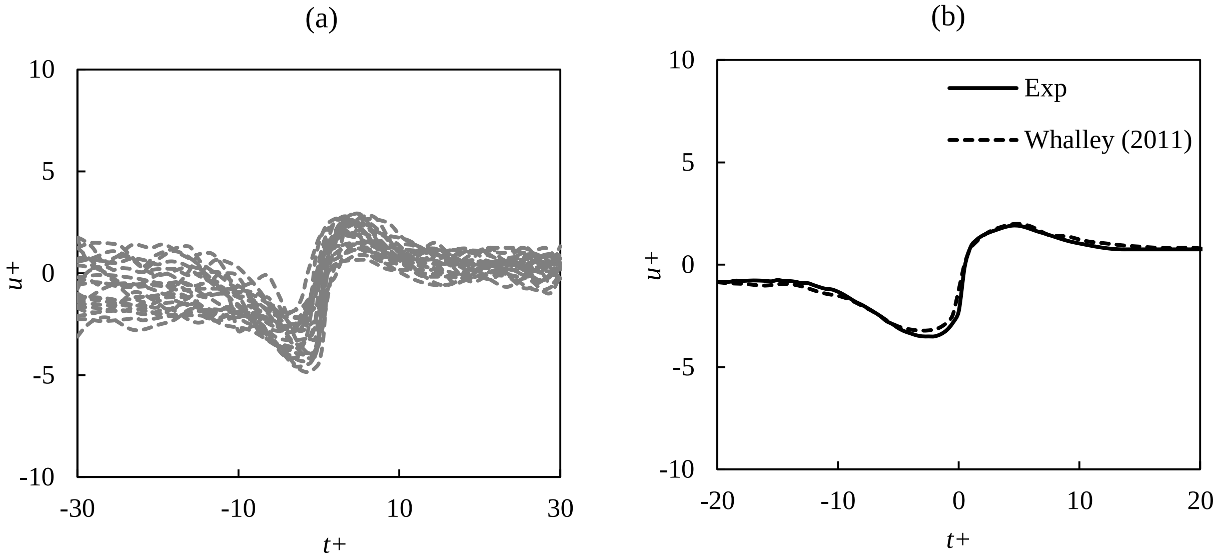


**Figure 11:** Experimental results for unexcited boundary layer VITA events at $y^{+} = 35$ and $\mathrm{Re}_{\tau} = 1785$; (a) sweep events and (b) averaged VITA sweep event.

The peak to peak value of the averaged VITA events reveals the intensity and the time difference between the peaks during the sweep events. In previous studies on flow control techniques, the investigations have focused on reducing the intensity and duration of the sweep events (Hooshmand et al. 1983; Choi 2002). For example, Figure 12 shows a reduction in the turbulent events outside of the viscous sublayer achieved by applying traveling waves, which reduce the intensity of the sweep events by up to 10% (Jukes et al. 2006). In the present study the sweep events have been calculated within the turbulent boundary layer downstream of the resonators with potential to stabilize the flow, HR2 and HR4. As shown in Figure 13(a), downstream of HR2 at $y^{+}$= 35, an 11% reduction in sweep intensity and a 5% reduction in sweep duration were observed. Figure 13(b) shows that moving further from the wall, at $y^{+}$= 100 the intensity and the duration are also reduced by 7% and 12% respectively. The results for HR4 also indicate that the sweep intensity at both locations, $y^{+}$= 35 and $y^{+}$= 100, is reduced by approximately 5% (Figure 13c & d). The duration of the sweep is also reduced by 8% downstream of HR4 at $y^{+}$= 100.

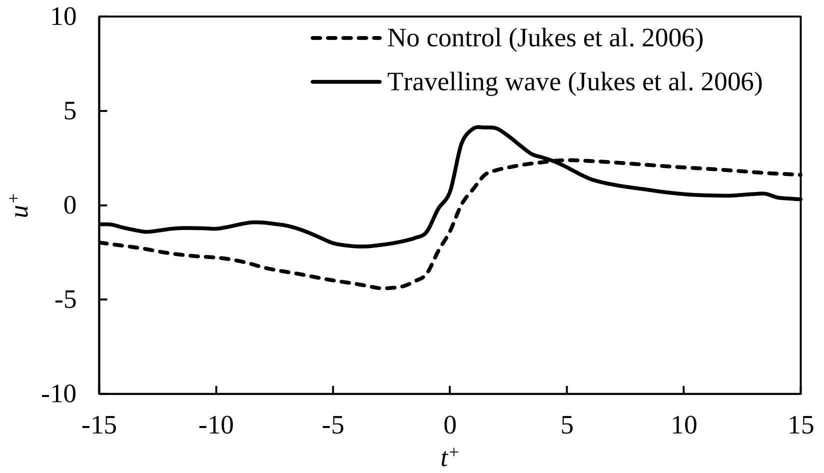


**Figure 12:** Averaged VITA events with and without travelling wave at $y^+$=30 (data based on Jukes et al. 2006).

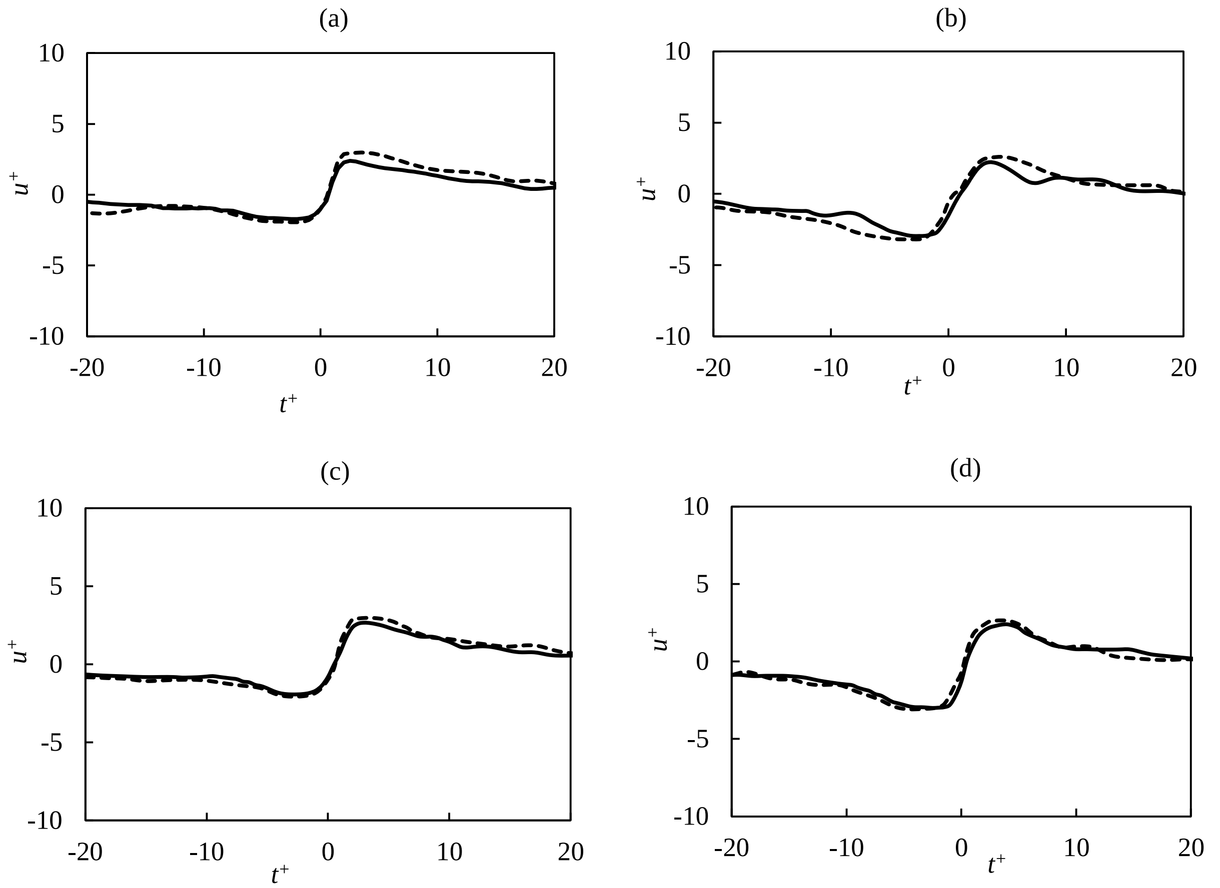


**Figure 13:** Averaged VITA sweep events; (solid line) with and (dashed line) without Helmholtz resonator at $\mathrm{Re}_\tau = 890$: (a) HR2 at $y^+$=35, (b) HR2 at $y^+$=100, (c) HR4 at $y^+$=35 and (d) HR4 at $y^+$=100.

Further increasing the free stream velocity has some effect on the sweep events. As can be seen in Figure 14(a), the sweep intensity downstream of HR2 within the logarithmic region is decreased at the two locations considered by approximately 7% when $\mathrm{Re}_\tau$= 1450. Downstream of HR2 the sweep duration remained unaltered at $y^+$= 35, whilst at $y^+$= 100 a slight reduction of approximately 10% is achieved (Figure 14b). However, for HR4 at $Re_\tau$= 1450, the resonator does not significantly change the structure of the sweep events, so a maximum of 3% and 4% reduction in the intensity and duration of sweep events at $y^+$= 35 and $y^+$= 100 was observed (Figure 14c & d). It can be concluded that at an increased flow velocity of $Re_\tau$ = 1450 the resonators investigated cannot significantly attenuate the turbulence energy. This is due to this fact that increasing the velocity of grazing flow amplifies the generation of the turbulent events.

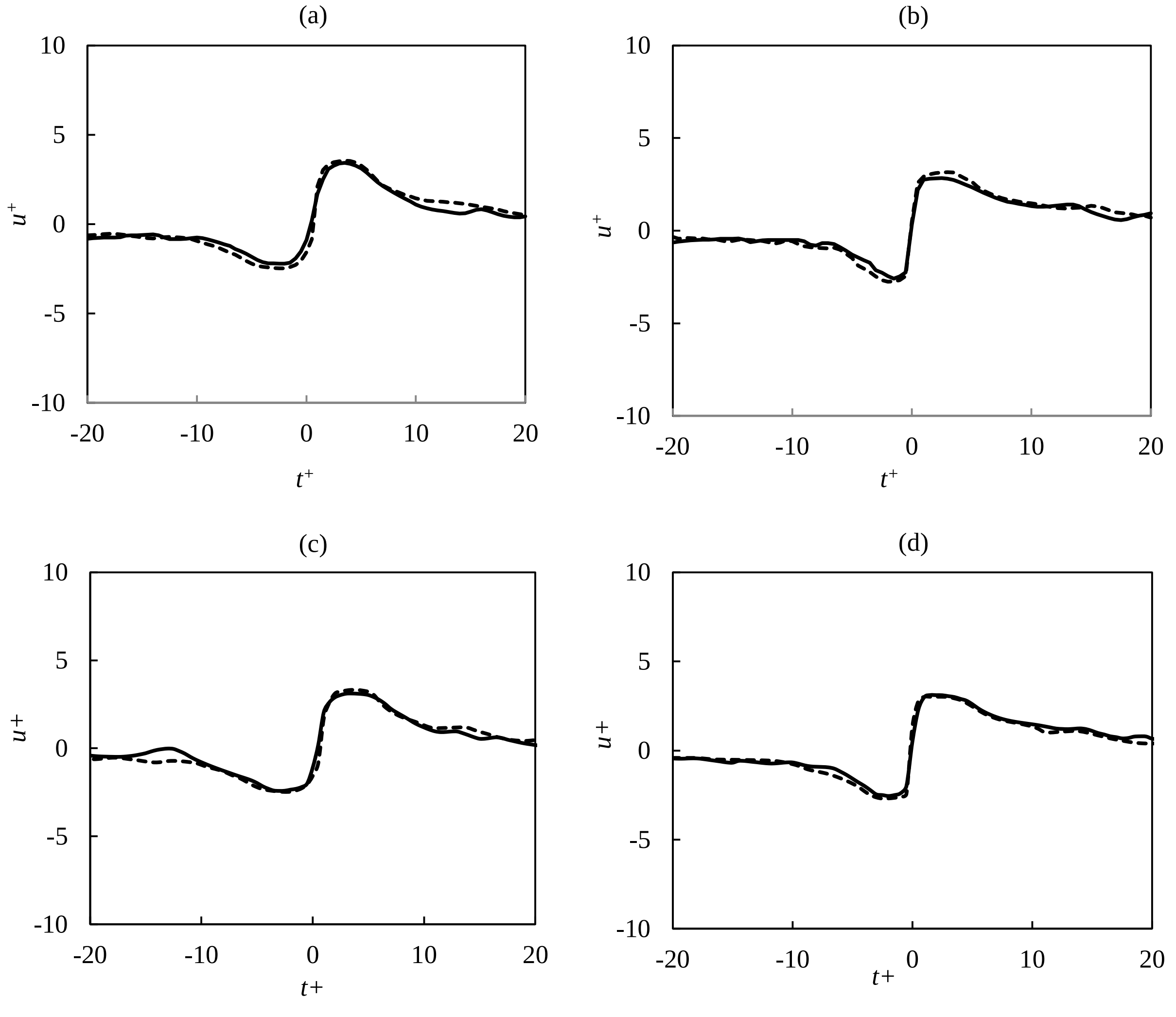


**Figure 14:** Averaged VITA sweep events; (line) with and (dash line) without Helmholtz resonator at $Re_\tau = 1450$: (a) HR2 at $y^+$=35, (b) HR2 at $y^+$=100, (c) HR4 at $y^+$=35 and (d) HR4 at $y^+$=100.

The effect of the resonators on the frequencies of the turbulent events has also been investigated. To this end, the sweep frequencies within the inner region of the boundary layer, up to $y^+$= 100, were calculated downstream of HR2 and HR4. It should be noted that the common feature of drag reduction techniques is an increase of 3 to 8 times greater in the sweep frequencies (Choi 1989; Whalley 2011). The sweep frequency was defined as the total number of sweep events which occur per unit time and non-dimensionalised with time scale, $f^+ = f\,\upsilon/u_\tau^2$. As can be seen in Figure 15, the frequencies obtained in the present study for the no-resonator case are very close to the results achieved by Blackwelder et al. (1983) and Whalley (2011). The sweep frequencies downstream of HR2 and HR4 were also investigated at $\mathrm{Re}_\tau$= 873. It was observed that there is an increase in the sweep frequencies, by up to 1.3 times, at $25 < y^+ < 50$, which indicates that the sweep duration has been reduced (Figure 15). The relationship between the resonance frequency of the resonators and the frequency of the turbulent events downstream of the resonators has also been investigated. As highlighted in Figure 15, the sweep frequencies are between 20% to 30% of the non-dimensional resonance frequency of the resonators, $f^+_{r,\mathrm{HR}}$.

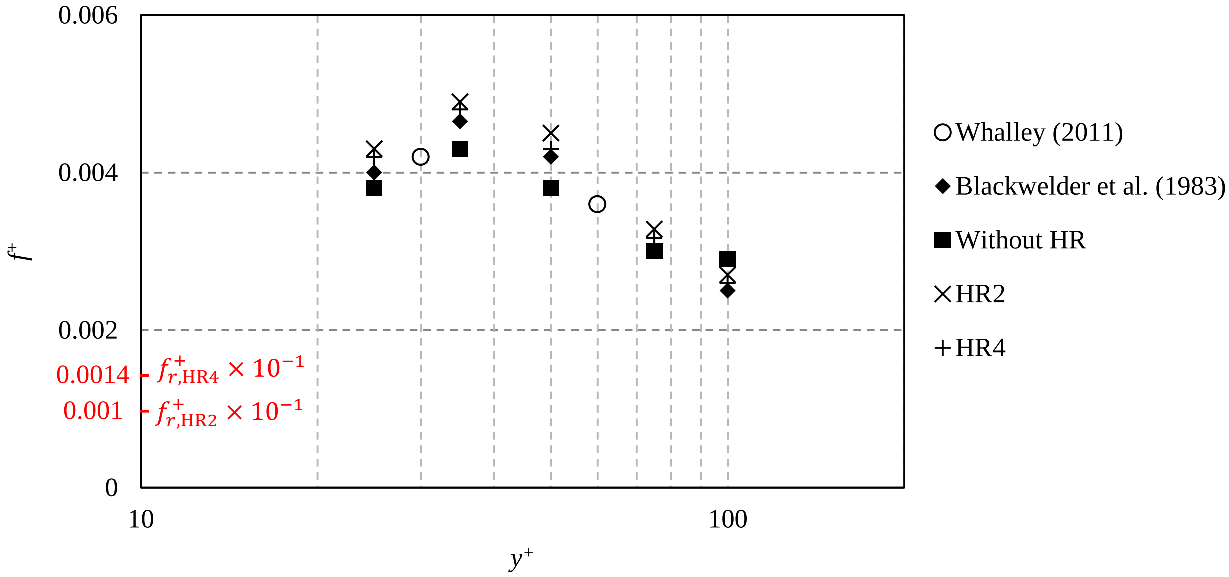


**Figure 15:** The frequency of sweep events downstream of HR2 and HR4 at $\mathrm{Re}_\tau$= 890.

Changes in the turbulence intensities can also be investigated by considering the probability density function (PDF) of the instantaneous streamwise velocities. Analysis of the PDF indicates alteration of the skewness and kurtosis associated with the $u$-component of the velocity. One usual characteristics of flow control techniques is an increase in skewness and kurtosis at $y^+ < 80$ (Choi & Clayton 2001), as shown in Figure 16.

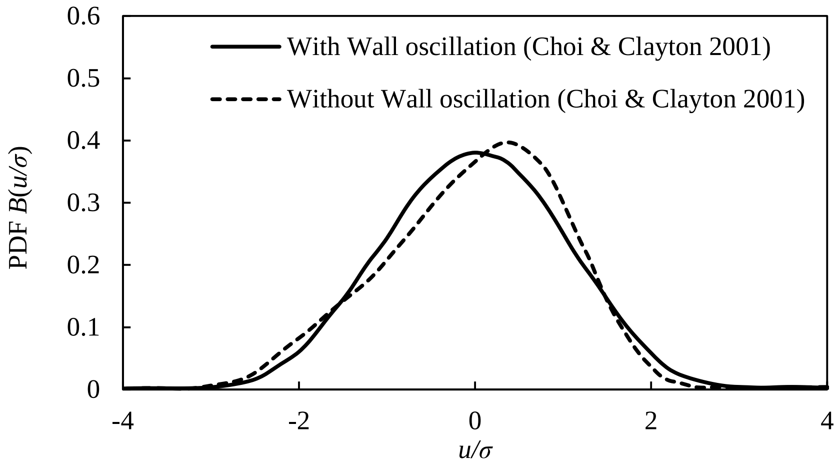


**Figure 16**: Probability density function of $u$-component velocity fluctuations at $y^+$=20 with and without wall oscillation (data based on Choi & Clayton 2001).

In the present study the PDFs have also been normalized by their own standard deviation at $y^+$= 35 downstream of HR2 and HR4. It can be seen in Figure 17 (a & c) that downstream of both HR2 and HR4 at $\mathrm{Re}_\tau = 890$ there is a long tail of positive probability, which results in an increase in skewness and kurtosis within the logarithmic region. It is hypothesized that the increase in the skewness and the kurtosis is associated with the streamwise vortices generated by the resonators. Figure 17(b) shows that further increasing the flow velocity to $\mathrm{Re}_\tau = 1450$, causes a small reduction in positive skewing downstream of HR2, whilst the kurtosis remains increased. Downstream of HR4 at $\mathrm{Re}_\tau = 1450$ there is also a slight increase in both the skewness and kurtosis in comparison to the no-resonator case (Figure 17d).

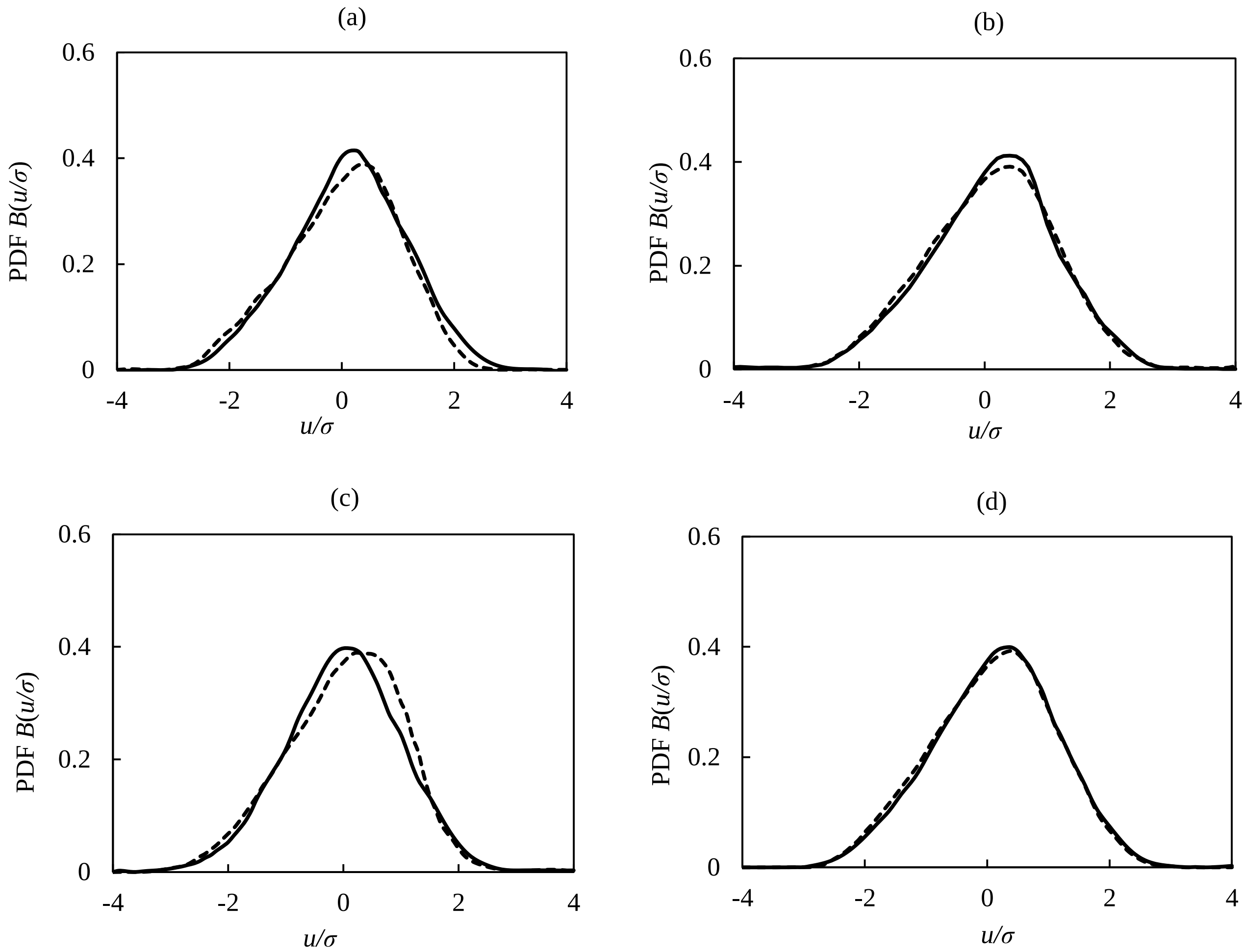


**Figure 17:** Probability density function of streamwise velocity fluctuations at $y^+ = 35$, (solid line) with and (dashed line) without Helmholtz resonator: (a) HR2 at $\mathrm{Re}_\tau$= 890, (b) HR2 at $\mathrm{Re}_\tau$= 1450, (c) HR4 at $\mathrm{Re}_\tau$= 890 and (d) HR4 at $\mathrm{Re}_\tau$= 1450.

## 9. Summary and Conclusion

As the oscillatory flow created by a flow-excited Helmholtz resonator is at the surface, the resonators are an ideal candidate for a wall based flow control method. An LES model and experiments have been undertaken to investigate the structure of a turbulent boundary layer downstream of four different cylindrical flow-excited Helmholtz resonators for a range of Reynolds numbers $800 < \mathrm{Re}_\tau < 2000$. This research provides an insight into how the resonators can attenuate the turbulence production in the boundary layer and also identifies the favourable parameters to stabilize the boundary layer. To validate the numerical analyses, as well as to evaluate uncertainties in the experimental data, the resonance frequency of each resonator, the mean streamwise velocity and turbulence intensity of the incoming boundary layer were compared against previously published data. A maximum difference of 10%

between the values shows excellent agreement and demonstrates that the incoming flow was a fully developed turbulent boundary layer with zero pressure gradient.

Disruption of the instantaneous velocity fields within the boundary layer was investigated downstream of all resonators. It was observed that when the orifice diameter equals the boundary layer thickness, the instabilities are amplified. When the orifice diameter is reduced to the thickness of the inner layer, $d \approx 300\upsilon/u_\tau$, a significant reduction of up to 16% occurs in the turbulence intensity downstream of the resonator. A slight reduction in the intensity and the duration of the sweep, of 11% and 5% respectively, also indicates the capability of this resonator to reduce turbulent energy production. The contour plots of the velocity fluctuations normal to the grazing flow demonstrate that a relatively low value of the velocity pulsation, up to 0.5m/s, disrupts the quasi-streamwise vortices which naturally occur within the boundary layer and thus modifies the turbulence regeneration cycle. However, it was also shown that increasing the flow velocity causes an increase in the instabilities for this resonator.

The orifice length is another important resonator parameter which affects the structure of the turbulent boundary layer, such that a significant amplification of up to 20% was observed downstream of the resonator with the shortest orifice length, $l \leq 150\upsilon/u_\tau$. This is thought to be due to the high value of the pressure fluctuations within this resonator, which amplifies the instabilities (Ghanadi et al 2014b). However, increasing the orifice length such that $l \approx \delta$ causes an energy transfer from the large eddies to the small eddies in the near wall region resulting in a slight suppression, up to 12%, of the velocity fluctuations downstream of the resonator. The PDF of the streamwise velocity fluctuations downstream of this resonator also demonstrates a slight positive skewing and narrowing in comparison with similar values in the no-resonator case, which indicates an attenuation of turbulence energy production within the boundary layer.

Therefore, it is suggested that when the orifice length of a Helmholtz resonator equals the boundary layer thickness and the orifice diameter approaches the thickness of the inner layer, the resonator can be used as a flow control device. The results presented in this paper are only the beginning of the development of a flow-excited Helmholtz resonator as a flow control device. Consequently a significant amount of work, such as varying different geometric parameters and flow conditions, still exists for future investigations.

**References**

Amandolese, X, Hemon, P & Regardin, C 2004, 'An experimental study of the acoustic oscillations by flows over cavities', *Journal of Vibration and Acoustics*, vol. 126, no. 2, pp. 190-195.

Berger, TW, Kim, J, Lee, C & Lim, J 2000, 'Turbulent boundary layer control utilizing the Lorentz force', *Physics of Fluids*, vol. 12, no. 3, pp. 631-649.

Bilanin, AJ & Covert, EE 1973, 'Estimation of possible excitation frequencies for shallow rectangular cavities', *AIAA Journal*, vol. 11, no. 3, pp. 347-351.

Blackwelder, RF & Kaplan, RE 1976, 'On the wall structure of the turbulent boundary layer', *Journal of Fluid Mechanics*, vol. 76, no.1, pp. 89–112.

Blackwelder, R. and Haritonidis, J 1983, 'Scaling of the bursting frequency in turbulent boundary layers', *Journal of Fluid Mechanics*, vol. 132, no. 1, pp. 87-103.

Bruggeman, J, Hirschberg, A, Van Dongen, M, Wijnands, A & Gorter, J 1991, 'Self-sustained aero-acoustic pulsations in gas transport systems: experimental study of the influence of closed side branches', *Journal of Sound and Vibration*, vol. 150, no. 3, pp. 371-393.

Candler, GEW 1996, 'Comparison of Baldwin-Lomax turbulence models for two-dimensional open cavity computations', *AIAA Journal*, vol. 34, no. 3, pp. 629-631.

Charwat, A & Walker, B 1983, 'Velocity perturbations above the orifice of an acoustically excited cavity in grazing flow', *Journal of Fluid Mechanics*, vol. 128, pp. 413-426.

Chatellier, L, Laumonier, J & Gervais, Y 2004, 'Theoretical and experimental investigations of low Mach number turbulent cavity flows', *Experiments in Fluids*, vol. 36, no. 5, pp. 728-740.

Choi, K 1989, 'Near-wall structure of a turbulent boundary layer with riblets', *Journal of Fluid Mechanics*, vol. 208, pp. 417-458.

Choi, KS 2002, 'Near-wall structure of turbulent boundary layer with spanwise-wall oscillation', *Physics of Fluids*, vol. 14, no. 7, pp. 2530-2542.

Choi, K & Clayton, B, R, 2001, 'The mechanism of turbulent drag reduction with wall oscillation', *International Journal of Heat and Fluid Flow*, vol. 22, no. 1, pp. 1-9.

Choi, KS, Jukes, T and Whalley, R 2011, 'Turbulent boundary-layer control with plasma actuators', *Philosophical Transactions of the Royal Society A: Mathematical, Physical and Engineering Sciences*, vol. 369, pp. 1443-1458.

Colonius, T, Basu, AJ & Rowley, CW 1999, 'Numerical investigation of the flow past a cavity', *5th AIAA/CEAS Aeroacoustics Conference*, Washington, USA.

Crouse, B, Senthooran, S, Freed, D, Balasubramanian, G, Gleason, M, Puskarz, M, Lew, P & Mongeau, L 2006, 'Experimental and numerical investigation of a flow induced cavity resonance with application to automobile buffeting', *27th AIAA Aeroacoustics Conference*, Massachusetts, USA.

de Jong, A, Bijl, H, Hazir, A & Wiedemann, J 2012, 'Aeroacoustic simulation of slender partially covered cavities using a Lattice Boltzmann method', *Journal of Sound and Vibration*, vol. 323, no. 7, pp. 1687-1703.

Dequand, S, Hulshoff, S, Kuijk, HV, Willems, J & Hirschberg, A 2003, 'Helmholtz-like resonator self-sustained oscillations, Part 2: Detailed flow measurements and numerical simulations', *AIAA Journal*, vol. 41, no. 3, pp. 416-423.

Dhanak, M & Si, C 1999, 'On reduction of turbulent wall friction through spanwise wall oscillations', *Journal of Fluid Mechanics*, vol. 383, pp. 175-195.

Du, Y, Symeonidis, V & Karniadakis, G 2002, 'Drag reduction in wall-bounded turbulence via a transverse travelling wave', *Journal of Fluid Mechanics*, vol. 457, pp. 1-34.

Elder, S, Farabee, T & DeMetz, F 1982, 'Mechanisms of flow-excited cavity tones at low Mach number', *Journal of the Acoustical Society of America*, vol. 72, pp. 532-549.

El-Samni, O, Chun, HH and Yoon, HS 2007, 'Drag reduction of turbulent flow over thin rectangular riblets', *International Journal of Engineering Science*, vol. 45, no. 2, pp. 436-454.

Flynn, KP & Panton, RL 1990, 'The interaction of Helmholtz resonators in a row when excited by a turbulent boundary layer', *Journal of the Acoustical Society of America*, vol. 87, no. 4, pp. 1482-1488.

Gad-el-Hak, M 2000, 'Flow control: passive, active, and reactive flow management', Cambridge University Press.

García-Mayoral, R and Jiménez, J 2011, 'Drag reduction by riblets', *Philosophical Transactions of the Royal Society A: Mathematical, Physical and Engineering Sciences*, vol. 369, pp. 1412-1427.

Georges, L, Winckelmans, G, Caro, S & Geuzaine, P 2006, 'Aeroacoustic simulation of the flow in a Helmholtz resonator', *Computational Fluid Dynamics 2006*, pp. 819-824, Ghent, Belgium.

Ghanadi, F, Arjomandi, M, Cazzolato, B & Zander, A 2013a 'Numerical simulation of grazing flow over a self-excited Helmholtz resonator', *Engineering Letters*, vol. 21, no 3, pp. 137-142.

Ghanadi, F, Arjomandi, M, Cazzolato, BS & Zander, AC 2013b, 'Velocity fluctuations within the turbulent flow over a flow-excited Helmholtz resonator', *The 2013 International Conference on Mechanical and Materials Engineering*, Stockholm, Sweden.

Ghanadi, F, Arjomandi, M, Cazzolato, BS & Zander, AC 2014a, 'Understanding of the flow behaviour on a Helmholtz resonator excited by grazing flow', *International Journal of Computational Fluid Dynamics*, published online (DOI: 10.1080/10618562.2014.922681).

Ghanadi, F, Arjomandi, M, Cazzolato, BS & Zander, AC 2014b, 'Interaction of a flow-excited Helmholtz resonator with a grazing turbulent boundary layer', *Experimental Thermal and Fluid Science*, vol. 58, pp. 80-92.

Hardin, JC & Mason, JP 1977, 'Broadband noise generation by a vortex model of cavity flow', *AIAA Journal*, vol. 15, no. 5, pp. 632-637.

Hefner, JN 1988, 'Dragging down fuel costs'. *Aerospace America*, vol. 26, no. 2, pp. 1-14.

Holmberg, A 2010, 'Experimental determination of aeracoustic sources in low Mach number internal flows', *Licentiate thesis*, KTH, Sweden.

Hooshmand, D, Youngs, R, Wallace, J & Balint, J 1983, 'An experimental study of changes in the structure of a turbulent boundary layer due to surface geometry changes', *AIAA 21st Aerospace Sciences Meeting*, AIAA-83-0230, Nevada, USA.

Howe, M 1981, 'Influence of mean shear on unsteady aperture flow, with application to acoustical diffraction and self-sustained cavity oscillations', *Journal of Fluid Mechanics*, vol. 109, pp. 125-146.

Inagaki, M, Murata, O, Kondoh, T & Abe, K 2002, 'Numerical prediction of fluid-resonant oscillation at low Mach number', *AIAA Journal*, vol. 40, no. 9, pp. 1823-1829.

Jukes, T.N 2007, 'Turbulent drag reduction using surface plasma', *Ph.D. thesis*, University of Nottingham.

Jukes, TN, Choi, KS, Johnson, GA and Scott, SJ 2006, 'Turbulent drag reduction by surface plasma through spanwise flow oscillation', *3rd AIAA Flow Contorl Conference, Paper No. AIAA-2006-3693*, California, USA.

Jung, W, Mangiavacchi, N, & Akhavan, R 1992, 'Suppression of turbulence in wall-bounded flows by high-frequency spanwise oscillations', *Physics of Fluids*, vol. 4, no. 8, pp. 1605-1607.

Kasagi, N, Suzuki, Y, and Fukagata, K 2009, 'Microelectromechanical systems-based feedback control of turbulence for skin friction reduction', *Annual Review of Fluid Mechanics*, vol. 41, pp. 231-251.

Kooijman, G 2007, 'Acoustical response of shear layers', *Ph.D. thesis*, Endhoven University of Technology.

Kook, H, Mongeau, L & Franchek, M 2002, 'Active control of pressure fluctuations due to flow over Helmholtz resonators', *Journal of Sound and Vibration*, vol. 255, no. 1, pp. 61-76.

Khosropour, R & Millet, P 1990, 'Excitation of a Helmholtz resonator by an air jet', *Journal of the Acoustical Society of America*, vol. 88, no. 3, pp. 1211-1221.

Kramer, MO 1961, 'The dolphin’s secret', *Naval Engineers Journal*, vol. 73, pp. 103–107.

Laadhari, F, Skandaji, L and Morel, R 1994, 'Turbulence reduction in a boundary layer by a local spanwise oscillating surface', *Physics of Fluids*, vol. 6, pp. 3218-3220.

Larchevêque, L, Sagaut, P, Mary, I, Labbé, O & Comte, P 2002, 'Large-eddy simulation of a compressible flow past a deep cavity', *Physics of Fluids*, vol. 15, no. 1, pp. 193-210.

Lee, SJ & Choi, YS 2008, 'Decrement of spanwise vortices by a drag-reducing riblet surface', *Journal of Turbulence*, vol. 9, no. 23, pp. 1–15.

Lockerby, D 2001, 'Numerical simulation of boundary-layer control using MEMS actuation', *Ph. D. Thesis*, The University of Warwick.

Meissner, M 2005, 'The response of Helmholtz resonator to external excitation. Part II: flow-induced resonance', *Archives of Acoustics*, vol. 30, no. 1, pp. 57–71.

Mallick, S, Shock, R & Yakhot, V 2003, 'Numerical simulation of the excitation of a Helmholtz resonator by a grazing flow', *Journal of the Acoustical Society of America*, vol. 114, no. 4, pp. 1833-1840.

Marusic, I & Kunkel, GJ 2003 'Streamwise turbulence intensity formulation for flat-plate boundary layers', *Physics of Fluids*, vol. 15, no. 8, pp. 2461–2464.

Mast, TD & Pierce, AD 1995, 'Describing-function theory for flow excitation of resonators', *The Journal of the Acoustical Society of America*, vol. 97, no.1, pp. 163-172.

Massenzio, M, Biaise, A & Lesueur, C 2008, 'Mechanisms of self-sustained oscillations induced by a flow over a cavity', *Journal of Vibration and Acoustics*, vol. 130, no. 5, pp. 1-8

Merkle, C and Deutsch, S 1989, 'Drag reduction in liquid boundary layers by gas injection. In: Viscous drag Reduction in Boundary layers', *AIAA paper*, AIAA-91-12688 02-34, pp. 351-412, Washington, USA.

Myose, RY & Blackwelder, RF 1995, 'Control of streamwise vortices using selective suction', *AIAA Journal*, vol. 33, no. 6, pp. 1076-1080.

Nelson, PA, Halliwell, NA & Doak, PE 1981, 'Fluid dynamics of a flow excited resonance, part I: Experiment', *Journal of Sound and Vibration*, vol. 78, no. 1, pp. 15-38.

Nelson, PA, Halliwell, NA & Doak, PE 1983, 'Fluid dynamics of a flow excited resonance, Part II: Flow acoustic interaction', *Journal of Sound and Vibration*, vol. 91, no. 3, pp. 375-402.

Nicoud, F & Ducros, F 1999, 'Subgrid-scale stress modelling based on the square of the velocity gradient tensor', *Flow, Turbulence and Combustion*, vol. 62, no. 3, pp. 183-200.

Pang, J & Choi, KS, 2004 'Turbulent drag reduction by Lorentz force oscillation', *Physics of Fluids*, vol. 16, no. 5, pp. 35-38.

Panton, R 1990, 'Effect of orifice geometry on Helmholtz resonator excitation by grazing flow', *AIAA Journal*, vol. 28, pp. 60-65.

Panton, RL & Miller, JM 1975, 'Excitation of a Helmholtz resonator by a turbulent boundary layer', *Journal of the Acoustical Society of America*, vol. 58, no. 4, pp. 800-806.

Ricot, D, Maillard, DRV & Bailly, C 2001, 'Numerical simulation of the unsteady flow past a cavity and application to the sunroof buffeting'. *7th AIAA/CEAS Aeroacoustics Conference*, Maastricht, Netherlands.

Rockwell, D & Naudascher, E 1978, 'Review-self-sustaining oscillations of flow past cavities', *ASME Transactions Journal of Fluids Engineering*, vol. 100, pp. 152-165.

Rossiter, J & Britain, G 1964, 'Wind tunnel experiments on the flow over rectangular cavities at subsonic and transonic speeds', Ministry of Aviation, Aeronautical Research Council Reports and Memoranda, Technical report 64307, RAE.

Savill, A & Mumford, J 1988, 'Manipulation of turbulent boundary layers by outer-layer devices: Skin-friction and flow-visualization results', *Journal of Fluid Mechanics*, vol. 191, pp. 389-418.

Selamet, A, Radavich, P, Dickey, N & Novak, J 1997, 'Circular concentric Helmholtz resonators', *The Journal of the Acoustical Society of America*, vol. 101, no. 1, pp. 41-51.

Sinha, N, Arunajatesan, S & Ukeiley, L 2000, 'High fidelity simulation of weapons bay aeroacoustics attenuation using active flow control', *6th AIAA/CEAS Aeroacoustics Conference*, Lahaina, Hawaii.

Sipp, D 2012, 'Open-loop control of cavity oscillations with harmonic forcings', *Journal of Fluid Mechanics*, vol. 708, pp. 439-468.

Tam, CKW & Block, P 1978, 'On the tones and pressure oscillations induced by flow over rectangular cavities', *Journal of Fluid Mechanics*, vol. 89, no. 2, pp. 373-399.

Toda, HB, Cabrit, O, Balarac, G, Bose, S, Lee, J, Choi, H & Nicoud, F 2010, 'A subgrid-scale model based on singular values for LES in complex geometries', *Proceedings of the Summer Program (Center for Turbulence Research, NASA Ames/Stanford University, Stanford, CA, 2010)*, pp. 193-202.

Tonon, D, Willems, J & Hirschberg, A 2010, 'Flow-induced pulsations in pipe systems with closed side branches: study of the effectiveness of detuning as remedial measure', *20th International Congress on Acoustics*, Sydney, Australia.

Viotti, C, Quadrio, M & Luchini, P 2009, 'Streamwise oscillation of spanwise velocity at the wall of a channel for turbulent drag reduction'. *Physics of Fluids*, vol. 21, pp. 1-9.

Virk, P 1975, 'Drag reduction fundamentals', *AIChE Journal*, vol. 21, pp. 625–656.

Wagner, CA, Huttl, T & Sagaut, P 2007, 'Large-eddy simulation for acoustics', Cambridge Univ Press.

Walsh, MJ, 1983 'Riblets as a viscous drag reduction technique', *AIAA Journal*, vol. 21, no. 4, pp. 485-486.

Whalley, RD 2011, 'Turbulent boundary-layer control with DBD plasma actuators using spanwise travelling-wave technique', *Ph.D. thesis*, University of Nottingham.

White, FM 1991, 'Viscous fluid flow', McGraw-Hill Professional Publishing.

Zhang, Q & Bodony, DJ 2013 'Impedance prediction of three-dimensional honeycomb liners with laminar/turbulent boundary layers using DNS', *19th AIAA/CEAS Aeroacoustics Conference*, Berline, Germany.

# Chapter 7

# Conclusions and Future Work

Turbulent boundary layer control employing a flow-excited Helmholtz resonator has been investigated in this study. To support the developed hypothesis, the research has included theoretical and numerical studies, along with experimental work, focusing on the design and performance assessment of Helmholtz resonators excited by an upstream turbulent boundary layer. The primary contribution of the thesis is analysis of the instantaneous flow fields within the cavity and the shear layer that develops over the orifice of the resonator. Further to this, the turbulence structures downstream of the resonator orifice have been investigated to provide an insight into the potential of the resonators for attenuation of the turbulent events. The required features of the resonator and the incoming flow to stabilise the turbulent flow downstream of the orifice have also been investigated. The following sections outline the specific conclusions, outcomes and achievements drawn from the different parts of the present research.

### 7.1 Instantaneous pressure field inside the resonator

To address the lack of information pertaining to the flow behaviour within a flow-excited Helmholtz resonator, the research commenced by first identifying the instantaneous pressure fields generated inside the resonator. The investigations illustrated that the maximum pressure fluctuation occurs at a frequency close to the resonance frequency of the resonator which implies that the resonator is self-excited. Predicting the pressure inside a Helmholtz resonator using an analytical model, based on combination of the vortex sheet and discrete vortex models, demonstrated that the pressure amplitudes inside the resonator are strongly affected by the resonator geometry. The outcome of the analyses provides refined estimates of the pressure fluctuations generated by the resonator and assesses the effects of the resonator geometry on the instantaneous pressure field within the cavity. The results showed that when the orifice length is increased, the pressure fluctuations within the resonator are reduced due to skin friction or increased velocity inside the orifice. In addition, it was shown that for an orifice with fixed dimensions, as the length-to-diameter ratio of the resonator cavity is decreased, the energy exchange between the air flow inside the cavity and the grazing flow over the orifice decreases, which reduces the likelihood of excitation occurring (explained in Chapter 3). The sensitivity of the pressure fluctuations to the resonator geometry and the characteristics of the incoming flow was also analysed using numerical and experimental investigations of 12 different cylindrical Helmholtz resonators, with freestream velocities up to 30m/s. It was observed that there is almost no excitation of the pressure field when the free stream velocity is less than 15m/s and the length-to-diameter ratio of the cavity is less than four. It was found that when the turbulent boundary layer thickness is close to the orifice diameter, a high value of the Power Spectral Density (PSD) of the pressure fluctuations up to 18dB occurs, as shown in Chapters 4 & 5 of this thesis. In fact, when $\delta \approx d$, eddies can easily penetrate the cavity and increase the pressure magnitude of the cavity flow. Conversely, when the orifice diameter is reduced to the thickness of the inner layer of the boundary layer, $d \approx 300\upsilon/u_\tau$, a significant reduction, of up to 16%, occurs in the maximum value of the instantaneous pressure (Chapter 5). It has been observed that the pressure distribution within the resonator is also affected by the changes in the orifice length, such that when the orifice length approaches the boundary layer thickness, the vortices within the grazing flow cannot induce significant force into the cavity flow and the amplitude of the pressure PSD is decreased by up to 22dB (Chapter 5). The results highlight the major parameters that have a significant impact on the flow behaviour within the resonator and resulted in the development of an appropriate system for flow control purposes.

## 7.2 Velocity fluctuations within the shear layer

The instantaneous values of the cross-stream component of the flow velocity within the shear layer over the Helmholtz resonator orifice were investigated. It was observed that with increasing free stream velocities, the region of maximum interaction of the grazing flow with the resonator moves towards the leading edge of the orifice for all of the resonators investigated. The maximum values of the velocity fluctuations were found to occur at frequencies close to the natural frequency of the resonator excited by the grazing flow (Chapter 4). For the resonator with $l \approx \delta$, the area of flow suction in the vicinity of the orifice is greater than the flow injection area. For this particular resonator, the maximum suction-velocity is greater than for the other resonators throughout the range of investigated flow velocities. It was postulated that this flow behaviour reduces the stretching of the longitudinal vortices within the boundary layer leading to a reduction in the instabilities. It was also observed that when the inner layer of the boundary layer equals the orifice diameter, low values of the velocity pulsation, up to 0.5m/s, penetrate the logarithmic region of the downstream boundary layer and extend up to a distance of $2d$ from the trailing edge of the resonator orifice (see Chapter 5). As a consequence, this process generates semi-longitudinal vorticity, which suppresses the instabilities within the boundary layer. The results discussed in this section explore the flow behaviour in the vicinity of the resonator orifice and thus provide an insight into how the resonators attenuate the instabilities within the boundary layer.

### 7.3 Manipulation of the turbulent boundary layer

The major objective of the present study is attenuation of the streamwise velocity fluctuations and the turbulence events within the viscous and logarithmic regions of the turbulent boundary layer. Therefore, the disrupted instantaneous velocity fields were investigated within the boundary layer downstream of all the resonators. It was observed that when the orifice diameter approaches the boundary layer thickness, the root mean square (RMS) of the turbulence intensity within the logarithmic region of the boundary layer was amplified. Moreover, the instabilities downstream of the resonator with the smallest orifice length, among other investigated resonators, $l \approx 100\upsilon/u_\tau$, are also significantly increased by a maximum of 20% (Chapter 3). This is due to strong excitation of the pressure fluctuations within the resonator. Another reason for the amplification of the instabilities is the injection of high velocity fluid from the cavity flow perpendicular to the grazing flow, which occurs very close to the trailing edge of the resonator orifice.

When the orifice length equals the boundary layer thickness or the orifice diameter approaches the thickness of the inner layer of the boundary layer, a reduction of up to 16% in the turbulence intensity of the streamwise velocity fluctuations occurs. This demonstrates the potential of the resonators to stabilise the grazing flow. Downstream of these resonators, an energy transfer from the larger eddies to the smaller eddies within the near wall region ($y^+ < 80$) also results in a slight suppression of the instabilities of the boundary layer. The modifications to the turbulence intensity caused by these two resonators were also considered through analysis of the changes in the turbulence regeneration cycles within the logarithmic region of the boundary layer (Chapter 5). It was postulated that the vortices in the vicinity of the orifice reduce the transport of high momentum fluid toward the surface. Using the variable interval time averaging (VITA) technique, a slight reduction in the intensity of sweep events by up to 11% was observed at two different spatial locations within the logarithmic region ($y^+$= 35 and $y^+$= 100). The sweep frequencies downstream of both resonators are also increased, by up to 1.3 times, at $25 < y^+ <50$. This indicates that the sweep duration is reduced. A slight positive skewing and narrowing in the streamwise velocity fluctuations was also observed in the flow downstream of the resonator, which also confirms the attenuation of turbulence energy production within the boundary layer. The relationship between the resonance frequency of the resonators and the frequency of the turbulent events also demonstrated that the sweep frequencies are between 20-30% of the resonance frequency of both resonators (Chapter 6). The results further illustrated that the reduction in the turbulence intensity of the streamwise velocity fluctuations and sweep events occurs immediately downstream of the resonator orifice, but that this effect dissipated further away from the resonator orifice. The disruption of turbulence-producing activities was thought to be due to thinning of the boundary layer thickness downstream of the resonator in the streamwise direction and the weakness of spanwise vortices generated by the resonator. The results demonstrated that the oscillatory flow at the surface created by a flow-excited Helmholtz resonator is an ideal candidate for a wall based flow control method.

In summary, the main outcomes of the research and advantages of the device are as follows:

- The capacity of the resonator to extract the energy required for attenuation of the instabilities from the grazing flow has been studied.
- A favourable flow induced pulsation in the vicinity of the resonator orifice was achieved to manipulate the downstream turbulent flow.
- A significant reduction in the turbulence intensity of the streamwise velocity fluctuations within the logarithmic region of the boundary layer was observed.

- The device resulted in disruption of the turbulence regeneration cycles and reduces the intensity and duration of the sweep events, but increases their frequency.
- The potential to stabilise the turbulent boundary layer with minimum manufacturing problems and energy consumption is demonstrated.
- An improved understanding for further development of adjacent resonators as potentially ideal system for the purpose of turbulent flow control is proposed.

These outcomes reveal that the aims of the project which were stated in the first chapter have been met.

### 7.4 Recommendations for future work

The results of this study provide the baseline for further development of flow-excited Helmholtz resonators as a flow control device, an area that warrants further investigation in the future. Manipulation of regenerated turbulent cycles using the flow-excited resonator is a complex phenomenon and the challenges involved in solving the problem are only just beginning to come to light. Therefore, a significant amount of potential work, such as varying the different geometric parameters and flow conditions, still exists for future investigations. The second section of this final chapter, therefore, presents the recommendations identified by the author, and discusses how these will complement and further the research presented in this thesis.

#### 7.4.1 Effects of the flow conditions on the resonator performance

Throughout this research, all experimental investigations were conducted at a limited range of Reynolds numbers. Therefore, it is suggested that further study needs to examine how robust the conclusions drawn are to the thickness of the boundary layer at the resonator location. The experimental arrangement for providing the conditions for such studies in a zero pressure gradient has also been designed and, hence, it is recommended to observe the effects of the resonators in a vast range of Reynolds numbers. Further studies can also focus on the laminar flow regime and assess the changes in the position of transition downstream of each resonator. In order to delay boundary layer transition, it is anticipated that the resonators must have low resonance frequencies and, therefore, the geometry of the resonators would need to be modified.

All investigations in this research have been conducted for flow over a flat plate at zero pressure gradient. The impact of other parameters like favourable or adverse pressure gradients on the effectiveness of the resonators to stabilise the boundary layer can also be investigated in greater detail. Therefore, possibilities for further work exist for using the flow-excited Helmholtz resonator under adverse pressure gradients, such as those encountered on turbine blades or wings. It should also be mentioned that the effects of other properties of the incoming flow such as turbulence intensity on pressure fluctuations within the cavity were ignored in the model developed in this study. Therefore, there is a need for further research to develop a comprehensive model that predicts the flow properties in the interior and exterior of a flow-excited Helmholtz resonator with various inflow conditions.

### 7.4.2 Shape and arrangement effects of the resonator on the grazing flow

Further work can also be done in order to determine the impact of the characteristics of the Helmholtz resonator. In all investigations conducted in the present study, the orifice and cavity of the resonators have sharp edges and circular cross-section and, hence, the effects of the orifice and the cavity shape on the turbulence structures were ignored. It is suggested that for the future numerical work that several resonators with different shapes of the orifice and the cavity of the resonator can be analysed to identify the ideal geometry for flow control purposes. This task is no small undertaking however, and will require a significant amount of time and effort. Further studies can also focus on the variation of the pressure field within the resonator when its cavity lower wall has a hole with different sizes. This can change the flow behaviour within the cavity and consequently the resonator effects on the boundary layer.

It is concluded that through the use of the flow-excited Helmholtz resonator the turbulent boundary layer is only stabilised close to the resonator orifice in both the streamwise and spanwise directions. It is anticipated that by incorporating subsequent and identical resonators close to the first in the streamwise and spanwise directions, the stability improvements could be maintained further downstream of the resonators. Hence, for future work the effects of multiple adjacent Helmholtz resonators on the turbulent boundary layer can be investigated.

### 7.4.3 Detailed flow measurements

In the present research the streamwise component of the flow velocity has been measured using a single hotwire. However, to accurately analyse all fluctuating components of the velocity it is required to use a hotwire with an X-probe. In spite of all the advantages of using hotwires for flow measurements, this device faces some issues when implementing it in the vicinity of the resonator orifice for boundary layer measurements, such as possible residual heating effects as well as intrusion in the free development of the flow. Furthermore, it is not possible to observe the flow pattern in the vicinity of the resonator orifice using hotwire anemometry. In order to better estimate the expected performance of the resonators and understand the vortex pattern within the boundary layer, the use of optical measurement techniques such as laser Doppler velocimetry (LDV) or particle image velocimetry (PIV) is recommended for future study. These techniques do not require physical intrusion into the boundary layer and can measure all three flow velocity components.

It is also recommended that in order to quantify the changes to skin friction, other measurement techniques, such as the Fibre-Bragg grating system (Segawa et al. 2003), be implemented rather than using hotwire anemometry for such estimates. However, using this measurement technique requires a considerable allocation of resources. The undertaking of the recommended work would provide the best direction forward for developing an ideal system to achieve the desired flow augmentation while also eventually addressing cost concerns in engineering applications requiring a low cost flow control device.

**Reference**

Segawa, T., Abe, H., Kikushima, Y., Yoshida, H. and Mizunuma, H. 2003, ‘Measurement of turbulent skin frictional drag using a fiber Bragg grating system’, *AIAA paper*, AIAA 2003-646, pp- 1-8.